U.S. DEPARTMENT OF ENERGY
Prepared for the U.S. Department of Energy
under Contract DE-AC05-76RL01830

PNNL-20774
EMSP-RPT-009

Formulation and Characterization of Waste Glasses with Varying Processing Temperature

D Kim
MJ Schweiger
CP Rodriguez
WC Lepry
JB Lang
JV Crum
JD Vienna
FC Johnson
JC Marra
DK Peeler

October 2011

Pacific Northwest
NATIONAL LABORATORY
Proudly Operated by Battelle Since 1965

DISCLAIMER

PACIFIC NORTHWEST NATIONAL LABORATORY
operated by
BATTELLE
for the
UNITED STATES DEPARTMENT OF ENERGY
under Contract DE-AC05-76RL01830

Printed in the United States of America

Available to DOE and DOE contractors from the
Office of Scientific and Technical Information,
P.O. Box 62, Oak Ridge, TN 37831-0062;
ph: (865) 576-8401
fax: (865) 576 5728
email: reports@adonis.osti.gov

Available to the public from the National Technical Information Service,
U.S. Department of Commerce, 5285 Port Royal Rd., Springfield, VA 22161
ph: (800) 553-6847
fax: (703) 605-6900
email: orders@nits.fedworld.gov
online ordering: http://www.ntis.gov/ordering.htm

PNNL-20774
EMSP-RPT-009

Formulation and Characterization of Waste Glasses with Varying Processing Temperature

D Kim
MJ Schweiger
CP Rodriguez
WC Lepry
JB Lang
JV Crum
JD Vienna
FC Johnson[1]
JC Marra[1]
DK Peeler[1]

October 2011

Prepared for
the U.S. Department of Energy
under Contract DE-AC05-76RL01830

Pacific Northwest National Laboratory
Richland, Washington 99352

[1] Savannah River National Laboratory

Summary

This report documents the preliminary results of glass formulation and characterization accomplished within the finished scope of the U.S. Department of Energy, Office of Environmental Management EM-31 technology development tasks for WP-4 and WP-5, including

- WP-4.1.2: Glass Formulation for Next Generation Melter
- WP-5.1.2.3: Systematic Glass Studies
- WP-5.1.2.4: Glass Formulation for Specific Wastes.

These tasks were prematurely closed during the early stage of the development. This report also presents the recommended studies for eventual restart of these tasks.

The initial glass formulation efforts for the cold crucible induction melter, operating at ≥1200°C, with selected high-level waste (AZ-101) and low-activity waste (AN-105), successfully developed glasses with significant increase of waste loading compared to that which is likely to be achieved based on expected reference Hanford Tank Waste Treatment and Immobilization Plant formulation. Three glasses formulated for AZ-101 high-level waste (with a waste loading of 39.8 wt% to 45.1 wt% compared to 37 wt% for WTP) and one glass for AN-105 low-activity waste (containing 24 wt% Na_2O at 31.3 wt% waste loading) were selected for the initial cold crucible induction melter demonstration tests; however, the melter tests were not performed due to an early closure of this task. Glass formulations for the cold crucible induction melter were expanded to cover additional high-level wastes that have a high potential to successfully demonstrate the unique advantages of the cold crucible induction melter technologies, based on projected composition of Hanford wastes. However, only the preliminary scoping tests were completed with selected wastes.

Advanced glass formulations for the reference Hanford Tank Waste Treatment and Immobilization Plant melter, operating at ~1150°C, were initiated with selected specific wastes to determine the estimated maximum waste loading. The preliminary results from these initial formulation efforts are summarized. In addition, a test matrix of 32 high-aluminum glasses was developed based on a new space filling methodology developed in this study to assess the potential for Al_2O_3 concentrations in glass exceeding 22 wt%. Although the test matrix was developed, no experimental work was initiated during FY11.

Acknowledgments

The authors are grateful to the U.S. Department of Energy's Environmental Management Office of Waste Processing (EM-31) for initial funding of the project and for the Office of River Protection and Washington River Protection Solutions for their continued support. Programmatic direction by Steve Schneider and Gary Smith at EM-31, technical support by Albert Kruger at the Office of River Protection, and technical guidance by Gene Ramsey at Washington River Protection Solutions are greatly appreciated. The authors also would like to acknowledge Catherine Veyer and Eric Tchemitcheff at AREVA Federal Services LLC, Nick Soelberg at Idaho National Laboratory, and Ian Pegg at Vitreous State Laboratory of The Catholic University of America for their helpful discussion and guidance.

Acronyms and Abbreviations

AJHM	advanced Joule-heated melter
CCC	canister centerline cooling
CCIM	cold crucible induction melter
CUA	Catholic University of America
DBVS	demonstration bulk vitrification system
DOE	U.S. Department of Energy
DWPF	Defense Waste Processing Facility
EM	U.S. Department of Energy, Office of Environmental Management
EM-31	U.S. Department of Energy, Office of Waste Processing
HBV	high-level waste blend vessel
HLP	Hanford LAW product
HLW	high-level waste
HTWOS	Hanford Tank Waste Operations Simulator
IHLW	immobilized high-level waste
ICP-AES	inductively coupled plasma-atomic emission spectroscopy
ICV	in-container vitrification
INL	Idaho National Laboratory
IWL	improved waste loading
JHM	Joule-heated melter
LAW	low-activity waste
LRM	low-activity reference material
MFPV	melter feed preparation vessel
MT	metric ton
NRC	National Research Council
OB	optical basicity
ORP	U.S. Department of Energy, Office of River Protection
PCT	product consistency test
PNNL	Pacific Northwest National Laboratory
PSAL	SRNL Process Science Analytical Laboratory
SEM	scanning electron microscope
SRNL	Savannah River National Laboratory
SRS	Savannah River Site
TCLP	toxicity characteristic leach procedure
VHT	vapor hydration test

VSL	Vitreous State Laboratory
WP	waste processing
WTP	Hanford Tank Waste Treatment and Immobilization Plant
XRD	x-ray diffraction

Contents

Figures

Tables

1.0 Introduction

Resolving the nation's high-level waste (HLW) legacy requires designing, constructing, and operating large and technically complex processing facilities coupled to equally complex waste treatment and vitrification facilities. Vitrification technology was chosen to treat HLW at the Hanford Site and Savannah River Site (SRS), as well as the low-activity waste (LAW) at the Hanford Site, and it may potentially be applied to other defense waste streams, such as Idaho National Laboratory (INL) tank waste or calcine. Joule-heated melters (JHMs) are being used at the Defense Waste Processing Facility (DWPF) at SRS and will be used at the Hanford Tank Waste Treatment and Immobilization Plant (WTP) to vitrify tank waste fractions (Perez et al. 2001).

The loading of waste into glass and the glass production rates at WTP and DWPF are limited by the current melter technology. Significant reductions in glass volumes for disposal and shorter mission life are only possible with advances in melter technology and glass formulations. These were discussed in the National Research Council report (NRC 2009) "Advice on the Department of Energy's Cleanup Technology Roadmap: Gaps and Bridges," Waste Processing Gap No. 4 (WP-4): "Increased vitrification capacity may be needed to meet schedule requirements of EM's high-level waste programs" and Waste Processing Gap No. 5 (WP-5): "The baseline tank waste vitrification process significantly increases the volume of high-level waste to be disposed." Based on the National Research Council's recommendations, the U.S. Department of Energy, Office of Environmental Management (EM) launched the EM-31 technology development tasks to address the waste processing gaps including WP-4 and WP-5.

This report documents the preliminary results from the FY2011 EM-31 WP-4 and WP-5 subtasks related to the formulation and characterization of glasses with varying processing temperature. These tasks were prematurely closed during the early stage of the development, without significant progress for some subtasks. This report summarizes all the results of glass formulation and characterization achieved prior to closure. Background information and scope covered in this report are described in the following subsections.

1.1 Glass Formulation for Cold Crucible Induction Melter (WP-4.1.2)

The rate of glass production and loading of waste in glass is strongly dependent on glass melter design and operation. Melters with a higher throughput rate may shorten the cleanup mission. Melters that allow for higher waste loading in glass may also significantly reduce lifecycle costs. Next-generation melter technologies with a higher waste throughput rate have been developed to support accelerating the cleanup mission and reducing the lifecycle cost within the U.S. Department of Energy (DOE) complex.

Two melter technologies have been considered (Bush 2010), an advanced Joule-heated melter (AJHM) equipped with more corrosion-resistant electrodes and refractory materials and a cold crucible induction melter (CCIM). In the CCIM design, the molten glass is in contact with a frozen "skull" of glass inside a water-cooled metal crucible; therefore, there are no glass-contact materials that can corrode (Roach et al. 2009). Both melter technologies enable higher melter operating temperatures that can lead to higher loading of waste in glass and a higher processing rate of melter feeds to achieve a higher waste throughput rate. However, it should be noted that the CCIM technologies offer the opportunity for much

higher process temperatures because of the formation of the skull layer. In addition to their capability to achieve higher operating temperatures, the bottom pouring configuration of the CCIM may make the CCIM more tolerant to crystallization within the melter and reduce some of the constraints associated with crystal formation in the JHM. However, a potential concern with higher operating temperatures of the CCIM is higher volatilization from the melter. Whereas the AJHM is significantly closer in design to currently installed/operating melters and so will have fewer challenges for retrofitting of DWPF or WTP.

Advanced glass formulations have been developed to highlight the unique benefits of the next-generation melter technologies while demonstrating reasonable estimates of increased waste loading and glass throughput rates under the WP-4.1.2: Glass Formulation for Next Generation Melter. This subtask focused on developing new glass formulations with higher waste loadings that can be successfully processed with the AJHM or advanced CCIM technologies. These glasses should possess melt properties adequate for processing and meet all product quality requirements. The glass formulations for the AJHM have been performed by the Vitreous State Laboratory (VSL) at Catholic University of America (CUA) (Kot et al. 2011). The glass formulations for the CCIM have been developed through joint efforts by the Pacific Northwest National Laboratory (PNNL) and the Savannah River National Laboratory (SRNL) and their results are presented in this report. Initial results of this subtask on CCIM formulation at PNNL and SRNL were reported in Kim et al. 2011. Detailed results achieved to date are summarized in Section 4.0.

1.2 Advanced Silicate Glass Development (WP-5.1.2)

Vitrification into borosilicate glass is a mature, efficient method to treat U.S. HLW and LAW. However, estimates of the quantity of glass produced by the current state-of-technology glass formulations are excessively high. Therefore, advanced silicate-based glass formulations are needed to reduce the volume of glass produced at both the Hanford and the Savannah River Sites. The possible advances are generally specific to the chemical nature of the waste being treated.

Recent developments in advanced silicate glasses suggest that step function improvements in HLW and LAW loading in glass are possible. The first of these advances include the use of crystal-tolerant glasses for HLW where sparingly insoluble components such as chromium are allowed to crystallize in the melter but are passed out of the melter before accumulating in a sludge layer (Matyas et al. 2010). Another advancement is the development of glasses with significantly higher aluminum content than what would be allowed by the current nepheline precipitation constraints, as well as a corresponding revision to those constraints (McCloy and Vienna 2010). Yet another advancement is the development of very-low silica glasses for ultra-high waste loadings (Marra et al. 2010; Matlack et al. 2010). They were planned to be further developed and demonstrated under WP-5.1.2 task.

The primary programmatic objective was to develop data to evaluate the impacts of advanced methods of silicate glass formulations and melter operations for step function increases in loading of Hanford and SRS wastes in glasses. Data were planned to be generated in this activity at the appropriate quality assurance level to allow for use in waste form qualification activities. However, qualification of these advanced silicate waste forms was not the immediate target of these studies. The WP-5.1.2 included following four subtasks initiated at PNNL:

- WP-5.1.2.1 – Crystal Tolerant Glasses
- WP-5.1.2.2 – Nepheline Model Development
- WP-5.1.2.3 – Systematic Glass Data for Models
- WP-5.1.2.4 – Optimization for Specific Wastes.

The subtask WP-5.1.2.1 – Crystal Tolerant Glasses was completed and the results were documented in Matyas et al. (2010), and the technology was transferred to the site for further development. The recent results from subtask WP-5.1.2.2 – Nepheline Model Development were summarized in Rodriguez et al. (2011). Section 5 of this report documents the initial results, which were completed before the task close out, from two subtasks—WP-5.1.2.3 – Systematic Glass Data for Models and WP-5.1.2.4 – Optimization for Specific Wastes.

1.3 Quality Assurance

A graded quality assurance approach was used for the WP-4 and WP-5 tasks performed under the DOE EM-31 Technology Development and Deployment program. The following work activities performed in the WP-4.1.2 and WP-5.1.2 subtasks were considered waste form quality impacting and were performed in accordance with the quality assurance plan for the EM-31 Support Project (EM-31SP-PQAP) under Quality Level 2. This work was conducted to the quality requirements of NQA-1-2008 as instituted through the PNNL Nuclear Project Quality Assurance Plan (Energy & Environment Directorate) [PNNL-NQA-EQAM-1].

- glass fabrication to prepare glass samples for product consistency test (PCT) and toxicity characteristic leach procedure (TCLP)
- Canister centerline cooling treatment to prepare glass samples for PCT and TCLP
- PCT and TCLP.

All other activities that are not waste form quality impacting (e.g., liquidus temperature, viscosity, and electrical conductivity) were performed in accordance with the quality assurance plan for the EM-31 Support Project (EM-31SP-PQAP) under Quality Level 3. This work was conducted in accordance with best laboratory practices (NQA-1-2000 based) as implemented through PNNL's standards-based management system (HDI) work flows and subject areas.

Quality assurance (QA) activities performed by SRNL are defined in the project specific quality assurance plan, SRNL-RP-2010-00932.

2.0 Waste Compositions

This section describes the waste compositions that were used in this study. Section 2.1 summarizes the selection of waste compositions used for initial glass formulation efforts for CCIM. Section 2.2 describes the projected Hanford waste compositions used for both CCIM glass formulation (Section 4.0) and advanced silicate glass formulation (Section 5.0). Section 2.2 also describes the cluster analyses of the projected Hanford wastes, glass formulation constraints used for estimation of maximum waste loading, and estimated waste loading and glass mass for each cluster.

2.1 Selection of Wastes for Initial Formulation for the Cold Crucible Induction Melter

Table 2.1 lists the wastes that were considered for use in initial CCIM glass formulations. The selection of wastes initially focused on Hanford waste streams because they are likely to show the highest cost benefit to implementation, considering the size and cost of the Hanford tank waste cleanup program and the timing of startup. INL treatment is likely to show a cost increase because of the low cost baseline options selected, and DWPF will be so far progressed in their program before CCIM implementation that it will have only moderate cost impacts.

Table 2.1. Wastes Considered for Glass Formulation for Next-Generation Melters

Waste ID	Site	Type	Comment
C-104 Actual	Hanford	HLW	Zr and Th rich
AZ-101 Actual	Hanford	HLW	Fe rich
Alumina	INL	Calcine/HLW	Al rich
Alumina-Na Blend	INL	Calcine/HLW	Al rich
Zirconia	INL	Calcine/HLW	Zr rich
Zirconia-Na Blend	INL	Calcine/HLW	Zr rich
SBW*	INL	SBW/HAW	Na rich
Bi Limited	Hanford	HLW	$BiPO_4$ waste
Cr Limited	Hanford	HLW	Redox/$BiPO_4$
Al Limited	Hanford	HLW	Al rich
Al and Na Limited	Hanford	HLW	Al rich
AN-105	Hanford	LAW	Low S, Cl rich
AN-102	Hanford	LAW	S and Cl rich
AZ-102	Hanford	LAW	S rich
AP-101	Hanford	LAW	K rich
High Al_2O_3	DWPF	HLW	Al rich
High Fe_2O_3	DWPF	HLW	Fe rich
High MnO and NiO	DWPF	HLW	Mn rich
*SBW is a sodium-bearing high-activity waste stored in INL tanks			

The compositions of the Hanford related wastes are given in Table 2.2 and are expressed in terms of wt% of oxides and halogens (referred to as “oxides” in this report).

Table 2.2. Waste Compositions (in wt% oxides) Considered for Next-Generation Melter Glass Formulation

Component	HLW						LAW			
	AZ-101	C-104	Bi-Limited	Cr-Limited	Al-Limited	Al&Na-Limited	AN-105	AN-102	AZ-102	AP-101
Al_2O_3	24.58	9.69	23.18	27.48	52.95	45.13	17.88	6.40	0.30	5.23
B_2O_3	0.00	0.00	0.60	0.57	0.42	0.77	0.08	0.03	0.00	0.01
BaO	0.00	0.00	0.02	0.03	0.12	0.06	0.00	0.00	0.00	0.00
Bi_2O_3	0.00	0.00	13.33	7.85	2.53	2.45	0.00	0.00	0.00	0.00
CaO	1.40	1.67	1.66	2.66	2.38	1.53	0.00	0.19	0.00	0.00
CdO	2.16	0.27	0.00	0.01	0.05	0.02	0.00	0.00	0.00	0.00
Ce_2O_3	0.80	0.30	0.00	0.00	0.00	0.00	0.00	0.00	0.00	0.00
Cl	0.00	0.00	0.00	0.00	0.00	0.00	2.17	1.33	0.07	0.79
Cr_2O_3	0.46	0.40	1.03	3.30	1.15	1.50	0.07	0.09	0.90	0.32
Cs_2O	0.50	0.50	0.50	0.50	0.50	0.50	0.50	0.50	0.50	0.50
F	0.00	0.00	1.63	2.15	1.47	0.48	0.01	0.70	0.56	0.31
Fe_2O_3	37.67	17.80	13.83	14.13	13.03	5.95	0.00	0.00	0.00	0.00
HfO_2	0.00	14.35	0.00	0.00	0.00	0.00	0.00	0.00	0.00	0.00
K_2O	0.00	0.00	0.92	0.40	0.31	1.40	1.72	0.66	3.32	19.49
La_2O_3	0.89	0.00	0.00	0.00	0.00	0.00	0.00	0.00	0.00	0.00
Li_2O	0.00	0.00	0.32	0.39	0.38	0.16	0.00	0.00	0.00	0.00
MgO	0.00	0.00	0.85	0.17	0.26	0.46	0.00	0.00	0.00	0.00
MnO	0.91	3.55	0.00	0.00	0.00	0.00	0.00	0.00	0.00	0.00
Na_2O	10.58	11.03	13.39	21.62	7.91	26.88	76.79	84.71	80.57	71.24
Nd_2O_3	0.65	9.97	0.00	0.00	0.00	0.00	0.00	0.00	0.00	0.00
NiO	1.66	1.01	3.83	1.14	0.88	0.21	0.00	0.15	0.00	0.03
P_2O_5	1.34	1.37	9.91	3.59	2.32	4.27	0.00	1.15	0.24	0.49
PbO	0.00	0.00	0.50	0.52	0.90	0.19	0.00	0.06	0.00	0.03
Re_2O_7	0.00	0.00	0.00	0.00	0.00	0.00	0.10	0.10	0.10	0.10
RuO_2	0.15	0.10	0.10	0.10	0.10	0.10	0.00	0.00	0.00	0.00
SiO_2	3.77	6.57	12.43	11.36	10.81	6.48	0.10	0.05	0.48	0.10
SnO_2	0.66	0.00	0.00	0.00	0.00	0.00	0.00	0.00	0.00	0.00
SO_3	0.38	0.19	0.94	1.64	0.44	0.46	0.59	3.89	12.98	1.38
TiO_2	0.00	0.00	0.31	0.01	0.02	0.36	0.00	0.00	0.00	0.00
ZnO	0.00	0.00	0.32	0.27	0.18	0.38	0.00	0.00	0.00	0.00
ZrO_2	11.44	21.21	0.41	0.12	0.87	0.26	0.00	0.00	0.00	0.00

Each of these wastes was adjusted slightly to ensure adequate analysis of key partially volatile radionuclides (Cs_2O, and Re_2O_7 as Tc_2O_7 surrogates) and noble metals to ensure adequate crystal nucleation in HLW simulant melts. The waste compositions were evaluated for their potential to successfully demonstrate the unique advantages of the CCIM technology over current reference technologies. The comments and waste loading targets from these evaluations are given below (note that these targets are very challenging and represent the high end of the likely results of laboratory scale formulation activities):

AZ-101: This waste is relatively high in aluminum, iron, and zirconium, which suggests that using a melter technology capable of higher melting temperature and increased tolerance to spinel crystals could increase loading and potentially increase the processing rate. In addition, the composition is at the high end of potential noble metal concentrations for Hanford tank wastes. The maximum expected waste loading for the reference WTP formulation is 37 wt%.

C-104: This waste represents a relatively small fraction of waste in the Hanford tanks with high thorium and zirconium (being found only in cluster #3, below). Although CCIM technology is likely to obtain significantly higher loadings of this waste than a Joule-heated melter because of higher operating temperatures, the impacts will not be as significant as for other wastes.

Bismuth-limited: This waste represents the $BiPO_4$ waste stream, which makes up a relatively large fraction of Hanford tank wastes. The waste loading is generally limited by phosphate content, which is not expected to be significantly higher in a CCIM than the reference melter type unless the composition is changed to either a phosphate-based glass or a glass ceramic where the phosphate is precipitated from the silicate melt.

Chromium-limited: This waste represents a mix of REDOX (Reduction-Oxidation Plant) and $BiPO_4$ wastes, which make up a large fraction of Hanford tank sludge. A melter with higher operating temperature and crystal tolerance has a potential to obtain higher loadings for this waste type. However, this waste also contains relatively high concentration of SO_3, suggesting that the waste loading may be limited by salt formation. In that case the CCIM may not have an advantage.

Aluminum-limited: There is a full range wastes with very high aluminum in the Hanford sludge because aluminum was a component of the fuel cladding that was dissolved and sent to the tank farm. This waste type makes up almost half of the Hanford HLW. Higher-temperature melting can generally tolerate higher aluminum loadings; however, in the case of this particular composition, nepheline precipitation on slow cooling (and its impact on durability) is the biggest challenge. The CCIM does not appear to have a strong advantage for these waste types; however, if lower alkali can be added to the glass, the resulting, partially crystallized waste form may pass durability constraints.

Aluminum- and sodium-limited: A subset of the high-aluminum wastes described above simultaneously includes high sodium. Glasses for these wastes include minimal alkali addition and are still limited by nepheline precipitation. It is not clear how a CCIM would show significant advantages over a JHM for this waste stream. It is worth noting, however, that this type of Hanford waste is closely related to the DWPF high Al_2O_3 composition from sludge batch 19 (Chew and Hamm 2009).

AN-105: This is a low-sulfur and high-chlorine LAW stream. Its loading is limited by Na_2O concentration in glass, which dictates the chemical durability of glass. The maximum expected waste loading for the reference WTP formulation is 27 wt% (yielding 21 wt% Na_2O in glass). This waste stream is also characterized by its high chlorine content, but its loading is not limited by chlorine because of its low sulfur content (the chlorine limit depends on the sulfur concentration in glass). The higher melting temperature of CCIM technologies would allow higher concentrations of refractory additive components that increase chemical durability, such as ZrO_2 and SnO_2, which may enable higher waste loading.

AN-102: This waste has elevated concentrations of both sulfur and chlorine. The loading in glass by CCIM is not expected be significantly higher than demonstrated in JHM because the waste loading is likely to be limited by salt formation.

AZ-102: This waste represents the highest sulfate wastes. Similar to AN-102, the CCIM is not expected to obtain significantly higher loadings for this waste in a silicate glass, although a phosphate glass is expected to achieve significant loading increases.

AP-101: This waste represents a relatively small fraction of Hanford LAW with high potassium, which is to be processed first in the WTP. Similar to AN-105, the higher melting temperature of CCIM technologies may enable higher waste loading.

Based on these preliminary informal evaluations, the AZ-101 HLW and AN-105 LAW were selected for initial glass formulations and demonstration for CCIM. The results of glass formulation tests are described in Sections 4.1 and 4.2.

2.2 Projected Hanford High-Level Waste Compositions

Information on the composition of the Hanford tank wastes for the entire mission is needed to estimate the impact of CCIM technologies on the glass volume, which is used to evaluate the impact on the duration and lifecycle costs of Hanford cleanup mission. The projected compositions of Hanford tank wastes generated by the WTP Dynamic Flowsheet Model (G2) were used. The G2 model run selected (MRQ 10-0063 Scenario 6.0.1a using adjusted System Plan Rev 3 feed vector [Certa et al. 2008]) represents one of the many recent G2 runs. The compositions of HLW at a node between high-level waste blend vessel (HBV, HLP-VSL-0028) and melter feed preparation vessel (MFPV, HFP-VSL-00001 and 5) were used. The G2 model output included 378 HLW batches for the entire mission with the first batch dated May 2018 and the last dated December 2033.

The G2 output given in the masses of elements and compounds were converted to concentrations of 63 oxides used in the glass formulation (i.e., in mass fraction of oxides and halogens) and to a total mass of oxides. The total oxide mass in metric tons (MT) from this particular G2 run was 11,075 metric tons (MT) (average 29.3 MT) with each batch ranging from 7.1 to 46.7 MT.

Figure 2.1 through Figure 2.4 show the concentrations of the components of interest as a function of time: Figure 2.1 for the 15 components that were used for cluster analyses in Section 2.2.1; Figure 2.2 for three major components that are present in high concentrations in Hanford wastes and have primary impact on the waste loading in glass; Figure 2.3 for three components that are important for the formation of spinel that has strong effect on waste loading; and Figure 2.4 for four components that are of interest for glass formulation related to potential phase separation and its effect on waste loading.

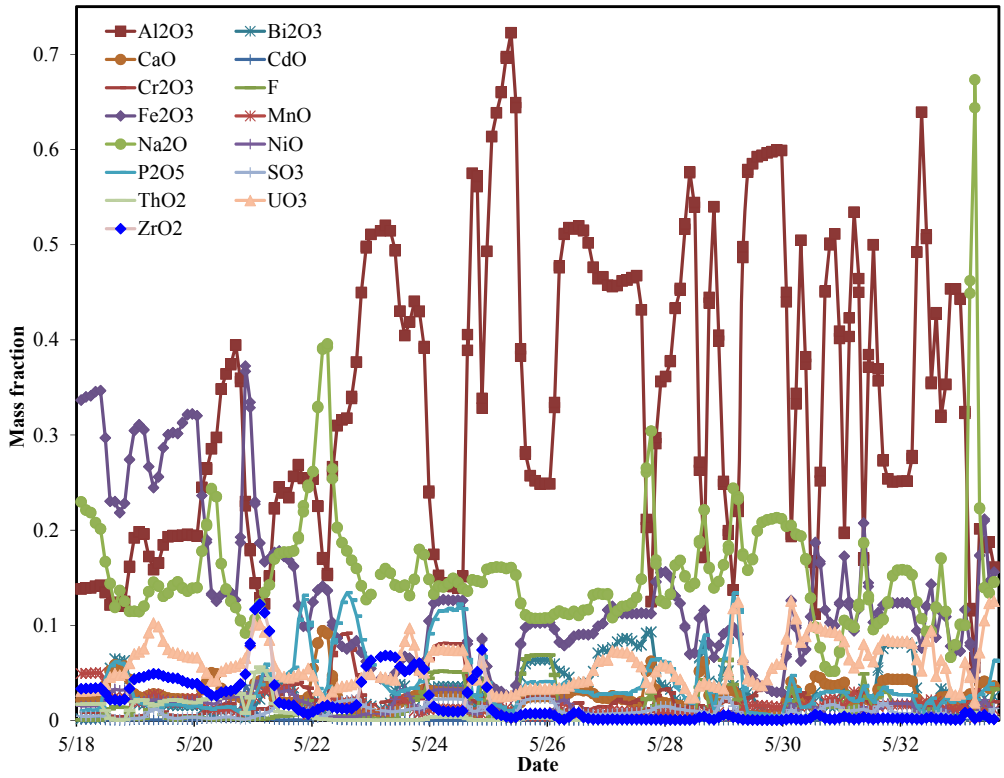

Figure 2.1. Composition of Projected Wastes for 15 Components of Interest for Glass Formulation

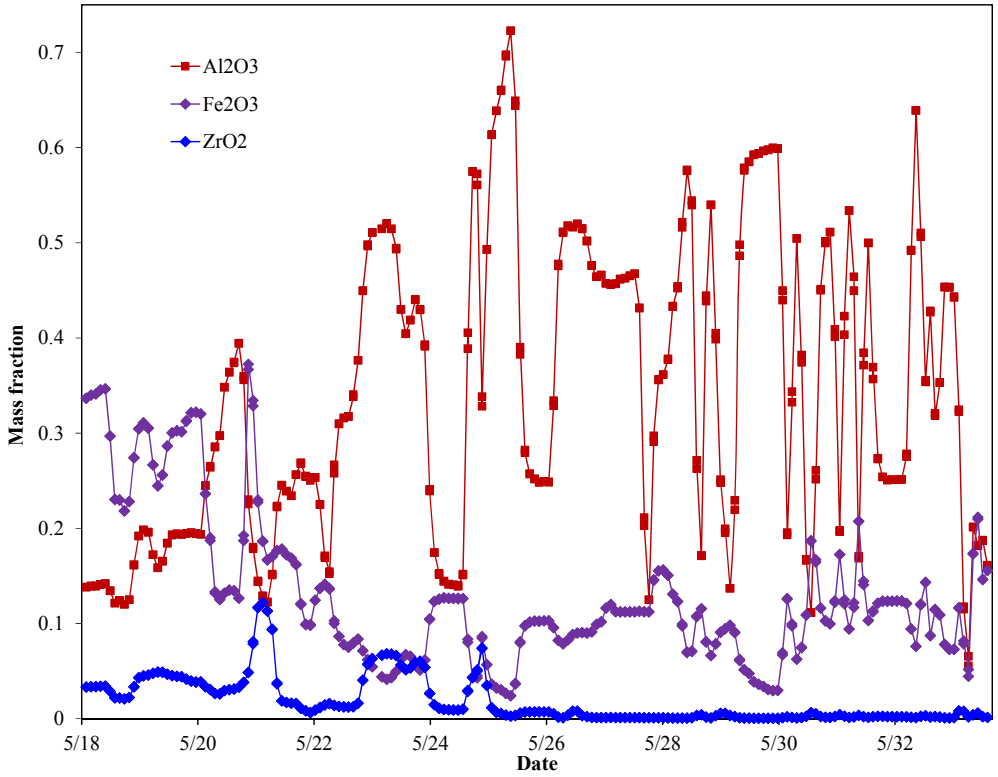

Figure 2.2. Composition of Projected Wastes for Three Major Components

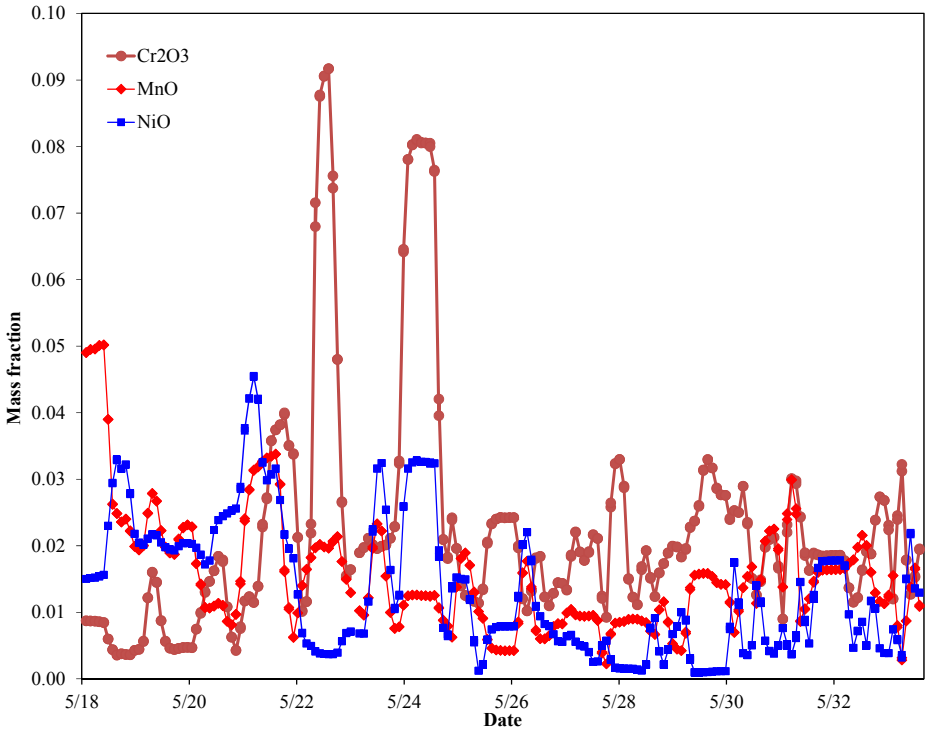

Figure 2.3. Composition of Projected Wastes for Three Components Important for Spinel Formation

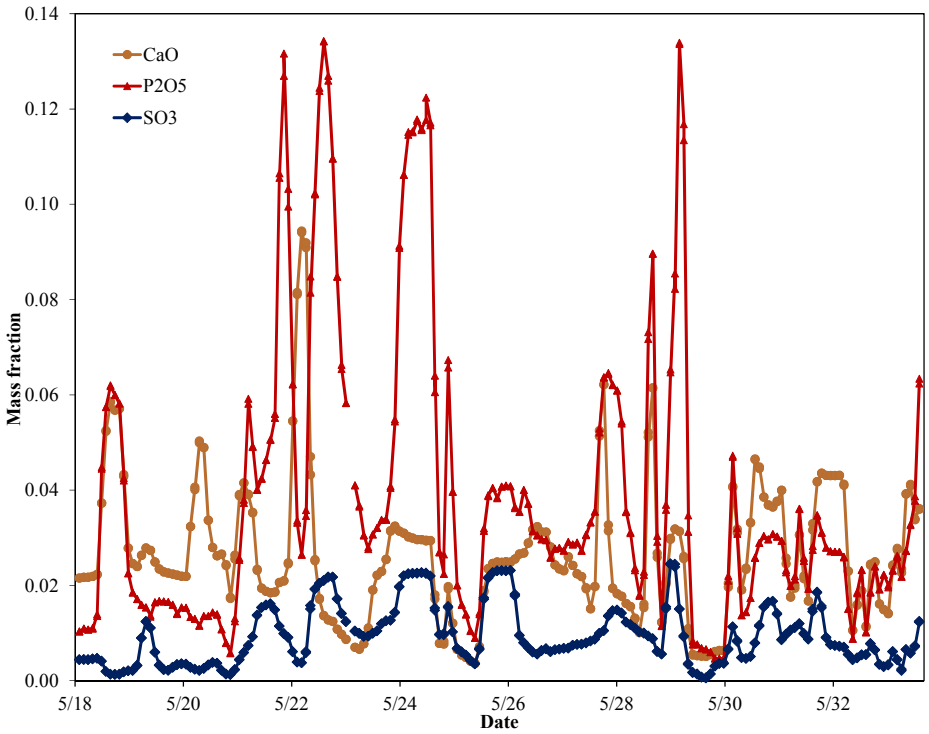

Figure 2.4. Composition of Projected Wastes for Four Components Important for Potential Phase Separation

2.2.1 Cluster Analysis

To keep the required glass formulations and glass mass estimation for each set of constraints manageable, K-Means cluster analysis was performed to sort 378 waste batches into waste clusters of like compositions using JMP® statistical software (Release 6.0.0, SAS Institute, Inc., Cary, NC). Waste batches were sorted according to their composition by mass of the 15 components: Al_2O_3, Bi_2O_3, CaO, CdO, Cr_2O_3, F, Fe_2O_3, MnO, Na_2O, NiO, P_2O_5, SO_3, ThO_2, UO_3, and ZrO_2, which represent the components that are present in large concentrations or have a strong effect on waste loading in glass.

In cluster analysis, as the number of clusters increases, the average distance (a measure of closeness of data points or waste compositions to the centroid of each cluster used by JMP® software) over all clusters analyzed decreases, i.e., the higher the number of clusters, the more accurate the partitioning of composition becomes. However, it is desirable to keep the number of clusters small so that the glass formulation is manageable. Figure 2.5 shows the decrease of the average distance as the number of clusters increases from 10 to 40. Figure 2.5 indicates that the decrease of average distance slows down after the number of clusters reaches about 20. The 20 clusters match reasonably well with the number used in previous studies of 17 clusters (Perez et al. 2001; Kim and Vienna 2002) and were chosen for the present study.

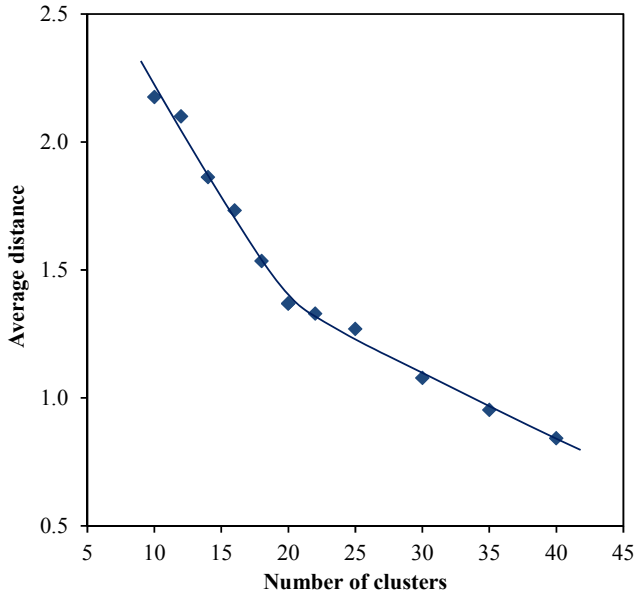

Figure 2.5. Average Distance versus Number of Clusters from K-Means Cluster Analysis

Figure 2.6 shows the parallel coordinate plots for the 20 clusters, generated by JMP® software. In Appendix A, Table A.1 lists the composition of 20 clusters in terms of 63 oxide components that are tracked in the G2 model. The glass formulation spreadsheet developed at PNNL uses 41 oxide components excluding the 22 minor components that are present in the wastes at very low concentrations. Table A.2 lists the composition of 20 clusters in terms of 41 oxide components (normalized mass fraction). Tables A.1 and A.2 also include the total oxide mass for each cluster, which is a sum of oxide masses for all batches that belong to each cluster.

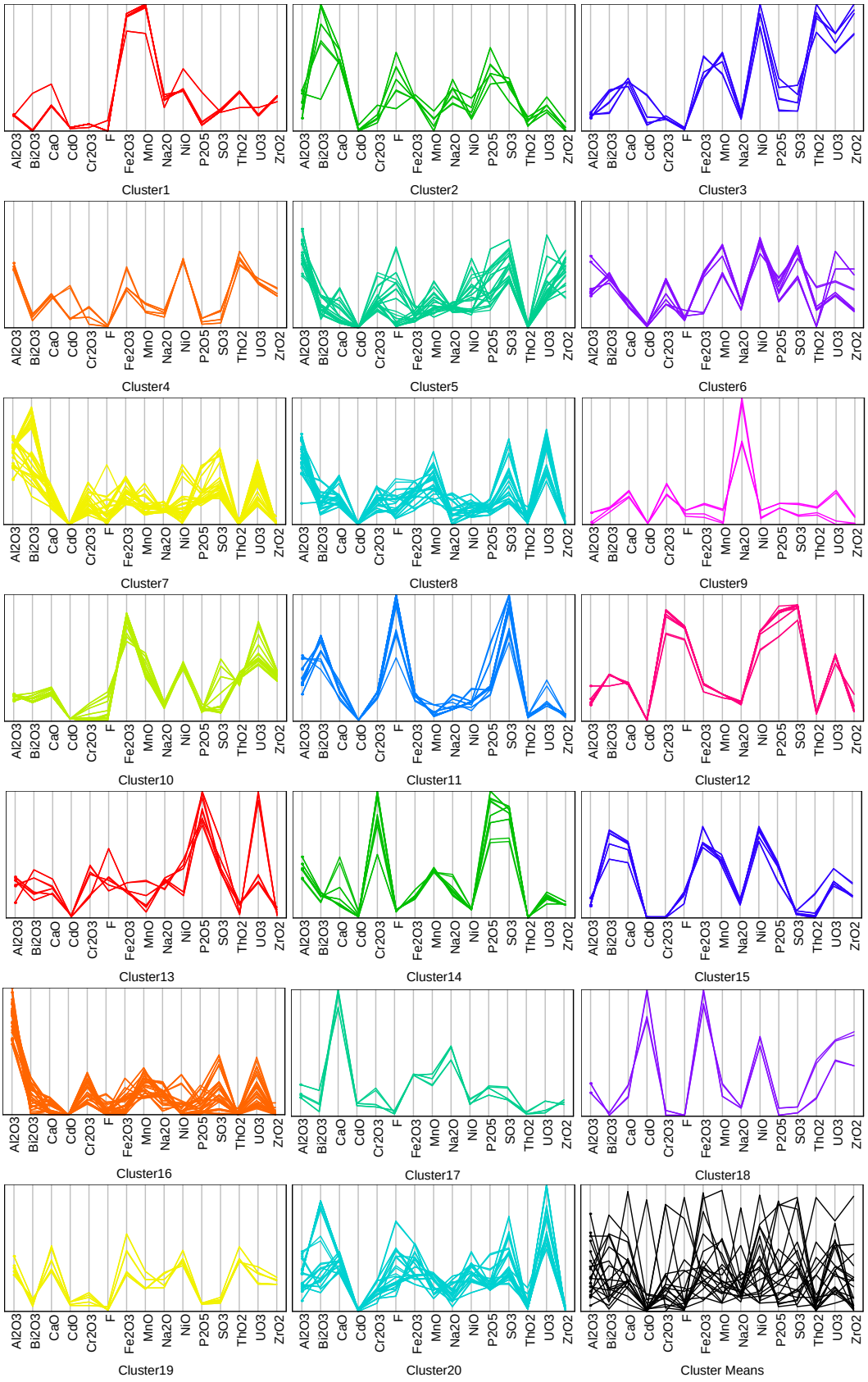

Figure 2.6. Parallel Coordinate Plots for 20 Clusters Based on 15 Components

2.2.2 High-Level Waste Glass Formulation Constraints for Waste Loading Estimation

Using the compositions of 20 waste clusters expressed in 41 oxide components (Table A.2), the maximum waste loading for each waste cluster was calculated by applying the constraints and glass property models developed for the WTP and those for the Hanford Tank Waste Operations Simulator (HTWOS). Table 2.3 through 2.5 summarize the preliminary constraints being developed for WTP, and Table 2.6 summarizes the HTWOS constraints. A detailed description of the preliminary glass formulation methods and constraints being developed for the operation of the WTP is in Vienna and Kim (2008). The HTWOS 2009 baseline constraints are summarized in Belsher and Meinert (2009) derived from Vienna et al. (2009) and the models used for the HTWOS are given in Vienna et al. (2009). Selected constraints for the HTWOS were revised and described in McCloy and Vienna (2010).

Table 2.3. WTP Glass Property and Solubility Constraints

Constraint Description	Lower limit	Upper limit
PCT normalized B release, r_B (g/L) PCT normalized Li release, r_{Li} (g/L) PCT normalized Na release, r_{Na} (g/L)		16.70 9.57 13.35
Nepheline rule, $N_{Si} = g_{SiO2}/(g_{Al2O3} + g_{Na2O} + g_{SiO2})$	0.62	
CdO concentration in glass, g_{CdO} (wt%) or TCLP Cd concentration, c_{Cd} (mg/L)		0.1 0.48
Tl_2O concentration in glass, g_{Tl2O} (wt%)		0.465
Temperature at 1 vol% spinel crystal, $T_{1\%}$ (°C)		950
Non spinel phase rule, $g_{Al2O3} + g_{ThO2} + g_{ZrO2}$ (wt%) Non spinel phase rule, $g_{ThO2} + g_{ZrO2}$ (wt%) Non spinel phase rule, g_{ZrO2} (wt%)		18 13 9.5
Viscosity at 1150°C, η_{1150} (Pa·s) Viscosity at 1100°C, η_{1100} (Pa·s)	2	8 15
Electrical conductivity at 1100°C, ε_{1100} (S/m) Electrical conductivity at 1200°C, ε_{1200} (S/m)	10	 70
SO_3 concentration in glass, g_{SO3} (wt%)		0.44
Phosphate phase rule, g_{P2O5} (wt%) Phosphate phase rule, $g_{P2O5} \times g_{CaO}$ (wt%^{2}) Phosphate phase rule, g_{Li2O} (wt%)		4.5 6.5 6.0

There are two groups of constraints, based on glass properties and concentrations, that are used when formulating glasses: acceptability constraints and processing constraints. Acceptability constraints are concerned with the acceptability of the final product, related to the resistance against corrosion to prevent the spread of the radioactive and toxic elements into the environment. The current regulation for immobilized HLW (IHLW) product uses two standard test methods—product consistency test (PCT) (ASTM 2008) and toxicity characteristic leach procedure (TCLP) (EPA 1997). The PCT normalized releases should be less than environmental assessment glass (Jantzen et al. 1993). See Table 2.3 for limiting values. As Hanford tank waste is a listed hazardous waste, a delisting action is required. A draft petition for delisting (see Vienna and Kim 2008) specifies that the CdO concentration in glass is below 0.1 wt% or the TCLP cadmium concentration is below 0.48 mg/L and the Tl_2O concentration in glass is

below 0.465 wt% (Table 2.3). However, the PCT and TCLP requirements are easily met for most Hanford HLW glasses, and therefore are sometimes not used as constraints (e.g., see Table 2.6).

Table 2.4. WTP Model Validity Constraints (in wt%)

Component	If $g_{CdO} \leq 0.1$ wt%		If $g_{CdO} > 0.1$ wt%	
	Lower limit	**Upper limit**	**Lower limit**	**Upper limit**
Al_2O_3	1.8	13.0	1.9	8.5
B_2O_3	4.5	15.0	4.8	14.0
CaO	0	1.0	0	1.0
CdO	0	1.6	0	1.6
Cr_2O_3	0	0.6	0	0.5
F	0	0.44	0	0.44
Fe_2O_3	1.4	15.0	1.9	14.0
K_2O	0	1.6	0	1.6
Li_2O	0	6.0	1.9	6.0
MgO	0	1.2	0	1.2
MnO	0	8.0	0	7.0
Na_2O	3.9	20.0	3.9	15.0
NiO	0	1.0	0	1.0
PbO	0	1.0	0	1.0
SiO_2	35.0	53.0	35.0	53.0
SrO	0	10.0	0	10.0
ThO_2	0	6.0	0	6.0
TiO_2	0	1.0	0	1.0
UO_3	0	6.5	0	6.3
ZnO	0	4.0	0	4.0
ZrO_2	0	9.6	0	9.1
Sum of Minors[(a)]	0	5.19	0	4.29

[(a)] For $g_{CdO} \leq 0.1$ wt%, the sum of all components not listed individually in this table. For $g_{CdO} > 0.1$ wt%, all components not listed individually in this table plus CaO, K_2O, MgO, PbO, and TiO_2.

Table 2.5. WTP Model Validity Constraints for Predicted PCT Normalized Releases

Component(s)	Upper limit, g/L
PCT r_B	6.61
PCT r_{Li}	4.27
PCT r_{Na}	5.53

Table 2.6. HTWOS Constraints

Constraint	Constraint Description	Baseline		Revised	
		Lower limit	Upper limit	Lower limit	Upper limit
Property Constraints	Viscosity at 1150°C, η_{1150} (Pa·s)	4	6		
	Temperature at 1 vol% spinel crystal, $T_{1\%}$ (°C)		950		
	Liquidus temperature of Zr-phase, T_L-Zrs (°C)		1050		
	Nepheline rule, $N_{Si} = g_{SiO2}/(g_{Al2O3} + g_{Na2O} + g_{SiO2})$ or Nepheline rule, OB	0.62			0.575[(a)]
Solubility Constraints	Cr_2O_3 concentration in glass, g_{Cr2O3} (wt%)		1.2		
	SO_3 concentration in glass, g_{SO3} (wt%)		0.5		0.6
	Noble metal oxides in glass, $g_{PdO} + g_{Rh2O3} + g_{RuO2}$ (wt%)		0.25		
	F concentration in glass, g_F (wt%)		2		
	Phosphate phase rule, g_{P2O5} (wt%) Phosphate phase rule, $g_{P2O5} \times g_{CaO}$ (wt%^{2}) Phosphate phase rule, g_{Li2O} (wt%)		2.5 6.5 6.0		4.5
Model Validity Constraints	Al_2O_3	1.9	20.0		
	B_2O_3	4.0	20.0		
	BaO		4.7		
	Bi_2O_3		3.2		7
	CaO		7.0		
	CdO		1.5		
	Fe_2O_3	4.0	17.4		
	K_2O		6.0		
	MgO		6.0		
	MnO		7.0		
	Na_2O	4.1	21.4		
	Nd_2O_3		5.9		
	NiO		3.0		
	SiO_2	30.3	53.0		
	SrO		10.1		
	ThO_2		6.0		
	TiO_2		3.1		
	UO_3		6.3		
	ZnO		4.0		
	ZrO_2		13.5		

Empty cells represent "not applicable" for baseline constraints and "no change" for revised constraints.
[(a)] For revised HTWOS constrains, the nepheline rule is met when either the N_{Si} or OB rule is satisfied.

The glass properties may strongly depend on the temperature history of the glass product. Slowly cooled glasses are more susceptible to amorphous phase separation or crystallization. Crystallization of the slowly cooled glass near the center of the canister, simulated by the canister centerline cooling (CCC) treatment, can result in a severe deterioration of glass chemical durability as determined by PCT, especially if nepheline ($NaAlSiO_4$) is formed (Kim et al. 1995; Li et al. 1997). It has been known that the

formation of spinel crystals in many HLW glasses does not affect the PCT durability (Bickford and Jantzen 1984). To formulate glasses without nepheline precipitation, empirical rules based on nepheline discriminator (N_{Si}) (Li et al. 2003) and optical basicity (OB) have been developed (see McCloy and Vienna 2010, for how to calculate OB from glass composition)

$$N_{Si} = \frac{g_{SiO_2}}{g_{SiO_2} + g_{Na_2O} + g_{Al_2O_3}} \geq 0.62 \tag{2.1}$$

$$\text{OB (Optical Basicity)} \leq 0.575 \tag{2.2}$$

where g_i is the mass fraction of the i^{th} oxide in glass. The WTP and Baseline HTWOS constraints use only the N_{Si} rule as a nepheline rule (Table 2.3 and Table 2.6), whereas the revised HTWOS constraints specify that the nepheline rule is met when either the N_{Si} or OB rule is satisfied (Table 2.6).

The processing constraints are used to make sure of adequate processability of glass in the melter, expressed in terms of either melt properties (viscosity and electrical conductivity, liquidus temperature, temperature at 1 vol% spinel) or component concentrations. The required ranges for melt properties differ for different melter types and operating strategies. The required ranges can also depend on the purpose of the constraints, e.g., for plant operation (WTP) or for glass mass estimation (HTWOS). The viscosity and electrical conductivity of the glass melt should be maintained within a certain range for acceptable processing (see Table 2.3). The permitted range for electrical conductivity of molten glass is wide and its requirement is met usually when the viscosity requirement is met and therefore often not used, especially when the narrow viscosity range is specified as in HTWOS constraints (Table 2.6).

An often limiting property of HLW glass is its liquidus temperature (T_L), the highest temperature at which a crystalline phase can exist in the melt at equilibrium. The glass with a T_L above a certain limit can precipitate the crystalline phase in the melter and may interfere with melter operation. To prevent a potential problem in the melter, the T_L is historically constrained to be 100°C lower than the nominal melter processing temperature. The WTP has developed a constraint to limit the equilibrium volume percent of spinel crystal at 950 °C to less than 1%, i.e. $T_{1\%} \leq 950$ °C (Vienna and Kim 2008). HTWOS constraints use the $T_{1\%} \leq 950$ °C and T_L-Zrs ≤ 1050 °C where T_L-Zrs is the liquidus temperature of the zirconium-containing crystalline phases. The current WTP constraints use the $T_{1\%} \leq 950$ °C requirement but apply a set of non-spinel phase rules (Table 2.3) instead of the T_L-Zrs constraint. Table 2.4.

In addition, the single or multiple component constraints are used to limit the concentrations of the potential troublesome components and thereby reduce the risk of their deleterious effects on glass processing. For WTP, the SO_3 concentration and a set of phosphate phase rules are applied (Table 2.3). Five sets of single or multiple component constraints are used for HTWOS, which are grouped as solubility constraints in Table 2.6. The constraints for both WTP and HTWOS also include constraints on concentration of individual components that are used to ensure that formulated glasses are within the composition region where the property models are valid (Table 2.4 and Table 2.6). The WTP constraints also apply the model validity upper bounds on predicted PCT normalized releases (see Table 2.5).

2.2.3 Waste Loading Estimates for 20 Waste Clusters

Table 2.7 shows the composition of waste clusters (same composition as in Appendix A, Table A.2 that lists all 41 components, but Table 2.7 lists only the 15 components used in cluster analysis) and estimated maximum waste loadings along with the constraints that limit the waste loading and resulting glass mass. The maximum waste loading calculations were performed separately for WTP, HTWOS baseline, and HTWOS revised constraints. Table 2.7 also shows the composition of waste clusters in six different waste groups discussed below.

The model validity composition ranges were the only constraints that limited the loading for all clusters in WTP formulation. This resulted in relatively low overall waste loadings and therefore large glass mass. The model validity constraints are somewhat artificial and are not real limits driven by processing or product requirements. There are three primary reasons for WTP's model validity constraints to be so constrictive. First, the current WTP models were developed for the first four tanks that were planned to be vitrified during the initial WTP contract, which represent a very small fraction of entire Hanford HLWs. Second, the current WTP models were developed based on the waste composition estimates made in early 2000, but the composition estimates have evolved significantly. Third, the WTP contract is focused on design, construction, and commissioning of the plant not on overall process optimization, so, maximizing waste loading was never a formal driver. Expansion of the valid composition region is needed to allow the waste loadings to be limited by constraints driven by the actual process and quality requirements.

When the waste loading is limited by glass properties or nepheline constraints, not limited by model validity or solubility constraints, the calculations for glass optimization continue until other property requirements are met and maximize the waste loading, i.e., there are always multiple constraints that limit the waste loading as shown in Table 2.7 for HTWOS.

Based on waste cluster composition and the constraints that limit waste loading for HTWOS baseline and revised constraints, the waste clusters were further grouped into six different waste groups described as follows. Note that these groupings are somewhat arbitrary and are used to picture the overall waste compositions trend.

High-Al_2O_3. These clusters contain 41.8 wt% Al_2O_3 or higher. The waste loading for these clusters is expected to be primarily limited by nepheline formation. At the same time, because of the strong effect of Al_2O_3 on increasing the $T_{1\%}$ and T_L-Zrs, glass needs to be formulated to avoid the crystallization. For the glasses formulated based on HTWOS baseline constraints, all four waste clusters were limited by three constraints, T_L-Zrs, N_{Si}, and VisU (VisU: viscosity upper limit, see the footnotes to Table 2.7 for abbreviations used for constraints). It should be noted that the prediction of waste loading limited by the T_L-Zrs constraint is not realistic considering that the ZrO_2 concentration in glass is very low (the highest was 1.8 wt% ZrO_2 for glasses formulated for Cluster 5, the rest less than 0.1 wt%). For the revised HTWOS constraints, the waste loading becomes limited by the constraints involving OB instead of N_{Si} and model validity for Al_2O_3. The primary factor for the increased waste loading going from baseline to revised constraint is the introduction of OB: for Clusters 5 and 8 the N_{Si} changes to OB and for Clusters 7 and 16 the waste loading become limited by model validity.

High-Fe_2O_3. These clusters contain 30 wt% Fe_2O_3 or higher and are similar to the AZ-101 composition given in Table 2.2, which was used for initial glass formulation for CCIM. The waste

loading is primarily limited by $T_{1\%}$. Table 2.7 shows that all three high-Fe_2O_3 clusters were limited by $T_{1\%}$, N_{Si}, and VisL (VisL: viscosity lower limit). A brief waste loading sensitivity study for these wastes showed that dramatic increase of waste loading results when the $T_{1\%}$ constraint is relaxed (i.e. $T_{1\%}$ is allowed to increase over the current limit of 950°C) whereas there is little change in waste loading when the other two constraints are relaxed.

Spinel-limited. These waste clusters do not have high aluminum or iron and are not limited by salt formation. They typically contain relatively high or moderate concentrations of "spinel components" (Fe_2O_3, Cr_2O_3, NiO, and MnO) that participate in the spinel structure and have therefore strong impact on $T_{1\%}$. The waste loading is primarily limited by spinel $T_{1\%}$ and like high-Fe_2O_3 clusters. Relaxing the $T_{1\%}$ constraint would increase the waste loading significantly. Table 2.7 shows that all four clusters were limited by $T_{1\%}$, N_{Si}, and VisL similar to high-Fe_2O_3 clusters.

Cr_2O_3-SO_3 limited. The two clusters (Clusters 12 and 14) contain highest Cr_2O_3 concentration at 7.7 wt% and 7.4 wt%. These two clusters also contain high SO_3 (one with highest SO_3 and the other with third highest among all clusters). The two other clusters (Clusters 6 and 11) do not have highest Cr_2O_3 or highest SO_3 but contain relatively high concentrations of both Cr_2O_3 and SO_3. Within this group, two clusters are limited by Cr_2O_3 and two limited by SO_3 based on baseline HTWOS constraints while three clusters are limited by Cr_2O_3 and one limited by SO_3 based on revised HTWOS constraints. Both Cr_2O_3 and SO_3 limits are related to salt formation, and formation of salt by either Cr_2O_3 or SO_3 is strongly affected by each other, which is why they are grouped together.

P_2O_5-CaO limited. These clusters are characterized by the limiting constraints involving P_2O_5 with the combination of relatively high concentration of CaO. The limiting mechanism is not well defined for this waste group, suspected to be limited either by salt formation or by crystallization of calcium phosphate phases in the cold-cap, forming a 'killer-scum." More studies are needed to clearly identify the limiting mechanism for these waste clusters.

High-Na_2O. Only a very small fraction of wastes represents this waste cluster with Na_2O at 54 wt%. The waste loading is limited by the model validity of Na_2O in glass but it would become ultimately limited by chemical durability.

In summary, the high-Al_2O_3 waste clusters are limited by nepheline and spinel crystallization, the high-Fe_2O_3 and spinel-limited clusters are limited by spinel crystallization, and the other Cr_2O_3-SO_3 limited and P_2O_5-CaO limited clusters are primarily limited by salt formation or potentially by the formation of crystals other than spinel. For the present waste projections discussed above, it is not likely that the waste loading is limited by the crystallization of zirconium-containing phases.

The overall picture can be somewhat different if glass formulation is performed for each waste batch as in Belsher and Meinert (2009). The estimation of waste loading and glass volume based on the cluster analyses provides a very rough approximation. For more rigorous glass volume estimations and sensitivity studies, waste loading calculations for each batch should be performed like in Belsher and Meinert (2009) and Vienna and Kim (2008).

Table 2.7. Composition of Waste Clusters and Estimated Maximum Waste Loading

Cluster #	**5**	**7**	**8**	**16**	**1**	**10**	**18**	**3**	**4**	**19**	**20**
Group	**High-Al_2O_3**				**High-Fe_2O_3**			**Spinel limited**			
Al_2O_3	47.06	44.94	41.75	57.34	13.96	18.94	20.12	13.73	37.32	28.51	23.41
Bi_2O_3	1.86	5.56	1.85	1.45	0.67	1.71	0.34	2.47	0.98	0.86	4.99
CaO	1.56	2.44	2.47	0.87	2.47	2.42	2.22	3.88	2.62	4.02	3.96
CdO	0.02	0.00	0.02	0.00	0.09	0.08	3.23	0.47	0.52	0.23	0.03
Cr_2O_3	2.28	1.85	2.00	2.03	0.82	0.67	0.62	1.24	1.31	1.18	1.85
F	1.42	0.53	1.09	0.26	0.15	0.45	0.12	0.16	0.13	0.17	2.26
Fe_2O_3	5.83	10.89	10.74	5.49	33.55	29.96	34.88	18.84	14.75	17.02	14.35
MnO	1.19	0.95	1.83	1.38	4.80	2.17	1.24	2.89	0.97	1.32	1.35
Na_2O	14.84	12.83	11.86	16.27	20.61	13.39	9.57	12.68	12.14	20.22	15.08
NiO	1.29	0.69	0.64	0.36	1.67	2.04	2.74	4.18	2.47	1.93	1.54
P_2O_5	4.53	3.58	2.16	1.40	1.74	1.66	0.97	4.28	1.16	1.30	3.30
SO_3	1.22	0.86	0.86	0.50	0.44	0.44	0.18	0.67	0.27	0.26	0.98
ThO_2	0.06	0.03	0.26	0.05	1.60	1.98	1.71	5.06	3.06	2.37	0.29
UO_3	5.34	5.32	7.88	3.90	3.28	7.61	7.49	9.49	5.72	4.92	9.29
ZrO_2	5.29	0.19	0.21	0.18	3.30	4.41	6.60	11.15	3.34	2.97	0.28
SUM	93.77	90.66	85.63	91.47	89.13	87.92	92.01	91.19	86.76	87.28	82.95
Oxide mass (MT)	719	1,840	1,183	1,454	405	734	124	266	221	249	1,351
	5,196				1,263			2,087			
Estimated maximum WL and glass mass based on WTP constraints											
Max WL	26.34	28.93	30.02	22.67	40.55	41.37	36.54	23.90	22.77	24.90	19.45
Limited by	MV (Cr_2O_3)	MV (Al_2O_3)	MV (Cr_2O_3)	MV (Al_2O_3)	MV (CaO)	MV (CaO)	MV (NiO)	MV (NiO)	MV (Al_2O_3)	MV (CaO)	MV (F)
Glass mass (MT)	2,730	6,359	3,941	6,412	999	1,774	339	1,114	970	1,001	6,945
	19,442				3,112			10,030			
Estimated maximum WL and glass mass based on HTWOS baseline constraints											
Max WL	33.69	37.86	40.36	30.82	43.70	42.20	38.25	42.81	40.99	45.94	50.42
Limited by	T_L-Zrs, N_{Si}, VisU	T_L-Zrs, N_{Si}, VisU	T_L-Zrs, N_{Si}, VisU	T_L-Zrs, N_{Si}, VisU	$T_{1\%}$, N_{Si}, VisL	$T_{1\%}$, N_{Si}, VisL	$T_{1\%}$, N_{Si}, VisL	$T_{1\%}$, N_{Si}, VisL	$T_{1\%}$, T_L-Zrs, N_{Si}, VisL	$T_{1\%}$, N_{Si}, VisL	$T_{1\%}$, N_{Si}, VisL
Glass mass (MT)	2,134	4,859	2,932	4,717	927	1,739	324	622	539	542	2,679
	14,642				2,990			4,382			
Estimated maximum WL and glass mass based on HTWOS revised constraints											
Max WL	41.33	44.50	47.19	34.88	No change	42.27	38.29	No change	43.86	47.76	52.15
Limited by	T_L-Zrs, OB, VisU	MV (Al_2O_3)	$T_{1\%}$, OB, VisL	MV (Al_2O_3)		$T_{1\%}$, OB, VisL	$T_{1\%}$, OB, VisL		$T_{1\%}$, OB, VisL	T_L-Zrs, OB, VisL	$T_{1\%}$, OB, VisL
Glass mass (MT)	1,740	4,134	2,507	4,168	927	1,736	324	622	504	522	2,589
	12,548				2,987			4,237			

Table 2.7. (Continued)

Cluster #	12	14	6	11	2	13	15	17	9	Total
Group	Cr_2O_3-SO_3 limited				P_2O_5-CaO limited				High-Na	
Al_2O_3	16.40	32.32	27.92	28.37	20.47	22.68	13.05	18.40	9.35	-
Bi_2O_3	3.41	1.77	3.81	5.73	7.26	2.47	5.77	1.23	1.31	-
CaO	3.01	2.17	2.00	2.49	5.63	2.49	5.36	8.91	2.58	-
CdO	0.02	0.08	0.06	0.03	0.05	0.05	0.02	0.36	0.04	-
Cr_2O_3	7.71	7.42	2.95	2.22	1.38	2.91	0.38	1.46	2.74	-
F	5.01	0.44	0.55	6.08	2.83	2.29	1.23	0.26	0.70	-
Fe_2O_3	12.25	8.52	14.86	9.57	11.41	10.15	23.62	13.86	6.70	-
MnO	1.23	2.04	3.04	0.53	0.58	0.88	2.42	1.62	0.59	-
Na_2O	14.27	19.37	16.83	12.36	24.81	22.81	12.86	37.18	54.16	-
NiO	3.14	0.39	3.08	0.78	0.78	1.55	3.08	0.57	0.49	-
P_2O_5	11.14	11.18	4.36	4.43	6.75	11.67	5.60	3.17	2.44	-
SO_3	2.20	1.99	1.41	2.14	0.91	1.10	0.15	0.45	0.35	-
ThO_2	0.38	0.03	0.81	0.22	0.38	0.44	0.29	0.14	0.63	-
UO_3	7.31	3.59	5.50	3.47	3.93	8.05	5.02	2.57	3.52	-
ZrO_2	1.30	1.37	2.83	0.63	0.34	0.61	2.40	1.39	0.52	-
SUM	88.79	92.67	90.02	79.05	87.50	90.15	81.26	91.58	86.13	-
Oxide mass (MT)	275	173	364	533	339	209	327	165	144	11,075
	1,346				1,040				144	11,075
Estimated maximum WL and glass mass based on WTP constraints										
Max WL	7.78	8.09	20.34	7.23	15.55	19.21	18.67	11.22	21.88	-
Limited by	MV (Cr_2O_3)	MV (Cr_2O_3)	MV (Cr_2O_3)	MV (F)	MV (F)	MV (F)	MV (CaO)	MV (CaO)	MV (Cr_2O_3)	-
Glass mass (MT)	3,538	2,143	1,790	7,369	2,179	1,090	1,752	1,468	657	54,572
	14,840				6,489				657	54,572
Estimated maximum WL and glass mass based on HTWOS baseline constraints										
Max WL	15.56	16.17	35.44	23.31	37.02	21.41	44.61	47.99	39.51	-
Limited by	Sol (Cr_2O_3)	Sol (Cr_2O_3)	Sol (SO_3)	Sol (SO_3)	Sol (P_2O_5)	Sol (P_2O_5)	Sol (P_2O_5)	Sol (CaO* P_2O_5)	MV (Na_2O)	-
Glass mass (MT)	1,769	1,072	1,028	2,286	916	978	734	343	364	31,503
	6,154				2,970				364	31,503
Estimated maximum WL and glass mass based on HTWOS revised constraints										
Max WL	No change	No change	40.68	27.98	41.36	38.54	46.53	No change	No change	-
Limited by			Sol (Cr_2O_3)	Sol (SO_3)	Sol (CaO* P_2O_5)	Sol (P_2O_5)	Sol (CaO* P_2O_5)			-
Glass mass (MT)	1,769	1,072	895	1,905	819	543	703	343	364	28,186
	5,641				2,409				364	28,186

"-" empty cell
Max WL: maximum waste loading given in wt%
MV("comp") or Sol("comp"): model validity or solubility constraint for a given component
T_L-Zrs: liquidus temperature for zirconium-containing phase; $T_{1\%}$: temperature at 1 vol% spinel; N_{Si}: nepheline discriminator; OB: optical basicity; VisL: viscosity lower limit; VisU: viscosity upper limit
No change: no change from the baseline constraints

Figure 2.7 shows a pie chart of the relative fraction of each waste group for the projected waste oxide mass, projected glass masses based on WTP, HTWOS baseline, and HTWOS revised constraints. The total mass of oxides and glass masses are also included in Figure 2.7.

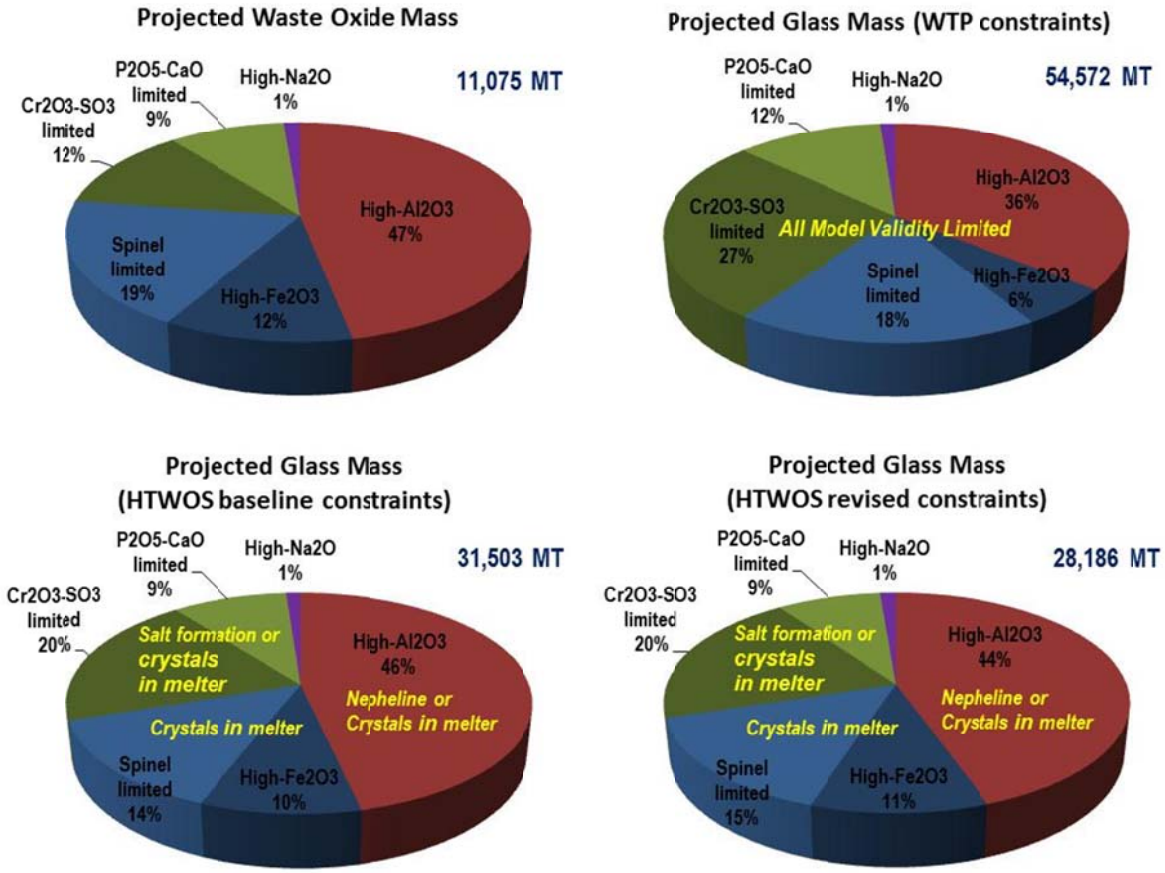

Figure 2.7. Projected Mass of Waste Oxides and Glass Based on Estimated Maximum Waste Loading based on Different Constraints

3.0 Experimental Procedures

3.1 Glass Fabrication

Glasses for property measurements were prepared in platinum-alloy crucibles with a lid following a two-step melting process while a quick meltability evaluation for some glasses was obtained from the first melt only. The first melt was of raw materials after mechanically mixing them in an agate milling chamber. Melting was performed nominally for 1 or 2 hours at a recommended melting temperature that was estimated based on model predicted viscosity (recommended melting temperature is given for all glasses formulated in this study in Sections 4.0 and 5.0). A second melt of the glass was performed after the quenched glass was ground to a fine powder in a tungsten carbide mill. Generally, the temperature of second melt was adjusted, based on the fluidity of the melt estimated during pouring of the first melt.

3.2 Canister Centerline Cooling Treatment

Selected glass melts were cooled according to the CCC profile for WTP HLW or LAW glasses as given in Table 3.1and Table 3.2, respectively. This cooling is intended to simulate the center line temperature/time profile of melts prepared at 1150 °C. For HLW glasses with recommended melting temperature between 1200 °C and 1300 °C, the melt was brought to 1150°C, cooled to 1050°C at -2°C/min, and then cooled following the profile given in Table 3.1. No adjustment was made to the CCC profile for LAW glasses as it starts at a relatively high temperature of 1114°C.

Table 3.1. CCC Profile for HLW Glasses

Segment	Time (min)	Start Temp (°C)	Rate (°C/min)
1	0-45	1050	-1.556
2	45-107	980	-0.806
3	107-200	930	-0.591
4	200-329	875	-0.388
5	329-527	825	-0.253
6	527-707	775	-0.278
7	707-1776	725	-0.304

Table 3.2. CCC Profile for LAW Glasses

Segment	Time (min)	Start Temp (°C)	Rate (°C/min)
1	0 – 16	1114	-7.125
2	16 – 73	1000	-1.754
3	73 – 195	900	-0.615
4	195 – 355	825	-0.312
5	355 – 640	775	-0.175
6	640 – 1600	725	-0.130
7	1600 – 3710	600	-0.095

3.3 Characterization of Glasses

3.3.1 Composition Analyses

To confirm that the "as-fabricated" glasses correspond to the defined target compositions, a representative sample of each glass was chemically analyzed at the SRNL Process Science Analytical Laboratory (PSAL). Two preparation methods were used in measuring these chemical compositions: lithium metaborate fusion followed by HNO_3 dissolution or HNO_3 dissolution. For each glass, measurements were obtained from samples prepared in duplicate. All of the prepared samples were analyzed (twice for each element of interest) by inductively coupled plasma-atomic emission spectroscopy (ICP-AES).

3.3.2 Product Consistency Test

PCT responses were measured in triplicate on each of the glasses, including quenched or CCC samples using Method A of the procedure (ASTM 2008). Also included in the experimental test matrix and tested in triplicate was the environmental assessment (Jantzen et al. 1993) glass, the Approved Reference Material (Mellinger and Daniel 1984) glass, and blanks from the sample cleaning batch. Glass samples were ground, washed, and prepared according to the standard PCT procedure. The resulting solutions were sampled (filtered and acidified) and analyzed. Normalized release rates were calculated based on target compositions using the average of the logs of the leachate concentrations.

The normalized elemental mass loss, r_i, is calculated from:

$$r_i \text{ (g/L)} = \frac{c_i}{f_i} \tag{3.1}$$

where c_i is the concentration of the i^{th} element in the leachate (g/m^3 = ppm = μg/ml = mg/L assuming a solution density of 1 g/mL) and is the mass fraction of the i^{th} element in glass (unitless), which is calculated from target glass composition.

3.3.3 Toxicity Characteristic Leaching Procedure

The TCLP was performed on quenched or CCC glass samples at Davis & Floyd[1] under an SRNL subcontract. The extraction and analyses were performed according to SW 846 Method 1311 (EPA 1997). Crushed glass pieces that passed through a 9.5-mm (0.4-inch) sieve and ≥ 100 g in mass, are placed in dilute acetic acid (pH value of 4.98 ± 0.05) and agitated at 30 ± 2 rpm for 18 ± 2 hours at room temperature. The concentrations of hazardous metals in solution were then measured by ICP-AES.

3.3.4 Vapor Hydration Test

The standard vapor hydration test (VHT) method (ASTM 2011) was employed to assess the durability of LAW glass products. Specimens were cut from rectangular glass bars with a diamond saw

[1] Davis & Floyd, Inc., 816 E. Durst Avenue, Greenwood, SC.

and all sides were polished with 600 grit SiC paper. The specimens (approximately 10 × 10 × 1.5 mm^3) were rinsed successively with acetone and deionized water, after which the dimensions and weight were measured to an accuracy of ±0.002 mm and ±0.01 mg, respectively. VHT specimens were suspended by a Teflon thread connected to a stainless steel support. The support along with the specimens was placed inside a Parr 22 ml T304 stainless steel vessel together with 0.25 ml of deionized water. The sealed vessel containing the sample was heated at 200 ± 2 °C in an automated temperature-controlled oven for a specified time. After removing the sample from the vessel, the sample was cross-sectioned and polished. The cross-section of each sample was examined and the thickness of the uncorroded part of the sample was measured with an accuracy of ±0.002 mm by an optical microscope.

The VHT alteration rate, r_{alt} ($g/m^2/d$), of the specimen is calculated from the equation:

$$r_{alt}(\mathrm{g/m^2/d}) = \frac{d_i \rho}{2t}\left(1 - \frac{d_r}{d_i}\right) = \frac{m_i}{2 w_i l_i t}\left(1 - \frac{d_r}{d_i}\right) \tag{3.2}$$

where d_i, w_i, and l_i are the initial thickness, width, and length of the specimen, respectively, d_r is the average thickness of the remaining glass, m_i is the initial specimen mass, t is the duration of test, and ρ is the density of glass. The average density of 2.7 g/cc was used for all LAW glasses used in this study.

3.3.5 Viscosity

The viscosity of glass was measured as a function of temperature following PNNL procedure GDL-VIS using a Brookfield rotating spindle digital viscometer (DV-III) staged above a high-temperature Deltech® furnace and equipped with a Pt/Rh spindle which fit through a hole in the top of the furnace. A 50 mL glass sample, measured by liquid displacement, was added into a Pt/Rh crucible and placed into the furnace set at 1150 °C. The spindle was immersed into the molten glass in the center of the crucible with its lower end of the rod at 5.1 mm above the bottom. A thermocouple was located directly under the bottom center of the crucible. The furnace was set to the required ramp/soak schedule and digital data collection of spindle torque and temperature commenced. The temperature sequence was 1150°C, 1100°C, 1050°C, 1000°C, 950°C, 1050°C, 1150°C, 1200°C, and then 1150°C. The soak time was 30 min. at each temperature, except the second soak at 1150°C was for 45 min. The hysteresis approach allows for the potential impacts of crystallization (at lower temperatures) to be assessed (via reproducibility) with duplicate measurements being taken in the range at which the melter is anticipated to be operating. Volatilization (at higher temperatures) is minimized by measuring viscosity at temperatures above 1150°C as the final viscosity measurement. The viscometer was calibrated with a standard glass (DWPF start-up frit) at specified intervals following PNNL procedure GDL-VSC.

3.3.6 Electrical Conductivity

The electrical conductivities of molten glasses were measured as a function of temperature using a probe with two platinum-10% rhodium blades according to the PNNL procedures GDL-ELC (for measurement) and GDL-ECC (for calibration). The 50 mL of glass used for viscosity measurements was added back into a platinum/rhodium crucible and placed into the furnace at 1100°C. The probe was then lowered through a hole in the top of the furnace and into the melt, making sure that the probe was in the center of the crucible. Using the automated Solartron Analytical 1455 Cell Test System which was

connected to the probe, the probe was lowered into the glass precisely 1.27 cm. The glass soaked at temperatures of 1200°C, 1100°C, 1000°C, and 900°C for 45 minutes at each temperature, allowing the program to collect impedance data at frequencies of 10000 Hz, 1000 Hz, 100 Hz, and 63 Hz 5 min. apart at the end of each temperature setting when the sample was at thermal equilibrium. Only the 1000 Hz frequency data were used in the conductivity calculation since these were the closest values to real impedance. Measured data were exported into Excel®, where the impedance data were converted into conductance.

The electrical conductivity system was checked at specified intervals in 0.1 and 1 M solutions of KCl at room temperature to determine a cell constant. Two measurements were taken at intervals of approximately 5 min. for each solution. The cell constant was then used to calculate the conductivity of each glass melt.

3.3.7 Equilibrium Crystal Fraction and Crystal Identification after Canister Centerline Cooling

The equilibrium crystal fraction as a function of temperature were measured in Pt-alloy crucibles and boats with tight fitting lids (to minimize volatility) according the PNNL procedure GDL-LQT. The heat treatment time was 24 ± 2 hours for 900-1250 °C to ensure equilibrium was achieved without excessive volatility. Selected glasses were subjected to simulated CCC treatments (roughly 150 g glass sample in Pt-alloy boats) according to the profiles described in Section 3.2. Samples were analyzed by x-ray diffraction (XRD) to determine the type and quantity of crystal fractions (quantitative analyses) according to the PNNL procedure GDL-XRD.

4.0 Glass Formulation for the Cold Crucible Induction Melter

This section deals with the EM-31 program WP-4.1.2 task on the formulation of glasses for CCIM with a processing temperature higher than 1150 °C. The primary objective of glass formulation effort for CCIM was to estimate the potential benefit in waste loading that can be achieved by CCIM compared to the baseline WTP technology using the 1150 °C JHM. For initial glass formulation efforts, two wastes, AZ-101 HLW and AN-105 LAW, were selected as described in Section 2.1. The initial formulation tests with these two wastes based on crucible melts were completed, glass compositions for melter tests were selected, and the recipes for melter feed were developed. However, the actual melter tests were not performed before this task was closed. The results of formulating the glasses for these two wastes are described in Sections 4.1 and 4.2.

The next step of glass formulation efforts was to use the projected Hanford waste compositions that were described in Section 2.2 to estimate the potential benefit of CCIM focusing only on HLWs. Only part of the formulation tests for selected waste clusters was completed before this task was closed. The glass formulations and some limited test results are in Section 4.3.

4.1 Cold Crucible Induction Melter Glass Formulation for AZ-101 HLW

The composition of AZ-101 HLW was presented in Table 2.1. As discussed in Section 2.1, AZ-101 was selected based on its potential to successfully demonstrate the unique advantages of the CCIM technology over current reference technologies. This waste is relatively high in aluminum, iron, and zirconium, which suggests that higher melting temperature and tolerance to spinel crystals for the CCIM technology could increase loading and potentially increase the processing rate.

4.1.1 Formulation Approach for AZ-101 HLW Glasses for the Cold Crucible Induction Melter

Various constraints that are being applied for WTP and HTWOS were discussed in Section 2.2.2. The glass formulations for specific waste compositions use the selected constraints that are critical for the specific waste and melter technology to screen the candidate glasses with maximum waste loading. The selection of glass for a melter demonstration test involves confirming that the selected glass will pass all the acceptance and processing requirements discussed in Section 2.2.2.

Table 4.1 summarizes the glass property requirements applied when designing the AZ-101 HLW glasses for testing for the CCIM. The requirements for crystal fraction versus temperature, CCC crystallinity, viscosity, and electrical conductivity were self-imposed for the glass development purpose. Available glass property models (Vienna et al 2002; Vienna et al. 2009) were used to predict these properties whenever possible. However, the predicted values were used primarily as guidelines for glass formulation because the high waste loaded glasses that are considered in this study are well outside the model validity composition range of these models or, any models that the authors are aware of.

Table 4.1. Glass Property Requirements[(a)] for HLW Glasses

Property	Requirements
Crystal fraction vs. temperature	As low as possible
CCC crystallinity	No nepheline formation after CCC
PCT normalized release for Q and CCC samples	B < 16.70, Li < 9.57, Na < 13.35 g/L
TCLP Cd response for Q and CCC samples	< 0.48 mg/L
Viscosity	4 Pa·s at a nominal melting temperature (T_m)
Electrical conductivity	10 – 100 S/m at T_m
[(a)]Self-imposed for the glass development purpose except for PCT and TCLP requirements Q stands for quenched and CCC canister centerline cooling	

Main difference for the CCIM formulation compared to that for WTP baseline melter is the potential increased melting temperature and tolerance to crystallization. For AZ-101 HLW, the most critical information for formulating glasses with maximum possible waste loading is the crystal fraction versus temperature because the waste loading is likely limited by the crystal content within the glass melts. However, currently the limit for crystal inclusions is not known. DoQuang et al. (2004) cite a 3 wt% limit on noble metals in the CCIM to be installed in LaHague for the production of R7/T7 glass. Currently, there is no practical model to predict the crystal fraction as a function of temperature except one by Hrma and Vienna (2003) that has very limited applicability. Instead, spinel [$(Fe^{2+},Ni)(Fe^{3+},Cr,Al)_2O_4$] liquidus temperature ($T_L$) and temperature at which 1 vol% spinel crystal exists ($T_{1\%}$) have been used as conservative constraints to prevent the potential accumulation of crystals in the melter. Models to predict the T_L and $T_{1\%}$ have been developed (Vienna et al 2002; Vienna et al. 2009); however, they have poor predictability, especially for the glasses outside the valid composition range. Therefore, these models were used only as qualitative guidelines in selecting glasses for testing. The models for PCT normalized releases and TCLP Cd response (Vienna et al 2009) were used to confirm that these requirements will be met. The PCT and TCLP models also suffer poor predictability outside the valid composition range. However, the performance of PCT and TCLP models is not of concern because PCT and TCLP rarely limit the waste loading of HLW glasses as long as nepheline doesn't precipitate on slow cooling. To estimate the potential for nepheline precipitation after CCC treatment, the nepheline rules based on both N_{Si} (see Eq. 2.1) and OB (see Eq. 2.2) were calculated. Whenever possible the glass formulation was performed to satisfy the nepheline constraint, but this constraint was not used to limit the waste loading as this constraint is known to be conservative (McCloy and Vienna 2010).

The model for viscosity (Vienna et al. 2009) was used to predict the nominal melting temperature at a predicted viscosity of 4 Pa·s. The model for electrical conductivity (Vienna et al. 2009) was used to confirm that the glasses have predicted electrical conductivity within the desired range of 10 to 100 S/m for CCIM (Marra et al. 2008) at a predicted nominal melting temperature.

Table 4.2 shows the target compositions and predicted properties for AZ-101 HLW (CCIM-AZ-xx[1]) glasses. Some initial compositions formulated with high waste loading did not result in homogeneous glasses because of severe crystallization during melting. The crystals formed did not dissolve into glass, even with increased temperature and time, as shown for CCIM-AZ-02 glass in Figure 4.1. The first seven glasses (CCIM-AZ-02 through 20) in Table 4.2 were melted but resulted in severe crystallization and therefore were not used for further property testing. The predicted nominal melting temperature (T_m) at a

[1] All glasses that were formulated and considered in this study were given unique ID numbers. However, only partial selected glasses were prepared, and the missing ID numbers represent the glasses that were considered but were not prepared for testing.

predicted viscosity of 4 Pa·s ranged from 1150 °C to 1300 °C. The predicted electrical conductivity was within the desired range of 10 S/m to 100 S/m at T_m for all CCIM-AZ glasses. The predicted normalized PCT releases and TCLP Cd response were all below the regulatory limits. The predicted T_L and $T_{1\%}$ were all higher than the traditional constraints (see footnotes in Table 4.2) that have been imposed to avoid crystal accumulation in the melter. The nepheline constraint was met for all CCIM-AZ glasses, primarily by satisfying the N_{Si} rule, except the CCIM-AZ-18 glass that failed both N_{Si} and OB rules.

Table 4.2. Target Composition and Predicted Properties of CCIM-AZ Glasses

Oxide	Glasses that were prepared but NOT tested for properties							Limits[a]
	CCIM-AZ-02	CCIM-AZ-03	CCIM-AZ-05	CCIM-AZ-06	CCIM-AZ-08	CCIM-AZ-19	CCIM-AZ-20	
Al_2O_3	0.12650	0.12650	0.11826	0.13050	0.11093	0.10440	0.10440	-
B_2O_3	0.16599	0.10000	0.15682	0.08000	0.08000	0.11000	0.11000	-
CaO	0.00720	0.00720	0.00674	0.02000	0.00632	0.00595	0.00595	-
CdO	0.01112	0.01112	0.01039	0.01147	0.00975	0.00917	0.00917	-
Ce_2O_3	0.00412	0.00412	0.00385	0.00425	0.00361	0.00340	0.00340	-
Cr_2O_3	0.00237	0.00237	0.00221	0.00244	0.00208	0.00195	0.00195	-
Cs_2O	0.00257	0.00257	0.00241	0.00265	0.00226	0.00212	0.00212	-
Fe_2O_3	0.19387	0.19387	0.18124	0.20000	0.17000	0.16000	0.16000	-
K_2O	0.00000	0.00000	0.00000	0.00000	0.00000	0.00000	0.04000	-
La_2O_3	0.00453	0.00453	0.00423	0.00467	0.00397	0.00374	0.00374	-
Li_2O	0.00979	0.03000	0.02517	0.02000	0.03500	0.05000	0.03000	-
MnO	0.00463	0.00463	0.00433	0.00478	0.00406	0.00382	0.00382	-
Na_2O	0.08337	0.07876	0.08104	0.08153	0.12117	0.06872	0.09037	-
Nd_2O_3	0.00335	0.00335	0.00313	0.00345	0.00293	0.00276	0.00276	-
NiO	0.00849	0.00849	0.00794	0.00876	0.00745	0.00701	0.00701	-
P_2O_5	0.00684	0.00684	0.00640	0.00706	0.00600	0.00565	0.00565	-
RuO_2	0.00077	0.00077	0.00072	0.00080	0.00068	0.00064	0.00064	-
SiO_2	0.30037	0.35076	0.32518	0.35149	0.37757	0.40775	0.36610	-
SO_3	0.00190	0.00190	0.00178	0.00196	0.00167	0.00157	0.00157	-
SnO_2	0.00340	0.00340	0.00318	0.00350	0.00298	0.00280	0.00280	-
ZrO_2	0.05882	0.05882	0.05499	0.06068	0.05158	0.04855	0.04855	-
Total	1.00000	1.00000	1.00000	1.00000	1.00000	1.00000	1.00000	-
Waste loading	0.515	0.515	0.481	0.531	0.451	0.425	0.425	-
T_m at 4 Pa·s, °C	1250	1250	1200	1300	1200	1200	1200	-
EC at T_m, S/m	24.2	29.3	26.6	26.9	38.8	34.4	29.6	10-100
Spinel T_L, °C	1405	1457	1319	1555	1274	1255	1192	$<T_m$–100[b]
Spinel $T_{1\%}$, °C	1332	1355	1250	1416	1176	1142	1107	$<T_m$–200[c]
PCT-B, g/L	0.317	0.179	0.405	0.102	0.327	0.305	0.451	<16.7
PCT-Li, g/L	0.325	0.193	0.385	0.138	0.330	0.309	0.399	<9.57
PCT-Na, g/L	0.232	0.134	0.273	0.103	0.307	0.206	0.333	<13.35
TCLP Cd, mg/L	0.218	0.127	0.227	0.101	0.170	0.131	0.190	<0.48
N_{Si}	0.589	0.631	0.620	0.624	0.619	0.702	0.653	≥0.62
OB	0.575	0.593	0.576	0.601	0.604	0.578	0.594	≤0.575

Table 4.2. Target Composition and Predicted Properties of CCIM-AZ Glasses (continued)

Oxide	Glasses that were tested for properties									Limits[a]
	CCIM-AZ-10	CCIM-AZ-17	CCIM-AZ-18	CCIM-AZ-16	CCIM-AZ-29	CCIM-AZ-30	CCIM-AZ-31	CCIM-AZ-32	CCIM-AZ-33	
Al_2O_3	0.11093	0.11093	0.11093	0.10440	0.09788	0.09788	0.09788	0.09788	0.09788	-
B_2O_3	0.11000	0.14000	0.14000	0.11000	0.11000	0.11000	0.07000	0.15000	0.11000	-
CaO	0.00632	0.00632	0.00632	0.00595	0.00557	0.00557	0.00557	0.00557	0.04000	-
CdO	0.00975	0.00975	0.00975	0.00917	0.00860	0.00860	0.00860	0.00860	0.00860	-
Ce_2O_3	0.00361	0.00361	0.00361	0.00340	0.00319	0.00319	0.00319	0.00319	0.00319	-
Cr_2O_3	0.00208	0.00208	0.00208	0.00195	0.00183	0.00183	0.00183	0.00183	0.00183	-
Cs_2O	0.00226	0.00226	0.00226	0.00212	0.00199	0.00199	0.00199	0.00199	0.00199	-
Fe_2O_3	0.17000	0.17000	0.17000	0.16000	0.15000	0.15000	0.15000	0.15000	0.15000	-
K_2O	0.00000	0.00000	0.00000	0.00000	0.00000	0.00000	0.00000	0.00000	0.00000	-
La_2O_3	0.00397	0.00397	0.00397	0.00374	0.00350	0.00350	0.00350	0.00350	0.00350	-
Li_2O	0.03000	0.03000	0.03000	0.03000	0.03000	0.05000	0.04500	0.03000	0.03000	-
MnO	0.00406	0.00406	0.00406	0.00382	0.00358	0.00358	0.00358	0.00358	0.00358	-
Na_2O	0.10781	0.08642	0.10781	0.11382	0.11991	0.07499	0.11992	0.09253	0.09122	-
Nd_2O_3	0.00293	0.00293	0.00293	0.00276	0.00259	0.00259	0.00259	0.00259	0.00259	-
NiO	0.00745	0.00745	0.00745	0.00701	0.00657	0.00657	0.00657	0.00657	0.00657	-
P_2O_5	0.00600	0.00600	0.00600	0.00565	0.00530	0.00530	0.00530	0.00530	0.00530	-
RuO_2	0.00068	0.00068	0.00068	0.00064	0.00060	0.00060	0.00060	0.00060	0.00060	-
SiO_2	0.36593	0.35732	0.33593	0.38264	0.39928	0.42419	0.42426	0.38665	0.39354	-
SO_3	0.00167	0.00167	0.00167	0.00157	0.00147	0.00147	0.00147	0.00147	0.00147	-
SnO_2	0.00298	0.00298	0.00298	0.00280	0.00263	0.00263	0.00263	0.00263	0.00263	-
ZrO_2	0.05158	0.05158	0.05158	0.04855	0.04551	0.04551	0.04551	0.04551	0.04551	-
Total	1.00000	1.00000	1.00000	1.00000	1.00000	1.00000	1.00000	1.00000	1.00000	-
Waste loading	0.451	0.451	0.451	0.425	0.398	0.398	0.398	0.398	0.398	-
T_m at 4 Pa·s, °C	1200	1200	1150	1200	1200	1200	1200	1200	1200	-
EC at T_m, S/m	33.1	28.9	36.6	34.3	35.7	35.5	43.6	30.2	27.1	10-100
Spinel T_L, °C	1272	1272	1226	1218	1165	1202	1182	1163	1232	$<T_m$–100[b]
Spinel $T_{1\%}$, °C	1178	1184	1160	1114	1049	1077	1057	1055	1093	$<T_m$–200[c]
PCT-B, g/L	0.358	0.389	0.583	0.399	0.448	0.344	0.363	0.512	0.259	<16.7
PCT-Li, g/L	0.330	0.360	0.516	0.364	0.405	0.345	0.400	0.488	0.276	<9.57
PCT-Na, g/L	0.261	0.257	0.386	0.296	0.338	0.235	0.382	0.350	0.230	<13.35
TCLP Cd, mg/L	0.184	0.193	0.280	0.181	0.178	0.129	0.143	0.194	0.170	<0.48
N_{Si}	0.626	0.644	0.606	0.637	0.647	0.710	0.661	0.670	0.675	≥0.62
OB	0.591	0.577	0.586	0.588	0.586	0.575	0.598	0.568	0.587	≤0.575

[a] Used as guidelines for formulating the glasses.
[b] Based on a traditional constraint used in Perez et al. (2001).
[c] Based on a constraint of $T_{1\%} < 950$°C for glasses with $T_m = 1150$°C (Vienna et al. 2009).
Shaded cells indicate that the predicted or calculated value is not within the limits.

Figure 4.1. Crystals Remaining Attached to the Crucible after Melting of CCIM-AZ-02

4.1.2 Test Results of AZ-101 HLW Glasses for Cold Crucible Induction Melter

Chemical analyses of glasses were performed for CCIM-AZ glasses primarily to confirm glass batching and melting preparation. Table 4.3 and Table 4.4 compare the target and analyzed compositions and provide their relative percent difference (RPD) values. The RPD values were calculated for components with concentration higher than 1 wt%. The analytical results matched well with the target concentrations for all eight CCIM-AZ glasses without any specific glasses that are suspected for any batching error.

Table 4.3. Comparison of Target and Analyzed Compositions of CCIM-AZ-10 through CCIM-AZ-18 Glasses and their Relative Percent Difference (RPD)

	Target (wt%)				Analyzed (wt%)[1]				RPD[2]			
Glass	**AZ-10**	**AZ-16**	**AZ-17**	**AZ-18**	**AZ-10**	**AZ-16**	**AZ-17**	**AZ-18**	**AZ-10**	**AZ-16**	**AZ-17**	**AZ-18**
Al_2O_3	11.09	10.44	11.09	11.09	11.10	10.43	11.04	11.16	0.1%	-0.1%	-0.4%	0.6%
B_2O_3	11.00	11.00	14.00	14.00	11.93	11.54	14.41	14.44	8.5%	4.9%	2.9%	3.2%
CaO	0.63	0.59	0.63	0.63	0.75	0.71	0.74	0.77				
CdO	0.97	0.92	0.97	0.97	0.66	0.61	0.59	0.64				
Ce_2O_3	0.36	0.34	0.36	0.36	0.33	0.31	0.32	0.33				
Cr_2O_3	0.21	0.20	0.21	0.21	0.20	0.16	0.17	0.16				
Cs_2O	0.23	0.21	0.23	0.23								
Fe_2O_3	17.00	16.00	17.00	17.00	17.37	15.94	16.59	16.80	2.2%	-0.3%	-2.4%	-1.2%
La_2O_3	0.40	0.37	0.40	0.40	0.31	0.29	0.30	0.31				
Li_2O	3.00	3.00	3.00	3.00	2.95	2.91	2.90	2.93	-1.8%	-2.9%	-3.2%	-2.2%
MnO	0.41	0.38	0.41	0.41	0.33	0.31	0.31	0.33				
Na_2O	10.78	11.38	8.64	10.78	11.11	11.63	8.71	11.25	3.1%	2.2%	0.8%	4.3%
Nd_2O_3	0.29	0.28	0.29	0.29	0.32	0.30	0.31	0.34				
NiO	0.74	0.70	0.74	0.74	0.72	0.65	0.66	0.69				
P_2O_5	0.60	0.56	0.60	0.60	0.51	0.49	0.48	0.50				
RuO_2	0.07	0.06	0.07	0.07								

Glass	Target (wt%)				Analyzed (wt%)[1]				RPD[2]			
	AZ-10	AZ-16	AZ-17	AZ-18	AZ-10	AZ-16	AZ-17	AZ-18	AZ-10	AZ-16	AZ-17	AZ-18
SiO_2	36.59	38.26	35.73	33.59	36.49	37.77	35.10	33.17	-0.3%	-1.3%	-1.8%	-1.3%
SO_3	0.17	0.16	0.17	0.17	0.16	0.14	0.12	0.15				
SnO_2	0.30	0.28	0.30	0.30	0.27	0.25	0.25	0.27				
ZrO_2	5.16	4.85	5.16	5.16	4.88	4.62	4.61	4.98	-5.4%	-4.9%	-10.6%	-3.4%
Total	100.00	100.00	100.00	100.00	100.40	99.07	97.62	99.21				

[1]Empty cells represent the components that were not analyzed or below detection limit.
[2]Calculated for components with target concentration > 1 wt%.

Table 4.4. Comparison of Target and Analyzed Compositions of CCIM-AZ-29 through CCIM-AZ-33 Glasses and their Relative Percent Difference (RPD)

Glass	Target (wt%)				Analyzed (wt%)[1]				RPD[2]			
	AZ-29	AZ-30	AZ-31	AZ-33	AZ-29	AZ-30	AZ-31	AZ-33	AZ-29	AZ-30	AZ-31	AZ-33
Al_2O_3	9.79	9.79	9.79	9.79	9.98	9.89	9.90	9.88	2.0%	1.1%	1.2%	1.0%
B_2O_3	11.00	11.00	7.00	11.00	10.82	11.08	7.02	11.04	-1.6%	0.7%	0.3%	0.4%
CaO	0.56	0.56	0.56	4.00	0.52	0.50	0.50	4.28				7.1%
CdO	0.86	0.86	0.86	0.86	0.75	0.74	0.73	0.75				
Ce_2O_3	0.32	0.32	0.32	0.32	0.31	0.30	0.30	0.30				
Cr_2O_3	0.18	0.18	0.18	0.18	0.16	0.14	0.17	0.14				
Cs_2O	0.20	0.20	0.20	0.20								
Fe_2O_3	15.00	15.00	15.00	15.00	14.87	14.94	14.73	14.80	-0.9%	-0.4%	-1.8%	-1.3%
La_2O_3	0.35	0.35	0.35	0.35	0.28	0.28	0.28	0.28				
Li_2O	3.00	5.00	4.50	3.00	2.97	4.91	4.42	2.99	-1.1%	-1.7%	-1.8%	-0.4%
MnO	0.36	0.36	0.36	0.36	0.32	0.31	0.31	0.31				
Na_2O	11.99	7.50	11.99	9.12	12.82	8.13	12.97	9.65	6.9%	8.4%	8.2%	5.8%
Nd_2O_3	0.26	0.26	0.26	0.26	0.27	0.27	0.27	0.26				
NiO	0.66	0.66	0.66	0.66	0.45	0.45	0.46	0.44				
P_2O_5	0.53	0.53	0.53	0.53	0.44	0.49	0.48	0.39				
RuO_2	0.06	0.06	0.06	0.06								
SiO_2	39.93	42.42	42.43	39.35	40.45	42.59	42.80	39.48	1.3%	0.4%	0.9%	0.3%
SO_3	0.15	0.15	0.15	0.15								
SnO_2	0.26	0.26	0.26	0.26	0.33	0.32	0.32	0.31				
ZrO_2	4.55	4.55	4.55	4.55	4.28	4.39	4.32	4.42	-6.0%	-3.5%	-5.1%	-2.9%
Total	100.00	100.00	100.00	100.00	100.00	99.74	99.98	99.75				

[1]Empty cells represent the components that were not analyzed or below detection limit.
[2]Calculated for components with target concentration > 1 wt%.

Table 4.5 summarizes the results of XRD analyses of CCC-treated samples of CCIM-AZ glasses. Crystals identified after CCC treatment included spinel [$(Fe^{2+},Ni)(Fe^{3+},Cr,Al)_2O_4$] as the major phase with a smaller fraction of baddeleyite (ZrO_2) only in glasses with 16 wt% or 17 wt% Fe_2O_3 (CCIM-AZ-10, 17, 18, and 16). As mentioned earlier, spinel crystals are known to have little impact on the PCT normalized releases (Bickford and Jantzen 1984). Nepheline ($NaAlSiO_4$) was not detected in any glasses, including the CCIM-AZ-18 glass that failed the nepheline constraint (i.e., failed both N_{Si} and OB rules, see Table 4.2. In summary, it is expected that the PCT releases of CCIM-AZ glasses are not likely to be affected by CCC treatment.

Table 4.5. Measured Crystal Vol% after CCC Treatment for CCIM-AZ Glasses

Crystal	AZ-10	AZ-17	AZ-18	AZ-16	AZ-29	AZ-30	AZ-31	AZ-32	AZ-33
Spinel	4.9	5.0	4.8	4.6	5.1	6.1	4.9	N/A	5.0
Baddeleyite	1.0	1.3	0.8	0.5	0	0	0	N/A	0
AZ-10, 17, and 18 have 17 wt% Fe2O3, AZ-16 has 16 wt% Fe2O3, and AZ-29 through AZ-33 have 15wt% Fe2O3, N/A: not analyzed									

Table 4.6 summarizes the PCT normalized releases and TCLP responses of quenched and CCC treated CCIM-AZ Glasses. Figure 4.2 displays the PCT normalized releases for boron, lithium and sodium (Figure 4.2) and Figure 4.3 shows the TCLP cadmium response for CCIM-AZ glasses. The PCT normalized releases of all the quenched and CCC-treated glasses were well below the limits of the Environmental Assessment glass (Jantzen et al. 2003). All quenched and CCC glasses passed the TCLP cadmium requirement of 0.48 mg/L. Note that the AZ-101 waste is one of the small number of Hanford waste streams with high cadmium content. For all PCT-normalized boron, lithium, and sodium releases and TCLP cadmium response, the measured values (for quenched samples) were equal to or slightly higher than the predicted. The CCC treatment had mixed effects on PCT normalized releases and the TCLP Cd response, but did not show a significant difference from quenched samples as expected from CCC crystallinity results.

Table 4.6. PCT Normalized Releases and TCLP Responses of Quenched and CCC Treated CCIM-AZ Glasses

Glass	AZ-10	AZ-17	AZ-18	AZ-16	AZ-29	AZ-30	AZ-31	AZ-33
PCT Normalized releases, g/L								
PCT-B, Q	0.4755	0.5728	0.7502	0.4810	0.4865	0.5362	0.4840	0.4810
PCT-Li, Q	0.6348	0.7960	0.8098	0.6515	0.6181	0.6896	0.5994	0.6495
PCT-Na, Q	0.3991	0.3500	0.5507	0.4307	0.3902	0.2571	0.4837	0.4119
PCT-B, CCC	0.4455	0.7318	1.0884	0.4404	0.4264	0.4401	0.4746	0.3288
PCT-Li, CCC	0.5615	0.9063	0.9668	0.5419	0.5311	0.5964	0.5496	0.4668
PCT-Na, CCC	0.3880	0.4240	0.6999	0.3936	0.3669	0.2139	0.4624	0.3038
TCLP responses, mg/L								
TCLP B, Q	1.4000	1.2900	1.8700	1.0500	1.4300	1.2100	<1	1.2500
TCLP Cd, Q	0.2760	0.2080	0.3040	0.1850	0.2490	0.2190	0.2240	0.2530
TCLP B,CCC	1.6800	2.0000	2.5400	1.6600	1.5700	1.1200	<1	1.3500
TCLP Cd, CCC	0.3330	0.3130	0.4170	0.3220	0.2940	0.1960	0.2240	0.2610

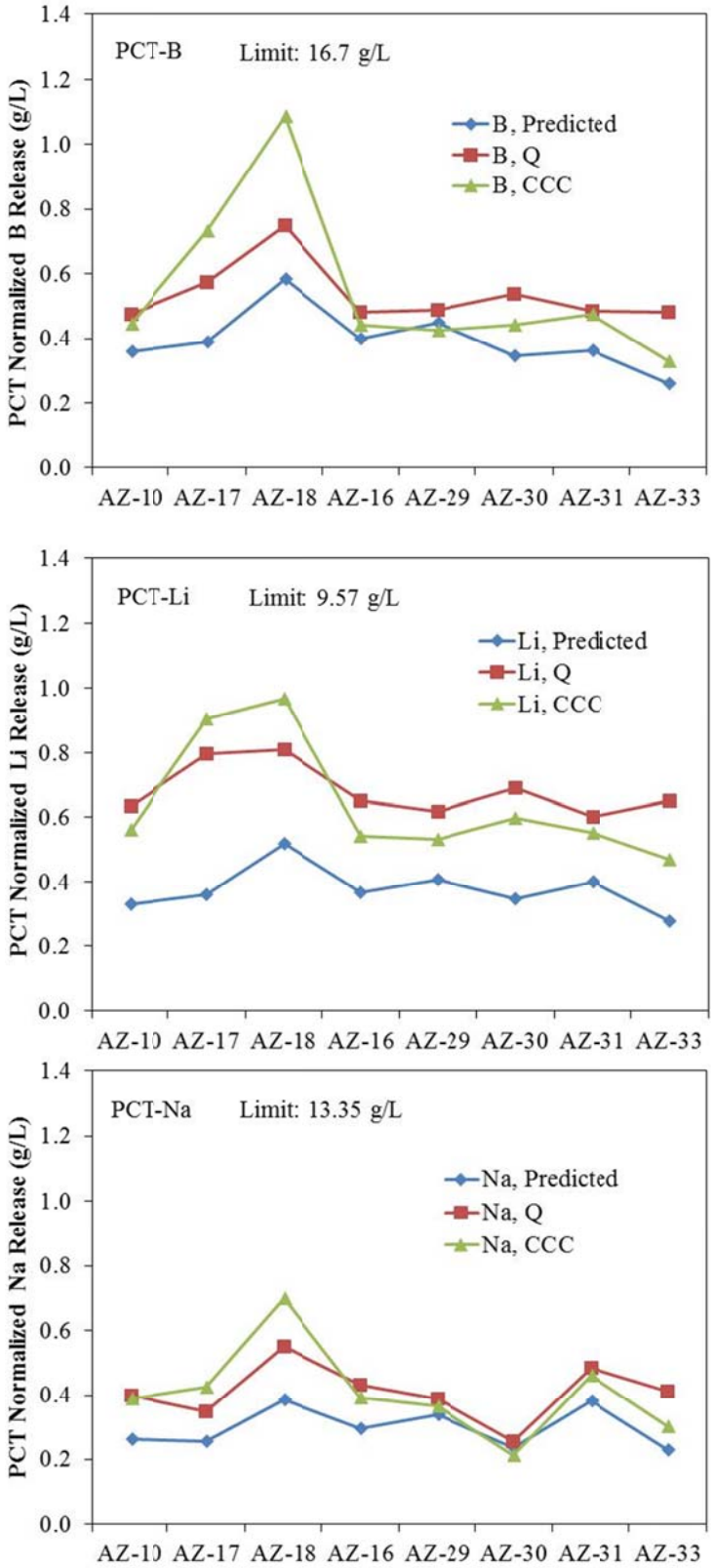

Figure 4.2. PCT Normalized Releases of CCIM-AZ Glasses (AZ-10, 17, and 18 glasses have 17 wt% Fe_2O_3, AZ-16 has 16 wt% Fe_2O_3, and AZ-29 through AZ-33 have 15 wt% Fe_2O_3)

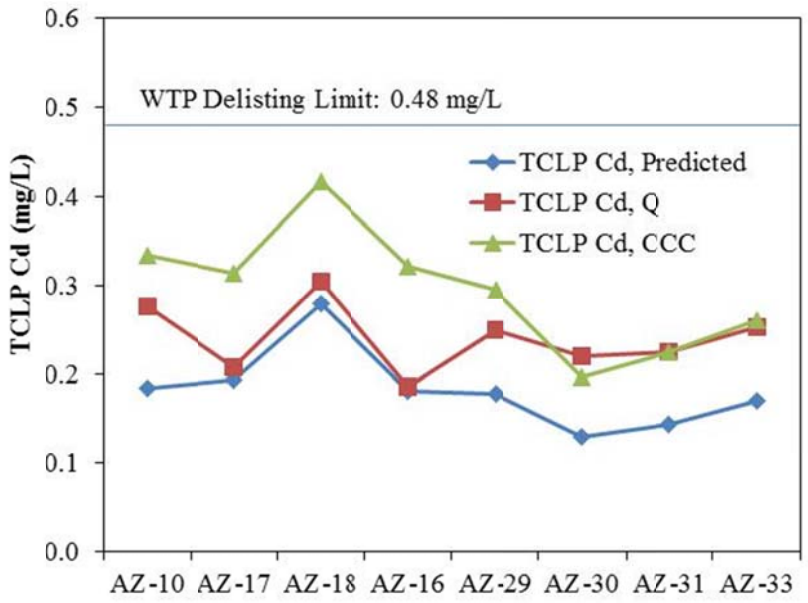

Figure 4.3. TCLP Cd of CCIM-AZ Glasses (AZ-10, 17, and 18 glasses have 17 wt% Fe_2O_3, AZ-16 has 16 wt% Fe_2O_3, and AZ-29 through AZ-33 have 15 wt% Fe_2O_3)

Table 4.7 summarizes the results of XRD analyses of isothermal heat-treated samples at temperatures from 900°C to 1250°C of CCIM-AZ glasses. Four crystalline phases were identified for isothermal heat-treated AZ-101 glasses: spinel and hematite (Fe_2O_3) that contain Fe_2O_3 as a main constituent and baddeleyite and zircon ($ZrSiO_4$) that contain ZrO_2. Spinel was a primary phase for all nine CCIM-AZ glasses.

Table 4.7. Crystal Vol% after Isothermal Heat Treatment for CCIM-AZ Glasses

T, °C	Crystal	AZ-10	AZ-17	AZ-18	AZ-16	AZ-29	AZ-30	AZ-31	AZ-32	AZ-33
900	Spinel	3.2	2.6	2.6	2.5	2.9	3.5	3.1	2.0	2.0
	Hematite	1.7	2.8	2.0	1.0	-	0.2	-	1.6	1.1
	Baddeleyite	0.9	0.3	0.9	0.5	-	-	-	-	-
	Zircon	-	1.6	-	-	-	0.3	-	0.3	0.1
1000	Spinel	2.7	1.7	2.1	2.2	1.3	1.8	1.4	1.5	1.5
	Hematite	1.0	2.1	1.1	-	-	-	-	0.2	-
	Baddeleyite	0.8	0.5	0.9	0.5	-	-	-		-
	Zircon	-	1.0	-		-	0.3	-	0.8	-
1100	Spinel	1.6	1.5	1.8	1.3	0.9	1.1	0.7	1.0	0.9
	Hematite	-	1.0	-	-	-	-	-	-	-
	Baddeleyite	0.6	0.8	0.7	0.2	-	-	-	-	-
1200	Spinel	1.5	1.9	1.5	0.8	-	-	-	0.8	-
	Hematite	-	0.3	-	-	-	-	-	-	-
	Baddeleyite	0.4	0.5	0.3	-	-	-	-	-	-
1250	Spinel	2.3	1.7	3.2	1.1	-	-	-	3.3	-
	Hematite	-	1.0	-	-	-	-	-	-	-
AZ-10, 17, and 18 have 17 wt% Fe_2O_3, AZ-16 has 16 wt% Fe_2O_3, and AZ-29 through AZ-33 have 15 wt% Fe_2O_3										

Figure 4.4 shows the effects of the heat-treating temperature on the total crystal vol% (a) and spinel vol% (b). The crystal content in general increased as the waste loading increased and decreased as the temperature increased. However, all glasses with 17 wt% and 16 wt% Fe_2O_3 (CCIM-AZ-10 through 18) and one glass with 15 wt% Fe_2O_3 (CCIM-AZ-32) exhibited the crystal content that increased as the temperature increased at higher temperatures. This unusual behavior is caused by formation of small crystals that occurred during "quenching" of the heat treated melts, but were not present at the higher heat-treatment temperature. The precipitation of these small spinel crystals makes it difficult to measure the T_L and $T_{1\%}$ values. Therefore, the T_L and $T_{1\%}$ values were estimated by extrapolating the crystal content data at lower temperatures.

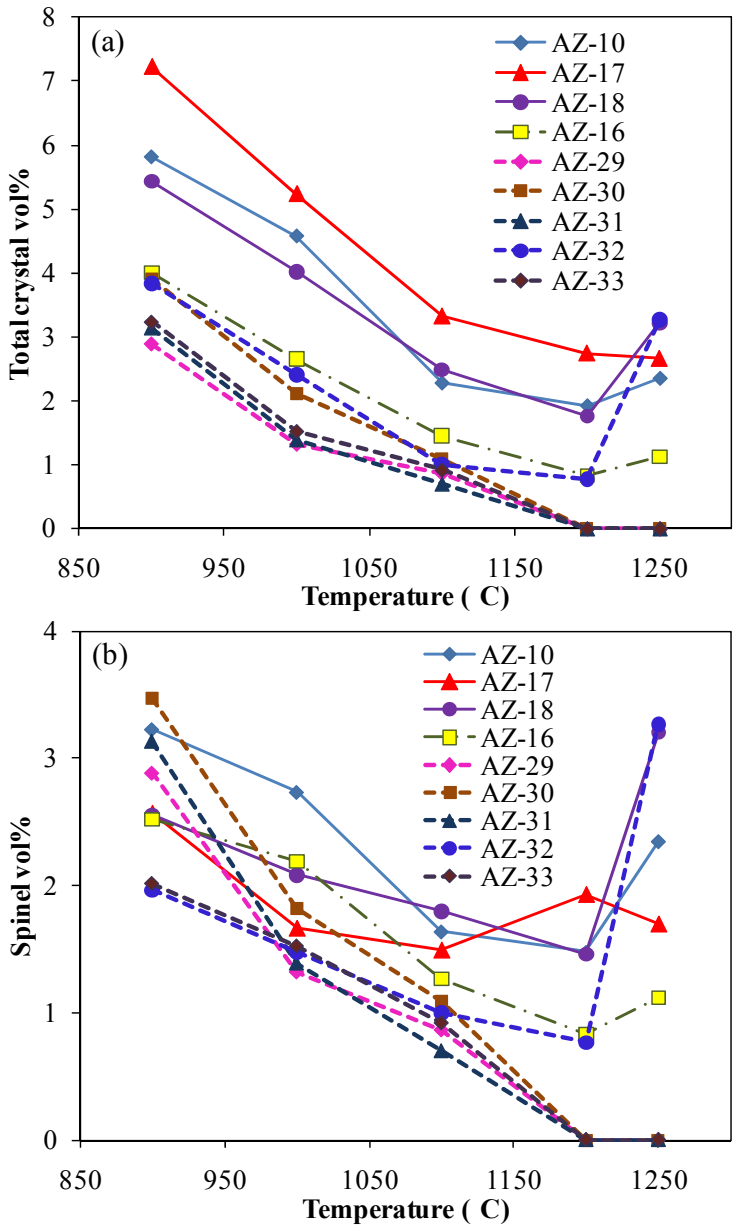

Figure 4.4. Total Crystal Vol% (a) and Spinel Vol% (b) As a Function of Temperature (AZ-10, 17, and 18 glasses have 17 wt% Fe_2O_3, AZ-16 has 16 wt% Fe_2O_3, and AZ-29 through AZ-33 have 15 wt% Fe_2O_3)

Figure 4.5 displays the estimated spinel T_L (a) and $T_{1\%}$ (b) for all CCIM-AZ glasses tested. The estimated spinel T_L and $T_{1\%}$ showed a similar general trend, except for three glasses marked in as high-B_2O_3 glasses. Both the estimated spinel T_L and $T_{1\%}$ were higher than the predicted values for 17 wt% Fe_2O_3 and 16 wt% Fe_2O_3 glasses but agreed reasonably well with the predicted for 15 wt% Fe_2O_3 glasses. It is likely that the outlying results for the three glasses with high B_2O_3 concentrations marked in Figure 4.5 were caused by the precipitation of small spinel crystals that interfered with the estimation of T_L and $T_{1\%}$. However, the reason for the high-B_2O_3 glasses to be more susceptible for these small spinel crystals is not clear.

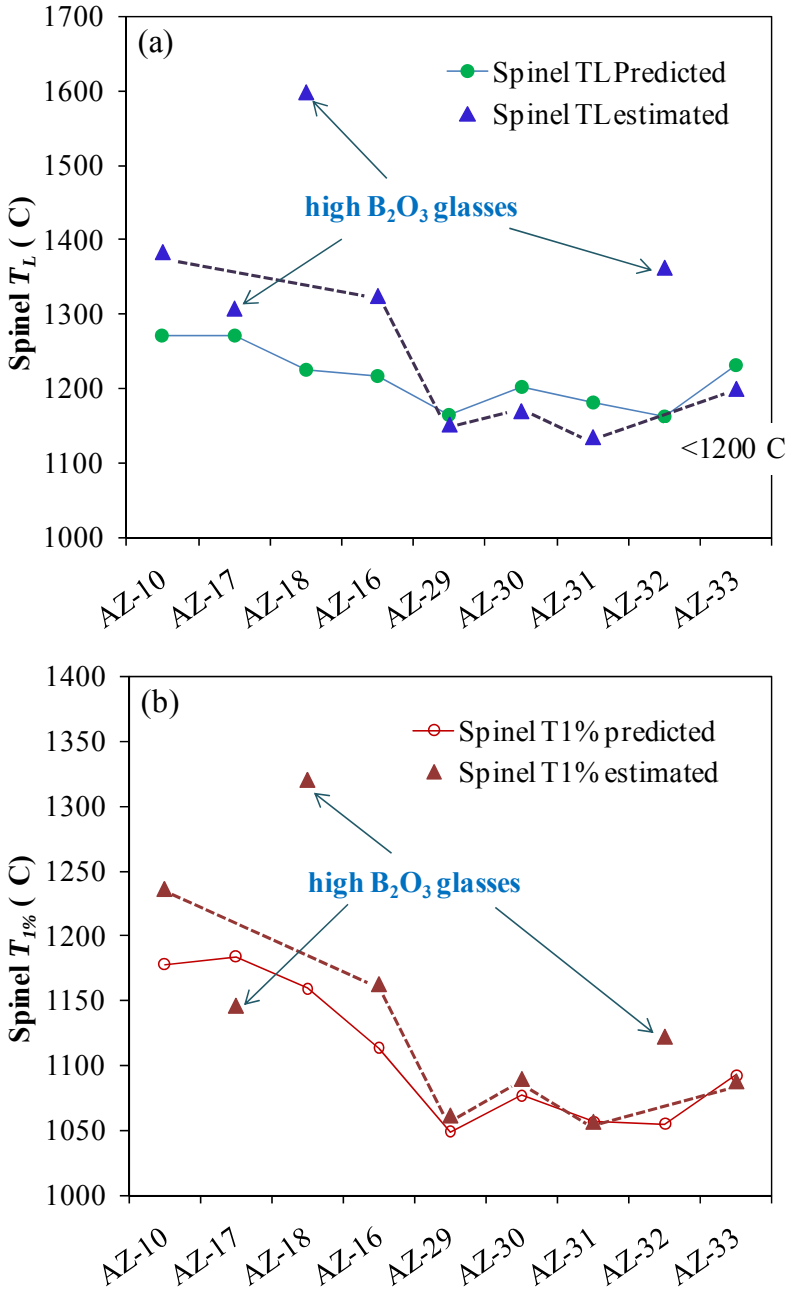

Figure 4.5. Estimated Spinel T_L (a) and $T_{1\%}$ (b) Compared with Predicted Values

Based on total crystal vol% and spinel vol% versus temperature data in Figure 4.4 and the estimated spinel T_L and $T_{1\%}$ in Figure 4.5, the three glasses with 17 wt%, 16 wt%, and 15 wt% Fe_2O_3, CCIM-AZ-10, 16, and 29, respectively, were selected for initial CCIM demonstration tests. The estimated spinel T_L and $T_{1\%}$ increase as waste loading increases in these three glasses (Figure 4.5). Figure 4.6 displays the total crystal vol% (a) and spinel vol% (b) as a function of temperature for the selected three glasses.

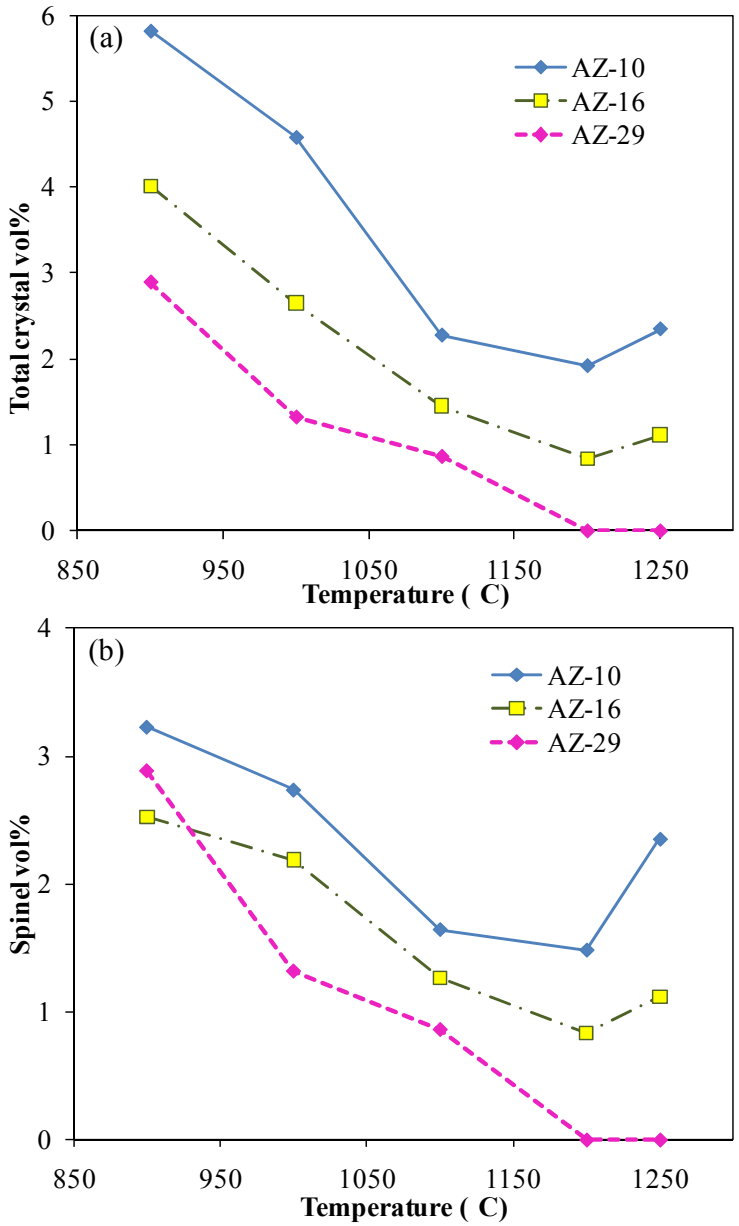

Figure 4.6. Total Crystal Vol% (a) and Spinel Vol% (b) As a Function of Temperature for Selected Three Glasses (AZ-10, 16, and 29 glasses have 17, 16, and 15 wt% Fe_2O_3, respectively)

Table 4.8 summarizes the composition of three selected glasses. They all have the same B_2O_3 and Li_2O concentrations. As the waste loading increases, the concentrations of major waste components (Al_2O_3, Fe_2O_3, and ZrO_2) increase, and the concentration of Na_2O, which was adjusted to keep the predicted viscosity constant, gradually decreases. Table 4.8 also includes estimated values for spinel T_L,

$T_{1\%}$, and total crystal and spinel vol% at 950 °C and 1150 °C. Figure 4.7 displays the total crystal vol% (a) and spinel vol% (b) as a function of waste loading for the selected three glasses, which shows that the crystal content increases as waste loading increases. The CCIM technologies possess the potential for higher tolerance to crystals in the melt. By processing these glasses during the CCIM demonstration tests starting at 39.8 wt% waste loading (15 wt% Fe_2O_3) and increasing to 42.5 wt% (16 wt% Fe_2O_3) and to 45.1 wt% (17 wt% Fe_2O_3), it would be possible to evaluate the CCIM's tolerance to crystals in the melt within the range of crystal contents summarized in Figure 4.7.

Table 4.8. Target Compositions of Major Components in Three Selected Glasses

Glass	**AZ-29**	**AZ-16**	**AZ-10**
Al_2O_3	9.79	10.44	11.09
B_2O_3	11.00	11.00	11.00
Fe_2O_3	15.00	16.00	17.00
Li_2O	3.00	3.00	3.00
Na_2O	11.99	11.38	10.78
SiO_2	39.93	38.26	36.59
ZrO_2	4.55	4.85	5.16
Subtotal[(a)]	95.26	94.94	94.63
Waste loading, wt%	39.8	42.5	45.1
Al_2O_3+Fe_2O_3+ZrO_2	29.3	31.3	33.3
T_m at 4 Pa·s, °C	1200	1200	1200
Estimated T_L	1152	1325	1384
Estimated $T_{1\%}$	1062	1163	1237
Estimated total crystal vol% at 950 °C[(b)]	2.2	3.3	5.1
Estimated total crystal vol% at 1050 °C[(b)]	0.2	0.8	1.6
Estimated spinel vol% at 950 °C[(b)]	2.2	2.3	3.0
Estimated spinel vol% at 1050 °C[(b)]	0.2	1.0	1.4

[(a)] Balance is remaining waste components.
[(b)] Obtained from linear fit of total crystal or spinel vol% versus temperature data up to 1100°C.

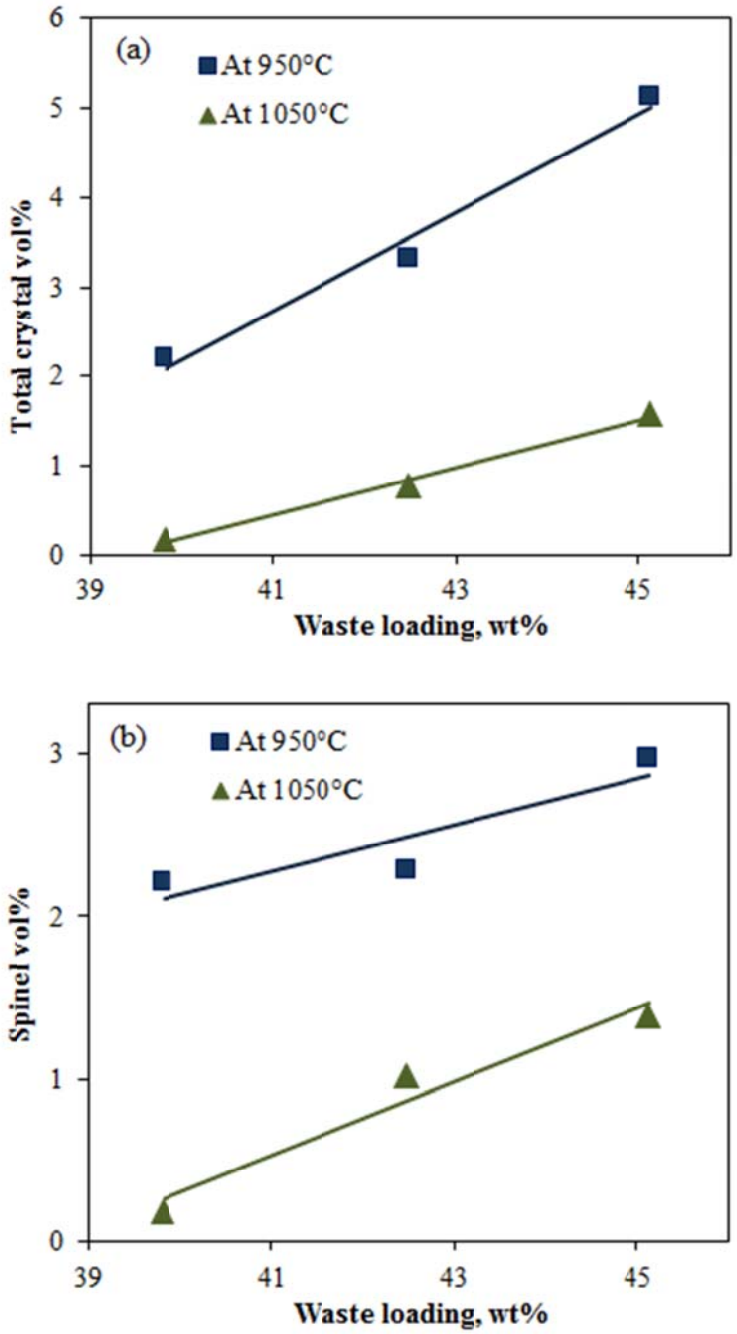

Figure 4.7. Total Crystal Vol% (a) and Spinel Vol% (b) As a Function of Waste Loading for Selected Three Glasses

Table 4.9 summarizes the viscosity and electrical conductivity of three glasses selected for the CCIM demonstration tests. Figure 4.8 displays the results of viscosity (a) and electrical conductivity (b) as a function of temperature for these three glasses. All three glasses had almost the same predicted viscosity (average predicted value is included in Figure 4.8a). The measured viscosities were reasonably well predicted for all three glasses at temperatures equal to or higher than 1150°C. The viscosities at lower temperatures were likely to be affected by the crystal contents given in Figure 4.6, i.e., the measured viscosities were higher than predicted, and the low-temperature viscosity increased as the waste loading

increased. The measured viscosity was ~4 Pa·s at 1200°C; i.e., the recommended melting temperature is 1200 °C for all three glasses. For electrical conductivity, three glasses had different predicted values as shown in Figure 4.8b. Figure 4.8b shows that the measured electrical conductivities were lower than predicted, and the measured differences between glasses were greater than predicted. However, the measured electrical conductivities for all three glasses were within the desired range of 10 S/m to 100 S/m at a recommended melting temperature of 1200 °C (Marra et al. 2008).

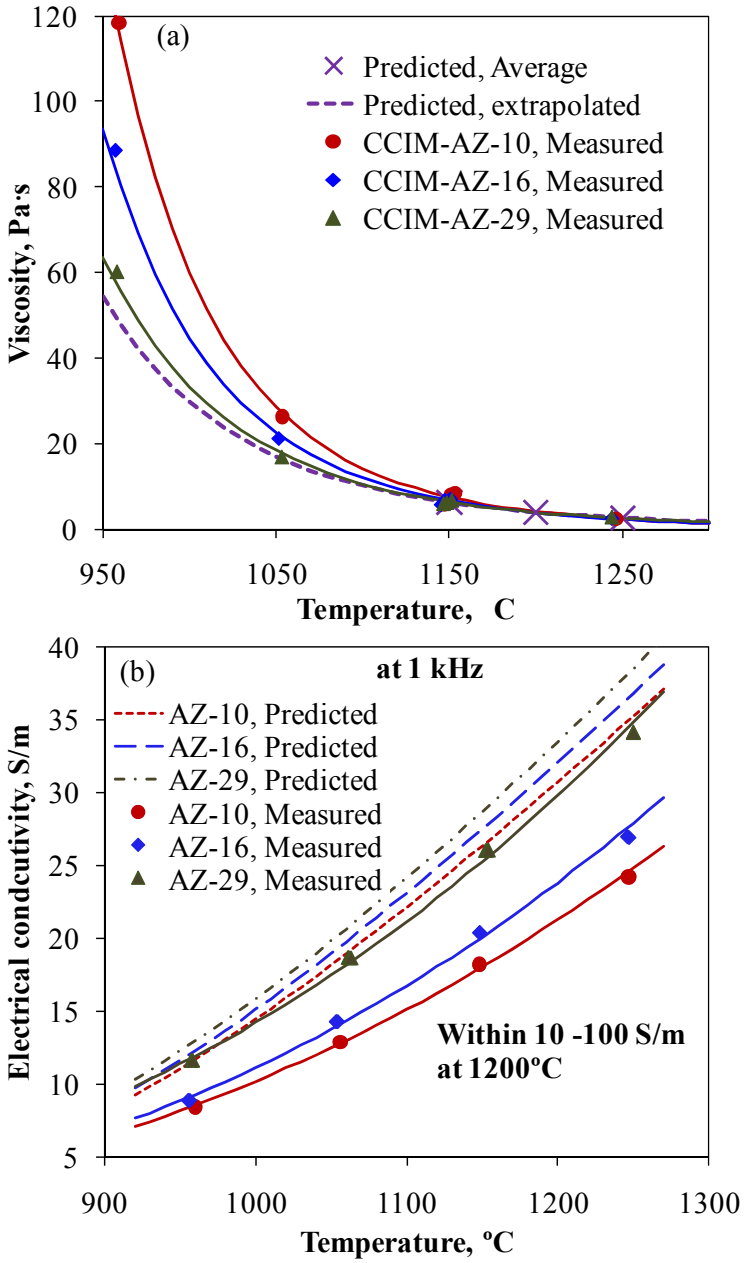

Figure 4.8. Viscosity (a) and Electrical Conductivity (b) of Three Glasses Selected for CCIM Tests (AZ-10, 16, and 29 glasses have 17, 16, and 15 wt% Fe_2O_3, respectively)

Table 4.9. Measured Viscosity and Electrical Conductivity of Three Selected Glasses

CCIM-AZ-10		CCIM-AZ-16		CCIM-AZ-29	
Viscosity (η) at a given temperature					
T, C	**η, Pa·s**	**T, C**	**η, Pa·s**	**T, C**	**η, Pa·s**
1151	8.14	1147	6.91	1148	6.20
1053	26.30	1051	21.34	1053	16.87
959	118.47	957	88.73	958	60.19
1153	8.36	1151	7.20	1151	6.75
1246	2.49	1244	2.63	1243	2.82
1147	5.89	1145	5.86	1146	5.97
Electrical conductivity (ε) at a given temperature (1 kHz)					
T, C	**ε, S/m**	**T, C**	**ε, S/m**	**T, C**	**ε, S/m**
960	8.47	955	8.90	957	11.59
1056	12.90	1053	14.29	1062	18.63
1148	18.20	1148	20.38	1153	26.00
1247	24.25	1246	26.93	1250	34.09

4.2 Cold Crucible Induction Melter Glass Formulation for AN-105 LAW

The composition of AN-105 LAW was given in Table 2.1. As discussed in Section 2.1, the loading of AN-105 is limited by Na_2O concentration in glass that dictates the chemical durability of glass. The higher melting temperature of CCIM technologies would allow higher concentrations of refractory additive components that increase chemical durability, such as ZrO_2 and SnO_2, which may enable higher waste loading.

4.2.1 Preliminary Vapor Hydration Test Model for High Alkali Glasses

For AN-105 LAW, the key properties that limit waste loading are the PCT normalized releases and the VHT alteration rate. Existing PCT normalized release models (Vienna et al. 2009) were used because the PCT models provide reasonable predictability for the present purpose. Although the recent models reported in Vienna et al. (2009) were developed primarily for estimating HLW glass volumes, they are considered global models and can be used for LAW glasses. They were developed from the compiled database that covers a large fraction of the region of waste glass compositions considered potentially of interest for Hanford including LAW glasses.

However, the performance of the VHT alteration rate model is in general poor compared to the PCT models. In addition, the recent models report (Vienna et al. 2009) does not include the model for VHT alteration rate. Therefore, existing data on the VHT response in glasses with high alkali oxides were collected and used to develop a preliminary VHT model suited for the high-waste-loaded AN-105 based glasses in this study.

The VHT alteration rate data were collected from a glass database that has been compiled at PNNL, which was also used for the development of the glass property models reported in Vienna et al. (2009). The VHT data reported in four data sets were considered:

- WTP glasses. This data set includes the glasses tested at VSL to develop the LAW glass property models for WTP. The data collection and model development are reported in Piepel et al. (2007).

The VHT alteration rate was based on 24-day tests at 200°C. One hundred eighty-one glasses had VHT alteration rate data.

- ORP glasses. This data set includes the glasses resulting from the glass formulation developments performed at VSL for ORP to increase the waste loading in LAW glasses, reported in Matlack et al. (2006, 2007b, and 2009). The VHT alteration rate was based on 24-day tests at 200°C. One hundred seventeen glasses had VHT alteration rate data.
- Hanford LAW product (HLP) acceptance glasses. This data set includes the HLP glasses developed and tested at PNNL to help determine the composition range of LAW glasses that will meet performance expectations of the Hanford site burial facility (Vienna et al 2001). The VHT alteration rate after 24 days was obtained from the plots of VHT alteration mass versus time. For some glasses, extrapolation was needed. Only the glasses with reasonable extrapolation were considered, i.e., the glasses with too much scatter or with test periods too far away from 24 days were excluded. Seventy-two glasses had the VHT data converted to 24-day rate.
- in-container vitrification (ICV) glasses: This data set includes the ICV glasses tested at PNNL under the demonstration bulk vitrification system (DBVS) to evaluate the bulk vitrification as a candidate technology for LAW supplement treatment (Kim et al. 2003). The VHT alteration rate was based on 14-day tests at 200°C. Ninety-three glasses had VHT alteration rate data.

As mentioned above, the VHT alteration rate was based on the 24-day tests except for the data set for ICV glasses. These 463 glasses were further sorted to collect the high-alkali borosilicate glasses, i.e., only the glasses that satisfy the following conditions were collected:

- $g_{B2O3} \geq 4$ wt%
- $g_{Na2O} + 0.66g_{K2O} + 2.07g_{Li2O} \geq 16$ wt%

Additional glasses were excluded as they were not adequate for the model:

- CCC treated glasses
- glasses that completely corroded before the end of test duration (24 days or 14 days)
- glasses with no corrosion after the end of test duration (24 days or 14 days)
- glasses that formed a significant fraction of crystals during melting (applicable to HLP glasses only).

Table 4.10 summarizes the glasses collected for VHT model development, including the number of glasses with VHT alteration data and those used for model development after excluding the glasses for the reasons described above. Table 4.10 also shows the range of concentrations for the components of interest including $g_{Na2O} + 0.66g_{K2O} + 2.07g_{Li2O}$ and the range of VHT alteration rates. Appendix B, Table B.1 lists the composition and VHT alteration rate for 257 glasses used for VHT model development.

Table 4.10. Summary of Glasses with VHT Data

Data Set	ORP Glasses		WTP Glasses		HLP Glasses		ICV Glasses		All Glasses	
# of glasses with VHT data	117		181		72		93		463	
# of glasses used for model	83		86		51		37		257	
Component concentration range (in mass fraction) of the glasses used for model										
Component	Min	Max	Min	Max	Min	Max	Min	Max	Min	Max
Al_2O_3	0.058	0.136	0.050	0.090	0.040	0.120	0.080	0.168	0.040	0.168
B_2O_3	0.061	0.128	0.061	0.130	0.060	0.126	0.040	0.060	0.040	0.130
CaO	0.000	0.105	0.000	0.100	0.000	0.050	0.025	0.055	0.000	0.105
Fe_2O_3	0.000	0.030	0.000	0.100	0.000	0.158	0.040	0.110	0.000	0.158
K_2O	0.001	0.059	0.000	0.054	0.003	0.050	0.000	0.025	0.000	0.059
Li_2O	0.000	0.036	0.000	0.045	0.000	0.001	0.000	0.000	0.000	0.045
MgO	0.000	0.034	0.000	0.037	0.000	0.043	0.000	0.030	0.000	0.043
Na_2O	0.130	0.260	0.131	0.240	0.160	0.236	0.170	0.240	0.130	0.260
SiO_2	0.343	0.433	0.383	0.491	0.360	0.598	0.390	0.501	0.343	0.598
SnO_2	0.000	0.050	0.000	0.000	0.000	0.000	0.000	0.000	0.000	0.050
SO_3	0.002	0.021	0.001	0.024	0.001	0.003	0.000	0.010	0.000	0.024
TiO_2	0.000	0.016	0.004	0.030	0.000	0.086	0.000	0.020	0.000	0.086
ZnO	0.010	0.037	0.010	0.050	0.000	0.043	0.000	0.000	0.000	0.050
ZrO_2	0.030	0.061	0.000	0.050	0.000	0.060	0.020	0.080	0.000	0.080
$Na_2O+0.66K_2O+2.07Li_2O$	0.205	0.264	0.171	0.245	0.162	0.239	0.170	0.251	0.162	0.264
VHT alteration rate range for the glasses used for model										
r_{alt}, ($g/m^2/d$)	2.0	130.0	0.2	108.2	0.4	87.8	0.3	147.1	0.2	147.1
$\ln(r_{alt})$, $\ln(g/m^2/d)$	0.69	4.87	-1.61	4.68	-1.00	4.47	-1.15	4.99	-1.61	4.99

A simple linear model form was applied for the 257 model glasses:

$$\ln(r_{alt}) = \sum_{n=1}^{14} g_i b_i \tag{4.1}$$

where r_{alt} is the VHT alteration rate ($g/m^2/d$), g_i is the mass fraction of the i^{th} component in glass, and b_i is the model coefficient for the i^{th} component. Table 4.11 lists the model coefficients and R^2 value for the 14 component model (13 oxide components plus "Others" component that represents the sum of all components not specifically listed in the 13). The poor predictability of this model is evident from the low R^2 value of 0.593, which suggests that the output of this model should be used with caution. The 2nd order model or any other model forms to improve the predictability were not explored for the present study as they are notorious for poor performance when extrapolated. Figure 4.9 shows the predicted versus measured VHT alteration rate for each data set. Except for the ORP glasses that had high alkali glasses only and therefore had overall high VHT alteration rates, the three data sets had similar range of the measured VHT rates.

Table 4.11. VHT Model Coefficients

Component	Coefficient
Al_2O_3	5.2
B_2O_3	-16.6
CaO	-16.4
Fe_2O_3	-11.6
K_2O	37.8
Li_2O	117.8
MgO	-15.7
Na_2O	45.4
SiO_2	-6.5
SnO_2	-24.4
TiO_2	-8.7
ZnO	-28.9
ZrO_2	-52.9
Others[(a)]	21.0
R^2	0.593
[(a)]Sum of concentrations for all remaining components	

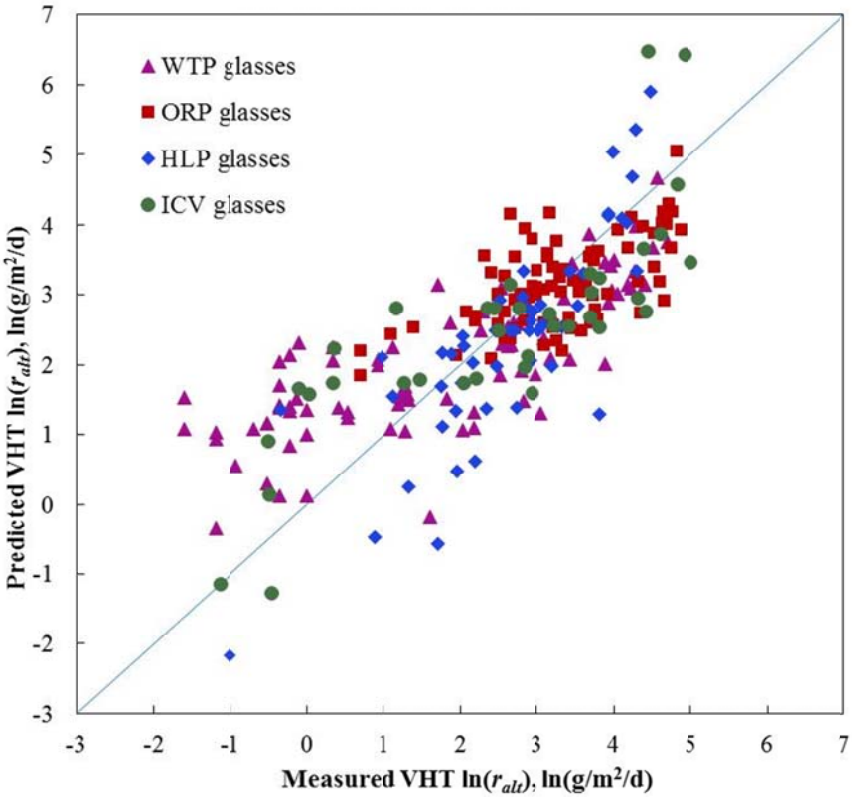

Figure 4.9. Predicted versus Measured VHT Alteration Rate

The preliminary model was used to plot the effect of glass composition on the VHT alteration rate in ln(g/m^2/d). The baseline glass was selected as a typical WTP glass containing:

- 20 wt% Na_2O

- fixed concentrations for Al_2O_3, B_2O_3, Fe_2O_3, TiO_2, ZnO, and ZrO_2 according to the WTP glass formulation rules (Vienna 2005)
- arbitrarily chosen concentration at 3 wt% for components with variable concentrations according to the WTP glass formulation rules (Vienna 2005), which include Li_2O, K_2O, CaO, and MgO
- SiO_2 concentration as a balance.

Table 4.12 shows the composition of the baseline glass.

Table 4.12. Composition of a Baseline Glass Used for Calculation of the Effect of Glass Composition on VHT Alteration Rate

Oxide	Mass fraction
Al_2O_3	0.061
B_2O_3	0.100
CaO	0.030
Fe_2O_3	0.055
K_2O	0.030
Li_2O	0.010
MgO	0.030
Na_2O	0.200
SiO_2	0.405
TiO_2	0.014
ZnO	0.035
ZrO_2	0.030
SUM	1.000

Figure 4.10 shows the change of predicted VHT alteration rate (in $\ln[g/m^2/d]$) as a function of mass% change of a glass component from the baseline glass calculated using the model given in Table 4.11. Figure 4.10 shows that alkali oxides strongly increase the VHT alteration rate while most other major LAW glass components, except for Al_2O_3, decrease the alteration rate. The addition of Al_2O_3 is predicted to slightly increase the alteration rate.

To compare the compositional effect for VHT with that for PCT, the PCT-Na model given in Vienna et al. (2009) was used to perform similar calculations. The results are shown in Figure 4.11 for PCT normalized sodium release. The PCT-Na models in Vienna et al. 2009 used the second order model form, with the second order terms for Al_2O_3 and B_2O_3. As shown in Figure 4.11, the B_2O_3 addition decreases the PCT release initially at low concentrations but increases the PCT release with further increase in B_2O_3 concentration after a minimum. The effect of Al_2O_3 is very strong at lower concentrations and becomes smaller as concentration of Al_2O_3 increases. There is similarity between VHT and PCT in that alkali oxides increase the glass corrosion while ZnO, SiO_2, Fe_2O_3, and ZrO_2 all decrease the glass corrosion. The major difference lies in the effect of Al_2O_3 and B_2O_3: Al_2O_3 has a strong positive effect on PCT with a slight negative effect on VHT, but B_2O_3 has a positive effect on VHT with relatively strong negative effect on PCT at higher B_2O_3 concentration range. Another difference to note is that both CaO and SnO_2 have positive effect on VHT but no effect on PCT. Glass formulation applies this information on the effect of the glass composition on PCT and VHT while keeping the viscosity and melting temperature within desired range.

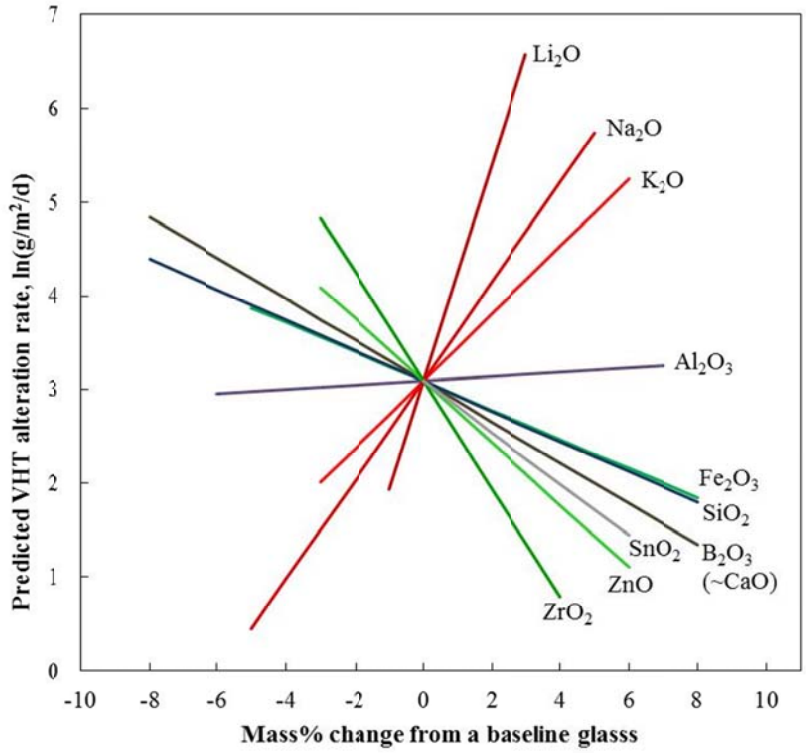

Figure 4.10. VHT Spider Plot for the Effect of Component Mass% Change on ln(r_{alt})

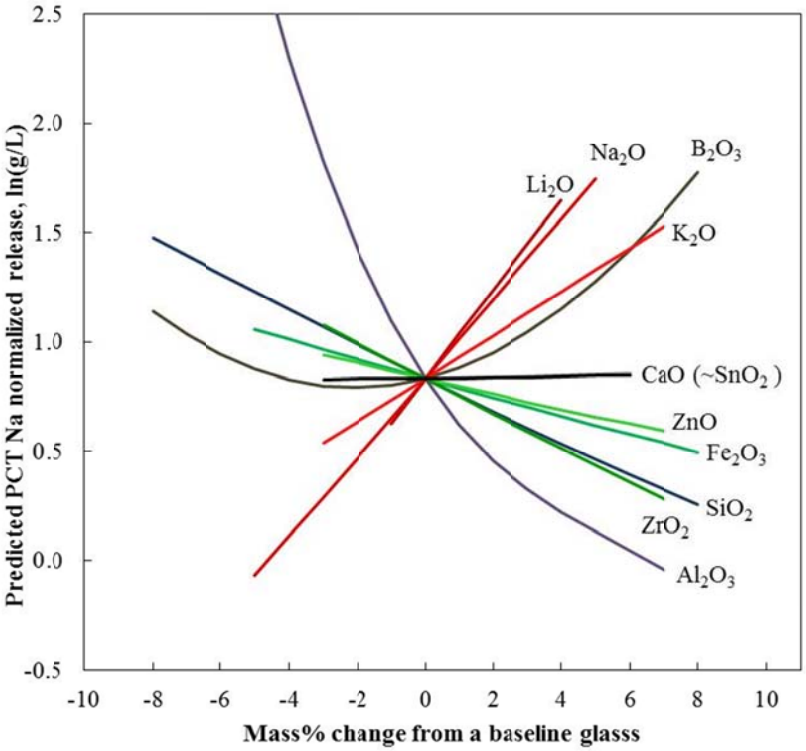

Figure 4.11. PCT Spider Plot for the Effect of Component Mass% Change on ln(r_{Na})

4.2.2 Formulation Approach for AN-105 LAW Glasses for the Cold Crucible Induction Melter

Table 4.13 summarizes the glass property requirements applied when designing the LAW glasses for CCIM testing. The requirements for CCC crystallinity, viscosity, and electrical conductivity were self-imposed for the glass development purpose. Available glass property models (Vienna et al. 2002; Vienna et al. 2009) were used to predict these properties whenever possible. However, the predicted values were used primarily as guidelines for glass formulation because the high waste loaded glasses that are considered in this study are outside the model validity composition range of these models.

Table 4.13. Glass Property Requirements[(a)] for LAW Glasses

Property	Requirements
CCC crystallinity	No nepheline formation after CCC
PCT normalized release of Q and CCC samples	B and Na < 4 g/L
VHT alteration rate of Q and CCC samples	< 50 $g/m^2/d$
Viscosity	4 Pa·s at a nominal melting temperature (T_m)
Electrical conductivity	10 – 100 S/m at T_m
[(a)]Self-imposed for the glass development purpose except for PCT and VHT requirements Q stands for quenched and CCC canister centerline cooling.	

Table 4.14 shows the target compositions and predicted properties for AN-105 LAW (CCIM-AN-xx) glasses. The glass formulation was performed in two steps. The second set of glasses was formulated after completing the testing and evaluation of the first set of glasses. The first set of glasses had 23 wt% to 25 wt% Na_2O in glass (30 wt% to 32.6 wt% waste loading) while the second set had 25 wt% and 26 wt% Na_2O (32.6 wt% and 33.9 wt% waste loading). The testing for the second set of glasses was not fully completed before the task close out.

The predicted nominal melting temperature (T_m) at a predicted viscosity of 4 Pa·s was from 1200°C to 1300°C. The predicted electrical conductivity was within the desired range of 10 S/m to 100 S/m at T_m for all CCIM-AN glasses. The predicted normalized PCT releases (Vienna et al. 2009) and predicted VHT alteration rate (by Table 4.11) are all below the waste acceptance criteria although the glasses with high Na_2O concentration (CCIM-AN-27, 28, 31) approach the limits especially for VHT. The nepheline constraint was met for two CCIM-AN glasses only, CCIM-AN-02 and 09, by satisfying the N_{Si} rule; all other glasses failed both the N_{Si} and OB rules.

Table 4.14. Target Composition and Predicted Properties of CCIM-AN Glasses

Oxide	1st set of glasses						Limits[(a)]
	CCIM-AN-02	CCIM-AN-04	CCIM-AN-09	CCIM-AN-11	CCIM-AN-18	CCIM-AN-20	
Al_2O_3	0.06000	0.06000	0.05589	0.05589	0.06000	0.05822	-
B_2O_3	0.10375	0.10032	0.09124	0.11582	0.07730	0.08053	-
CaO	0.00000	0.03000	0.00000	0.00000	0.02000	0.00000	-
Cl	0.00649	0.00649	0.00677	0.00677	0.00677	0.00706	-
Cr_2O_3	0.00021	0.00021	0.00022	0.00022	0.00022	0.00023	-
Cs_2O	0.00150	0.00150	0.00156	0.00156	0.00156	0.00163	-
F	0.00003	0.00003	0.00003	0.00003	0.00003	0.00003	-
K_2O	0.00515	0.00515	0.00537	0.00537	0.00537	0.00560	-
Na_2O	0.23000	0.23000	0.24000	0.24000	0.24000	0.25000	-
Re_2O_7	0.00030	0.00030	0.00031	0.00031	0.00031	0.00033	-
SiO_2	0.48082	0.45425	0.48676	0.45218	0.47659	0.48447	-
SO_3	0.00176	0.00176	0.00183	0.00183	0.00183	0.00191	-
SnO_2	0.02500	0.02500	0.02500	0.02500	0.02000	0.02500	-
ZnO	0.02500	0.02500	0.02500	0.02500	0.02000	0.02500	-
ZrO_2	0.06000	0.06000	0.06000	0.07000	0.07000	0.06000	-
Total	1.00000	1.00000	1.00000	1.00000	1.00000	1.00000	-
Waste loading	0.300	0.300	0.313	0.313	0.313	0.326	-
T_m at 4 Pa·s, °C	1250	1200	1250	1200	1250	1250	-
EC at T_m, S/m	54.3	52.5	59.8	56.9	61.0	66.3	10-100
PCT-B, g/L	1.83	1.73	2.00	2.89	1.35	1.93	<4
PCT-Na, g/L	1.78	1.99	2.13	2.56	1.89	2.33	<4
VHT r_{alt}, g/m^2/d	6.1	4.7	11.3	5.6	8.6	22.3	<50
N_{Si}	0.624	0.610	0.622	0.604	0.614	0.611	≥0.62
OB	0.582	0.595	0.588	0.587	0.600	0.595	≤0.575

Oxide	2nd set of glasses				Limits[(a)]
	CCIM-AN-23	CCIM-AN-27	CCIM-AN-28	CCIM-AN-31	
Al_2O_3	0.05822	0.06055	0.06055	0.07500	-
B_2O_3	0.06674	0.07046	0.05746	0.05519	-
CaO	0.02000	0.00000	0.02000	0.00000	-
Cl	0.00706	0.00734	0.00734	0.00734	-
Cr_2O_3	0.00023	0.00024	0.00024	0.00024	-
Cs_2O	0.00163	0.00169	0.00169	0.00169	-
F	0.00003	0.00003	0.00003	0.00003	-
K_2O	0.00560	0.00582	0.00582	0.00582	-
Na_2O	0.25000	0.26000	0.26000	0.26000	-
Re_2O_7	0.00033	0.00034	0.00034	0.00034	-
SiO_2	0.47827	0.48155	0.47454	0.48236	-
SO_3	0.00191	0.00199	0.00199	0.00199	-
SnO_2	0.02000	0.02500	0.02000	0.02000	-
ZnO	0.02000	0.02500	0.02000	0.02000	-
ZrO_2	0.07000	0.06000	0.07000	0.07000	-
Total	1.00000	1.00000	1.00000	1.00000	-
Waste loading	0.326	0.339	0.339	0.339	-
T_m at 4 Pa·s, °C	1250	1250	1250	1300	-
EC at T_m, S/m	67.8	73.7	75.7	77.4	10-100
PCT-B, g/L	1.44	1.89	1.43	1.09	<4
PCT-Na, g/L	2.31	2.63	2.68	1.99	<4
VHT r_{alt}, g/m^2/d	16.1	43.5	31.3	46.3	<50
N_{Si}	0.608	0.600	0.597	0.590	≥0.62
OB	0.606	0.602	0.613	0.607	≤0.575

[(a)] Used as guidelines for formulating the glasses.
Shaded cells indicate that the predicted or calculated value is not within the limits.

4.2.3 Test Results of AZ-105 LAW Glasses for the Cold Crucible Induction Melter

Chemical analyses of glasses were performed for all CCIM-AN glasses primarily to confirm glass batching and melting preparation. Table 4.15 and Table 4.16 compare the target and analyzed compositions and provide their relative percent difference (RPD) values for the first and second set of glasses. For the first set of glasses, the analytical results matched well with the target concentrations for all glasses except for CCIM-AN-20, which had the analyzed Na_2O concentration 7.7 RPD lower than the target (23.09 wt% compared to 25 wt% Na_2O in glass). It was not clear whether the difference was caused by glass batching/preparation or analytical error. The second set of glasses showed relatively larger differences between target and analyzed concentrations for most components in general compared to the first set. However, there was no specific glass that showed major difference from other glasses and the Na_2O results were consistent and matched the target values very well.

Table 4.15. Comparison of Target and Analyzed Compositions of First Set of CCIM-AN Glasses and their Relative Percent Difference (RPD)

	Target (wt%)						Analyzed (wt%)[1]					
Comp.	**AN-02**	**AN-04**	**AN-09**	**AN-11**	**AN-18**	**AN-20**	**AN-02**	**AN-04**	**AN-09**	**AN-11**	**AN-18**	**AN-20**
Al_2O_3	6.00	6.00	5.59	5.59	6.00	5.82	6.14	6.14	5.76	5.77	6.25	6.27
B_2O_3	10.37	10.03	9.12	11.58	7.73	8.05	10.01	9.93	9.55	11.74	8.00	8.15
CaO	0.00	3.00	0.00	0.00	2.00	0.00	0.00	3.21	0.00	0.00	2.12	0.00
Cl	0.65	0.65	0.68	0.68	0.68	0.71						
Cr_2O_3	0.02	0.02	0.02	0.02	0.02	0.02	0.04	0.03	0.03	0.03	0.03	0.02
Cs_2O	0.15	0.15	0.16	0.16	0.16	0.16						
F	0.003	0.003	0.003	0.003	0.003	0.003						
K_2O	0.52	0.52	0.54	0.54	0.54	0.56	0.53	0.57	0.57	0.55	0.58	0.60
Na_2O	23.00	23.00	24.00	24.00	24.00	25.00	22.28	22.61	23.29	23.83	23.29	23.09
Re_2O_7	0.03	0.03	0.03	0.03	0.03	0.03						
SiO_2	48.08	45.42	48.68	45.22	47.66	48.45	48.26	45.69	48.79	45.58	47.83	49.65
SO_3	0.18	0.18	0.18	0.18	0.18	0.19						
SnO_2	2.50	2.50	2.50	2.50	2.00	2.50	2.71	2.76	2.67	2.72	2.13	2.72
ZnO	2.50	2.50	2.50	2.50	2.00	2.50	2.42	2.40	2.40	2.42	1.90	2.47
ZrO_2	6.00	6.00	6.00	7.00	7.00	6.00	5.60	5.68	5.64	6.59	6.66	5.78
Total	100.0	100.0	100.0	100.0	100.0	100.0	97.98	99.03	98.69	99.23	98.78	98.74
	RPD[2]											
Comp.	**AN-02**	**AN-04**	**AN-09**	**AN-11**	**AN-18**	**AN-20**						
Al_2O_3	2.4%	2.4%	3.0%	3.3%	4.1%	7.6%						
B_2O_3	-3.5%	-1.0%	4.6%	1.3%	3.5%	1.2%						
CaO		7.1%			6.0%							
Cl												
Cr_2O_3												
Cs_2O												
F												
K_2O	1.9%	9.8%	6.3%	2.0%	7.5%	6.7%						
Na_2O	-3.2%	-1.7%	-3.0%	-0.7%	-3.0%	-7.7%						
Re_2O_7												
SiO_2	0.4%	0.6%	0.2%	0.8%	0.4%	2.5%						
SO_3												
SnO_2	8.2%	10.5%	6.9%	8.7%	6.4%	9.0%						
ZnO	-3.0%	-4.0%	-4.0%	-3.3%	-4.8%	-1.0%						
ZrO_2	-6.6%	-5.3%	-6.1%	-5.8%	-4.8%	-3.7%						

[1]Empty cells represent the components that were not analyzed or below detection limit

[2]Calculated for components with target concentration > 0.5 wt%

Table 4.16. Comparison of Target and Analyzed Compositions of Second Set of CCIM-AN Glasses and their Relative Percent Difference (RPD)

	Target (wt%)				Analyzed (wt%)[1]				RPD[2]			
Comp.	**AN-23**	**AN-27**	**AN-28**	**AN-31**	**AN-23**	**AN-27**	**AN-28**	**AN-31**	**AN-23**	**AN-27**	**AN-28**	**AN-31**
Al_2O_3	5.82	6.05	6.05	7.50	6.07	6.23	6.42	7.61	4.3%	2.9%	6.0%	1.5%
B_2O_3	6.67	7.05	5.75	5.52	6.57	6.30	5.23	4.73	-1.6%	-10.7%	-8.9%	-14.2%
CaO	2.00	0.00	2.00	0.00	2.13	0.05	2.20	0.05	6.6%		10.1%	
Cl	0.71	0.73	0.73	0.73								
Cr_2O_3	0.023	0.024	0.024	0.024	0.034	0.037	0.035	0.035				
Cs_2O	0.16	0.17	0.17	0.17								
F	0.003	0.003	0.003	0.003								
K_2O	0.56	0.58	0.58	0.58	0.55	0.55	0.60	0.59	-2.5%	-6.3%	3.6%	1.4%
Na_2O	25.00	26.00	26.00	26.00	25.87	26.57	26.64	26.53	3.5%	2.2%	2.4%	2.0%
Re_2O_7	0.033	0.034	0.034	0.034								
SiO_2	47.83	48.15	47.45	48.24	48.26	49.54	48.79	49.33	0.9%	2.9%	2.8%	2.3%
SO_3	0.19	0.20	0.20	0.20	0.14	0.18	0.15	0.18				
SnO_2	2.00	2.50	2.00	2.00	1.63	2.00	1.62	1.63	-18.6%	-19.9%	-18.8%	-18.7%
ZnO	2.00	2.50	2.00	2.00	2.02	2.46	1.99	1.96	0.8%	-1.4%	-0.7%	-2.0%
ZrO_2	7.00	6.00	7.00	7.00	6.60	5.70	6.54	6.55	-5.7%	-5.1%	-6.6%	-6.5%
Total	100.0	100.0	100.0	100.0	99.86	99.61	100.21	99.19				

[1]Empty cells represent the components that were not analyzed or below detection limit.
[2]Calculated for components with target concentration > 0.5 wt%.

All CCIM-AN glasses from both first and second sets were crystal-free after CCC treatment, although only two glasses, CCIM-AN-02 and 09, satisfied the nepheline constraint (i.e., met either N_{Si} or OB rule, see Table 4.14). This lack of nepheline crystallization in these glasses that are predicted to crystallize the nepheline indicates the conservativeness of the current constraint. As a result, CCC treatment is not likely to have a significant impact on PCT normalized releases and VHT responses.

Negligible corrosion was observed after 7-day and 24-day VHTs at 200°C for the first set of glasses for all quenched and CCC-treated samples based on optical microscopic examination. All 7-day VHT samples were observed by scanning electron microscopy (SEM) to confirm the negligible corrosion by optical microscopy. Figure 4.12 and Figure 4.13 show thin-section VHT samples after 7-day tests at 200 °C for the first set of quenched (Figure 4.12) and CCC-treated (Figure 4.13) glasses prepared for the optical microscopy and SEM examination.

Table 4.17 summarizes the results of VHT alteration rates measured by SEM after 7-day tests at 200 °C for the first set of glasses. The alteration rate was more than an order of magnitude smaller than the limit of 50 $g/m^2/d$ and significantly lower than predicted by the model (Table 4.11) for all quenched and CCC glasses. Figure 4.14 is an example SEM micrograph showing the VHT alteration layer formed on the CCIM-AN-09 CCC glass after the 7-day VHT at 200°C. SEM micrographs of the VHT alteration for the first set of glasses for all quenched and CCC-treated samples are given in Appendix C. Because of negligible corrosion by VHT for the first set of glasses, the second set of glasses were formulated based on the PCT normalized releases, discussed below.

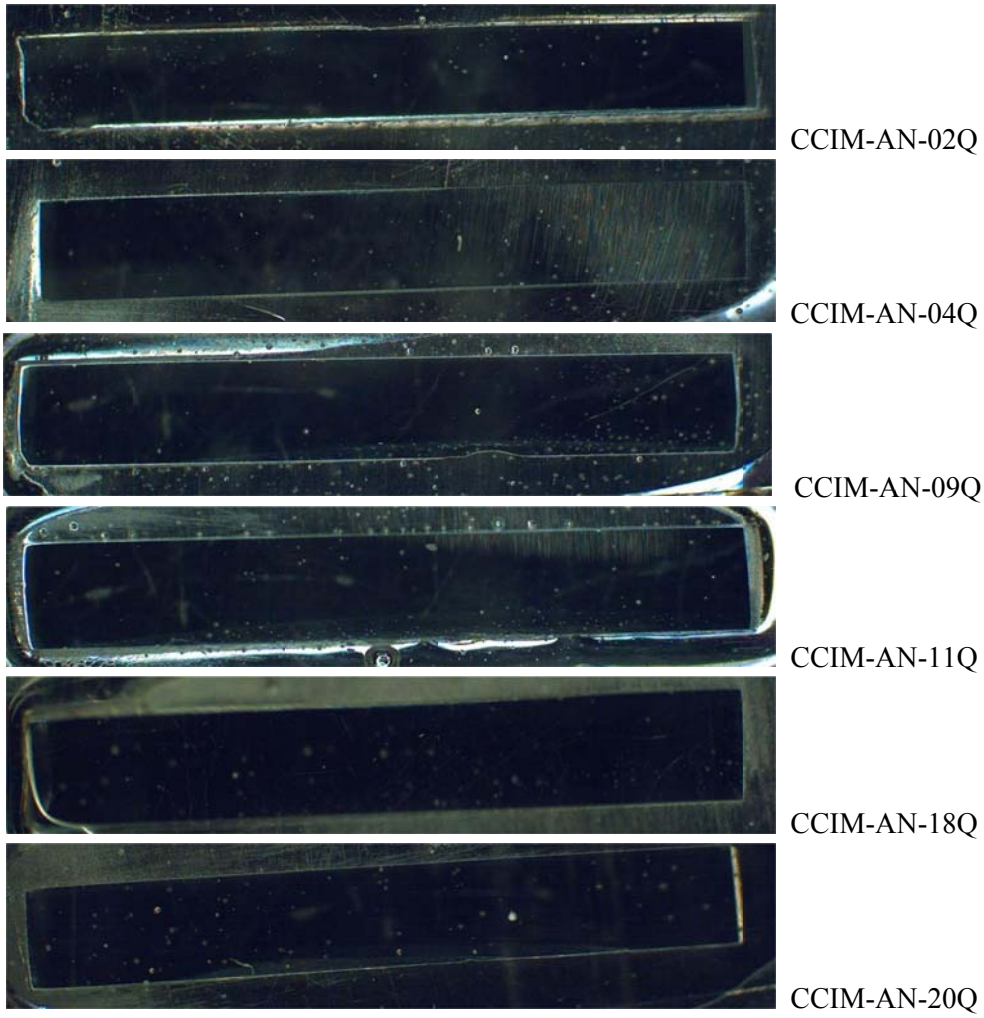

Figure 4.12. Thin Section of VHT Samples after 7-day Tests at 200°C for the First Set of Quenched CCIM-AN Glasses

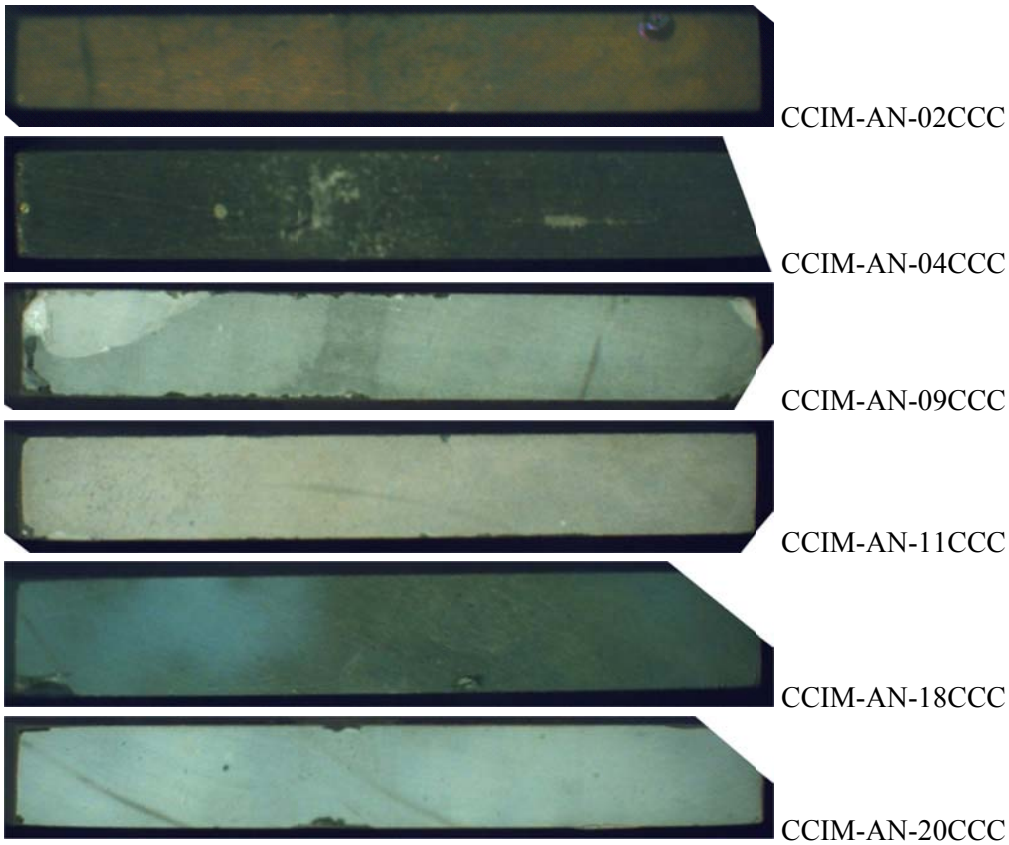

Figure 4.13. Thin Section of VHT Samples after 7-day Tests at 200°C for the First Set of CCC-Treated CCIM-AN Glasses

Table 4.17. VHT Alteration Rates for the First Set of CCIM-AN Glasses after 7-Day Test at 200°C

Glass	CCIM-AN-02	CCIM-AN-04	CCIM-AN-09	CCIM-AN-11	CCIM-AN-18	CCIM-AN-20
Quenched, $g/m^2/d$	0.7	0.4	2.9	2.3	0.6	2.4
CCC, $g/m^2/d$	1.0	<0.4	3.0	1.9	2.6	1.0
AN-02 and 04 glasses have 23 wt% Na_2O, AN-09, 11, 18 have 24 wt% Na_2O, and AN-20 has 25 wt% Na_2O.						

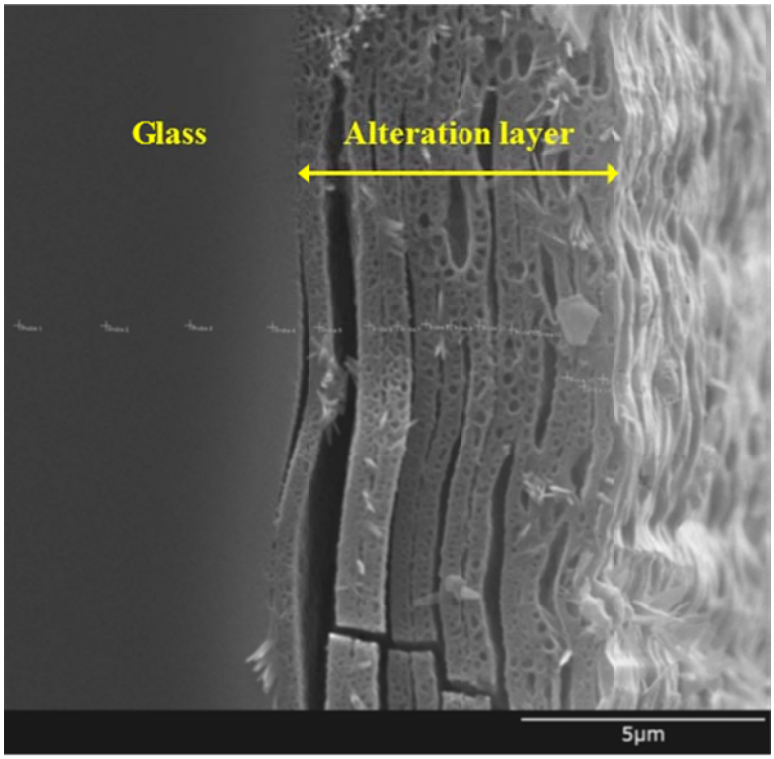

Figure 4.14. SEM Micrograph Showing the VHT Alteration Layer of CCIM-AN-09CCC Sample After 7-day VHT at 200°C (average alteration thickness of 8 µm)

Figure 4.15 shows the results of PCT normalized boron (Figure 4.15a) and sodium (Figure 4.15b) releases from both the first and second set of quenched and CCC-treated CCIM-AN glasses. All glasses but one (CCIM-AN-11 quenched) passed the PCT requirements for normalized boron and sodium releases. The information on the effect of glass composition on PCT for the first set of glasses (up to CCIM-AN-20) was used to formulate second set of four glasses at 25 wt% and 26 wt% Na_2O.

Table 4.18. PCT Normalized Releases (in g/L) from Quenched and CCC Treated CCIM-AN Glasses

Glass	CCIM-AN-02	CCIM-AN-04	CCIM-AN-09	CCIM-AN-11	CCIM-AN-18	CCIM-AN-20	CCIM-AN-23	CCIM-AN-27	CCIM-AN-28	CCIM-AN-31
PCT-B, Q	2.124	0.915	1.787	4.176	0.804	1.046	0.855	1.538	0.947	0.691
PCT-Na, Q	1.467	1.048	1.413	2.865	1.073	1.043	1.575	1.854	1.913	1.596
PCT-Si, Q	0.379	0.366	0.460	0.479	0.378	0.405	0.445	0.530	0.501	0.425
PCT-B, CCC	1.342	0.744	1.138	3.017	0.680	0.698	0.498	0.389	0.360	< 0.01
PCT-Na, CCC	1.032	0.910	1.052	2.064	0.998	0.880	1.568	1.618	1.867	1.593
PCT-Si, CCC	0.336	0.329	0.412	0.418	0.363	0.358	0.488	0.500	0.547	0.456

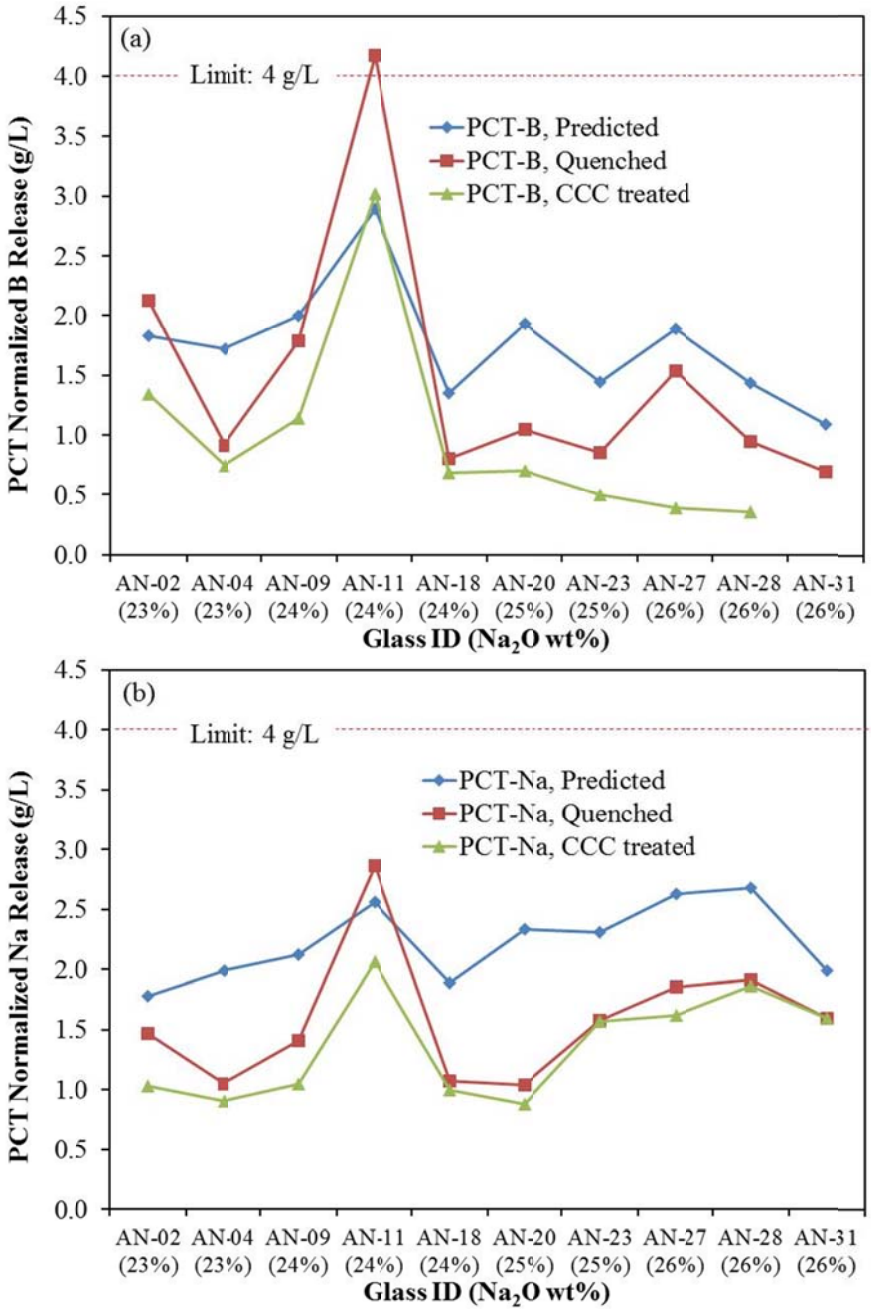

Figure 4.15. PCT Normalized Releases for CCIM-AN Glasses after 7-Day Test at 90°C

The PCT boron and sodium releases from the second set of glasses with 25 wt% and 26 wt% Na_2O were comparable to those from the first set of glasses with 23 wt% and 24 wt% Na_2O as shown in Figure 4.15. The measured PCT normalized releases showed reasonable agreement with the predicted values, and there were no undesirable effects on PCT by CCC treatment, i.e., the CCC-treated samples showed equal to or slightly lower PCT boron and sodium releases than quenched samples for all glasses.

The VHT results for the second set of glasses were similar to those for the first set of glasses in that negligible corrosion was observed after 7-day VHTs at 200 °C except for one sample, CCIM-AN-27CCC. Figure 4.16 shows the pictures of thin section VHT samples after 7-day tests at 200°C for the second set

of CCC treated glasses prepared for the optical microscopy and SEM examination. The negligible corrosion in seven out of eight 7-day VHT samples from the second set of quenched and CCC glasses by optical microscopy were confirmed by SEM examination. Further evaluation of VHT samples to determine the exact VHT alteration rate (similar to Table 4.17 for the first set of glasses) was not performed for the second set of CCIM-AN glasses.

As shown in Figure 4.16, CCIM-AN-27CCC had severe and irregular corrosion. Additional cross-section samples were prepared and Figure 4.17 displays these samples and confirms the severe and irregular corrosion. The cause of this dramatic difference in VHT corrosion of the CCIM-AN-27CCC compared to all other CCIM-AN VHT samples is not clear. The comparison between target and analyzed composition for the second set of glasses given in Table 4.16 does not show any potential indication for this irregular behavior, i.e., there was no unusual feature on the analytical result of the CCIM-AN-27 glass. Investigation to understand the erratic VHT behavior in CCIM-AN-27CCC sample, such as a potential for amorphous phase separation that cannot not be detected by XRD, OM, and SEM observations, was not performed in this study.

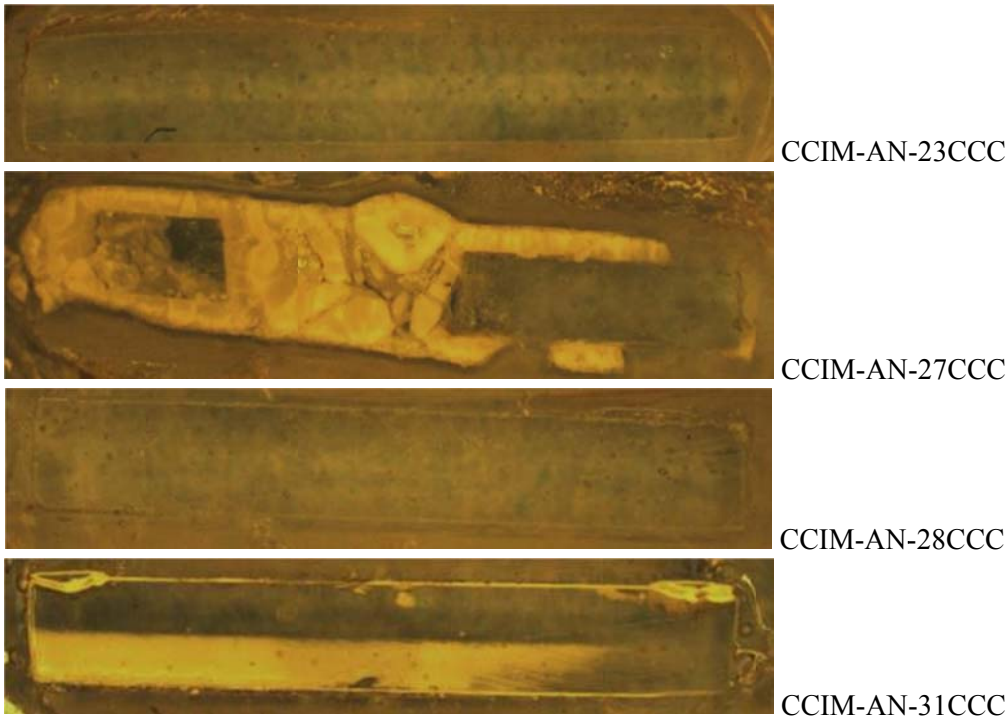

Figure 4.16. Thin Section of VHT Samples after 7-day Tests at 200 °C for the Second Set of CCC-Treated CCIM-AN Glasses

Figure 4.17. Cross-Sections of VHT Samples After 7-day Test at 200 °C for the CCIM-AN-27CCC

Based on PCT results from the first set of glasses, two glasses, CCIM-AN-09 and 18, were selected for further testing for viscosity and electrical conductivity. The CCIM-AN-20 glass with 25 wt% Na_2O passed all requirements, but its analyzed composition significantly deviated from the target composition (see Table 4.15) and was not selected for further testing. Additional tests to identify the source of composition discrepancy were not performed.

Table 4.19 summarizes the viscosity and electrical conductivity of two selected glasses. Figure 4.18 displays the results of viscosity (Figure 4.18a) and electrical conductivity (Figure 4.18b) as a function of temperature for two selected glasses compared with the predicted values. Both glasses had almost the same predicted viscosity (average predicted value is included in Figure 4.18a). The measured viscosities agree reasonably well with the predicted value for both glasses within the temperatures tested. The measured viscosity was ~4 Pa·s at 1250 °C; i.e., the recommended melting temperature was 1250 °C for both glasses.

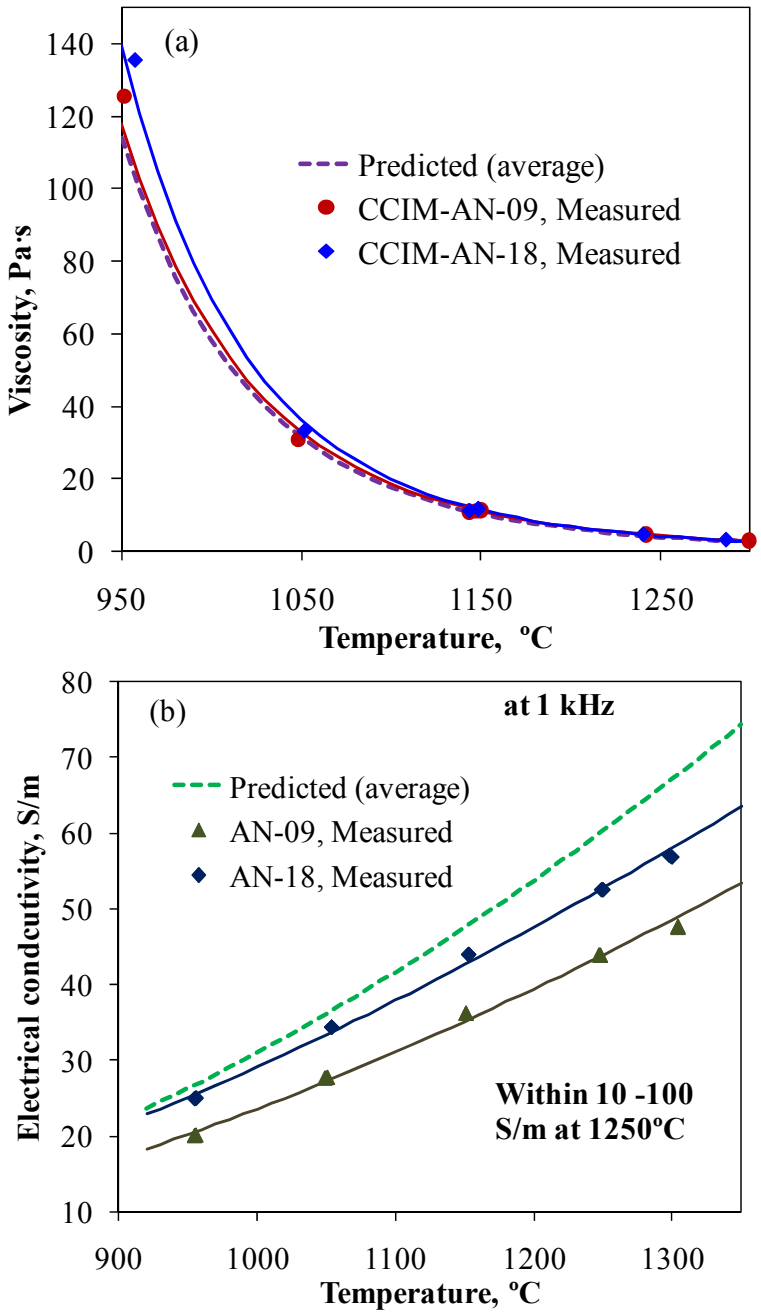

Figure 4.18. Viscosity and Electrical Conductivity of Selected Two CCIM-AN Glasses with 24 wt% Na_2O

Table 4.19. Viscosity and Electrical Conductivity of Selected CCIM-AN Glasses

CCIM-AN-09		CCIM-AN-18	
Viscosity (η) at a given temperature			
T, C	**η, Pa·s**	**T, C**	**η, Pa·s**
1147	11.09	1148	11.63
1048	30.82	1052	33.25
952	125.64	957	135.73
1150	11.29	1148	11.77
1242	4.65	1240	4.71
1299	2.94	1286	3.19
1143	10.92	1143	11.18
Electrical conductivity (ε) at a given temperature (1 kHz)			
T, C	**ε, S/m**	**T, C**	**ε, S/m**
955	20.07	956	25.03
1050	27.69	1054	34.39
1151	36.20	1153	43.95
1248	43.89	1250	52.47
1304	47.62	1299	56.88

Both glasses also had very similar predicted electrical conductivities (average predicted value is included in Figure 4.18b). Figure 4.18b shows that measured electrical conductivities were lower than the predicted value for both glasses with a significant measured difference between these two glasses. However, the measured electrical conductivities for both glasses were well within the desired range of 10 S/m to 100 S/m (Marra et al. 2008) at a recommended melting temperature of 1250°C.

Since there was no preference between these two glasses based on viscosity or electrical conductivity, the CCIM-AN-18 glass that had slightly better performance for PCT than CCIM-AN-09 was selected for the CCIM demonstration test. The melter feed recipe was prepared for the demonstration CCIM tests but they were not performed before the closure of the project.

The results of PCT and VHT on the second set of CCIM-AN glasses discussed above suggest that it is likely possible to formulate the acceptable glasses containing even higher than 26 wt% Na_2O. Testing glasses with 27 wt% Na_2O or higher would have been the next step of this study if the project had continued.

4.3 Cold Crucible Induction Melter Glass Formulation for Selected Waste Clusters

One of the objectives of glass formulation testing for the CCIM is to estimate the potential benefit of CCIM compared to the WTP baseline formulation. As mentioned in Section 2.1, AZ-101 HLW was selected for initial demonstration testing, based on potential for significant increase of waste loading by CCIM. The results presented in Section 4.1 clearly suggest that significant increase of waste loading is expected from CCIM for AZ-101 compared to the WTP baseline formulation for the JHM. To estimate the potential benefit for the entire Hanford mission, expected increase of waste loading needs to be estimated. Since it is not practical to estimate the waste loading for each waste batch, waste loading estimation was performed based on cluster compositions discussed in Section 2.2.

Out of six groups of wastes discussed in Section 2.2.3, the high-iron waste clusters have similar composition as AZ-101, so the AZ-101 formulation results can be applied to estimate the expected increase of waste loading for high-iron clusters. The high-aluminum wastes, though the most dominant wastes at Hanford site, were not selected in the initial stages because the nepheline precipitation after CCC has a strong effect on waste loading for high-aluminum wastes, which suggest that the CCIM may not have significant benefit. The next waste groups following AZ-101 most likely to be limited by spinel or similar crystal formation, and therefore are likely to be benefitted by CCIM, were chosen: spinel-limited and Cr_2O_3-SO_3 limited wastes. Among Cr_2O_3-SO_3 limited wastes, the initial focus was for high Cr_2O_3 waste cluster that has a potential to be limited by spinel crystallization rather than salt formation. The P_2O_5-CaO limited and salt-limited high Cr_2O_3-SO_3 wastes require laboratory experimental setup designed for evaluation of salt phase formation during cold cap melting. The initial results of glass formulation for spinel-limited and high Cr_2O_3 wastes obtained before the project discontinuation are summarized in the following subsections.

The compositions of waste clusters in terms of 41 oxide components given in Table A.2 (a simplified version sorted by waste group is presented in Table 2.7) were modified as follows for use in glass formulation and testing in this section and in Section 5.1. The two radioactive components (ThO_2 and UO_3) and minor components that are present in low concentrations (<0.4 wt% in all 20 clusters) and are not important for glass formulation were deleted. For noble metal oxides, PdO and Rh_2O_3 were replaced by the same mass fraction of RuO_2. For the same reason discussed in Section 2.1, the concentration of Cs_2O was fixed at 0.5 wt% for all clusters. The resulting normalized composition of 20 clusters in terms of 23 oxide components is given in Table 4.20.

Table 4.20. Composition of Waste Clusters in Terms of 23 Oxide Components

Cluster #	**5**	**7**	**8**	**16**	**1**	**10**	**18**	**3**	**4**	**19**	**20**
Group	**High-Al_2O_3**				**High-Fe_2O_3**			**Spinel limited**			
Al_2O_3	0.49789	0.47450	0.45532	0.59632	0.14764	0.21142	0.22312	0.16139	0.40988	0.30812	0.25944
B_2O_3	0.00250	0.00146	0.00695	0.00219	0.00259	0.00348	0.00297	0.00979	0.00144	0.00121	0.00409
Bi_2O_3	0.01967	0.05866	0.02020	0.01507	0.00706	0.01906	0.00373	0.02909	0.01073	0.00925	0.05524
CaO	0.01650	0.02579	0.02696	0.00900	0.02608	0.02698	0.02458	0.04556	0.02882	0.04341	0.04390
CdO	0.00018	0.00005	0.00025	0.00004	0.00091	0.00086	0.03580	0.00556	0.00569	0.00248	0.00030
Cr_2O_3	0.02410	0.01955	0.02180	0.02110	0.00864	0.00746	0.00685	0.01457	0.01439	0.01277	0.02051
Cs_2O	0.00500	0.00500	0.00500	0.00500	0.00500	0.00500	0.00500	0.00500	0.00500	0.00500	0.00500
F	0.01507	0.00562	0.01184	0.00268	0.00160	0.00501	0.00131	0.00190	0.00137	0.00179	0.02507
Fe_2O_3	0.06164	0.11502	0.11712	0.05709	0.35484	0.33449	0.38683	0.22156	0.16195	0.18398	0.15896
K_2O	0.00620	0.00479	0.00398	0.00226	0.00841	0.00723	0.01066	0.01220	0.00594	0.00520	0.00471
La_2O_3	0.00224	0.00105	0.00073	0.00099	0.00196	0.00279	0.00935	0.00792	0.00295	0.00197	0.00355
MgO	0.00194	0.00109	0.00367	0.00201	0.00366	0.00892	0.00287	0.00480	0.00147	0.00253	0.00622
MnO	0.01257	0.01001	0.01991	0.01440	0.05076	0.02426	0.01370	0.03403	0.01069	0.01426	0.01498
Na_2O	0.15696	0.13542	0.12938	0.16917	0.21797	0.14952	0.10610	0.14910	0.13336	0.21849	0.16704
Nd_2O_3	0.00037	0.00030	0.00107	0.00078	0.00335	0.00228	0.00712	0.00127	0.00211	0.00209	0.00067
NiO	0.01365	0.00730	0.00697	0.00373	0.01768	0.02283	0.03035	0.04920	0.02710	0.02084	0.01712
P_2O_5	0.04791	0.03781	0.02356	0.01453	0.01838	0.01854	0.01074	0.05033	0.01277	0.01410	0.03651
PbO	0.00262	0.00444	0.00873	0.00271	0.01388	0.01764	0.00753	0.00741	0.00635	0.00752	0.00910

Cluster #	5	7	8	16	1	10	18	3	4	19	20
Group	High-Al_2O_3				High-Fe_2O_3			Spinel limited			
RuO_2	0.00003	0.00000	0.00000	0.00000	0.00170	0.00193	0.00026	0.00031	0.00105	0.00138	0.00000
SiO_2	0.03629	0.07915	0.12087	0.07212	0.06749	0.07482	0.03509	0.04851	0.11486	0.08729	0.14241
SO_3	0.01291	0.00912	0.00941	0.00520	0.00469	0.00490	0.00204	0.00792	0.00296	0.00284	0.01084
SrO	0.00778	0.00188	0.00397	0.00172	0.00080	0.00133	0.00076	0.00152	0.00244	0.02140	0.01130
ZrO_2	0.05597	0.00198	0.00232	0.00189	0.03491	0.04924	0.07322	0.13105	0.03667	0.03212	0.00305
SUM	1.00000	1.00000	1.00000	1.00000	1.00000	1.00000	1.00000	1.00000	1.00000	1.00000	1.00000
Oxide mass (MT)	719.0	1,839.6	1,183.1	1,453.8	405.2	734.0	123.9	266.3	220.9	249.2	1,350.5

Table 4.20. (Continued)

Cluster #	12	14	6	11	2	13	15	17	9
Group	Cr_2O_3-SO_3 limited				P_2O_5-CaO limited				High-Na
Al_2O_3	0.17779	0.33611	0.29919	0.29532	0.21406	0.24823	0.13806	0.18983	0.09786
B_2O_3	0.00232	0.00328	0.00459	0.00224	0.00223	0.00259	0.00210	0.00147	0.00562
Bi_2O_3	0.03701	0.01838	0.04084	0.05967	0.07589	0.02704	0.06107	0.01267	0.01372
CaO	0.03268	0.02253	0.02146	0.02588	0.05881	0.02723	0.05667	0.09194	0.02703
CdO	0.00026	0.00083	0.00062	0.00033	0.00050	0.00050	0.00018	0.00372	0.00043
Cr_2O_3	0.08364	0.07716	0.03161	0.02311	0.01448	0.03181	0.00404	0.01508	0.02871
Cs_2O	0.00500	0.00500	0.00500	0.00500	0.00500	0.00500	0.00500	0.00500	0.00500
F	0.05431	0.00458	0.00593	0.06331	0.02958	0.02507	0.01303	0.00263	0.00734
Fe_2O_3	0.13276	0.08857	0.15918	0.09960	0.11931	0.11112	0.24999	0.14292	0.07010
K_2O	0.01138	0.00757	0.00805	0.00581	0.00513	0.00507	0.02261	0.01025	0.02653
La_2O_3	0.00522	0.00079	0.01041	0.00036	0.00046	0.00202	0.00035	0.00224	0.00019
MgO	0.00222	0.00123	0.00659	0.00149	0.00172	0.00260	0.00207	0.00116	0.00411
MnO	0.01333	0.02118	0.03259	0.00552	0.00605	0.00963	0.02565	0.01672	0.00614
Na_2O	0.15475	0.20147	0.18036	0.12861	0.25938	0.24975	0.13604	0.38352	0.56687
Nd_2O_3	0.00022	0.00111	0.00125	0.00030	0.00079	0.00051	0.00040	0.00342	0.00083
NiO	0.03403	0.00403	0.03301	0.00810	0.00815	0.01693	0.03257	0.00593	0.00510
P_2O_5	0.12081	0.11627	0.04671	0.04609	0.07061	0.12780	0.05931	0.03266	0.02554
PbO	0.00429	0.00437	0.00797	0.00291	0.00657	0.00453	0.01299	0.00323	0.00612
RuO_2	0.00003	0.00021	0.00055	0.00001	0.00013	0.00024	0.00039	0.00088	0.00001
SiO_2	0.06362	0.04502	0.05449	0.19198	0.09788	0.06740	0.14883	0.02488	0.08925
SO_3	0.02380	0.02069	0.01512	0.02232	0.00948	0.01202	0.00163	0.00464	0.00367
SrO	0.02641	0.00543	0.00412	0.00552	0.01024	0.01619	0.00165	0.03083	0.00432
ZrO_2	0.01411	0.01420	0.03038	0.00651	0.00354	0.00671	0.02539	0.01438	0.00549
SUM	1.00000	1.00000	1.00000	1.00000	1.00000	1.00000	1.00000	1.00000	1.00000
Oxide mass (MT)	275.2	173.3	364.1	533.0	338.9	209.4	327.2	164.7	143.8

4.3.1 Cold Crucible Induction Melter Glass Formulation for Spinel-Limited Waste Clusters

There were four waste clusters (Clusters 3, 4, 19, and 20) grouped as spinel-limited as shown in Table 2.7. The primary property constraint to watch for in these wastes is the $T_{1\%}$, however, some clusters (Clusters 19 and 20) also contain relatively high concentration of Al_2O_3 and therefore the nepheline precipitation may become a limiting constraint.

Table 4.21 summarizes the composition and predicted properties of the glasses formulated for spinel-limited clusters. The first step of glass development was to prepare small batches of glass and examine melting characteristics visually to sort out the glasses that form severe crystallization during melting, which will prevent preparing reasonable glasses for property characterization. Initial glass calculations showed that there is similarity between Clusters 4 and 19 in terms of maximum achievable waste loading. Therefore, it was decided that the glass formulations to determine maximum waste loading that make reasonable glass for property measurements will be performed for three clusters (Clusters 3, 4, and 20) and that of Cluster 19 can be estimated from the glass formulation results for Cluster 4.

At high waste loadings the additives are limited to B_2O_3, Li_2O, and Na_2O with the SiO_2 as a balance. The starting composition for each cluster was formulated at:

- Al_2O_3+Fe_2O_3+ZrO_2 content estimated to be close to maximum based on formulation experience with AZ-101 HLW in Section 4.1
- fixed target concentrations of 11 wt% B_2O_3 and 3 wt% Li_2O in glass (the same as used in AZ-101 glasses selected for melter demonstration tests)
- predicted viscosity of 4 Pa·s at a target melting temperature of 1200°C.

For Cluster 3, the first glass (CCIM-SLC3-3) tested had 27 wt% of Al_2O_3+Fe_2O_3+ZrO_2 (52.5 wt% WL) with 11 wt% B_2O_3. The maximum Li_2O that can be used was 2.6 wt% to keep the melting temperature at 1200 °C. This melt made a reasonable glass that can be used for property testing although it appeared that the waste loading limit was reached based on relatively high crystallinity. The next glass (CCIM-SLC3-4) was modified without increasing waste loading to have lower B_2O_3 at 8 wt% and higher Li_2O at 3 wt% than CCIM-SLC3-3 glass. Then, the concentration of Na_2O was adjusted to keep the melting temperature at 1200°C. This melt resulted in much higher crystallinity than CCIM-SLC3-3, to the extent not adequate for property characterization, and therefore, the CCIM-SLC3-3 composition was selected as a glass for further characterization.

For Cluster 4, the first glass tested (CCIM-SLC4-4) had 33 wt% of Al_2O_3+Fe_2O_3+ZrO_2 (54.2 wt% waste loading) with 11 wt% B_2O_3 and 3 wt% Li_2O. The concentration of Na_2O was adjusted to keep the melting temperature at 1200°C. This melt had only small fraction of crystals. The next three glasses tested (CCIM-SLC4-7, 8, and 9) had 35 wt% of Al_2O_3+Fe_2O_3+ZrO_2 (57.5 wt% WL) with varying concentrations of B_2O_3 and Li_2O in glass:

- CCIM-SLC4-7 had 11 wt% B_2O_3 and 3 wt% Li_2O
- CCIM-SLC4-8 had 14 wt% B_2O_3 and 3 wt% Li_2O
- CCIM-SLC4-9 had 14 wt% B_2O_3 and 4.5 wt% Li_2O, while Na_2O addition was adjusted to keep the 1200°C melting temperature.

Table 4.21. Glasses Formulated for Spinel-Limited Waste Clusters and Their Predicted Properties

Glass ID	Cluster 3		Cluster 4					Limits[a]
	CCIM-SLC3-3	CCIM-SLC3-4	CCIM-SLC4-4	CCIM-SLC4-7	CCIM-SLC4-8	CCIM-SLC4-9	CCIM-SLC4-10	
	Selected	Bad	Good	Selected	Selected	Bad	Bad	
Al_2O_3	0.08478	0.08478	0.22228	0.23575	0.23575	0.23575	0.24923	-
B_2O_3	0.11000	0.08000	0.11000	0.11000	0.14000	0.14000	0.11000	-
Bi_2O_3	0.01528	0.01528	0.00582	0.00617	0.00617	0.00617	0.00652	-
CaO	0.02393	0.02393	0.01563	0.01658	0.01658	0.01658	0.01752	-
CdO	0.00292	0.00292	0.00309	0.00327	0.00327	0.00327	0.00346	-
Cr_2O_3	0.00766	0.00766	0.00780	0.00827	0.00827	0.00827	0.00875	-
Cs_2O	0.00263	0.00263	0.00271	0.00288	0.00288	0.00288	0.00304	-
F	0.00100	0.00100	0.00075	0.00079	0.00079	0.00079	0.00084	-
Fe_2O_3	0.11638	0.11638	0.08783	0.09315	0.09315	0.09315	0.09848	-
K_2O	0.00641	0.00641	0.00322	0.00342	0.00342	0.00342	0.00361	-
La_2O_3	0.00416	0.00416	0.00160	0.00169	0.00169	0.00169	0.00179	-
Li_2O	0.02644	0.03000	0.03000	0.03000	0.03000	0.04500	0.03000	-
MgO	0.00252	0.00252	0.00080	0.00084	0.00084	0.00084	0.00089	-
MnO	0.01787	0.01787	0.00580	0.00615	0.00615	0.00615	0.00650	-
Na_2O	0.07832	0.09464	0.15705	0.15355	0.12646	0.09022	0.14996	-
Nd_2O_3	0.00067	0.00067	0.00115	0.00121	0.00121	0.00121	0.00128	-
NiO	0.02584	0.02584	0.01470	0.01559	0.01559	0.01559	0.01648	-
P_2O_5	0.02644	0.02644	0.00693	0.00734	0.00734	0.00734	0.00776	-
PbO	0.00389	0.00389	0.00344	0.00365	0.00365	0.00365	0.00386	-
RuO_2	0.00016	0.00016	0.00057	0.00061	0.00061	0.00061	0.00064	-
SiO_2	0.36889	0.37901	0.29604	0.27487	0.27196	0.29320	0.25379	-
SO_3	0.00416	0.00416	0.00161	0.00170	0.00170	0.00170	0.00180	-
SrO	0.00080	0.00080	0.00132	0.00140	0.00140	0.00140	0.00148	-
ZrO_2	0.06884	0.06884	0.01989	0.02109	0.02109	0.02109	0.02230	-
Total	1	1	1	1	1	1	1	-
Waste loading	0.525	0.525	0.542	0.575	0.575	0.575	0.608	-
Al_2O_3+Fe_2O_3+ZrO_2	0.270	0.270	0.330	0.350	0.350	0.350	0.370	-
T_m at 4 Pa·s, °C	1200	1200	1200	1200	1200	1200	1200	-
EC at T_m, S/m	20.5	25.7	44.2	43.1	33.3	31.9	42.0	10-100
Spinel T_L, °C	1450	1450	1377	1436	1449	1477	1496	$<T_m$–100[b]
Spinel $T_{1\%}$, °C	1343	1339	1260	1331	1344	1368	1403	$<T_m$–200[c]
PCT-B, g/L	0.109	0.101	0.046	0.017	0.016	0.013	0.005	<16.7
PCT-Li, g/L	0.155	0.166	0.059	0.025	0.027	0.022	0.009	<9.57
PCT-Na, g/L	0.115	0.138	0.049	0.020	0.018	0.013	0.007	<13.35
TCLP Cd, mg/L	0.085	0.080	0.190	0.206	0.196	0.148	0.222	<0.48
N_{Si}	0.693	0.679	0.438	0.414	0.429	0.474	0.389	≥0.62
OB	0.583	0.597	0.605	0.609	0.592	0.583	0.613	≤0.575

[a] Used as guidelines for formulating the glasses.
[b] Based on a traditional constraint used in Perez et al. (2001).
[c] Based on a constraint of $T_{1\%}$ < 950°C for glasses with T_m = 1150°C (Vienna et al. 2009).
Shaded cells indicate that the predicted or calculated value is not within the limits.

Table 4.21. (Continued)

Glass ID	Cluster 20					Limits[a]
	CCIM-SLC20-2	CCIM-SLC20-4	CCIM-SLC20-6	CCIM-SLC20-7	CCIM-SLC20-8	
	Good	Good	Selected	Bad	Bad	
Al_2O_3	0.15390	0.16621	0.17852	0.17852	0.19083	-
B_2O_3	0.11000	0.11000	0.11000	0.08000	0.11000	-
Bi_2O_3	0.03277	0.03539	0.03801	0.03801	0.04063	-
CaO	0.02604	0.02812	0.03021	0.03021	0.03229	-
CdO	0.00018	0.00019	0.00021	0.00021	0.00022	-
Cr_2O_3	0.01217	0.01314	0.01411	0.01411	0.01509	-
Cs_2O	0.00297	0.00320	0.00344	0.00344	0.00368	-
F	0.01487	0.01606	0.01725	0.01725	0.01844	-
Fe_2O_3	0.09429	0.10184	0.10938	0.10938	0.11692	-
K_2O	0.00279	0.00301	0.00324	0.00324	0.00346	-
La_2O_3	0.00211	0.00228	0.00244	0.00244	0.00261	-
Li_2O	0.02414	0.01646	0.00896	0.01988	0.00162	-
MgO	0.00369	0.00398	0.00428	0.00428	0.00457	-
MnO	0.00889	0.00960	0.01031	0.01031	0.01102	-
Na_2O	0.09909	0.10702	0.11494	0.11494	0.12287	-
Nd_2O_3	0.00040	0.00043	0.00046	0.00046	0.00050	-
NiO	0.01015	0.01096	0.01178	0.01178	0.01259	-
P_2O_5	0.02166	0.02339	0.02512	0.02512	0.02686	-
PbO	0.00540	0.00583	0.00626	0.00626	0.00669	-
RuO_2	0.00000	0.00000	0.00000	0.00000	0.00000	-
SiO_2	0.35956	0.32674	0.29373	0.31281	0.26057	-
SO_3	0.00643	0.00695	0.00746	0.00746	0.00798	-
SrO	0.00670	0.00724	0.00777	0.00777	0.00831	-
ZrO_2	0.00181	0.00195	0.00210	0.00210	0.00224	-
Total	1	1	1	1	1	-
Waste loading	0.593	0.641	0.688	0.688	0.736	-
Al_2O_3+Fe_2O_3+ZrO_2	0.250	0.270	0.290	0.290	0.310	
T_m at 4 Pa·s, °C	1200	1200	1200	1200	1200	-
EC at T_m, S/m	23.9	22.8	22.0	26.7	21.6	10-100
Spinel T_L, °C	1417	1493	1570	1580	1649	$<T_m$–100[b]
Spinel $T_{l\%}$, °C	1191	1268	1346	1352	1424	$<T_m$–200[c]
PCT-B, g/L	0.230	0.202	0.164	0.139	0.120	<16.7
PCT-Li, g/L	0.321	0.289	0.243	0.235	0.188	<9.57
PCT-Na, g/L	0.223	0.205	0.176	0.186	0.139	<13.35
TCLP Cd, mg/L	0.008	0.010	0.012	0.010	0.015	<0.48
N_{Si}	0.587	0.545	0.500	0.516	0.454	≥0.62
OB	0.578	0.585	0.592	0.602	0.599	≤0.575

[a] Used as guidelines for formulating the glasses.
[b] Based on a traditional constraint used in Perez et al. (2001).
[c] Based on a constraint of $T_{l\%}$ < 950°C for glasses with T_m = 1150°C (Vienna et al. 2009).
Shaded cells indicate that the predicted or calculated value is not within the limits.

The two melts (CCIM-SLC4-7 and 8) had indication of small amount of crystals but in general made homogenous glass. However, the CCIM-SLC4-9 contained lots of crystals after the first melt. The second melt contained a little less, but still a large amount of crystals and it was difficult to pour the glass

apparently because of the high crystal content. With two good glasses successfully prepared at 35 wt% Al_2O_3+Fe_2O_3+ZrO_2 (57.5 wt% waste loading), the next test melt (CCIM-SLC4-10) was prepared at 37 wt% Al_2O_3+Fe_2O_3+ZrO_2 (60.8 wt% waste loading) with the similar composition as CCIM-SLC4-7, i.e., 11 wt% B_2O_3 and 3 wt% Li_2O with Na_2O adjusted to make the 1200 °C melting temperature. This melt had visually very high crystallinity with severe melt inhomogeneity and not adequate for property measurements. The two reasonable glasses (CCIM-SLC4-7 and 8) with different B_2O_3 concentration at 11 wt% and 14 wt%, were selected for further evaluation.

For Cluster 20, the first glass tested (CCIM-SLC20-2) had 25 wt% of Al_2O_3+Fe_2O_3+ZrO_2 (59.3 wt% waste loading) with 11 wt% B_2O_3. The maximum Li_2O that can be used to keep the melting temperature at 1200 °C was 2.4 wt%. Na_2O was not added for this glass. This melt had little crystals. The next glass was CCIM-SLC20-4 containing 27 wt% of Al_2O_3+Fe_2O_3+ZrO_2 (64.1 wt% waste loading), 11 wt% B_2O_3, and 1.65 wt% Li_2O had indication of small amount of crystals but made a typical homogenous glass. Then, two glasses (CCIM-SLC20-6 and 7) were formulated at 29 wt% of Al_2O_3+Fe_2O_3+ZrO_2 (68.8 wt% waste loading) with 11 wt% B_2O_3 and 0.9 wt% Li_2O and 8 wt% B_2O_3 and 1.99 wt% Li_2O, respectively. CCIM-SLC20-6 had relatively high crystals in the bulk of the glass but made into in general a homogeneous glass. However, the CCIM-SLC20-7 glass with lower B_2O_3 (and higher Li_2O) than CCIM-SLC20-6 had very high crystallinity with severe melt inhomogeneity not adequate for property measurements. The CCIM-SLC20-8 melt with higher waste loading at 31 wt% of Al_2O_3+Fe_2O_3+ZrO_2 (73.6 wt% waste loading) was also prepared but was full of crystals. The CCIM-SLC20-6 was selected for further characterization.

The maximum waste loadings estimated for spinel-limited clusters to make reasonable glass for property measurements are summarized in Table 4.22. Table 4.22 also provides the estimated maximum Al_2O_3+Fe_2O_3+ZrO_2 in glass and glass compositions selected for property testing. The estimated maximum waste loading for Cluster 19 was obtained by assuming that Cluster 19 has the same Al_2O_3+Fe_2O_3+ZrO_2 loading in glass as Cluster 4. Note that these estimated maximum waste loadings are not those that can be processed in the CCIM, which need to be determined based on measured crystal vol% at a fixed temperature or as a function of temperature.

Table 4.22. Summary of Results for the Initial Glasses Formulated for Spinel-Limited Clusters

Cluster	Estimated Maximum		Selected for property testing
	Waste loading	Al_2O_3+Fe_2O_3+ZrO_2 in glass	
3	52.5 wt%	27 wt%	CCIM-SLC3-3
4	57.5 wt%	35 wt%	CCIM-SLC4-7 and 8
19	66.8 wt%	35 wt%	Not applicable
20	68.8 wt%	29 wt%	CCIM-SLC20-6

4.3.2 Cold Crucible Induction Melter Glass Formulation for High-Chromium Waste Clusters

The waste loading for the Cr_2O_3-SO_3 limited clusters can be limited either by spinel crystallization or salt formation, depending on the concentration of SO_3 compared to Cr_2O_3 and other spinel components (typically Fe_2O_3, NiO, and MnO). For the development of glasses for the CCIM, the wastes that are limited by salt formation are not likely benefited significantly by high melter operation temperature of CCIM. Therefore, it is preferable to select waste with a low SO_3 to Cr_2O_3 ratio so that potential maximum benefit of CCIM can be evaluated. Among four Cr_2O_3-SO_3 limited clusters (Clusters 12, 14, 6, and 11), the two clusters (Clusters 12 and 14) are characterized by high Cr_2O_3 at 8.36 wt% and 7.72 wt% (see Table 4.20) with a slightly lower SO_3 to Cr_2O_3 ratio for Cluster 14. Therefore, Cluster 14 was selected for initial formulation studies for CCIM.

Table 4.23 summarizes the composition and predicted properties formulated and melted for one of the Cr_2O_3-SO_3 limited clusters, Cluster 14. The first set of four glasses was formulated at a fixed Cr_2O_3 concentration of 3 wt% (corresponding to 38.9 wt% waste loading) with varying concentrations of B_2O_3, K_2O, Li_2O, and Na_2O. The concentration of Na_2O was adjusted last to make the predicted viscosity at 1200 °C to 5 Pa·s after choosing the concentrations for B_2O_3, K_2O and Li_2O. The main focus of melting test with these high-chromium glasses was the presence of salt phase after melting.

Figure 4.19 shows the pictures of the crucible wall of the first set of four CCIM-HCC14 glasses after melting at 1200°C. The yellow salt layer was formed on three glasses with most significant amount observed by CCIM-HCC14-6 and much less by CCIM-HCC14-1 and CCIM-HCC14-4. The CCIM-HCC14-2 did not form any salt. The most noticeable difference in the composition of CCIM-HCC14-2 glass (with no salt) was that it had higher concentration of B_2O_3 at 14 wt% compared to 11 wt% in other glasses. The CCIM-HCC14-6 glass that had most salt formation had no Li_2O and consequently contained higher concentrations of K_2O and Na_2O to keep the viscosity the same as 4 Pa·s at 1200°C.

Based on the information from the first set of glasses, the first glass (CCIM-HCC14-8) of the second set was formulated at increased Cr_2O_3 loading of 3.5 wt% (corresponding to 45.4 wt% waste loading) with 14 wt% B_2O_3 and 3 wt% Li_2O. The B_2O_3 concentration was increased to 17 wt% for the next glass (CCIM-HCC14-10) while Na_2O was decreased to keep the viscosity the same. The third glass (CCIM-HCC14-12) of the second set was formulated to have 6 wt% K_2O at 14 wt% B_2O_3 and 3 wt% Li_2O without adding Na_2O (9.14 wt% Na_2O is from waste). The last glass (CCIM-HCC14-15) was formulated with the same B_2O_3, Li_2O and K_2O as the first glass (CCIM-HCC14-8), but the predicted temperature at 4 Pa·s was increased to 1250 °C by decreasing Na_2O concentration.

The melting of the second set containing 3.5 wt% Cr_2O_3 with varying additive concentrations did not form any salt layer in all four glasses. In summary, the glasses without salt formation at 3 wt% Cr_2O_3 and 3.5 wt% Cr_2O_3 were successfully formulated so that they can be used for further characterization to determine the maximum waste loading.

Table 4.23. Glasses Formulated for a High-Cr_2O_3 Waste Cluster and Their Predicted Properties

	First Set				Second Set				
Glass ID	**CCIM-HCC14-1**	**CCIM-HCC14-2**	**CCIM-HCC14-4**	**CCIM-HCC14-6**	**CCIM-HCC14-8**	**CCIM-HCC14-10**	**CCIM-HCC14-12**	**CCIM-HCC14-15**	**Limits[a]**
Al_2O_3	0.13068	0.13068	0.13068	0.13068	0.15246	0.15246	0.15246	0.15246	-
B_2O_3	0.11000	0.14000	0.11000	0.11000	0.14000	0.17000	0.14000	0.14000	-
Bi_2O_3	0.00715	0.00715	0.00715	0.00715	0.00834	0.00834	0.00834	0.00834	-
CaO	0.00876	0.00876	0.00876	0.00876	0.01022	0.01022	0.01022	0.01022	-
CdO	0.00032	0.00032	0.00032	0.00032	0.00037	0.00037	0.00037	0.00037	-
Cr_2O_3	0.03000	0.03000	0.03000	0.03000	0.03500	0.03500	0.03500	0.03500	-
Cs_2O	0.00194	0.00194	0.00194	0.00194	0.00227	0.00227	0.00227	0.00227	-
F	0.00178	0.00178	0.00178	0.00178	0.00208	0.00208	0.00208	0.00208	-
Fe_2O_3	0.03444	0.03444	0.03444	0.03444	0.04018	0.04018	0.04018	0.04018	-
K_2O	0.00294	0.00294	0.06000	0.06000	0.00343	0.00343	0.06000	0.00343	-
La_2O_3	0.00031	0.00031	0.00031	0.00031	0.00036	0.00036	0.00036	0.00036	-
Li_2O	0.03000	0.03000	0.03000	0.00000	0.03000	0.03000	0.03000	0.03000	-
MgO	0.00048	0.00048	0.00048	0.00048	0.00056	0.00056	0.00056	0.00056	-
MnO	0.00823	0.00823	0.00823	0.00823	0.00961	0.00961	0.00961	0.00961	-
Na_2O	0.16060	0.13565	0.12300	0.19450	0.12746	0.10629	0.09139	0.10912	-
Nd_2O_3	0.00043	0.00043	0.00043	0.00043	0.00050	0.00050	0.00050	0.00050	-
NiO	0.00157	0.00157	0.00157	0.00157	0.00183	0.00183	0.00183	0.00183	-
P_2O_5	0.04521	0.04521	0.04521	0.04521	0.05274	0.05274	0.05274	0.05274	-
PbO	0.00170	0.00170	0.00170	0.00170	0.00198	0.00198	0.00198	0.00198	-
RuO_2	0.00008	0.00008	0.00008	0.00008	0.00010	0.00010	0.00010	0.00010	-
SiO_2	0.40770	0.40265	0.38824	0.34674	0.36223	0.35339	0.34173	0.38056	-
SO_3	0.00805	0.00805	0.00805	0.00805	0.00939	0.00939	0.00939	0.00939	-
SrO	0.00211	0.00211	0.00211	0.00211	0.00246	0.00246	0.00246	0.00246	-
ZrO_2	0.00552	0.00552	0.00552	0.00552	0.00644	0.00644	0.00644	0.00644	-
Total	1	1	1	1	1	1	1	1	-
Waste loading	0.389	0.389	0.389	0.389	0.454	0.454	0.454	0.454	-
T_m at 4 Pa·s, °C	1200	1200	1200	1200	1200	1200	1200	1250	-
EC at T_m, S/m	49.1	38.9	36.3	52.1	37.3	30.9	28.0	35.1	10-100
Spinel T_L, °C	1320	1328	1295	1235	1479	1478	1454	1520	$<T_m$–100[b]
Spinel $T_{1\%}$, °C	982	992	978	931	1142	1147	1136	1163	$<T_m$–200[c]
PCT-B, g/L	1.083	1.101	1.194	1.917	0.924	1.009	1.041	0.653	<16.7
PCT-Li, g/L	1.359	1.571	1.455	1.965	1.409	1.806	1.417	1.034	<9.57
PCT-Na, g/L	1.027	0.942	1.120	2.084	0.783	0.918	0.873	0.552	<13.35
TCLP Cd, mg/L	0.028	0.028	0.028	0.048	0.037	0.039	0.037	0.027	<0.48
N_{Si}	0.583	0.602	0.605	0.516	0.564	0.577	0.584	0.593	≥0.62
OB	0.569	0.555	0.575	0.593	0.558	0.546	0.565	0.551	≤0.575

[a] Used as guidelines for formulating the glasses.
[b] Based on a traditional constraint used in Perez et al. (2001).
[c] Based on a constraint of $T_{1\%} < 950$ °C for glasses with $T_m = 1150$ °C (Vienna et al. 2009).
Shaded cells indicate that the predicted or calculated value is not within the limits.

CCIM-HCC14-1

CCIM-HCC14-2

CCIM-HCC14-4

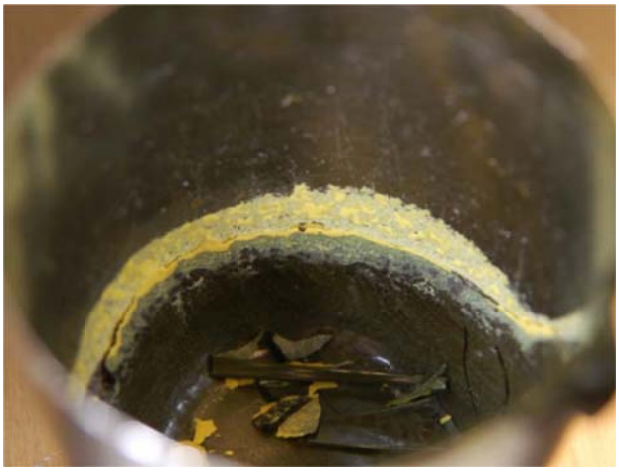

CCIM-HCC14-6

Figure 4.19. Salt Phase that Remained on Crucible Wall after Melting of Four CCIM-HCC14 Glasses

5.0 Advanced Silicate Glass Formulation

This section summarizes the results of formulation and characterization of glasses with the nominal processing temperature of 1150°C for current WTP baseline melter. The results from two subtasks of the EM-31 Advanced Silicate Glass Development (WP-5.1.2) task, WP-5.1.2.3 – Systematic Glass Data for Models and WP-5.1.2.4 – Optimization for Specific Wastes, are presented in this section.

5.1 Glass Formulation for Specific Wastes (WP-5.1.2.4)

One of the objectives of this subtask WP-5.1.2.4 – Optimization for Specific Wastes was to determine the maximum achievable waste loading for each cluster and then calculate the estimated reduction of glass volume by producing waste loading optimized glasses. Candidate glasses were formulated for three waste groups that cover the majority of Hanford HLW and represent the largest resulting glass mass: high-iron, spinel-limited, and high-aluminum waste cluster groups.

Glass formulations were performed based on the cluster compositions in terms of 23 oxide components given in Table 4.20. It is expected that at least two or more iterations of glass formulation and characterization will be required to find the maximum waste loading reasonably achievable. Only the first iteration was completed before the task closure.

5.1.1 Advanced Silicate Glass Formulation for High-Iron Waste Clusters

The high-iron waste clusters (Clusters 1, 10, and 18) have compositions similar to AZ-101 HLW used in glass formulations for CCIM discussed in Section 4.1. The waste loading for these waste clusters is primarily limited by the spinel crystallization, i.e., the requirement for $T_{1\%} < 950$°C.

Table 5.1 shows the target compositions and predicted properties for improved waste loading-high ion cluster IWL-HICx-y glasses. The cluster number is represented by x, and y is a serial number. For the first set, five glasses were formulated for Clusters 1 and 18. There is reasonable similarity between Clusters 10 and 18 so it is assumed that the maximum loading for Cluster 10 can be estimated from the glass formulation results for Cluster 18.

For glasses formulated for Cluster 1, the IWL-HIC1-1 glass was as formulated based on HTWOS revised constraints given in Table 2.6. As shown in Table 5.1, the waste loading is limited by $T_{1\%}$ and nepheline discriminator, N_{Si}. The IWL-HIC1-2 glass was also formulated to meet the revised HTWOS constraints but was forced to meet the nepheline constraint by meeting the OB requirement instead of N_{Si}. This resulted in slightly lower waste loading but significantly different concentrations for main additive components, B_2O_3 and alkali oxides. The IWL-HIC1-3 glass uses the same concentrations for B_2O_3 and Li_2O as in the glasses selected for CCIM demonstration tests (Table 4.8) at the same waste loading as in IWL-HIC1-1. The IWL-HIC1-3 glass had B_2O_3 concentration in between the IWL-HIC1-1 and IWL-HIC1-2 glasses, and had highest Li_2O and lowest Na_2O concentrations among three IWL-HIC1 glasses.

For glasses formulated for Cluster 18, the IWL-HIC18-1 glass was as formulated based on HTWOS revised constraints given in Table 2.6. As shown in Table 5.1, this waste loading is limited by $T_{1\%}$ and

OB. This glass had similar compositional features as the IWL-HIC1-2 glass that was limited by $T_{1\%}$ and OB and therefore high B_2O_3 concentration. The IWL-HIC18-3 glass uses the same concentrations for B_2O_3 and Li_2O in glass as those selected for CCIM demonstration tests (Table 4.8) and so as in the IWL-HIC1-3 glass.

Table 5.1. Glasses Melting at 1150 °C Formulated for High-Iron Clusters and Their Predicted and Measured Properties

	Cluster 1			Cluster 18		
Comp.	**IWL-HIC1-1**	**IWL-HIC1-2**	**IWL-HIC1-3**	**IWL-HIC18-1**	**IWL-HIC18-3**	**Limits[(a)]**
Al_2O_3	0.06229	0.06126	0.06229	0.07970	0.07970	-
B_2O_3	0.04000	0.14477	0.11000	0.16537	0.11000	-
Bi_2O_3	0.00298	0.00293	0.00298	0.00133	0.00133	-
CaO	0.01100	0.01082	0.01100	0.00878	0.00878	-
CdO	0.00038	0.00038	0.00038	0.01279	0.01279	-
Cr_2O_3	0.00365	0.00359	0.00365	0.00245	0.00245	-
Cs_2O	0.00211	0.00207	0.00211	0.00179	0.00179	-
F	0.00068	0.00066	0.00068	0.00047	0.00047	-
Fe_2O_3	0.14971	0.14723	0.14971	0.13817	0.13817	-
K_2O	0.00355	0.00349	0.00355	0.00381	0.00381	-
La_2O_3	0.00083	0.00081	0.00083	0.00334	0.00334	-
Li_2O	0.02054	0.00000	0.03000	0.00000	0.03000	-
MgO	0.00155	0.00152	0.00155	0.00102	0.00102	-
MnO	0.02142	0.02106	0.02142	0.00489	0.00489	-
Na_2O	0.20423	0.15594	0.11443	0.15973	0.13505	-
Nd_2O_3	0.00141	0.00139	0.00141	0.00254	0.00254	-
NiO	0.00746	0.00734	0.00746	0.01084	0.01084	-
P_2O_5	0.00775	0.00763	0.00775	0.00384	0.00384	-
PbO	0.00586	0.00576	0.00586	0.00269	0.00269	-
RuO_2	0.00072	0.00070	0.00072	0.00009	0.00009	-
SiO_2	0.43485	0.40388	0.44518	0.36920	0.41925	-
SO_3	0.00198	0.00195	0.00198	0.00073	0.00073	-
SrO	0.00034	0.00033	0.00034	0.00027	0.00027	-
ZrO_2	0.01473	0.01448	0.01473	0.02615	0.02615	-
Total	1.00000	1.00000	1.00000	1.00000	1.00000	-
Waste Loading	0.422	0.415	0.422	0.357	0.357	-
Al_2O_3+Fe_2O_3+ZrO_2	0.227	0.223	0.227	0.244	0.244	-
η_{1150}, Pa·s	4	4	4	4	4	2 - 8
ε_{1150}, S/m	61.4	26.6	27.3	27.8	33.1	10 - 100
Spinel $T_{1\%}$, °C	950	950	998	950	978	950
PCT-B, g/L	0.831	1.018	0.626	1.305	0.801	<16.7
PCT-Li, g/L	0.777	1.140	0.668	1.389	0.636	<9.57
PCT-Na, g/L	1.926	0.942	0.556	1.075	0.600	<13.35
TCLP Cd, mg/L	0.013	0.014	0.009	0.637	0.381	<0.48
N_{Si}	0.620	0.650	0.716	0.607	0.661	≥0.62
OB	0.625	0.575	0.577	0.575	0.586	≤0.575
Measured spinel vol% after 24 h heat treatment at 950°C						
Spinel vol%	0.6	1.1	1.2	1.6	1.4	1

[(a)] Used as guidelines for formulating the glasses.
Shaded cells indicate that the predicted or calculated value is not within the limits.

None of the five IWL-HIC glasses in Table 5.1 failed the nepheline constraint. For the first iteration of glass formulation and testing for the high-iron waste clusters, the primary focus was on the spinel crystallization and the glasses were initially tested only for crystal fraction after a 24-hour heat treatment at 950°C.

The results of XRD measurement for the spinel vol% after the 24-hour heat treatment at 950°C were included in Table 5.1. The IWL-HIC1-1 was the only glass that passed the $T_{1\%} < 950$ °C. This glass had low concentration of B_2O_3 at 4 wt% while the other four glasses had 11 wt% or higher. The predicted $T_{1\%}$ did not show any correlation with the measured spinel vol%, suggesting that the models do not work well for these glasses. No successful glass resulted from Cluster 18. Additional formulation and testing are needed for both high-iron clusters to determine the estimated maximum waste loadings.

5.1.2 Advanced Silicate Glass Formulation for Spinel-Limited Waste Clusters

The spinel-limited waste clusters (Clusters 3, 4, 19, and 20) have Fe_2O_3 lower than the high-iron clusters, but relatively high overall concentrations of spinel-forming components (Fe_2O_3, Cr_2O_3, NiO, and MnO) and the waste loading for these waste clusters is primarily limited by the requirement of $T_{1\%} < 950$ °C.

Table 5.2 shows the target compositions and predicted properties for improved waste loading-spinel-limited cluster (IWL-SLCx-y) glasses where x is the cluster number, and y is a serial number". For the first set, 10 glasses were formulated for three clusters, Clusters 3, 4, and 20. There is reasonable similarity between Clusters 19 and 4 so it is assumed that the maximum loading for Cluster 19 can be estimated from glass formulation results for Cluster 4.

The glasses were formulated following similar pattern used for high-iron cluster glasses. The first glasses for each cluster (IWL-SLC3-1, IWL-SLC4-1, and IWL-SLC20-1) were formulated based on HTWOS revised constraints given in Table 2.6. As shown in Table 5.2, the waste loading is limited by $T_{1\%}$ and nepheline constraint. The glass for Cluster 3 (IWL-SLC3-1) met the nepheline constraint based on N_{Si} and the (IWL-SLC4-1 and IWL-SLC 20-1) met the OB requirement. The lower loading of these major waste components in IWL-SLC3-1 glass compared to other two glasses is attributed to high overall concentrations for spinel components in Cluster 3.

The second glasses for each cluster (IWL-SLC3-2, IWL-SLC 4-2, and IWL-SLC 20-2) were also formulated to meet the HTWOS revised constraints, but were forced to meet the other nepheline constraint, i.e., IWL-SLC3-1 glass was forced to meet the OB requirement and the IWL-SLC4-1 and IWL-SLC20-1 glasses were forced to meet the N_{Si} requirement. This change resulted in slightly lower waste loading for all three glasses with significantly different concentrations for main additive components, B_2O_3 and alkali oxides. The third glasses for each cluster (IWL-SLC3-3, IWL-SLC4-3, and IWL-SLC20-3) use the same concentrations for B_2O_3 and Li_2O as in the glasses selected for CCIM demonstration tests (Table 4.8) at the same waste loading as in the first glasses for each cluster (IWL-SLC3-1, IWL-SLC4-1, and IWL-SLC20-1). The concentration of Na_2O was adjusted to keep the viscosity at 1150°C at 4 Pa·s. One additional (fourth) glass (IWL-SLC4-4) was formulated for Cluster 4 only. This glass had the same waste loading and Li_2O concentration in glass as the IWL- SLC4-4 glass, but had increased B_2O_3 concentration of 14 wt%. The concentration of Na_2O was adjusted to keep the viscosity at 1150 °C at 4 Pa·s.

All glasses for spinel limited clusters were tested for crystallinity after a 24-hour heat treatment at 950°C. The glasses for Cluster 3 (IWL-SLC3-1, IWL-SLC3-2, and IWL-SLC3-3) contain low concentration of Al_2O_3 but the glasses for Clusters 4 and 20 contain relatively high concentration of Al_2O_3 and therefore have a potential to precipitate the nepheline. These glasses were CCC-heat treated and

tested for crystallinity. However, the crystallinity results were not obtained in time for inclusion in this report.

Table 5.2. Glasses Melting at 1150°C Formulated for Spinel-Limited Waste Clusters and Their Predicted and Measured Properties

	Cluster 3			Cluster 4				
Comp.	**IWL-SLC3-1**	**IWL-SLC3-2**	**IWL-SLC3-3**	**IWL-SLC4-1**	**IWL-SLC4-2**	**IWL-SLC4-3**	**IWL-SLC4-4**	**Limits[(a)]**
Al_2O_3	0.06220	0.06189	0.06220	0.17163	0.15812	0.17163	0.17163	-
B_2O_3	0.04000	0.15437	0.11000	0.19241	0.16484	0.11000	0.14000	-
Bi_2O_3	0.01121	0.01115	0.01121	0.00449	0.00414	0.00449	0.00449	-
CaO	0.01756	0.01747	0.01756	0.01207	0.01112	0.01207	0.01207	-
CdO	0.00214	0.00213	0.00214	0.00238	0.00220	0.00238	0.00238	-
Cr_2O_3	0.00562	0.00559	0.00562	0.00602	0.00555	0.00602	0.00602	-
Cs_2O	0.00193	0.00192	0.00193	0.00209	0.00193	0.00209	0.00209	-
F	0.00073	0.00073	0.00073	0.00058	0.00053	0.00058	0.00058	-
Fe_2O_3	0.08539	0.08496	0.08539	0.06782	0.06248	0.06782	0.06782	-
K_2O	0.00470	0.00468	0.00470	0.00249	0.00229	0.00249	0.00249	-
La_2O_3	0.00305	0.00304	0.00305	0.00123	0.00114	0.00123	0.00123	-
Li_2O	0.03001	0.00000	0.03000	0.00138	0.05770	0.03000	0.03000	-
MgO	0.00185	0.00184	0.00185	0.00061	0.00057	0.00061	0.00061	-
MnO	0.01311	0.01305	0.01311	0.00448	0.00412	0.00448	0.00448	-
Na_2O	0.19875	0.16293	0.13032	0.18901	0.08741	0.18950	0.16264	-
Nd_2O_3	0.00049	0.00049	0.00049	0.00088	0.00081	0.00088	0.00088	-
NiO	0.01896	0.01887	0.01896	0.01135	0.01045	0.01135	0.01135	-
P_2O_5	0.01940	0.01930	0.01940	0.00535	0.00493	0.00535	0.00535	-
PbO	0.00286	0.00284	0.00286	0.00266	0.00245	0.00266	0.00266	-
RuO_2	0.00012	0.00012	0.00012	0.00044	0.00041	0.00044	0.00044	-
SiO_2	0.42576	0.37876	0.42419	0.30300	0.40060	0.35630	0.35316	-
SO_3	0.00305	0.00304	0.00305	0.00124	0.00114	0.00124	0.00124	-
SrO	0.00059	0.00058	0.00059	0.00102	0.00094	0.00102	0.00102	-
ZrO_2	0.05051	0.05025	0.05051	0.01536	0.01415	0.01536	0.01536	-
Total	1.00000	1.00000	1.00000	1.00000	1.00000	1.00000	1.00000	-
Waste Loading	0.385	0.383	0.385	0.419	0.386	0.419	0.419	-
$Al_2O_3+Fe_2O_3+ZrO_2$	0.198	0.197	0.198	0.255	0.235	0.255	0.255	-
η_{1150}, Pa·s	4	4	4	4	4	4	4	2 – 8
ε_{1150}, S/m	60.1	27.5	30.1	38.6	34.9	53.1	40.7	10 – 100
Spinel $T_{1\%}$, °C	950	950	984	950	950	968	980	950
PCT-B, g/L	0.921	1.254	0.788	1.818	1.044	1.111	1.088	<16.7
PCT-Li, g/L	0.945	1.613	0.853	3.696	1.116	0.917	1.095	<9.57
PCT-Na, g/L	2.221	1.282	0.762	2.035	0.730	0.943	0.834	<13.35
TCLP Cd, mg/L	0.118	0.157	0.097	0.311	0.113	0.190	0.182	<0.48
N_{Si}	0.620	0.628	0.688	0.457	0.620	0.497	0.514	≥0.62
OB	0.624	0.575	0.581	0.575	0.557	0.600	0.584	≤0.575
Measured spinel vol% after 24 h heat treatment at 950°C and Crystallinity after CCC								
950°C Spinel vol% (vol% of other crystals)	1.7	0.9	1.5	1.5	1.8	1.5 (1.8 Np)	1.7 (3.7 Ap)	1 (NA)
CCC Crystallinity	NM	NM	NM	2.4 Sp	2.7 Sp	2.3 Sp 48.7 Np	2.4 Sp	No Np

[(a)] Used as guidelines for formulating the glasses.
Shaded cells indicate that the predicted or calculated value is not within the limits.
NM: not measured (see text).
Ap: apatite; Sp: spinel; Np: nepheline.
No Np: no nepheline formation; NA: not applicable.

Table 5.2. (Continued)

Comp.	Cluster 20			Limits[(a)]
	IWL-SLC20-1	IWL-SLC20-2	IWL-SLC20-3	
Al_2O_3	0.12767	0.12299	0.12767	-
B_2O_3	0.15220	0.17151	0.11000	-
Bi_2O_3	0.02718	0.02619	0.02718	-
CaO	0.02160	0.02081	0.02160	-
CdO	0.00015	0.00014	0.00015	-
Cr_2O_3	0.01009	0.00972	0.01009	-
Cs_2O	0.00246	0.00237	0.00246	-
F	0.01234	0.01189	0.01234	-
Fe_2O_3	0.07822	0.07535	0.07822	-
K_2O	0.00232	0.00223	0.00232	-
La_2O_3	0.00175	0.00168	0.00175	-
Li_2O	0.00000	0.02194	0.03000	-
MgO	0.00306	0.00295	0.00306	-
MnO	0.00737	0.00710	0.00737	-
Na_2O	0.16543	0.10657	0.12985	-
Nd_2O_3	0.00033	0.00032	0.00033	-
NiO	0.00842	0.00811	0.00842	-
P_2O_5	0.01797	0.01731	0.01797	-
PbO	0.00448	0.00431	0.00448	-
RuO_2	0.00000	0.00000	0.00000	-
SiO_2	0.34456	0.37455	0.39234	-
SO_3	0.00534	0.00514	0.00534	-
SrO	0.00556	0.00535	0.00556	-
ZrO_2	0.00150	0.00145	0.00150	-
Total	1.00000	1.00000	1.00000	-
Waste Loading	0.492	0.474	0.492	-
$Al_2O_3+Fe_2O_3+ZrO_2$	0.207	0.200	0.207	-
η_{1150}, Pa·s	4	4	4	2 - 8
ε_{1150}, S/m	29.4	21.3	31.0	10 - 100
Spinel $T_{1\%}$, °C	950	950	982	950
PCT-B, g/L	1.482	1.237	0.917	<16.7
PCT-Li, g/L	2.017	1.801	1.072	<9.57
PCT-Na, g/L	1.495	1.206	0.876	<13.35
TCLP Cd, mg/L	0.015	0.011	0.009	<0.48
N_{Si}	0.540	0.620	0.604	≥0.62
OB	0.575	0.555	0.579	≤0.575
Measured spinel vol% after 24 h heat treatment at 950°C and Crystallinity after CCC				
950°C Spinel vol%, %	1.4 (2.3 Sp)	1.6 (1.8 Ap)	1.3	1 (NA)
CCC Crystallinity	2.1 Sp 4.3 Ap	3.5 Sp 3.7 Ap	2.5 Sp 3.3 Ap	No Np

[(a)] Used as guidelines for formulating the glasses.
Shaded cells indicate that the predicted or calculated value is not within the limits.
Ap: apatite; Sp: spinel; Np: nepheline.
No Np: no nepheline formation; NA: not applicable.

The results of XRD measurement for the spinel vol% after a 24-hour heat treatment at 950°C and CCC treatment were included in Table 5.2. Among three clusters, only the formulation with Cluster 3 (IWL-SLC3-2) produced a glass that pass the $T_{1\%}$ requirement. Out of six glasses for Clusters 4 and 20 that contain relatively high concentration of Al_2O_3, one glass (IWL-SLC4-3) formed nepheline. This

glass had lower concentration of B_2O_3 and higher Na_2O compared to IWL-SLC4-4. Additional formulation and testing are needed to determine the estimated maximum waste loading for each cluster.

5.1.3 Advanced Silicate Glass Formulation for High-Al Waste Clusters

Past glass formulation studies with high-aluminum wastes (Matlack et al. 2007a; Matlack et al. 2008; Matlack et al. 2010; Kim et al. 2008; Marra et al. 2010) suggest that the loading of high-alumina wastes in glass is limited by both nepheline constraint and spinel $T_{1\%}$. Therefore the maximum loading of Al_2O_3 achievable in glass depends on the concentration of spine forming components and also ZrO_2 that has strong effect on spinel formation. Among four high-aluminum waste clusters (Clusters 5, 7, 8, and 16), Cluster 5 is characterized by higher ZrO_2, Clusters 7 and 8 by higher Fe_2O_3, and Cluster 16 by low zirconium and iron (see Table 4.20). The NiO was highest in Cluster 5. Based on this firsthand information it is likely that Cluster 16 will have highest Al_2O_3 loading.

Table 5.3 shows the target compositions and predicted properties for IWL-HACx-y glasses where IWL-HAC represents "improved waste loading-high-alumina cluster." For the first set, 10 glasses were formulated for Clusters 5, 8, and 16. Similar to the high-iron and spinel-limited cluster glass formulations, there is reasonable similarity between Clusters 7 and 8, so it is assumed that the maximum loading of Al_2O_3 in the glasses for Cluster 7 is similar to that obtained from Cluster 8.

The glasses were formulated following similar pattern used for high-iron cluster glasses. The first glasses for each cluster (IWL-HAC5-1, 8-1, and 16-1) were formulated based on HTWOS revised constraints given in Table 2.6. As shown in Table 5.3, the waste loading is limited by $T_{1\%}$ and nepheline constraint. All three glasses met the nepheline constraint by satisfying the OB requirement. The loading of Al_2O_3 in these glasses ranged from 21.1 wt% to 27 wt%, and loading of Al_2O_3+Fe_2O_3+ZrO_2 ranged from 26.7 wt% to 29.7 wt%. Although there is significant difference in Al_2O_3 loading between these three glasses, there is only a relatively small difference in loading of Al_2O_3+Fe_2O_3+ZrO_2. These glasses are formulated without any manual adjustments and all contain high concentrations of Na_2O at 19.3 wt% to 20.1 wt%.

All the first glasses for each cluster (IWL-HAC5-1, 8-1, and 16-1) have the high concentrations of B_2O_3 (19.5 wt% or 20.0 wt%) and Na_2O (19.3 wt% to 20.1 wt%). The high B_2O_3 concentration in high Al_2O_3 glasses was also used in past glass formulation studies with high-aluminum wastes (Kim et al. 2008; Marra et al. 2010). The next two glasses for Clusters 5 and 8 (IWL-HAC5-4, 6 and IWL-HAC8-4, 6) were formulated with increased Al_2O_3 concentration at one wt% increment while decreasing the B_2O_3 concentration by the same wt% at a fixed concentration of Li_2O. The Na_2O was not used as additive and the viscosity changed accordingly. These changes decreased the viscosity to the range of 2.3 Pa·s to 2.5 Pa·s from 4 Pa·s and 4.5 Pa·s at 1150 °C. In next three glasses for Cluster 16 (IWL-HAC16-5, 6, and 7), the IWL-HAC16-5 glass was formulated at the same Al_2O_3 loading as the IWL-HAC16-1 glass while keeping the B_2O_3 the same at 20 wt% and adding 4 wt% Li_2O. The Na_2O was not used as additive and the viscosity changed accordingly.

Table 5.3. Glasses Melting at 1150°C Formulated for High-Aluminum Waste Clusters and Their Predicted and Measured Properties

Comp.	Cluster 5			Cluster 8			Limits[(a)]
	IWL-HAC5-1	IWL-HAC5-4	IWL-HAC5-6	IWL-HAC8-1	IWL-HAC8-4	IWL-HAC8-6	
Al_2O_3	0.22160	0.23000	0.24000	0.21137	0.22000	0.23000	-
B_2O_3	0.20000	0.19000	0.18000	0.19536	0.19000	0.18000	-
Bi_2O_3	0.00876	0.00909	0.00948	0.00938	0.00976	0.01020	-
CaO	0.00734	0.07000	0.07000	0.01251	0.07000	0.07000	-
CdO	0.00008	0.00008	0.00008	0.00012	0.00012	0.00013	-
Cr_2O_3	0.01073	0.01113	0.01162	0.01012	0.01053	0.01101	-
Cs_2O	0.00223	0.00231	0.00241	0.00232	0.00242	0.00253	-
F	0.00671	0.00696	0.00727	0.00550	0.00572	0.00598	-
Fe_2O_3	0.02743	0.02847	0.02971	0.05437	0.05659	0.05916	-
K_2O	0.00276	0.03000	0.03000	0.00185	0.03000	0.03000	-
La_2O_3	0.00100	0.00103	0.00108	0.00034	0.00035	0.00037	-
Li_2O	0.00000	0.04000	0.04000	0.00000	0.04000	0.04000	-
MgO	0.00086	0.00089	0.00093	0.00170	0.00177	0.00185	-
MnO	0.00559	0.00581	0.00606	0.00924	0.00962	0.01006	-
Na_2O	0.20139	0.07251	0.07566	0.19320	0.06252	0.06536	-
Nd_2O_3	0.00017	0.00017	0.00018	0.00050	0.00052	0.00054	-
NiO	0.00608	0.00631	0.00658	0.00324	0.00337	0.00352	-
P_2O_5	0.02132	0.02213	0.02309	0.01094	0.01138	0.01190	-
PbO	0.00116	0.00121	0.00126	0.00405	0.00422	0.00441	-
RuO_2	0.00001	0.00001	0.00002	0.00000	0.00000	0.00000	-
SiO_2	0.24067	0.23646	0.22761	0.26663	0.26353	0.25506	-
SO_3	0.00575	0.00597	0.00622	0.00437	0.00455	0.00475	-
SrO	0.00346	0.00359	0.00375	0.00184	0.00192	0.00200	-
ZrO_2	0.02491	0.02586	0.02698	0.00108	0.00112	0.00117	-
Total	1.00000	1.00000	1.00000	1.00000	1.00000	1.00000	-
Waste Loading	0.445	0.462	0.482	0.464	0.483	0.505	-
Al_2O_3+Fe_2O_3+ZrO_2	0.274	0.284	0.297	0.267	0.278	0.290	-
η_{1150}, Pa·s	4.53	2.43	2.49	4.00	2.29	2.32	2 - 8
ε_{1150}, S/m	46.5	22.9	23.5	41.9	21.1	21.6	10 - 100
Spinel $T_{1\%}$, °C	950	1087	1130	950	1086	1130	950
PCT-B, g/L	0.930	0.186	0.076	1.347	0.312	0.145	<16.7
PCT-Li, g/L	3.608	0.442	0.195	4.091	0.616	0.303	<9.57
PCT-Na, g/L	1.403	0.302	0.128	1.853	0.466	0.220	<13.35
TCLP Cd, mg/L	0.019	0.015	0.015	0.021	0.016	0.016	<0.48
N_{Si}	0.363	0.439	0.419	0.397	0.483	0.463	≥0.62
OB	0.575	0.576	0.582	0.575	0.574	0.579	≤0.575
Measured spinel vol% after 24 h heat treatment at 950°C and Crystallinity after CCC							
950°C Spinel vol% (vol% of other crystals)	1.7 (3.6 Ap, 0.6 Bd)	1.6 (3.4 Ap, 0.6 Bd)	2.6 (3.5 Ap, 0.9 Bd)	1.1	1.9	1.9	1 (NA)
CCC Crystallinity, vol%	5.2 Np, 1.5 Ap, 1.6 Sp	4.0 Ap, 1.8 Sp, 0.9 Bd	5.1 Ap, 2.6 Sp, 1.3 Bd	15.8 Np, 1.9 Sp	2.8 Sp, 2.0 Ap	3.0 Sp, 2.2 Ap	No Np

[(a)] Used as guidelines for formulating the glasses.
Shaded cells indicate that the predicted or calculated value is not within the limits.
Ap: apatite; Bd: baddeleyite; Sp: spinel; Np: nepheline.
No Np: no nepheline formation; NA: not applicable.

Table 5.3. (Continued)

Comp.	Cluster 16				Limits[(a)]
	IWL-HAC16-1	IWL-HAC16-5	IWL-HAC16-6	IWL-HAC16-7	
Al_2O_3	0.27036	0.27036	0.28000	0.29000	-
B_2O_3	0.20000	0.20000	0.20000	0.20000	-
Bi_2O_3	0.00683	0.00683	0.00708	0.00733	-
CaO	0.00408	0.07000	0.07000	0.07000	-
CdO	0.00002	0.00002	0.00002	0.00002	-
Cr_2O_3	0.00957	0.00957	0.00991	0.01026	-
Cs_2O	0.00227	0.00227	0.00235	0.00243	-
F	0.00122	0.00122	0.00126	0.00131	-
Fe_2O_3	0.02588	0.02588	0.02680	0.02776	-
K_2O	0.00103	0.03000	0.03000	0.03000	-
La_2O_3	0.00045	0.00045	0.00047	0.00048	-
Li_2O	0.01039	0.04000	0.04000	0.04000	-
MgO	0.00091	0.00091	0.00094	0.00098	-
MnO	0.00653	0.00653	0.00676	0.00700	-
Na_2O	0.19674	0.07670	0.07943	0.08227	-
Nd_2O_3	0.00036	0.00036	0.00037	0.00038	-
NiO	0.00169	0.00169	0.00175	0.00181	-
P_2O_5	0.00659	0.00659	0.00682	0.00707	-
PbO	0.00123	0.00123	0.00127	0.00132	-
RuO_2	0.00000	0.00000	0.00000	0.00000	-
SiO_2	0.24989	0.24542	0.23063	0.21530	-
SO_3	0.00236	0.00236	0.00244	0.00253	-
SrO	0.00078	0.00078	0.00081	0.00084	-
ZrO_2	0.00085	0.00085	0.00089	0.00092	-
Total	1.00000	1.00000	1.00000	1.00000	-
Waste Loading	0.453	0.453	0.470	0.486	-
$Al_2O_3+Fe_2O_3+ZrO_2$	0.297	0.297	0.308	0.319	-
η_{1150}, Pa·s	6.00	3.28	3.09	2.91	2 - 8
ε_{1150}, S/m	46.5	22.2	23.0	23.9	10 - 100
Spinel $T_{1\%}$, °C	950	1049	1078	1107	950
PCT-B, g/L	0.008	0.003	0.001	0.000	<16.7
PCT-Li, g/L	0.057	0.014	0.005	0.001	<9.57
PCT-Na, g/L	0.023	0.010	0.003	0.001	<13.35
TCLP Cd, mg/L	0.004	0.003	0.004	0.004	<0.48
N_{Si}	0.349	0.414	0.391	0.366	≥0.62
OB	0.575	0.574	0.577	0.580	≤0.575
Measured spinel vol% after 24 h heat treatment at 950°C and Crystallinity after CCC					
950°C Spinel vol% (vol% of other crystals)	0.8	0.9	3.0 (4.2 Ap, 1.8 Bd)	1.2	1 (NA)
CCC Crystallinity, vo%	45.2 Np, 1.7Sp, 0.1 Bd	1.4 Sp	1.6 Sp	1.8 Sp 1.8	No Np

[(a)] Used as guidelines for formulating the glasses.
Shaded cells indicate that the predicted or calculated value is not within the limits.
Ap: apatite; Bd: baddeleyite; Sp: spinel; Np: nepheline.
No Np: no nepheline formation; NA: not applicable.

The results of XRD measurement for the spinel vol% after a 24-hour heat treatment at 950°C and CCC treatment were included in Table 5.3. Among three clusters, the formulation with Cluster 16 produced two glasses that pass the $T_{1\%}$ requirement. All three as-formulated glasses for each cluster

(IWL-HAC5-1, 8-1, and 16-1) based on HTWOS revised constraints precipitated nepheline after CCC treatment, which is likely to be attributed to their high Na_2O concentration. These glasses passed the OB constraint at the maximum value of 0.575. This suggests that the current OB constraint, unlike N_{Si}, may not be conservative for these high-aluminum glasses. All the other glasses manually adjusted by adding K_2O and/or Li_2O replacing Na_2O did not form nepheline. Additional formulation and testing are needed to determine the estimated maximum Al_2O_3 loading for each cluster.

5.2 Systematic Glass Studies: High-Al_2O_3 Test Matrix Glasses

In addition to the approach of glass formulation described in Section 5.1, some test objectives may rely on defining specific glass compositions that cover a generic compositional region of interest. For example, assume that a specific process control model (e.g., $T_{1\%}$) is limiting access to higher waste loadings. A review of the compositional range over which that model was either developed or validated may identify compositional gaps that need to be covered from an experimental perspective. These data can then be used to revise the existing model or develop a new model. To accomplish this through a matrix design study, the general approach is to define the glass composition region of interest. As previously mentioned, this region may be defined based on compositional gaps identified by the review of the model or validation range as compared to the glass composition region covered by higher waste loadings. Other approaches may simply set minimum and maximum limits to the glass region of interest independent of model or validation ranges. Regardless of the approach, minimum and maximum values for the major and/or minor oxides of interest are needed.

Among 20 waste clusters discussed in Section 2.2, the high-alumina clusters represent nearly a half of Hanford wastes (on a waste oxides basis or a glass basis). In addition, glasses with Al_2O_3 content of up to 27 wt% have been demonstrated while current models are sparsely populated with data going only to 20 wt%. Therefore, the first glass matrix for advanced silicate glass formulation studies was developed to cover a glass composition region of high Al_2O_3.

Typically, glass composition matrices have been developed using statistical design approaches (Piepel et al. 2004). However, these approaches tend to push a majority (e.g., all) of the glasses to the boundaries of composition space. One approach to avoid this has been to define multiple sets of boundaries forming concentric circles of compositions with all glasses on one of the boundaries. This approach is not deemed appropriate for high-alumina glasses as there are specific formulation directions that do not make acceptable glasses for further characterization and the highly non-linear and unknown nature of composition effects on glass properties at their waste loading boundaries. Therefore, a new design approach is needed at least for the first high-alumina glass matrix. This approach is to evenly fill composition space with compositions that are all predicted to successfully produce glasses that can be characterized. This ‘space filling’ design is described below.

Design of space filling matrix for high-alumina glasses was performed according to the following steps:

1. Collect existing data on high-Al_2O_3 glasses (Section 5.2.1)
2. Define single component constraints, multicomponent constraints, and property constraints (Section 5.2.2)
3. Formulate random-generated glasses within the predetermined single component constraints (Section 5.2.3)

4. Select matrix glasses by (Section 5.2.4):
   - sorting out the glasses outside the multicomponent and property constraints
   - performing distance calculations compared to existing data and sorting out the glasses that are too close to the existing glasses
   - performing distance calculations between matrix glasses and sorting out the glasses that are too close each other.

5.2.1 Existing Data on High-Al_2O_3 Glasses

Recent efforts to increase waste loading beyond that is estimated based on WTP formulation algorithm and HTWOS constraints (Vienna et al 2009) have focused on high-aluminum wastes. The studies at VSL (Matlack et al. 2007a, 2008, 2010) and PNNL (Kim et al. 2008; Marra et al. 2010; Schweiger et al. 2011) applied iterative approach of repeating the formulation and testing of a set of few glasses to finally select glasses for scaled melter tests. In this approach, only selected properties are tested for all glasses and only selected glasses are fully characterized and tested in scaled melter runs.

The loading of wastes in high-alumina glasses is primarily limited by nepheline formation after CCC treatment and spinel $T_{1\%}$ constraint. The other property requirements such as PCT and TCLP are easily met. Among these two critical constraints, most of the high-Al_2O_3 glasses in the studies mentioned above were tested for the nepheline formation, but limited number of glasses was tested for $T_{1\%}$. Instead, most glasses were tested for the vol% of spinel crystal after a 950 °C heat treatment so that the pass/fail determination of $T_{1\%} \leq 950$°C can be made. The limited glasses with >21 wt% Al_2O_3 and $T_{1\%}$ data were collected and used as a set of existing data in the design of matrix glasses. Table 5.4 summarizes the glass composition, measured $T_{1\%}$, and key predicted properties for the 14 glasses with measured $T_{1\%}$ data. The measured $T_{1\%}$ was obtained by interpolating or extrapolating the spinel vol% versus temperature data for multiple temperatures given in the literature. Some glasses that had less than three data points or did not show reasonable linear fit between the spinel vol% versus temperature were excluded.

Figure 5.1 shows the predicted versus measured $T_{1\%}$ data for the 14 high-Al_2O_3 glasses given in Table 5.4. The $T_{1\%}$ model developed for the glasses with lower Al_2O_3 concentration (≤20 wt%) (Vienna et al. 2009) showed a tendency to overpredict the measured values for these high-Al_2O_3 glasses.

Three glasses out of 14 existing glasses had predicted viscosity at 1150 °C outside the WTP required range (2–8 Pa·s). The predicted melting temperature ranged from 991 °C to 1226°C, based on predicted viscosity of 5 Pa·s. All 14 glasses fail the N_{Si} requirement but seven glasses pass the OB requirement and thereby passing the nepheline constraint (see Equations 2.1 and 2.2 in Section 2.2.2).

Table 5.4. Existing High-Al_2O_3 Glasses with Measured $T_{1\%}$ Data

Reference	Matlack et al. (2007a)							Matlack et al. (2008)						
Glass ID	**HLW-E-Al-12**	**HLW-E-Al-27**	**HLW-E-ANa-05**	**HLW-E-ANa-06**	**HLW-E-ANa-09**	**HLW-E-ANa-24**	**HLW-E-ANa-25**	**HWI-AL-7**	**HWI-AL-9**	**HWI-AL-13**	**HWI-AL-17**	**HWI-AL-18(G)**	**HWI-AL-19**	**HWI-AL-20**
Al_2O_3	0.23971	0.23971	0.23608	0.25878	0.25878	0.22700	0.22700	0.23970	0.21310	0.23970	0.23250	0.22570	0.23970	0.23970
B_2O_3	0.20190	0.15190	0.14406	0.14445	0.14445	0.18390	0.19390	0.15190	0.18170	0.15190	0.14730	0.20130	0.19190	0.18190
BaO	0.00054	0.00054	0.00031	0.00034	0.00034	0.00030	0.00030	0.00050	0.00050	0.00050	0.00050	0.00050	0.00050	0.00050
Bi_2O_3	0.01145	0.01145	0.01279	0.01402	0.01402	0.01230	0.01230	0.01140	0.01020	0.01140	0.01110	0.01080	0.01140	0.01140
CaO	0.14076	0.06076	0.00801	0.00878	0.00878	0.00770	0.00770	0.03080	0.00960	0.06080	0.05890	0.05720	0.05580	0.01080
CdO	0.00024	0.00024	0.00010	0.00011	0.00011	0.00010	0.00010	0.00020	0.00020	0.00020	0.00020	0.00020	0.00020	0.00020
Cr_2O_3	0.00521	0.00521	0.00785	0.00861	0.00861	0.00755	0.00755	0.00520	0.00460	0.00520	0.00510	0.00490	0.00520	0.00520
F	0.00667	0.00667	0.00250	0.00274	0.00274	0.00240	0.00240	0.00670	0.00590	0.00670	0.00650	0.00630	0.00670	0.00670
Fe_2O_3	0.05899	0.05899	0.03115	0.03414	0.03414	0.02995	0.02995	0.05900	0.05240	0.05900	0.05720	0.05560	0.05900	0.05900
K_2O	0.00141	0.00141	0.00733	0.00804	0.00804	0.00705	0.00705	0.00140	0.00130	0.04140	0.03140	0.00130	0.00140	0.05140
Li_2O	0.05171	0.03571	0.03583	0.02811	0.05091	0.03080	0.03080	0.03570	0.03150	0.03570	0.03460	0.03360	0.03570	0.03170
MgO	0.00117	0.00117	0.00239	0.00262	0.00262	0.00230	0.00230	0.03120	0.00100	0.00120	0.00110	0.00110	0.00120	0.00120
Na_2O	0.03580	0.09580	0.14061	0.15413	0.15413	0.13520	0.13520	0.09580	0.13180	0.06080	0.09290	0.09020	0.09580	0.08580
NiO	0.00400	0.00400	0.00109	0.00120	0.00120	0.00105	0.00105	0.00400	0.00360	0.00400	0.00390	0.00380	0.00400	0.00400
P_2O_5	0.01052	0.01052	0.02236	0.02451	0.02451	0.02150	0.02150	0.01050	0.00940	0.01050	0.01020	0.00990	0.01050	0.01050
PbO	0.00409	0.00409	0.00099	0.00108	0.00108	0.00095	0.00095	0.00410	0.00360	0.00410	0.00400	0.00390	0.00410	0.00410
SiO_2	0.21896	0.30496	0.33890	0.29996	0.27716	0.32260	0.31260	0.30500	0.33350	0.30000	0.29580	0.28720	0.27000	0.28900
SO_3	0.00200	0.00200	0.00239	0.00262	0.00262	0.00230	0.00230	0.00200	0.00180	0.00200	0.00190	0.00190	0.00200	0.00200
TiO_2	0.00010	0.00010	0.00192	0.00211	0.00211	0.00185	0.00185	0.00010	0.00010	0.00010	0.00010	0.00010	0.00010	0.00010
ZnO	0.00083	0.00083	0.00198	0.00217	0.00217	0.00190	0.00190	0.00080	0.00070	0.00080	0.00080	0.00080	0.00080	0.00080
ZrO_2	0.00395	0.00395	0.00135	0.00148	0.00148	0.00130	0.00130	0.00390	0.00350	0.00390	0.00380	0.00370	0.00390	0.00390
Total	1	1	1	1	1	1	1	1	1	1	1	1	1	1
Measured spinel $T_{1\%}$ and Crystallinity after CCC Treatment														
$T_{1\%}$-Sp, °C	988	953	922	965	935	783	750	1144	827	1066	960	968	969	1067
Predicted properties (Vienna et a. 2009)														
η_{1150}, Pa.s	1.06	5.17	8.49	9.20	3.32	6.72	5.89	6.13	5.50	5.91	4.33	3.76	3.39	6.56
T at 5 Pas, °C	991	1154	1216	1226	1092	1187	1171	1173	1162	1171	1132	1116	1103	1183
$T_{1\%}$-Sp, °C	1121	1078	925	994	967	881	875	1173	909	1084	1033	1004	1051	1017
Nepheline formation criteria														
N_{Si}	0.443	0.476	0.474	0.421	0.402	0.471	0.463	0.476	0.492	0.500	0.476	0.476	0.446	0.470
OB	0.581	0.577	0.570	0.577	0.587	0.558	0.557	0.578	0.560	0.578	0.585	0.562	0.569	0.567

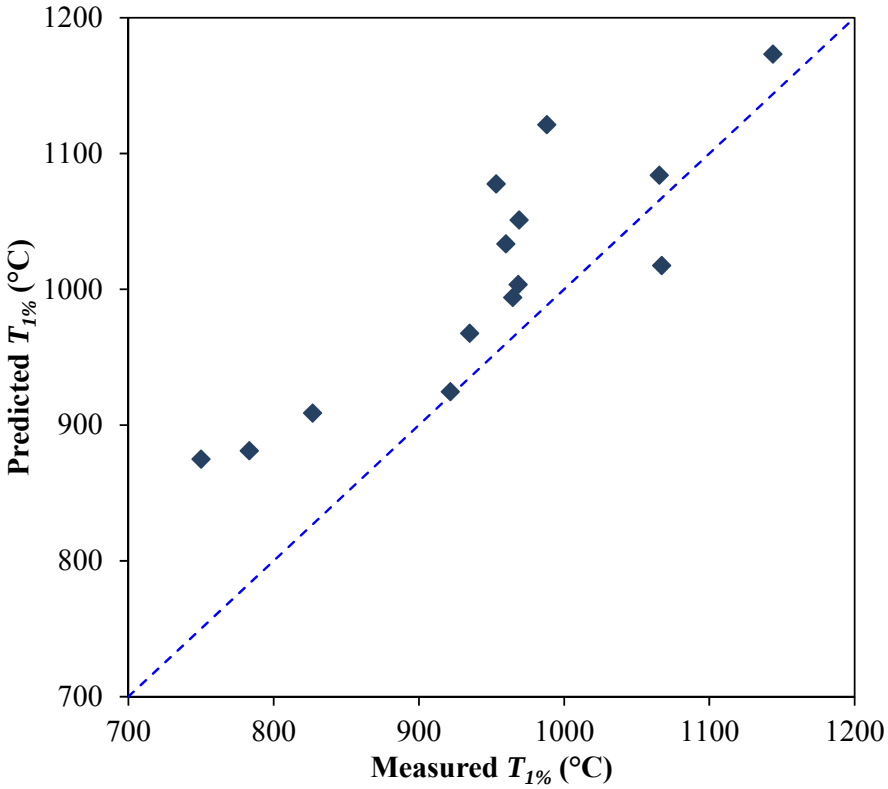

Figure 5.1. Predicted Versus Measured $T_{1\%}$ for High-Al_2O_3 Glasses with $T_{1\%}$ Data

5.2.2 Matrix Design Constraints

The glass composition constraints on single component concentrations were obtained by evaluating the compositional information on the high-Al_2O_3 glasses studied at VSL (Matlack et al. 2007a, 2008, 2010) and PNNL (Kim et al. 2008; Marra et al. 2010; Schweiger et al. 2011). Table 5.5 through Table 5.7 list the compositions and predicted properties with limited data on measured properties for the glasses evaluated for matrix design constraints. A brief discussion on these glasses is given below.

Table 5.5 list the glasses selected for and demonstrated through scaled melter tests. All glasses passed the PCT constraints for both quenched and CCC treated glasses. Theses glasses did not form nepheline after CCC treatment although three glasses, HAL-17, HAL-24, and HLW-E-Al-27, fail the nepheline constraint. All glasses met the electrical conductivity and viscosity requirements except HWI-Al-28, which had a measured viscosity of 1.6 Pa·s at 1150°C (compared to ≥ 2 Pa·s). Note that the HAL-24 and HWI-Al-28 were designed to have low a viscosity to improve the melter processing rate (Marra et al. 2010, Matlack et al. 2010). The three glasses, HAL-17, HAL-24, and HLW-E-Al-27, were designed to meet the $T_{1\%}$ requirement (<1 vol% spinel after 24-hour heat treatment at 950°C).[1] However, in later VSL studies (Matlack et al. 2008, 2010), the WTP crystallinity limit (<1 vol% spinel after 24-hour heat treatment at 950°C or $T_{1\%} \leq 950$°C) was "relaxed slightly as a waste loading constraint for the crucible melts based on experience form the melter test that the melter typically can tolerate high vol%

[1] The $T_{1\%}$ requirement was not met for HAL-24, but this glass was selected for melter test as being close to meeting the requirement so as not to perform additional iteration of glass formulation and testing (Marra et al. 2010).

crystals" (HWI-Al-19 and HWI-Al-28). This is in line with the approach at PNNL to develop the model that can predict crystal accumulation as a constraint for formulating crystal tolerant glasses for higher waste loading (Matyas et al. 2010).

Table 5.6 lists the glasses formulated and tested in a recent VSL study (Matlack et al. 2010) to select the high-Al_2O_3 glass for melter tests. The HWI-Al-28 was also included in Table 5.5 as it was selected for melter tests from this study. Nepheline was not detected after CCC treatment in all glasses as expected from that all glasses pass the nepheline constraint. Selected glasses tested met the electrical conductivity requirements, but the two glasses (HWI-AL-27 and HWI-AL-28) had a measured viscosity lower than 2 Pa·s at 1150 °C.[2] All the glasses in Table 5.6 had spinel vol% larger than 1% at 950°C (or $T_{1\%}$ higher than 950°C) as this requirement was relaxed as mentioned above (note that all glasses had $T_{1\%}$ even higher than 1050°C).

Table 5.7 lists glasses formulated as a part of advanced silicate formulation described in Section 5.1. These glasses were not tested at the time of the matrix design. The glasses formulated solely by optimization based on HTWOS constraints without manual adjustments of compositions (IWL-HAC5-1, IWL-HAC8-1, and IWL-HAC-16-1) were excluded. The glasses in Table 5.7 represent those that have potentially maximum waste loading for each high-Al_2O_3 cluster, i.e., formulated to determine the waste loading limits. All the glasses had predicted viscosity at 1150 °C higher than 2 Pa·s and predicted $T_{1\%}$ higher than 1049 °C. Two glasses (IWL-HAC8-4 and IWL-HAC16-5) out of seven pass the nepheline constraint.

[2] The report by Matlack et al. 2010 stated that these glasses "have acceptable viscosity" suggesting that lower minimum viscosity requirement than 2 Pa·s at 1150 °C was assumed.

Table 5.5. High-Al_2O_3 Glasses Processed in Scaled Melter Tests

Reference	Kim et al. (2008)	Marra et al. (2010)	Matlack et al. (2010)	Matlack et al. (2008)	Matlack et al. (2010)
Glass ID	**HAL-17**	**HAL-24**	**HLW-E-Al-27**	**HWI-Al-19**	**HWI-Al-28**
Al_2O_3	0.25889	0.25889	0.23971	0.23970	0.26633
B_2O_3	0.16139	0.20299	0.15190	0.19190	0.20212
BaO	0.00058	0.00058	0.00054	0.00050	0.00060
Bi_2O_3	0.01236	0.01236	0.01145	0.01140	0.01270
CaO	0.07331	0.07331	0.06076	0.05580	0.09201
CdO	0.00026	0.00026	0.00024	0.00020	0.00030
Cr_2O_3	0.00563	0.00563	0.00521	0.00520	0.00580
Cs_2O	-	-	-	-	-
F	0.00721	0.00721	0.00667	0.00670	0.00740
Fe_2O_3	0.06371	0.06371	0.05899	0.05900	0.06551
K_2O	0.02723	0.02723	0.00141	0.00140	0.00160
La_2O_3	-	-	-	-	-
Li_2O	0.04000	0.04000	0.03571	0.03570	0.05011
MgO	0.00126	0.00126	0.00117	0.00120	0.00130
MnO	-	-	-	-	-
Na_2O	0.06067	0.06067	0.09580	0.09580	0.04980
Nd_2O_3	-	-	-	-	-
NiO	0.00431	0.00431	0.00400	0.00400	0.00440
P_2O_5	0.01136	0.01136	0.01052	0.01050	0.01170
PbO	0.00442	0.00442	0.00409	0.00410	0.00450
RuO_2	-	-	-	-	-
SiO_2	0.25999	0.21840	0.30496	0.27000	0.21622
SO_3	0.00216	0.00216	0.00200	0.00200	0.00220
SrO	-	-	-	-	-
TiO_2	0.00011	0.00011	0.00010	0.00010	0.00010
ZnO	0.00089	0.00089	0.00083	0.00080	0.00090
ZrO_2	0.00426	0.00426	0.00395	0.00390	0.00440
Total	1.00000	1.00000	1.00000	1.00000	1.00000
Predicted properties (Vienna et al 2009)					
η_{1150}, Pa.s	3.93	2.44	5.17	3.39	1.90
T at 5 Pas, °C	1121	1065	1154	1103	1040
$T_{1\%}$-Sp, °C	1160	1134	1078	1051	1189
Nepheline formation criteria					
N_{Si}	0.449	0.406	0.476	0.446	0.406
OB	0.582	0.576	0.577	0.569	0.574
Measured viscosity at 1150°C					
η_{1150}, Pa.s	5.8	2.1	4.6	3.3	1.6
Measured Spinel vol% after heat treatment at each temperature					
800°C	-	-	7.2	3.7	4.6[a]
850°C	-	-	3.4	3.0	-
900°C	-	-	3.8	2.1	-
950°C	1.0	1.1	1.0	1.3	2.4[b]
1050°C	-	-	-	-	2.5

"-" represents empty cells.
[a] Spinel and Apatite.
[b] Spinel, Phosphate and Al-rich dendritic crystal.

Table 5.6. High-Al_2O_3 Glasses Formulated and Tested to Select the Glass for Melter Test

Reference	Matlack et al. (2010)							
Glass ID	**HWI-Al-21**	**HWI-Al-22**	**HWI-Al-23**	**HWI-Al-24**	**HWI-Al-25**	**HWI-Al-26**	**HWI-Al-27**	**HWI-Al-28**
Al_2O_3	0.25025	0.25035	0.25035	0.26633	0.25035	0.25035	0.25035	0.26633
B_2O_3	0.20006	0.20996	0.21896	0.19192	0.19996	0.20196	0.20196	0.20212
BaO	0.00060	0.00060	0.00060	0.00060	0.00060	0.00060	0.00060	0.00060
Bi_2O_3	0.01200	0.01200	0.01200	0.01270	0.01200	0.01200	0.01200	0.01270
CaO	0.03019	0.02020	0.01120	0.02000	0.04019	0.05619	0.08118	0.09201
CdO	0.00030	0.00030	0.00030	0.00030	0.00030	0.00030	0.00030	0.00030
Cr_2O_3	0.00540	0.00540	0.00540	0.00580	0.00540	0.00540	0.00540	0.00580
Cs_2O	-	-	-	-	-	-	-	-
F	0.00700	0.00700	0.00700	0.00740	0.00700	0.00700	0.00700	0.00740
Fe_2O_3	0.06159	0.06159	0.06159	0.06551	0.06159	0.06159	0.06159	0.06551
K_2O	0.00150	0.00150	0.00150	0.00160	0.00150	0.00150	0.00150	0.00160
La_2O_3	-	-	-	-	-	-	-	-
Li_2O	0.03579	0.03579	0.03579	0.03250	0.03179	0.03579	0.04999	0.05011
MgO	0.00120	0.00120	0.00120	0.00130	0.00120	0.00120	0.00120	0.00130
MnO	-	-	-	-	-	-	-	-
Na_2O	0.09638	0.09638	0.09638	0.09581	0.09338	0.08738	0.05739	0.04980
Nd_2O_3	-	-	-	-	-	-	-	-
NiO	0.00420	0.00420	0.00420	0.00440	0.00420	0.00420	0.00420	0.00440
P_2O_5	0.01100	0.01100	0.01100	0.01170	0.01100	0.01100	0.01100	0.01170
PbO	0.00430	0.00430	0.00430	0.00450	0.00430	0.00430	0.00430	0.00450
RuO_2	-	-	-	-	-	-	-	-
SiO_2	0.27105	0.27105	0.27105	0.27003	0.26805	0.25205	0.24285	0.21622
SO_3	0.00210	0.00210	0.00210	0.00220	0.00210	0.00210	0.00210	0.00220
SrO	-	-	-	-	-	-	-	-
TiO_2	0.00010	0.00010	0.00010	0.00010	0.00010	0.00010	0.00010	0.00010
ZnO	0.00090	0.00090	0.00090	0.00090	0.00090	0.00090	0.00090	0.00090
ZrO_2	0.00410	0.00410	0.00410	0.00440	0.00410	0.00410	0.00410	0.00440
Total	1.00000	1.00000	1.00000	1.00000	1.00000	1.00000	1.00000	1.00000
Predicted properties (Vienna et al 2009)								
η_{1150}, Pa.s	4.71	5.06	5.42	7.13	5.00	3.43	2.11	1.90
T at 5 Pas, °C	1143	1152	1160	1192	1150	1105	1050	1040
$T_{1\%}$-Sp, °C	1076	1067	1058	1141	1087	1093	1119	1189
Nepheline formation criteria								
N_{Si}	0.439	0.439	0.439	0.427	0.438	0.427	0.441	0.406
OB	0.562	0.557	0.553	0.561	0.562	0.567	0.570	0.574
Measured viscosity at 1150°C								
η_{1150}, Pa.s	-	-	-	7.5	-	-	1.7	1.6
Measured Spinel vol% after heat treatment at each temperature								
800°C	-	-	-	-	-	4.2[a]	4.0[a]	4.6[a]
850°C	-	-	-	-	-	-	-	-
900°C	-	-	-	-	-	-	-	-
950°C	1.8	2.4	2.9	3.0	2.3	1.8	1.8	2.4[b]
1050°C	1.3	1.4	1.5	2.3	1.9	1.1	1.4	2.5

"-" represents empty cells.
[a] Spinel and Apatite.
[b] Spinel, Phosphate and Al-rich dendritic crystal.

Table 5.7. High-Al_2O_3 Glasses Formulated Based on High-Al Clusters

Component	IWL-HAC5-4	IWL-HAC5-6	IWL-HAC8-4	IWL-HAC8-6	IWL-HAC16-5	IWL-HAC16-6	IWL-HAC16-7
Al_2O_3	0.23000	0.24000	0.22000	0.23000	0.27036	0.28000	0.29000
B_2O_3	0.19000	0.18000	0.19000	0.18000	0.20000	0.20000	0.20000
BaO	-	-	-	-	-	-	-
Bi_2O_3	0.00909	0.00948	0.00976	0.01020	0.00683	0.00708	0.00733
CaO	0.07000	0.07000	0.07000	0.07000	0.07000	0.07000	0.07000
CdO	0.00008	0.00008	0.00012	0.00013	0.00002	0.00002	0.00002
Cr_2O_3	0.01113	0.01162	0.01053	0.01101	0.00957	0.00991	0.01026
Cs_2O	0.00231	0.00241	0.00242	0.00253	0.00227	0.00235	0.00243
F	0.00696	0.00727	0.00572	0.00598	0.00122	0.00126	0.00131
Fe_2O_3	0.02847	0.02971	0.05659	0.05916	0.02588	0.02680	0.02776
K_2O	0.03000	0.03000	0.03000	0.03000	0.03000	0.03000	0.03000
La_2O_3	0.00103	0.00108	0.00035	0.00037	0.00045	0.00047	0.00048
Li_2O	0.04000	0.04000	0.04000	0.04000	0.04000	0.04000	0.04000
MgO	0.00089	0.00093	0.00177	0.00185	0.00091	0.00094	0.00098
MnO	0.00581	0.00606	0.00962	0.01006	0.00653	0.00676	0.00700
Na_2O	0.07251	0.07566	0.06252	0.06536	0.07670	0.07943	0.08227
Nd_2O_3	0.00017	0.00018	0.00052	0.00054	0.00036	0.00037	0.00038
NiO	0.00631	0.00658	0.00337	0.00352	0.00169	0.00175	0.00181
P_2O_5	0.02213	0.02309	0.01138	0.01190	0.00659	0.00682	0.00707
PbO	0.00121	0.00126	0.00422	0.00441	0.00123	0.00127	0.00132
RuO_2	1.45E-05	1.51E-05	5.53E-07	5.78E-07	1.36E-06	1.41E-06	1.46E-06
SiO_2	0.23646	0.22761	0.26353	0.25506	0.24542	0.23063	0.21530
SO_3	0.00597	0.00622	0.00455	0.00475	0.00236	0.00244	0.00253
SrO	0.00359	0.00375	0.00192	0.00200	0.00078	0.00081	0.00084
TiO_2	-	-	-	-	-	-	-
ZnO	-	-	-	-	-	-	-
ZrO_2	0.02586	0.02698	0.00112	0.00117	0.00085	0.00089	0.00092
Total	1.00000	1.00000	1.00000	1.00000	1.00000	1.00000	1.00000
Predicted properties (Vienna et al 2009)							
η_{1150}, Pa.s	2.43	2.49	2.29	2.32	3.28	3.09	2.91
T at 5 Pas, °C	1065	1067	1056	1057	1093	1084	1076
$T_{1\%}$-Sp, °C	1087	1130	1086	1130	1049	1078	1107
Nepheline formation criteria							
N_{Si}	0.439	0.419	0.483	0.463	0.414	0.391	0.366
OB	0.576	0.582	0.574	0.579	0.574	0.577	0.580
"-" represents empty cells.							

Table 5.8 summarizes the single component concentration constraints developed based on information on the composition and predicted and measured properties given in Table 5.5 through Table 5.7. For three major waste components (Al_2O_3, Fe_2O_3, and ZrO_2) and five additive components (B_2O_3,

CaO, K_2O, Li_2O, and Na_2O) other than SiO_2, the base approach was to set the lower and upper limits slightly outside the range from Table 5.5 through Table 5.7. See notes in Table 5.8 for additional consideration for each component. For SiO_2, the lower limit was set slightly lower than the minimum from Table 5.5 through Table 5.7 like other additives but no upper limit was used as it is calculated as a balance.

For minor components (waste components other than Al_2O_3, Fe_2O_3, and ZrO_2), the base approach was to set the upper limit at least 1.5 times (150%) larger than the maximum from Table 5.5 through Table 5.7. However, smaller upper limits were used for those components that are considered troublesome and may affect the waste loading at higher concentrations, Cr_2O_3, F, P_2O_5, and SO_3. The lower limits for these minor components would be all zero if the similar approach as the upper limits is applied, i.e., to set the lower limit smaller than the minimum from Table 5.5 through Table 5.7. However, for all minor components except P_2O_5 and RuO_2, the lower limit was set at 0.001 so that the random generated concentration (see Section 5.2.3) is not too small for batching but close to zero. For P_2O_5, non-zero lower limit was used to reflect the fact that the minimum P_2O_5 from Table 5.5 through Table 5.7 was 0.007. For RuO_2, which is present at very low concentrations but may have impact on crystallization of glass, the upper and lower limits were set outside the range with a non-zero lower limit. Special care needs to be taken to batch the glasses with RuO_2 concentration close to the lower limit.

Table 5.8. Single Component Concentration Constraints Developed for Matrix Design

Comp.	Lower Limit	Upper Limit	Notes
Al_2O_3	0.18	0.26	Maximum Al_2O_3 loading achievable in glass was estimated to be ~26 wt%. Upper limit was set at 26 wt% based on the considerations that the practical maximum loading will be lower than this if various uncertainties are accounted for but the model should be valid above the practical maximum. Lower limit was set at 4 wt% below the minimum from Table 5.5 through Table 5.7 so that the resulting model can also cover the glasses with lower waste loadings potentially constrained by some other limiting components.
B_2O_3	0.14	0.22	Upper limit was set at the maximum from Table 5.5 through Table 5.7. Lower limit was set at 1 wt% below the minimum from Table 5.5 through Table 5.7.
Bi_2O_3	0.001	0.03	Upper limit was set at ≥150% of the maximum from Table 5.5 through Table 5.7.
CaO	0	0.1	Upper and lower limits were set ~1 wt% outside the concentration range from Table 5.5 through Table 5.7.
CdO	0.001	0.003	Upper limit was set three times higher than the WTP upper limit below which the model calculation is not required (0.1 wt% CdO) although the maximum expected is only 0.03 wt% from glasses in Table 5.5 through Table 5.7. This was to make the TCLP model, which uses Cd as major leach component, valid for high-Al_2O_3 glasses.
Cr_2O_3	0.001	0.013	Upper limit was set at ~110% of the maximum from Table 5.5 through Table 5.7.
F	0.001	0.01	Upper limit was set at ~130% of the maximum from Table 5.5 through Table 5.7.

Comp.	Lower Limit	Upper Limit	Notes
Fe_2O_3	0.01	0.07	Lower and upper limits were set slightly outside the range from Table 5.5 through Table 5.7. Setting the lower limit to zero was not considered because it is unlikely and there is a potential sudden change of glass properties with small addition of Fe_2O_3 compared to no-Fe glass.
K_2O	0	0.04	Upper limit was set at 1 wt% higher than the maximum from Table 5.5 through Table 5.7.
La_2O_3	0.001	0.01	Upper limit was set at ≥150% of the maximum from Table 5.5 through Table 5.7.
Li_2O	0	0.06	Upper limit was set slightly higher than the maximum from Table 5.5 through Table 5.7.
MgO	0.001	0.01	Upper limit was set at ≥150% of the maximum from Table 5.5 through Table 5.7.
MnO	0.001	0.015	Upper limit was set at ≥150% of the maximum from Table 5.5 through Table 5.7.
Na_2O	0.05	0.12	Lower and Upper limit were set slightly outside the range from Table 5.5 through Table 5.7 after excluding the glasses formulated for high Al/Na waste that had higher Na_2O than the glasses formulated for any high-Al wastes.
Nd_2O_3	0.001	0.002	Upper limit was set at ≥150% of the maximum from Table 5.5 through Table 5.7.
NiO	0.001	0.01	Upper limit was set at ≥150% of the maximum from Table 5.5 through Table 5.7.
P_2O_5	0.005	0.025	Upper limit was set at ~110% of the maximum from Table 5.5 through Table 5.7.
PbO	0.001	0.01	Upper limit was set at ≥150% of the maximum from Table 5.5 through Table 5.7.
RuO_2	0.00001	0.00005	Upper limit was set at ≥150% of the maximum from Table 5.5 through Table 5.7.
SiO_2	0.2	None	SiO_2 is calculated as a balance. Lower limit was set slightly lower than the minimum from Table 5.5 through Table 5.7 (too low a SiO_2 concentration may not produce reasonable glass). No upper limit was used.
SO_3	0.001	0.007	Upper limit was set at ~110% of the maximum from Table 5.5 through Table 5.7.
SrO	0.001	0.01	Upper limit was set at ≥150% of the maximum from Table 5.5 through Table 5.7.
ZrO_2	0	0.04	Lower and Upper limit were set slightly outside the range from Table 5.5 through Table 5.7.

From past formulation studies with the wastes that contain high concentration of refractory components (Al_2O_3, Fe_2O_3, and ZrO_2) (see Sections 4.1 and 4.3), it was found that the total concentration of these components play a role in liming waste loading in glass. The glass calculation approach discussed later in Section 5.2.3 can result in an unlikely high combined concentration of these components, which will be unlikely from actual formation for each waste cluster. To avoid testing glasses that are unlikely from each waste cluster, multicomponent constraints are applied as summarized in Table 5.9. Table 5.9 lists the maximum possible from maximum concentration of each component from single component constraints in Table 5.8 and the maximum in high-Al_2O_3 glasses listed in Table

5.5 through Table 5.7. The matrix constraint was set as the maximum in high- Al_2O_3 glasses except Fe_2O_3+ZrO_2 constraint because the maximum in high- Al_2O_3 glasses was found to be too restrictive during preliminary formulation trials.

To avoid formulating glasses that are too far away from the glass property requirements, the property constraints are used for key properties. The viscosity at 1150 °C and $T_{1\%}$ were selected as summarized in Table 5.10. Viscosity is a key processing property that represents the processing temperature. The upper limit for viscosity was set at two times the requirement maximum, and the lower limit was set at one fourth of the requirement minimum considering that the recent trend is to formulate the glasses at the lower end of the acceptable viscosity range to improve the melter processing rate. The upper limit for $T_{1\%}$ was set at 1175°C, which is 225°C higher than the 950°C requirement considering that the current model tends to over predict by roughly 60°C (Figure 5.1) and that the maximum measured $T_{1\%}$ in existing glasses was 1170°C (Table 5.4).

Table 5.9. Multicomponent Constraints Used in Matrix Design Compared with Maximum Possible[a] and Maximum in High-Al_2O_3 Glasses[b]

Components	Maximum Possible[a]	Maximum in High-Al_2O_3 Glasses[b]	Matrix Upper Limit
Al_2O_3+Fe_2O_3+ZrO_2	0.37	0.34	0.34
Al_2O_3+ Fe_2O_3	0.33	0.33	0.33
Al_2O_3+ ZrO_2	0.30	0.29	0.29
Fe_2O_3+ ZrO_2	0.11	0.07	0.08

[a] Maximum possible from maximum concentration of each component from single component constraints in Table 5.8.
[b] Maximum value in the high-Al_2O_3 glasses listed in Table 5.5 through Table 5.7.

Table 5.10. Property Constraints Used in Matrix Design Compared with Their Requirements

Property	Requirements		Matrix Constraints	
	Min	Max	Lower Limit	Upper Limit
Predicted η_{1150}, Pa·s	2	8	0.5	16
Predicted $T_{1\%}$, °C		950		1175

Comparing the matrix design constraints summarized above with the existing glasses given in Table 5.4 revealed that eight glasses are outside the matrix constraints leaving only six glasses for use in the design of a new matrix. The six glasses that meet matrix design constraints are presented in Table 5.11.

Table 5.11. Existing High-Al_2O_3 Glasses That Have Measured $T_{1\%}$ Data and Meet Matrix Design Constraints

Reference	Matlack et al. (2007a)	Matlack et al. (2008)				
Glass ID	**HLW-E-Al-27**	**HWI-AL-7**	**HWI-AL-13**	**HWI-AL-17**	**HWI-AL-18(G)**	**HWI-AL-19**
Al_2O_3	0.23971	0.23970	0.23970	0.23250	0.22570	0.23970
B_2O_3	0.15190	0.15190	0.15190	0.14730	0.20130	0.19190
BaO	0.00054	0.00050	0.00050	0.00050	0.00050	0.00050
Bi_2O_3	0.01145	0.01140	0.01140	0.01110	0.01080	0.01140
CaO	0.06076	0.03080	0.06080	0.05890	0.05720	0.05580
CdO	0.00024	0.00020	0.00020	0.00020	0.00020	0.00020
Cr_2O_3	0.00521	0.00520	0.00520	0.00510	0.00490	0.00520
F	0.00667	0.00670	0.00670	0.00650	0.00630	0.00670
Fe_2O_3	0.05899	0.05900	0.05900	0.05720	0.05560	0.05900
K_2O	0.00141	0.00140	0.04140	0.03140	0.00130	0.00140
Li_2O	0.03571	0.03570	0.03570	0.03460	0.03360	0.03570
MgO	0.00117	0.03120	0.00120	0.00110	0.00110	0.00120
Na_2O	0.09580	0.09580	0.06080	0.09290	0.09020	0.09580
NiO	0.00400	0.00400	0.00400	0.00390	0.00380	0.00400
P_2O_5	0.01052	0.01050	0.01050	0.01020	0.00990	0.01050
PbO	0.00409	0.00410	0.00410	0.00400	0.00390	0.00410
SiO_2	0.30496	0.30500	0.30000	0.29580	0.28720	0.27000
SO_3	0.00200	0.00200	0.00200	0.00190	0.00190	0.00200
TiO_2	0.00010	0.00010	0.00010	0.00010	0.00010	0.00010
ZnO	0.00083	0.00080	0.00080	0.00080	0.00080	0.00080
ZrO_2	0.00395	0.00390	0.00390	0.00380	0.00370	0.00390
Total	1	1	1	1	1	1
Measured T1%						
$T_{1\%}$-Sp, °C	953	1144	1066	960	968	969
Predicted properties (Vienna et a. 2009)						
η_{1150}, Pa.s	5.17	6.13	5.91	4.33	3.76	3.39
T at 5 Pas, °C	1154	1173	1171	1132	1116	1103
$T_{1\%}$-Sp, °C	1078	1173	1084	1033	1004	1051
Nepheline formation criteria						
Si/(Si+Al+Na)	0.476	0.476	0.500	0.476	0.476	0.446
Optical basicity	0.577	0.578	0.578	0.585	0.562	0.569

5.2.3 Calculation of Candidate Glasses

Glass composition is calculated applying the random number

$$g_i = g_i^{min} + R_i(g_i^{max} - g_i^{min}), i \neq \mathrm{SiO_2} \tag{5.1}$$

$$g_{SiO_2} = 1 - \sum_{i=1}^{n-1} g_i \tag{5.2}$$

where g_i is the mass fraction of i^{th} component in the candidate glass, R_i is the random number between 0 and 1 for i^{th} component, g_i^{max} and g_i^{min} are the maximum and minimum concentrations for i^{th} component defined for matrix design (Table 5.8). From as-calculated glasses resulting from Equations 5.1 and 5.2, the glasses that satisfy the minimum SiO_2 requirement, the multicomponent constraints (Table 5.9), and property constraints (Table 5.10) calculated using the glass model (Vienna et al 2009) are selected as candidate glasses for matrix design. After generating 94 as-calculated glasses, 50 candidate glasses that meet all the constraints were selected. In addition, a centroid glass was calculated as:

$$g_i^{centroid} = \frac{(g_i^{max} + g_i^{min})}{2}, i \neq \mathrm{SiO_2} \tag{5.3}$$

$$g_{SiO_2}^{centroid} = 1 - \sum_{i=1}^{n-1} g_i^{centroid} \tag{5.4}$$

where $g_i^{centroid}$ is the mass fraction of i^{th} component in the centroid glass. In Appendix D Table D.1 lists the composition of these 51 candidate glasses and their predicted properties including the two key properties that were used for property constraints (viscosity, $T_{1\%}$), electrical conductivity, temperature at 5 Pa·s that is used as reference temperature for crucible glass melting, and nepheline criteria.

5.2.4 Selection of Matrix Glasses

To further select matrix glasses two steps of calculating the normalized distances between the candidate glasses and existing glasses and between candidate glasses were performed. The normalized distance between two glasses was defined as:

$$d^{x,y} = \sqrt{\sum_{i=1}^{n} \frac{\left(g_i^x - g_i^y\right)^2}{\sigma_i^2}} \tag{5.5}$$

where g_i^x and g_i^y are the mass fraction of i^{th} component in two glasses "x" and "y", $d^{x,y}$ is the normalized distance between two glasses, σ_i is the standard deviation of i^{th} component mass fraction over the candidate glasses. The normalized distance was calculated based on nine major components only including three major waste components (Al_2O_3, Fe_2O_3, and ZrO_2) and six additive components (B_2O_3, CaO, K_2O, Li_2O, Na_2O, and SiO_2). The selection process removed initially eight glasses that had distances $d^{x,y} < 2.27$ between existing and candidate glasses and then 11 glasses that had $d^{x,y} < 2.27$ between remaining candidate glasses. This resulted in 32 independent glasses as a test matrix including one centroid glass. Table 5.12 lists the composition of these 32 matrix glasses and their predicted properties. The IWL-HAM in the glass identification (ID) column represents "improved waste loading-high-alumina matrix."

Table 5.12. Composition and Predicted Properties of 32 Matrix Glasses

Glass ID	IWL-HAM-01	IWL-HAM-02	IWL-HAM-03	IWL-HAM-04	IWL-HAM-05	IWL-HAM-06	IWL-HAM-07	IWL-HAM-08	IWL-HAM-09
# in Table D.1	**4**	**5**	**6**	**7**	**9**	**10**	**11**	**12**	**13**
Al_2O_3	0.19789	0.18136	0.19367	0.18392	0.18969	0.23499	0.19171	0.20149	0.21108
B_2O_3	0.14580	0.14241	0.21385	0.20329	0.17301	0.15461	0.14234	0.17230	0.21673
Bi_2O_3	0.01046	0.01932	0.02111	0.00497	0.00419	0.02037	0.01789	0.00427	0.00756
CaO	0.05825	0.07286	0.01180	0.01083	0.08416	0.03888	0.08265	0.09341	0.03618
CdO	0.00199	0.00242	0.00102	0.00267	0.00131	0.00228	0.00166	0.00145	0.00109
Cr_2O_3	0.00441	0.00583	0.01206	0.00461	0.00779	0.01261	0.01269	0.00899	0.00254
F	0.00439	0.00966	0.00353	0.00724	0.00985	0.00889	0.00900	0.00777	0.00693
Fe_2O_3	0.02316	0.02644	0.03043	0.04174	0.04938	0.01012	0.04468	0.05142	0.06467
K_2O	0.02855	0.01360	0.00433	0.01283	0.02501	0.01394	0.02792	0.03371	0.01755
La_2O_3	0.00270	0.00543	0.00200	0.00221	0.00139	0.00454	0.00764	0.00548	0.00352
Li_2O	0.01344	0.04822	0.01322	0.04986	0.05272	0.03145	0.05455	0.04188	0.05106
MgO	0.00955	0.00465	0.00917	0.00583	0.00900	0.00816	0.00787	0.00838	0.00428
MnO	0.01184	0.00949	0.00589	0.00343	0.01432	0.00420	0.00541	0.01193	0.00397
Na_2O	0.08455	0.09204	0.11495	0.05159	0.05268	0.05440	0.06146	0.08187	0.08884
Nd_2O_3	0.00130	0.00151	0.00109	0.00183	0.00178	0.00154	0.00160	0.00176	0.00140
NiO	0.00118	0.00477	0.00695	0.00393	0.00525	0.00279	0.00649	0.00572	0.00788
P_2O_5	0.00544	0.01928	0.02142	0.01828	0.00653	0.00888	0.01412	0.01120	0.01132
PbO	0.00108	0.00839	0.00576	0.00158	0.00521	0.00934	0.00405	0.00366	0.00515
RuO_2	0.00001	0.00002	0.00004	0.00005	0.00003	0.00003	0.00005	0.00002	0.00004
SiO_2	0.35733	0.27966	0.27634	0.35169	0.27566	0.36647	0.29425	0.23356	0.24027
SO_3	0.00433	0.00690	0.00516	0.00221	0.00389	0.00537	0.00578	0.00482	0.00384
SrO	0.00291	0.00880	0.00738	0.00899	0.00358	0.00110	0.00254	0.00797	0.00743
ZrO_2	0.02944	0.03693	0.03884	0.02641	0.02356	0.00504	0.00366	0.00692	0.00666
Total	1	1	1	1	1	1	1	1	1
Multicomponent constraints									
Al_2O_3+Fe_2O_3+ZrO_2	0.25049	0.24473	0.26294	0.25208	0.26263	0.25015	0.24004	0.25983	0.28241
Al_2O_3+ Fe_2O_3	0.22105	0.20780	0.22410	0.22566	0.23907	0.24511	0.23639	0.25291	0.27576
Al_2O_3+ ZrO_2	0.22733	0.21829	0.23251	0.21033	0.21325	0.24003	0.19536	0.20841	0.21774
Fe_2O_3+ ZrO_2	0.05260	0.06337	0.06926	0.06816	0.07294	0.01516	0.04834	0.05834	0.07133
Predicted properties (Vienna et a. 2009)									
η_{1150}, Pa.s	14.06	1.25	6.38	6.27	1.22	13.86	1.37	0.84	1.13
T at 5 Pas, °C	1268.5	1008.1	1174.0	1175.2	1000.9	1263.7	1005.2	958.7	970.0
$T_{1\%}$-Sp, °C	940.3	940.5	1047.8	919.7	1064.7	1074.3	1088.6	1063.4	989.6
ε_{1150}, S/m	11.4	33.4	19.4	22.9	26.6	12.5	29.7	27.6	37.0
Nepheline formation criteria									
N_{Si}	0.559	0.506	0.472	0.599	0.532	0.559	0.538	0.452	0.445
OB	0.572	0.594	0.556	0.542	0.585	0.553	0.591	0.599	0.571

Table 5.12. (Continued)

Glass ID	IWL-HAM-10	IWL-HAM-11	IWL-HAM-12	IWL-HAM-13	IWL-HAM-14	IWL-HAM-15	IWL-HAM-16	IWL-HAM-17	IWL-HAM-18
# in Table D.1	**15**	**17**	**20**	**24**	**25**	**26**	**28**	**29**	**32**
Al_2O_3	0.24868	0.23021	0.22837	0.20646	0.23783	0.21598	0.25920	0.22360	0.19754
B_2O_3	0.16750	0.14291	0.20640	0.19927	0.21524	0.17618	0.17329	0.14351	0.18371
Bi_2O_3	0.01494	0.01832	0.01096	0.00254	0.02269	0.02731	0.02311	0.01774	0.01686
CaO	0.09086	0.03119	0.01669	0.01140	0.01549	0.02327	0.04830	0.08156	0.07407
CdO	0.00250	0.00280	0.00231	0.00207	0.00150	0.00290	0.00134	0.00203	0.00190
Cr_2O_3	0.00145	0.00249	0.00279	0.00532	0.00402	0.00332	0.00250	0.00141	0.00581
F	0.00438	0.00412	0.00622	0.00330	0.00769	0.00166	0.00483	0.00140	0.00723
Fe_2O_3	0.01824	0.02279	0.01911	0.01206	0.04794	0.04081	0.04805	0.05170	0.02006
K_2O	0.03933	0.00208	0.00552	0.03972	0.01975	0.00898	0.03015	0.01435	0.01799
La_2O_3	0.00946	0.00315	0.00542	0.00849	0.00871	0.00711	0.00563	0.00935	0.00599
Li_2O	0.01622	0.02545	0.04925	0.05421	0.01723	0.05977	0.02536	0.01570	0.03318
MgO	0.00422	0.00990	0.00225	0.00885	0.00221	0.00508	0.00824	0.00517	0.00771
MnO	0.00443	0.00704	0.00679	0.00705	0.00570	0.00517	0.00622	0.01193	0.00915
Na_2O	0.11700	0.11996	0.07708	0.09176	0.09241	0.05072	0.08094	0.05236	0.11334
Nd_2O_3	0.00107	0.00130	0.00154	0.00181	0.00168	0.00138	0.00114	0.00133	0.00135
NiO	0.00461	0.00308	0.00203	0.00619	0.00930	0.00159	0.00635	0.00921	0.00106
P_2O_5	0.01070	0.01515	0.00888	0.02045	0.01940	0.00998	0.00867	0.02067	0.02144
PbO	0.00852	0.00816	0.00626	0.00288	0.00489	0.00788	0.00531	0.00382	0.00371
RuO_2	0.00003	0.00002	0.00005	0.00005	0.00004	0.00001	0.00002	0.00005	0.00004
SiO_2	0.21230	0.31257	0.31536	0.28230	0.22645	0.32795	0.24242	0.30693	0.25504
SO_3	0.00428	0.00556	0.00138	0.00113	0.00565	0.00142	0.00219	0.00146	0.00254
SrO	0.00869	0.00411	0.00576	0.00330	0.00990	0.00386	0.00321	0.00659	0.00304
ZrO_2	0.01061	0.02762	0.01958	0.02941	0.02426	0.01767	0.01353	0.01815	0.01726
Total	1	1	1	1	1	1	1	1	1
Multicomponent constraints									
Al_2O_3+Fe_2O_3+ZrO_2	0.27753	0.28062	0.26705	0.24792	0.31003	0.27447	0.32077	0.29345	0.23486
Al_2O_3+ Fe_2O_3	0.26692	0.25300	0.24748	0.21851	0.28577	0.25680	0.30724	0.27530	0.21760
Al_2O_3+ ZrO_2	0.25929	0.25783	0.24794	0.23586	0.26209	0.23365	0.27273	0.24175	0.21480
Fe_2O_3+ ZrO_2	0.02885	0.05041	0.03869	0.04147	0.07220	0.05848	0.06158	0.06985	0.03732
Predicted properties (Vienna et a. 2009)									
η_{1150}, Pa.s	2.15	7.94	4.51	2.11	5.93	4.07	5.33	12.05	1.37
T at 5 Pas, °C	1055.0	1197.2	1138.6	1046.2	1167.9	1128.4	1157.3	1246.3	1006.4
$T_{1\%}$-Sp, °C	943.9	973.5	880.2	875.2	1100.3	958.8	1131.1	1172.4	858.9
ε_{1150}, S/m	20.9	23.1	27.5	38.1	16.9	29.9	16.5	8.5	29.9
Nepheline formation criteria									
N_{Si}	0.367	0.472	0.508	0.486	0.407	0.552	0.416	0.527	0.451
OB	0.603	0.577	0.551	0.569	0.561	0.560	0.583	0.575	0.585

Table 5.12. (Continued)

Glass ID	IWL-HAM-19	IWL-HAM-20	IWL-HAM-21	IWL-HAM-22	IWL-HAM-23	IWL-HAM-24	IWL-HAM-25	IWL-HAM-26	IWL-HAM-27
# in Table D.1	**35**	**37**	**38**	**39**	**40**	**41**	**44**	**45**	**46**
Al_2O_3	0.25384	0.18696	0.24973	0.25923	0.19551	0.20295	0.22875	0.20433	0.23901
B_2O_3	0.18840	0.19466	0.21567	0.16126	0.17537	0.21556	0.18993	0.21262	0.20708
Bi_2O_3	0.02508	0.00888	0.02257	0.02873	0.01883	0.02486	0.00362	0.00120	0.01926
CaO	0.02794	0.05617	0.03965	0.08985	0.01745	0.05148	0.09434	0.08060	0.00733
CdO	0.00202	0.00251	0.00216	0.00102	0.00204	0.00286	0.00178	0.00219	0.00198
Cr_2O_3	0.00394	0.00320	0.00370	0.00897	0.00726	0.00328	0.00946	0.00279	0.01071
F	0.00217	0.00980	0.00147	0.00188	0.00957	0.00460	0.00981	0.00315	0.00173
Fe_2O_3	0.03159	0.02524	0.01244	0.01168	0.06158	0.03107	0.02764	0.03774	0.06817
K_2O	0.01369	0.01467	0.01795	0.00203	0.03183	0.03983	0.03979	0.02951	0.02445
La_2O_3	0.00693	0.00549	0.00738	0.00854	0.00761	0.00164	0.00990	0.00875	0.00512
Li_2O	0.03347	0.02312	0.04004	0.01320	0.00348	0.04628	0.02464	0.03715	0.03556
MgO	0.00242	0.00182	0.00913	0.00890	0.00275	0.00259	0.00465	0.00619	0.00158
MnO	0.00130	0.01071	0.00605	0.00776	0.01301	0.00187	0.01484	0.01187	0.00525
Na_2O	0.10604	0.06551	0.11328	0.10069	0.09427	0.06020	0.05154	0.07742	0.11187
Nd_2O_3	0.00132	0.00170	0.00197	0.00193	0.00193	0.00146	0.00183	0.00160	0.00165
NiO	0.00311	0.00229	0.00729	0.00297	0.00189	0.00998	0.00422	0.00800	0.00483
P_2O_5	0.01457	0.00758	0.01995	0.01314	0.01682	0.01568	0.00575	0.01459	0.01985
PbO	0.00420	0.00484	0.00259	0.00601	0.00222	0.00825	0.00334	0.00280	0.00497
RuO_2	0.00004	0.00004	0.00001	0.00002	0.00004	0.00003	0.00002	0.00005	0.00002
SiO_2	0.24743	0.34072	0.21303	0.25942	0.31453	0.26192	0.25280	0.20954	0.21784
SO_3	0.00402	0.00165	0.00604	0.00688	0.00195	0.00568	0.00126	0.00475	0.00245
SrO	0.00125	0.00896	0.00270	0.00213	0.00506	0.00412	0.00963	0.00452	0.00921
ZrO_2	0.02524	0.02348	0.00520	0.00377	0.01501	0.00382	0.01046	0.03866	0.00008
Total	1	1	1	1	1	1	1	1	1
Multicomponent constraints									
Al_2O_3+Fe_2O_3+ZrO_2	0.31066	0.23568	0.26736	0.27468	0.27209	0.23784	0.26685	0.28073	0.30727
Al_2O_3+ Fe_2O_3	0.28543	0.21220	0.26217	0.27091	0.25708	0.23402	0.25639	0.24207	0.30718
Al_2O_3+ ZrO_2	0.27907	0.21045	0.25493	0.26300	0.21052	0.20677	0.23921	0.24299	0.23909
Fe_2O_3+ ZrO_2	0.05683	0.04872	0.01763	0.01545	0.07659	0.03489	0.03810	0.07640	0.06826
Predicted properties (Vienna et a. 2009)									
η_{1150}, Pa.s	4.68	6.95	1.72	6.21	12.89	1.69	3.09	1.25	2.28
T at 5 Pas, °C	1142.5	1185.2	1016.6	1175.3	1252.2	1027.3	1092.6	1005.0	1048.8
$T_{1\%}$-Sp, °C	999.4	874.1	950.8	1095.9	1021.7	923.3	1085.0	1007.0	1101.7
ε_{1150}, S/m	26.4	12.5	34.3	14.4	12.1	25.0	12.0	23.6	33.8
Nepheline formation criteria									
N_{Si}	0.407	0.574	0.370	0.419	0.520	0.499	0.474	0.427	0.383
OB	0.573	0.553	0.574	0.582	0.562	0.563	0.580	0.584	0.574

Table 5.12. (Continued)

Glass ID	IWL-HAM-28	IWL-HAM-29	IWL-HAM-30	IWL-HAM-31	IWL-HAM-32	Min	Max
# in Table D.1	47	48	49	50	Centroid		
Al_2O_3	0.22314	0.21019	0.24000	0.23315	0.22000	0.18136	0.25923
B_2O_3	0.21072	0.20103	0.16638	0.17948	0.18000	0.14234	0.21673
Bi_2O_3	0.00628	0.00773	0.02974	0.00419	0.01550	0.00120	0.02974
CaO	0.07134	0.04770	0.09639	0.01832	0.05000	0.00733	0.09639
CdO	0.00267	0.00229	0.00127	0.00220	0.00200	0.00102	0.00290
Cr_2O_3	0.00572	0.01119	0.00144	0.00697	0.00700	0.00141	0.01269
F	0.00272	0.00841	0.00853	0.00120	0.00550	0.00120	0.00985
Fe_2O_3	0.02998	0.01140	0.03177	0.01732	0.04000	0.01012	0.06817
K_2O	0.03183	0.01091	0.02879	0.02906	0.02000	0.00203	0.03983
La_2O_3	0.00227	0.00365	0.00266	0.00810	0.00550	0.00139	0.00990
Li_2O	0.00803	0.04206	0.04598	0.03927	0.03000	0.00348	0.05977
MgO	0.00472	0.00842	0.00825	0.00781	0.00550	0.00158	0.00990
MnO	0.00491	0.01114	0.00786	0.00992	0.00800	0.00130	0.01484
Na_2O	0.09668	0.10029	0.07741	0.05257	0.08500	0.05072	0.11996
Nd_2O_3	0.00198	0.00103	0.00167	0.00147	0.00150	0.00103	0.00198
NiO	0.00172	0.00294	0.00905	0.00643	0.00550	0.00106	0.00998
P_2O_5	0.00902	0.02250	0.00564	0.01955	0.01500	0.00544	0.02250
PbO	0.00183	0.00109	0.00897	0.00279	0.00550	0.00108	0.00934
RuO_2	0.00004	0.00005	0.00002	0.00002	0.00003	0.00001	0.00005
SiO_2	0.23658	0.25727	0.20686	0.31925	0.26897	0.20686	0.36647
SO_3	0.00660	0.00501	0.00344	0.00499	0.00400	0.00113	0.00690
SrO	0.00888	0.00141	0.00781	0.00608	0.00550	0.00110	0.00990
ZrO_2	0.03235	0.03230	0.01006	0.02986	0.02000	0.00008	0.03884
Total	1	1	1	1	1	1	1
Multicomponent constraints							
Al_2O_3+Fe_2O_3+ZrO_2	0.28547	0.25388	0.28183	0.28032	0.28000	0.23486	0.32077
Al_2O_3+ Fe_2O_3	0.25312	0.22159	0.27177	0.25046	0.26000	0.20780	0.30724
Al_2O_3+ ZrO_2	0.25549	0.24249	0.25006	0.26301	0.24000	0.19536	0.27907
Fe_2O_3+ ZrO_2	0.06233	0.04369	0.04184	0.04717	0.06000	0.01516	0.07659
Predicted properties (Vienna et a. 2009)							
η_{1150}, Pa.s	5.16	1.99	0.84	10.68	3.72	0.84	14.06
T at 5 Pas, °C	1153.5	1043.8	964.7	1237.4	1117.1	958.7	1268.5
$T_{1\%}$-Sp, °C	969.2	968.8	1057.6	1066.5	1057.3	858.9	1172.4
ε_{1150}, S/m	13.7	31.2	28.0	16.4	19.7	8.5	38.1
Nepheline formation criteria							
N_{Si}	0.425	0.453	0.395	0.528	0.469	0.367	0.599
OB	0.573	0.570	0.606	0.555	0.574	0.542	0.606

Figure 5.2 show the range of concentrations for nine major components and major predicted properties. There are four set of glasses: 94 as-formulated glasses, 51 candidate glasses that meet all the matrix design constraints, six existing glasses that meet all the matrix design constraints, and 32 matrix glasses, showing the change of glass composition and property coverage with the progress of matrix design. Figure 5.3 through Figure 5.5 show the scatter plots for all as formulated glasses (Figure 5.3), matrix glasses only (Figure 5.4), and matrix and existing glasses (Figure 5.5).

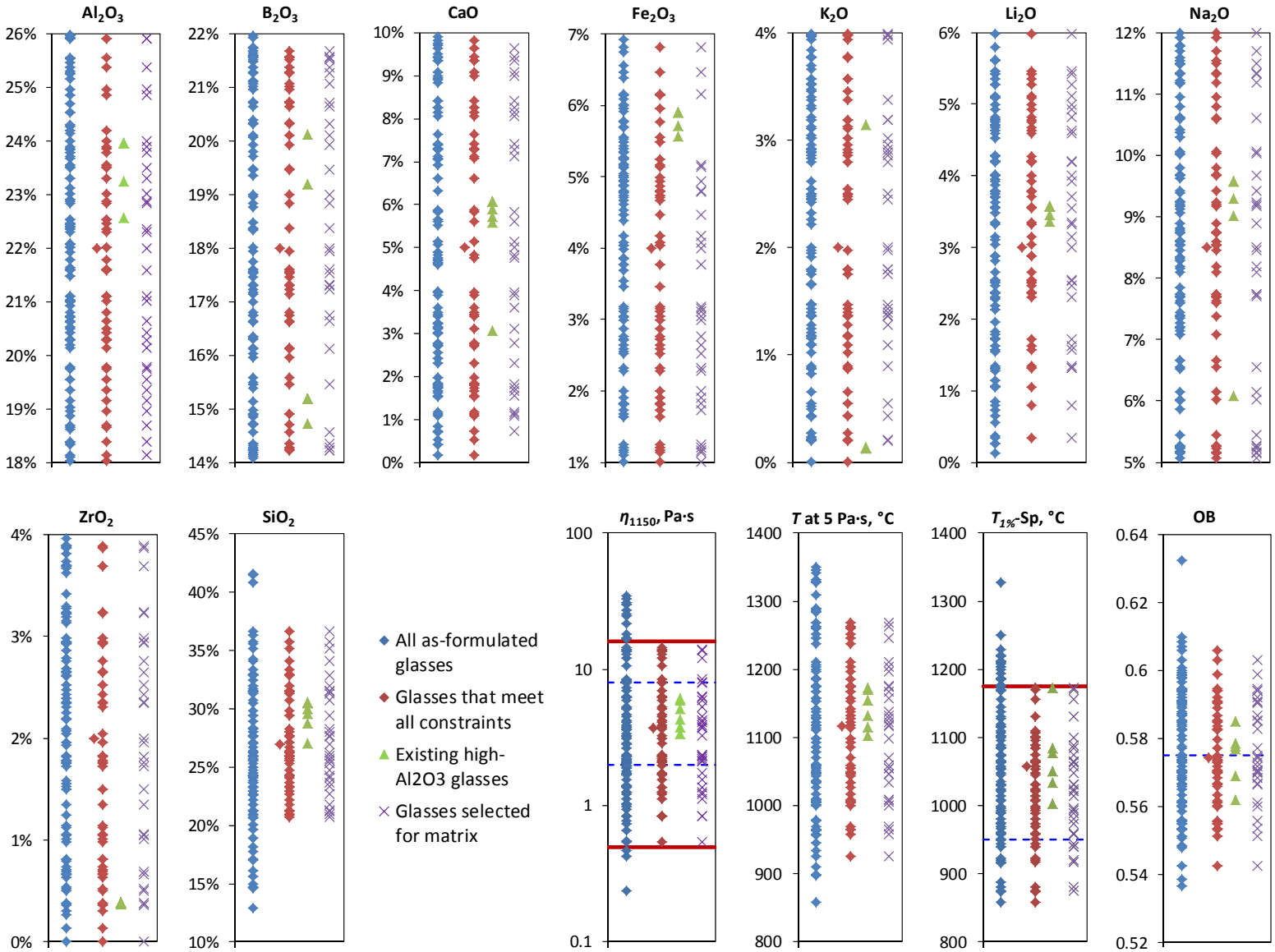

Figure 5.2. Concentration and Predicted Property Range

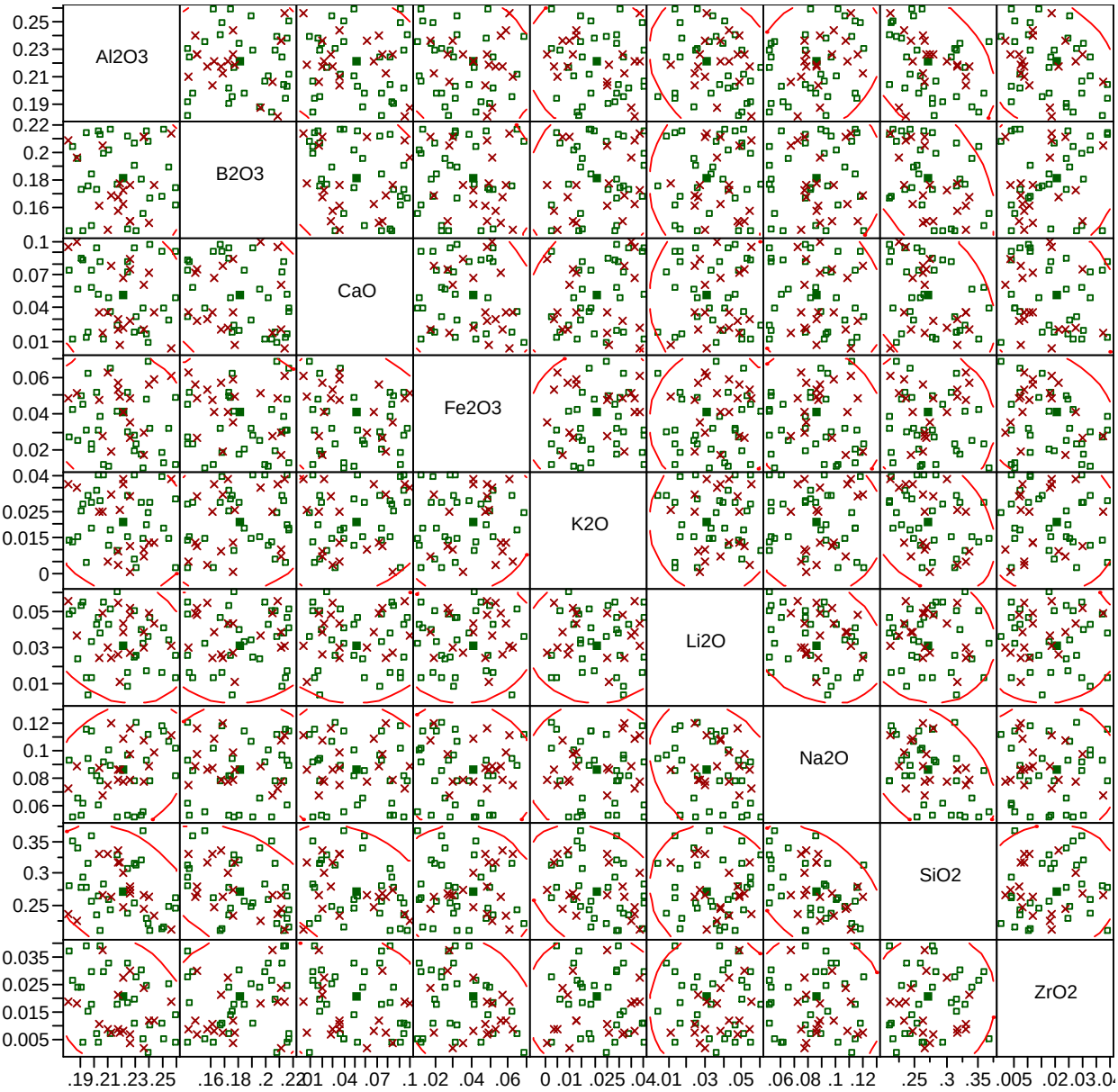

Figure 5.3. Scatter Plot for All Candidate Glasses (Square: selected, X: deleted)

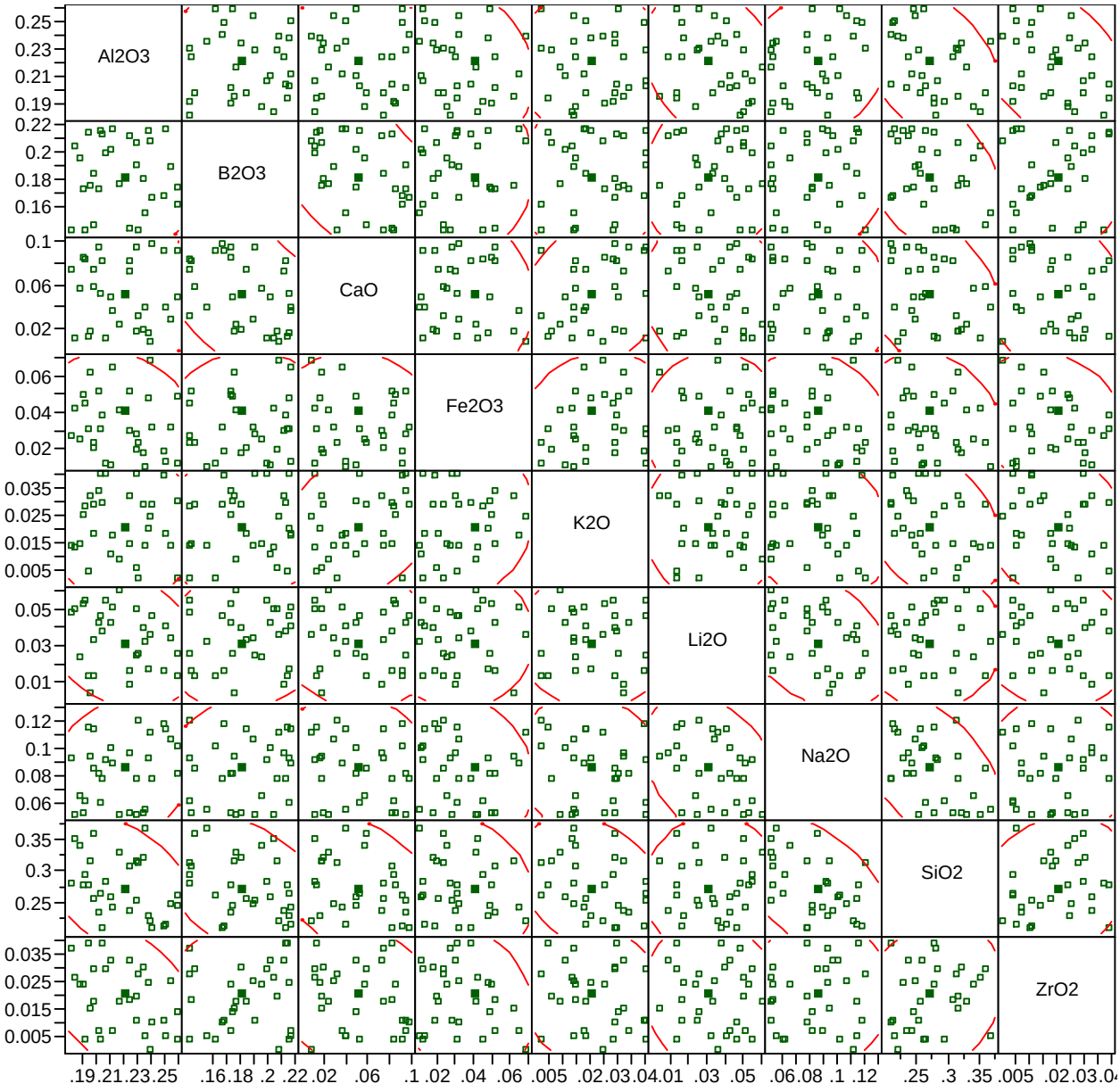

Figure 5.4. Scatter Plot for Matrix Glasses

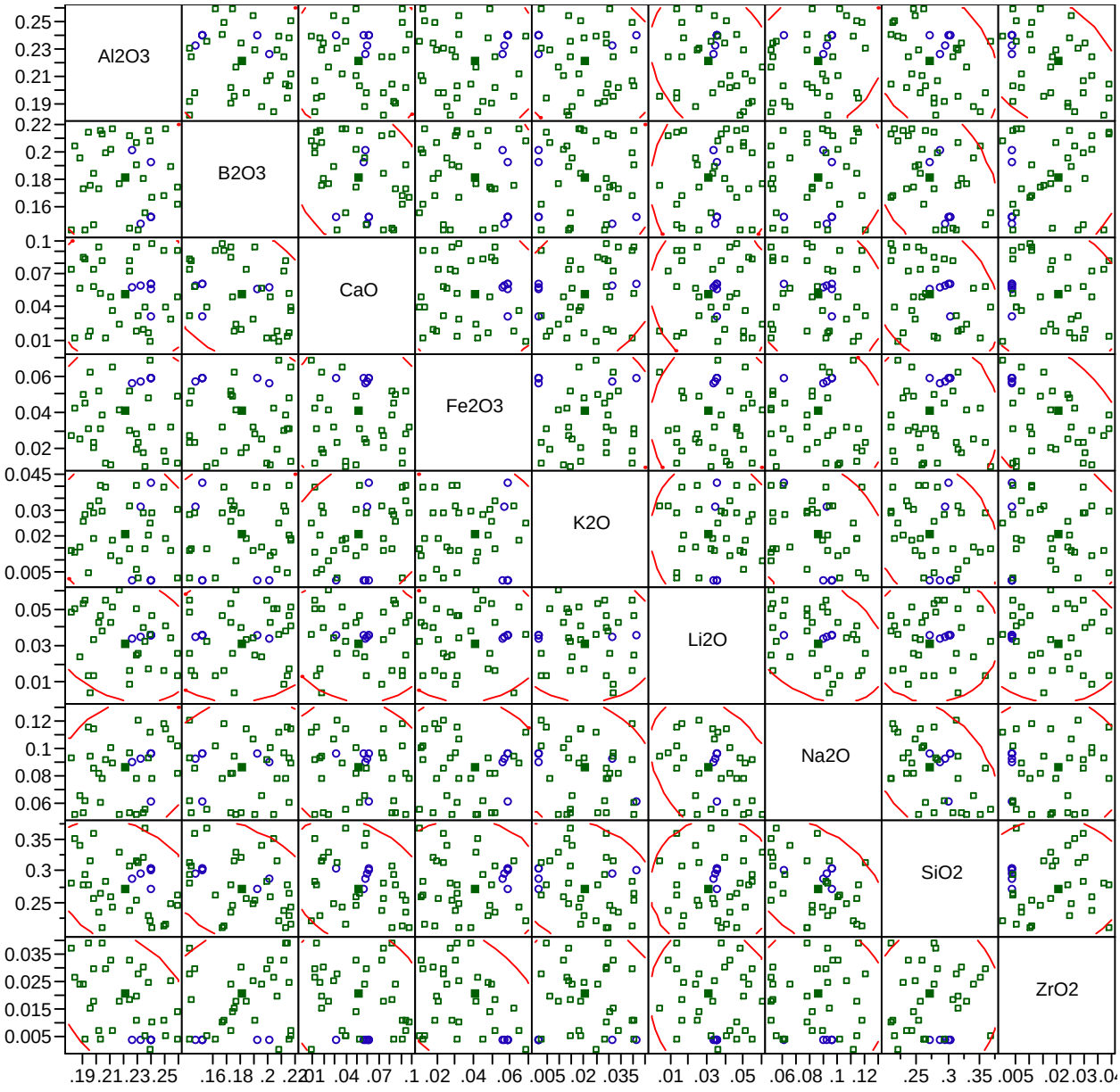

Figure 5.5. Scatter Plot for Matrix and Existing Glasses (Square: matrix, Circle: existing)

6.0 Conclusions

The glass formulation and testing results achieved from the finished scope of the EM-31 technology development tasks for WP-4 and WP-5 are summarized and future work for continued glass formulation development are recommended.

6.1 Summary of Glass Formulation for Cold Crucible Induction Melter (WP-4.1.2)

From glass formulation and testing with AZ-101 simulated HLW, the three glasses, CCIM-AZ-29, CCIM-AZ-16, and CCIM-AZ-10, were selected for the initial CCIM demonstration. The target Fe_2O_3 concentration and waste loading of these glasses are summarized in Figure 6.1.

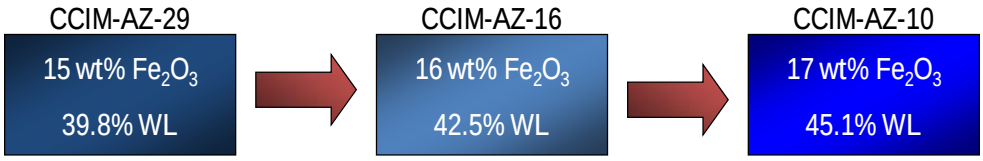

Figure 6.1. Fe_2O_3 Concentration and Waste Loading in Three AZ-101 Glasses Selected for Initial CCIM Demonstration Testing from This Study

The CCIM-AZ-10 glass at 45.1 wt% waste loading corresponds to a 22% increase from 37 wt%, which is the maximum waste loading that is likely to be achieved based on expected reference WTP formulation. However, it involves the assumption that the high-waste loaded glass with more crystals can be successfully processed in the CCIM, which needs be demonstrated. The recommended nominal processing temperature for all three glasses is 1200 °C based on a measured viscosity of 4 Pa·s for all three glasses. The measured electrical conductivities at 1200 °C is 30 S/m, 24 S/m, and 21 S/m for CCIM-AZ-29, 16, and 10 glasses, respectively, which are within the desired range of 10 to 100 S/m. All three glasses meet the PCT and TCLP requirements regardless of thermal history (quenched or CCC treated glasses).

The CCIM tests with AZ-101-simulated HLW were planned to start with the CCIM-AZ-29 glass to evaluate the glass melting characteristics (e.g., processing rates, cold cap behavior, pour stability, etc.) at lower waste loading (39.8 wt%). When successful at this waste loading (39.8 wt%), it was planned to make a transition to target the higher waste loaded (42.5 wt%) CCIM-AZ-16 glass, and then ultimately the CCIM-AZ-10 (45.1 wt%) glass. In this approach, the capability of CCIM technologies to tolerate the crystals in the melt, which increases as the waste loading increases (summarized in Figure 6.2), can be evaluated. Preparation of melter feeds was completed but the demonstration melter run was not started before the closure of the project.

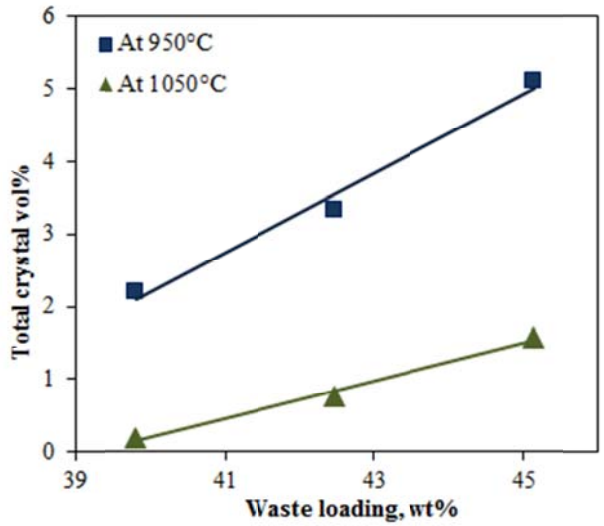

Figure 6.2. Total Crystal Vol% As a Function of Waste Loading for Selected Three Glasses

From initial glass formulation and testing with AN-105 simulated LAW, the CCIM-AN-18 glass targeting 24 wt% Na_2O with a waste loading of 31.3 wt% was selected for the initial CCIM demonstration test. This waste loading is a 14% increase from the reference WTP formulation maximum of 21 wt% Na_2O in glass. The 24 wt% Na_2O loading was also achieved by ORPLA20 glass that was developed by ORP for processing at 1150 °C and was demonstrated to have good processing characteristics. The recommended nominal processing temperature for CCIM-AN-18 glass is 1250°C, based on a measured viscosity of ~4 Pa·s. The measured electrical conductivity at 1250°C is 53 S/m, which is within the recommended range of 10 S/m to 100 S/m. The CCIM-AN-18 glass meets the PCT and VHT requirements for both quenched and CCC-treated glasses. This work was discontinued during the preparation for demonstration CCIM tests and melter feeds were not prepared.

Additional glass development efforts with AN-105-simulated LAW successfully formulated acceptable glasses containing up to 26 wt% Na_2O before the closure of this project. The present results of PCT and VHT from the glasses with 24 wt% to 26 wt% Na_2O suggest that it may be possible to formulate acceptable glasses containing even higher than 26 wt% Na_2O. Therefore, when the project restarts, the CCIM tests will be performed with the newly developed glasses containing ≥26 wt% Na_2O rather than CCIM-AN-18.

The high waste loading (up to 26 wt% Na_2O) achieved in this study with AN-105 is attributed to two factors: (1) finding of new composition region with good VHT performance and (2) use of higher temperature. The information on the effect of glass composition on PCT and VHT gained from the present study for the AN-105 LAW glasses melting at ≥ 1200°C can also be used to formulate higher waste loaded glasses for the baseline WTP melter operated at 1150°C.

After completing the initial formulations with AZ-101 HLW and AN-105 LAW, glass formulations for CCIM were expanded to cover the additional HLWs that have a high potential to successfully demonstrate the unique advantages of the CCIM technologies. The selected two waste groups were spinel-limited and high-chromium wastes. Only the preliminary scoping tests were completed with these wastes to find the maximum waste loadings at which reasonable glass can be made without severe

crystallization (for spinel-limited wastes) or salt formation (for high-chromium waste) so that they can be used for glass property characterization.

For spinel-limited wastes, the maximum concentrations of Al_2O_3+Fe_2O_3+ZrO_2 that can be in glass without severe crystallization ranged from 27 wt% to 35 wt% (corresponding to 52.5 wt% to 68.8 wt% waste loading). These Al_2O_3+Fe_2O_3+ZrO_2 loading are significantly higher than those predicted as maximum based on revised HTWOS constraints, which ranged from 19.8 wt% to 25.5 wt%. For high-chromium waste, the glasses without salt formation were successfully formulated at 3 wt% and 3.5 wt% Cr_2O_3 so that they can be used for further characterization to determine the estimated maximum waste loading to be evaluated through scaled melter tests.

6.2 Summary of Advanced Silicate Glass Development (WP-5.1.2)

For glass formulations for specific wastes, limited testing with high-iron, spinel-limited, and high-aluminum waste clusters was completed before the closure of the project. Additional iterations of glass formulation and property testing are needed to determine the estimated maximum waste loading for these waste clusters. The incomplete results from this first initial iteration are summarized in this report for eventual restart of the task. For high-iron waste clusters, the loading of Al_2O_3+Fe_2O_3+ZrO_2 in glasses for Cluster 1 will be higher than 22.7 wt%, based on one successful glass formulated with 0.6 vol% spinel at 950°C. However, no successful glass resulted from the first set of glasses formulated for Cluster 18. Among three high-aluminum clusters, one glass for Cluster 16 (IWL-HAC16-5) passed both the $T_{1\%}$ requirement and CCC crystallinity requirements.

For systematic glass studies, a test matrix of 32 high-aluminum glasses was generated based on a new space filling method developed in this study. The new matrix approach involves formulating random-generated glasses within the predetermined single component constraints, and then sorting out the glasses outside the multicomponent and property constraints and the glasses that have compositions close to each other. The development of test matrix was described in detail for eventual restart of the project and for application to similar matrices for glasses with different composition regions, e.g., high-iron or spinel-limited glasses.

6.3 Suggested Studies

Suggested studies are briefly summarized as below.

Formulation of CCIM Glasses Melting at >1200°C

- Perform CCIM demonstration tests with three AZ-101 glasses selected.
- Perform additional crucible tests to determine the maximum Na_2O loading in AN-105 glasses, select a new glass (with higher Na_2O than CCIM-AN-18) for a CCIM test, and perform CCIM demonstration tests.
- Complete the determination of the waste loadings that would result in reasonable crystal contents that can be tolerated by CCIM for spinel-limited and high-chromium waste clusters.
- Develop an inexpensive test method to determine the tendency of salt formation during melting of HLW feeds.

- Determine the estimated maximum waste loading for all Cr_2O_3-SO_3 limited and P_2O_5-CaO limited waste clusters.
- Determine the potential waste loading benefit by CCIM for high-aluminum waste clusters.
- Complete pre-conceptual design for CCIM retrofit for Hanford HLW and Hanford LAW.
- Perform a cost/benefit/risk analysis on CCIM retrofit for Hanford HLW and Hanford LAW.

Formulation of Advanced Silicate Glasses Melting at 1150℃

- Complete the determination of the maximum loadings for high-iron, spinel-limited, and high-aluminum waste clusters.
- Determine the estimated maximum waste loading for all Cr_2O_3-SO_3 limited and P_2O_5-CaO limited waste clusters using the test method developed to determine the tendency of salt formation.
- Complete the estimation of glass volume reduction that can be achieved by applying the advanced glass formulation for improved waste loadings.
- Refine the crystal limits using the crystal tolerant glass formulation approach.
- Perform testing the high-aluminum test matrix glasses.
- Develop additional test matrices for glasses with different composition regions.
- Develop expanded glass property models to cover the entire glass composition region.

7.0 References

ASTM—American Society of Testing and Materials. 2008. *Standard Test Methods for Determining Chemical Durability of Nuclear, Hazardous, and Mixed Waste Glasses and Multiphase Glass Ceramics: The Product Consistency Test (PCT),* ASTM C 1285-02(2008), American Society of Testing and Materials.

ASTM—American Society of Testing and Materials. 2009. *Standard Test Methods for Measuring Waste Glass or Glass Ceramic Durability by Vapor Hydration Test),* ASTM C 1663-09, American Society of Testing and Materials.

Belsher JD and FL Meinert. 2009. *High-Level Waste Glass Formulation Model Sensitivity Study 2009 Glass Formulation Model versus 1996 Glass Formulation Model,* RPP-RPT-42649, Rev. 0, Washington River Protection Solutions, Richland, Washington.

Bickford DF and CM Jantzen. 1984. *Devitrification of SRL Defense Waste Glass*, in *Sci. Basis for Nuclear Waste Management VII*, ed. GL McVay, Elsevier, New York, pp. 557-565.

Bush SR. 2010. *US DOE Office of Environmental Management Technology Development Report Fiscal Year 2010,* SRNS-STI-2010-00700, Savannah River National Laboratory, Aiken, South Carolina.

Certa PJ, GK Allen, TW Crawford, TM Hohl, KN Jordan, RA Kirkbride, and RL Lytle. 2008. River Protection Project System Plan – Revision 3A, ORP-11242, CH2M Hill Hanford Group, Richland, Washington.

Chew DP and BA Hamm. 2009. *Liquid Waste System Plan, Revision 16*, Savannah River Remediation, Aiken, South Carolina.

DoQualng R, E Pluche, C Ladirat, and A Prod'Homme. 2004. *Review of the French Vitrification Program*, in Waste Management 2004, WM-4320, Tucson, Arizona.

EPA—U.S. Environmental Protection Agency. 1997. *Test Methods for Evaluation of Solid Waste Physical/Chemical Methods*, SW-846, 3rd. ed., as amended, U. S. Environmental Protection Agency, Washington, D.C.

Hrma P, and JD Vienna. 2003. *Relationship Between Liquidus Temperature and Solubility*, in *Ceramic Transactions,* **143**, pp. 159-167, American Ceramic Society, Westerville, Ohio.

Jantzen CM, NE Bibler, DC Beam, CL Crawford, and MA Pickett. 1993. *Characterization of the Defense Waste Processing Facility (DWPF) Environmental Assessment (EA) Glass Standard Reference Material*, WSRC-TR-92-346, Revision 1, Westinghouse Savannah River Company, Aiken, South Carolina.

Kim D, DK Peeler, and P Hrma. 1995. *Effect of Crystallization on the Chemical Durability of Simulated Nuclear Waste Glasses*, in *Environmental Issues and Waste Management Technologies*, *Ceramic Transactions*, Vol. 61, 177-185.

Kim D and JD Vienna. 2002. *Influence of Glass Property Restrictions on Hanford HLW Glass Volume*, in *Environmental Issues and Waste Management Technologies VII, Ceramic Transactions*, Vol. 132, 105-115.

Kim D, JD Vienna, P Hrma, MJ Schweiger, J Matyas, JV Crum, DE Smith, WC Buchmiller, JS Tixier, Jr., JD Yeager, and KB Belew. 2003. *Development and Testing of ICV Glasses for Hanford LAW*, PNNL-14351, Pacific Northwest National Laboratory, Richland, Washington.

Kim D, JD Vienna, DK Peeler, KM Fox, A Aloy, AV Trofimenko, and KD Gerdes. 2008. *Improved Alumina Loading in High-Level Waste Glasses*, in WM'08 proceedings, *HLW, TRU, LLW/ILW, Mixed, Hazardous Wastes & Environmental Management, February 24-28, 2008, Phoenix, Arizona*, WM Symposia Inc., Tucson, Arizona.

Kim D, MJ Schweiger, JD Vienna, FC Johnson, JC Marra, DK Peeler, and GL Smith. 2011. *Glass Formulation for Next Generation Cold Crucible Induction Melter*, in WM2011 proceedings, *Global Achievements and Challenges in Waste Management, February 27 – March 3, 2011, Phoenix, Arizona*., WM Symposia Inc., Tucson, Arizona (in press).

Kot WK, H Gan, M Chaudhuri, and IL Pegg. 2011. *Glass Formulation for Next Generation Melters*, VSL-11R2310-1, Vitreous State Laboratory, The Catholic University of America, Washington, DC.

Li H, JD Vienna, P Hrma, DE Smith, and MJ Schweiger. 1997. *Nepheline Precipitation in High-Level Waste Glasses: Compositional Effects and Impact on the Waste Form Acceptability*, *Scientific Basis for Nuclear Waste Management,* Vol. 465, 261-268.

Li H, P Hrma, JD Vienna, M Quin, Y Su, and DE Smith. 2003. "Effects of Al_2O_3, B_2O_3, Na_2O, and SiO_2 on Nepheline Formation in Borosilicate Glasses: Chemical and Physical Correlations." *Journal of Non-Crystalline Solids.* Vol. 331, 202-216.

Marra JM, A Youchak-Billings, M Stone, DK Peeler, T Edwards, C Girold, and J Dussossoy. 2008. *Glass Formulation Development and Testing for Cold Crucible Induction Melter Technology Retrofit and Deployment Project, Phase II-A – Demonstrations: Lab-Scale Evaluation and Assessment Report*, SRN-STI-2008-00036, Savannah River National Laboratory, Aiken, South Carolina.

Marra JC, KM Fox, GT Jannik, EB Farfan, D Kim, JD Vienna, JA Roach, AS Aloy, SV Stefanovsky, DP Lopukh, MD Bondarkov, KD Gerdes and AM Han. 2010. *The DOE Office of Environmental Management International Cooperative Program: Overview of Technical Tasks and Results*, in WM2010 proceedings, *HLW, TRU, LLW/ILW, Mixed, Hazardous Wastes & Environmental Management, March 7-11, 2010, Phoenix, Arizona,* WM Symposia Inc., Tucson, Arizona.

Matlack KS, W Gong, IS Muller, I Joseph, and IL Pegg. 2006. *LAW Envelope A and B Glass Formulation Testing to Increase Waste Loading*, VSL-06R6900-1, Rev. 0, Vitreous State Laboratory, The Catholic University of America, Washington, DC.

Matlack KS, H Gan, W Gong, and I L Pegg. 2007a. *High Level Waste Vitrification System Improvements*, VSL-07R1010-1, Rev. 0, Vitreous State Laboratory, The Catholic University of America, Washington, DC.

Matlack KS, I Joseph, W Gong, IS Muller, and IL Pegg. 2007b. *Enhanced LAW Glass Formulation Testing*, VSL-07R1130-1, Rev. 0, Vitreous State Laboratory, The Catholic University of America, Washington, DC.

Matlack KS, H Gan, M Chaudhuri, W Kot, W Gong, T Bardakci, and IL Pegg. 2008. *Melt Rate Enhancement for High Aluminum HLW Glass Formulations*, VSL-08R1360-1, Vitreous State Laboratory, The Catholic University of America, Washington, DC.

Matlack KS, I Joseph, W Gong, IS Muller, and IL Pegg. 2009. *Glass Formulation Development and DM10 Melter Testing with ORP LAW Glasses*, VSL-09R1510-2, Rev. 0, Vitreous State Laboratory, The Catholic University of America, Washington, DC.

Matlack KS, H Gan, M Chaudhuri, W Kot, W Gong, T Bardakci, IL Pegg, and I Joseph. 2010. *DM100 and DM1200 Melter Testing with High Waste Loading Glass Formulations for Hanford High-Aluminum HLW Streams,* VSL-10R1690-1, Vitreous State Laboratory, The Catholic University of America, Washington, DC.

Matyas J, JV Crum, JD Vienna, A Arrigoni, M Schaible, R Tate, and CP Rodriguez. 2010. *Development of Crystal-Tolerant High-Level Waste Glasses*, PNNL-20072, Pacific Northwest National Laboratory, Richland, Washington.

Mellinger GB and JL Daniel. 1984. *Approved Reference and Testing Materials for Use in Nuclear Waste Management Research and Development Programs*, PNL-49552, Pacific Northwest Laboratory, Richland, Washington.

McCloy JS and JD Vienna. 2010. *Glass Composition Constraint Recommendations for Use in Life-Cycle Mission Modeling*, PNNL-19372, Pacific Northwest National Laboratory, Richland, Washington.

NRC—National Research Council. 2009. "Advice on the Department of Energy's Cleanup Technology Roadmap: Gaps and Bridges," Committee on Development and Implementation of a Cleanup Technology Roadmap, National Academies Press, Washington, DC.

Perez Jr. JM, DF Bickford, DE Day, D Kim, SL Lambert, SL Marra, DK Peeler, DM Strachan, MB Triplett, JD Vienna, and RS Wittman. 2001. *High-Level Waste Melter Study Report*, PNNL-13582, Pacific Northwest National Laboratory, Richland, Washington.

Piepel GF, SK Cooley, and B Jones. 2004. *Construction of a 21-Component Layered Mixture Experimental Design*, PNNL-14862, Pacific Northwest National Laboratory, Richland, Washington.

Piepel GF, SK Cooley, I Muller, H Gan, I Joseph, and IL Pegg. 2007. *ILAW PCT, VHT, Viscosity, and Electrical Conductivity Model Development*, VSL-07R1230-1 (PNNL-16621), Vitreous State Laboratory, The Catholic University of America, Washington, DC.

Roach J, N Soelberg, M Ancho, E Tchemitcheff, and J Richardson. 2009. *Cold Crucible Induction Melter Testing at the Idaho National Laboratory for the Advanced Remediation Technologies Program - 9337*, in WM2009 proceedings, *HLW, TRU, LLW/ILW, Mixed, Hazardous Wastes & Environmental Management, March 1-5, 2009, Phoenix, Arizona*, WM Symposia Inc., Tucson, Arizona.

Rodriguez CP, JS McCloy, MJ Schweiger, JV Crum, and A Winschell. 2011. *Optical Basicity and Nepheline Crystallization in High Alumina Glasses*, PNNL-20184, Pacific Northwest National Laboratory, Richland, Washington.

Schweiger MJ, BJ Riley, JV Crum, PR Hrma, CP Rodriguez, BM Arrigoni, JB Lang, D Kim, JD Vienna, FC Raszewski, DK Peeler, TB Edwards, DR Best, IA Reamer, WT Riley, PT Simmons, and RJ Workman. 2011. *Expanded High-Level Waste Glass Property Data Development: Phase I*, PNNL-17950, Pacific Northwest National Laboratory, Richland, Washington.

Vienna JD, P Hrma, A Jiricka, DE Smith, TH Lorier, IA Reamer, and RL Schulz. 2001. *Hanford Immobilized LAW Product Acceptance Testing: Tanks Focus Area Results*, PNNL-13744, Pacific Northwest National Laboratory, Richland, Washington.

Vienna JD, D Kim, and PR Hrma. 2002. *Database and Interim Glass Property Models for Hanford HLW and LAW Glasses*, PNNL-14060, Pacific Northwest National Laboratory, Richland, Washington.

Vienna JD. 2005. *Preliminary ILAW Formulation Algorithm Description*, 24590-LAW-RPT-RT-04-0003, Rev 0, River Protection Project, Hanford Tank Waste Treatment and Immobilization Plant, Richland, Washington.

Vienna JD and D Kim. 2008. *Preliminary IHLW Formulation Algorithm Description*, 24590-HLW-RPT-RT-05-001, Rev. 0, River Protection Project, Hanford Tank Waste Treatment and Immobilization Plant, Richland, Washington.

Vienna JD, A Fluegel, D Kim, and P Hrma. 2009. *Glass Property Data and Models for Estimating High-Level Waste Glass Volume*, PNNL-18501, Pacific Northwest National Laboratory, Richland, Washington.

Appendix A

Composition of Waste Clusters

Appendix A: Composition of Waste Clusters

Table A.1. Composition of 20 Clusters in Terms of Full 63 "Oxide" Components that Are Tracked in the G2 Model (components in bold represent the 15 components used in cluster analysis)

Cluster #	1	2	3	4	5	6	7
Ac_2O_3	7.734E-12	4.350E-12	2.403E-11	3.208E-11	3.270E-12	5.572E-12	1.705E-12
Ag_2O	1.328E-03	1.438E-04	1.521E-03	2.011E-04	2.371E-04	5.591E-04	9.104E-05
Al_2O_3	1.392E-01	2.044E-01	1.370E-01	3.726E-01	4.700E-01	2.783E-01	4.489E-01
Am_2O_3	4.828E-06	1.882E-06	8.150E-06	1.854E-05	2.386E-06	6.828E-06	9.615E-07
As_2O_5	2.998E-04	5.556E-04	5.204E-04	2.744E-04	3.077E-04	7.217E-04	3.088E-04
B_2O_3	2.445E-03	2.128E-03	8.312E-03	1.310E-03	2.356E-03	4.273E-03	1.383E-03
BaO	1.588E-03	4.264E-04	6.909E-04	6.319E-04	2.338E-04	1.355E-03	8.467E-04
BeO	4.914E-05	3.710E-04	2.206E-04	1.634E-04	1.802E-04	7.381E-04	7.889E-05
Bi_2O_3	6.655E-03	7.246E-02	2.469E-02	9.754E-03	1.857E-02	3.799E-02	5.549E-02
CaO	2.459E-02	5.615E-02	3.867E-02	2.620E-02	1.558E-02	1.996E-02	2.440E-02
CdO	8.533E-04	4.800E-04	4.718E-03	5.175E-03	1.652E-04	5.774E-04	4.742E-05
Ce_2O_3	2.682E-03	8.378E-04	6.895E-04	8.690E-04	2.444E-04	9.507E-04	2.679E-04
Cl	1.716E-03	1.731E-03	2.010E-03	2.450E-03	2.149E-03	1.618E-03	1.705E-03
Cm_2O_3	1.033E-09	6.266E-11	3.164E-10	5.286E-10	2.471E-11	1.914E-10	1.745E-11
CoO	1.011E-04	1.020E-04	1.022E-04	1.293E-04	7.140E-05	2.019E-04	8.890E-05
Cr_2O_3	8.147E-03	1.382E-02	1.237E-02	1.308E-02	2.275E-02	2.940E-02	1.850E-02
Cs_2O	9.631E-05	1.548E-04	2.170E-04	3.539E-04	3.313E-04	1.858E-04	1.296E-04
CuO	7.157E-04	1.668E-04	3.605E-04	2.303E-04	1.697E-04	3.538E-04	6.236E-05
Eu_2O_3	2.506E-08	3.156E-09	1.009E-08	2.843E-08	1.313E-09	5.905E-09	9.084E-10
F	1.510E-03	2.824E-02	1.611E-03	1.250E-03	1.423E-02	5.520E-03	5.312E-03
Fe_2O_3	3.345E-01	1.139E-01	1.881E-01	1.472E-01	5.818E-02	1.481E-01	1.088E-01
HgO	5.291E-04	1.203E-04	1.397E-04	3.828E-05	8.747E-05	1.136E-04	1.576E-04
I	1.881E-06	1.159E-06	2.830E-06	3.361E-06	9.455E-07	1.378E-06	2.137E-07
K_2O	7.930E-03	4.897E-03	1.035E-02	5.398E-03	5.854E-03	7.485E-03	4.535E-03
La_2O_3	1.846E-03	4.405E-04	6.722E-03	2.678E-03	2.115E-03	9.682E-03	9.890E-04
Li_2O	1.971E-04	4.094E-04	2.455E-04	3.416E-04	3.866E-04	8.209E-04	2.124E-04
MgO	3.454E-03	1.647E-03	4.078E-03	1.335E-03	1.828E-03	6.126E-03	1.031E-03
MnO	4.785E-02	5.780E-03	2.888E-02	9.717E-03	1.187E-02	3.032E-02	9.469E-03
MoO_3	1.152E-04	3.733E-04	3.213E-04	2.235E-04	2.754E-04	5.377E-04	2.712E-04
Na_2O	2.055E-01	2.477E-01	1.265E-01	1.212E-01	1.482E-01	1.678E-01	1.281E-01
Nb_2O_5	2.025E-10	6.334E-10	4.959E-10	5.123E-10	9.847E-10	1.854E-09	9.763E-10
Nd_2O_3	3.161E-03	7.523E-04	1.076E-03	1.920E-03	3.529E-04	1.165E-03	2.862E-04
NiO	1.667E-02	7.781E-03	4.176E-02	2.463E-02	1.289E-02	3.070E-02	6.909E-03
NpO_2	1.710E-05	6.820E-06	2.775E-05	5.094E-05	9.077E-06	1.800E-05	7.029E-06
P_2O_5	1.733E-02	6.742E-02	4.272E-02	1.161E-02	4.523E-02	4.345E-02	3.577E-02
Pa_2O_5	2.739E-09	9.092E-09	8.297E-09	8.231E-09	8.421E-09	6.972E-09	3.669E-09
PbO	1.308E-02	6.277E-03	6.292E-03	5.774E-03	2.471E-03	7.410E-03	4.199E-03
PdO	2.466E-05	1.969E-05	1.295E-06	2.562E-04	4.543E-06	3.035E-06	1.026E-07
Pr_2O_3	7.926E-04	4.669E-05	9.009E-05	2.791E-04	8.270E-06	1.029E-04	1.199E-06
PuO_2	1.205E-04	2.420E-05	1.848E-04	2.273E-04	9.442E-05	1.505E-04	3.648E-05
RaO	6.810E-12	1.951E-12	2.202E-11	1.427E-11	9.471E-13	6.725E-12	5.707E-13
Rb_2O	9.194E-05	1.320E-05	2.946E-04	1.385E-04	4.436E-06	4.902E-05	2.131E-07
Rh_2O_3	1.175E-04	2.020E-05	2.010E-04	6.269E-05	6.218E-06	5.569E-05	5.625E-07
RuO_2	1.457E-03	8.653E-05	6.312E-05	6.386E-04	1.882E-05	4.524E-04	3.058E-06
SO_3	4.422E-03	9.053E-03	6.726E-03	2.695E-03	1.219E-02	1.406E-02	8.629E-03
Sb_2O_3	7.350E-05	2.763E-04	2.540E-04	9.040E-05	1.664E-04	2.587E-04	1.451E-04
SeO_2	1.224E-05	3.244E-05	4.592E-05	2.349E-05	1.074E-05	4.421E-05	1.352E-05
SiO_2	6.363E-02	9.346E-02	4.117E-02	1.044E-01	3.426E-02	5.068E-02	7.488E-02
Sm_2O_3	9.041E-06	4.391E-06	1.146E-05	1.452E-05	5.250E-06	1.880E-05	6.275E-06
SnO_2	3.369E-06	9.744E-07	7.309E-07	7.273E-07	1.489E-06	2.488E-06	1.367E-06
SrO	7.576E-04	9.782E-03	1.293E-03	2.218E-03	7.342E-03	3.830E-03	1.778E-03

Cluster #	1	2	3	4	5	6	7
Ta_2O_5	6.268E-06	6.185E-07	2.207E-06	2.256E-06	1.955E-07	1.198E-06	2.170E-08
Tc_2O_7	1.623E-05	2.915E-05	3.544E-05	3.085E-05	3.333E-05	5.708E-05	3.367E-05
TeO_2	2.814E-04	1.727E-05	3.602E-05	1.345E-04	2.635E-06	7.729E-05	4.667E-07
ThO_2	1.599E-02	3.749E-03	5.045E-02	3.054E-02	5.828E-04	8.115E-03	2.545E-04
TiO_2	6.064E-04	1.507E-04	3.796E-04	1.223E-04	2.316E-04	2.763E-04	6.727E-05
Tl_2O	5.974E-04	2.685E-04	1.861E-04	1.291E-04	3.530E-04	5.376E-04	3.568E-04
UO_3	3.267E-02	3.919E-02	9.467E-02	5.714E-02	5.331E-02	5.479E-02	5.310E-02
V_2O_5	9.330E-05	3.511E-04	2.560E-04	1.564E-04	2.390E-04	4.575E-04	2.239E-04
WO_3	2.054E-06	3.010E-05	3.209E-05	9.988E-05	2.738E-05	3.841E-04	3.366E-07
Y_2O_3	3.198E-04	3.216E-05	6.178E-05	1.006E-04	1.619E-05	8.724E-05	6.012E-06
ZnO	8.606E-04	3.641E-04	1.423E-03	2.864E-04	9.486E-04	8.190E-04	2.020E-04
ZrO_2	3.291E-02	3.384E-03	1.112E-01	3.334E-02	5.284E-02	2.826E-02	1.876E-03
SUM	1	1	1	1	1	1	1
Oxide mass (MT)	405.155	338.933	266.291	220.917	719.021	364.147	1,839.578

Table A.1. (Continued)

Cluster #	8	9	10	11	12	13	14
Ac_2O_3	2.861E-12	5.760E-12	9.465E-12	6.502E-12	1.139E-11	8.172E-12	2.518E-12
Ag_2O	2.826E-04	4.437E-04	1.190E-03	1.786E-04	2.609E-04	1.905E-04	1.896E-04
Al_2O_3	4.167E-01	9.320E-02	1.889E-01	2.831E-01	1.638E-01	2.263E-01	3.221E-01
Am_2O_3	1.995E-06	1.006E-06	8.212E-06	6.320E-07	6.970E-07	2.509E-06	1.095E-05
As_2O_5	9.659E-04	1.008E-03	2.835E-04	2.842E-04	2.200E-04	4.618E-04	7.141E-04
B_2O_3	6.356E-03	5.349E-03	3.106E-03	2.148E-03	2.138E-03	2.364E-03	3.147E-03
BaO	8.513E-04	6.097E-04	3.713E-03	7.178E-04	4.849E-04	5.198E-04	3.282E-04
BeO	1.110E-04	1.139E-04	8.029E-05	1.108E-03	7.391E-05	2.446E-04	9.526E-04
Bi_2O_3	1.849E-02	1.306E-02	1.703E-02	5.720E-02	3.411E-02	2.465E-02	1.761E-02
CaO	2.467E-02	2.574E-02	2.411E-02	2.481E-02	3.012E-02	2.483E-02	2.159E-02
CdO	2.322E-04	4.117E-04	7.696E-04	3.183E-04	2.406E-04	4.534E-04	7.921E-04
Ce_2O_3	8.569E-04	8.024E-04	1.621E-03	3.961E-04	2.183E-04	3.294E-04	7.618E-04
Cl	1.138E-03	1.728E-03	2.354E-03	2.315E-03	2.011E-03	2.534E-03	2.323E-03
Cm_2O_3	2.526E-11	1.690E-11	4.751E-10	8.168E-12	8.389E-12	5.225E-11	1.597E-10
CoO	1.871E-04	1.635E-04	1.117E-04	2.947E-04	1.198E-04	1.262E-04	1.447E-04
Cr_2O_3	1.995E-02	2.734E-02	6.665E-03	2.215E-02	7.707E-02	2.901E-02	7.395E-02
Cs_2O	7.785E-05	1.801E-04	4.815E-04	1.563E-04	1.583E-04	2.630E-04	3.100E-04
CuO	2.131E-04	1.842E-04	7.862E-04	1.453E-04	9.759E-05	2.628E-04	1.431E-04
Eu_2O_3	1.197E-09	4.184E-10	1.282E-08	9.064E-10	1.925E-09	3.323E-09	7.215E-09
F	1.084E-02	6.990E-03	4.475E-03	6.069E-02	5.005E-02	2.286E-02	4.385E-03
Fe_2O_3	1.072E-01	6.675E-02	2.988E-01	9.548E-02	1.223E-01	1.013E-01	8.489E-02
HgO	1.845E-04	1.027E-04	1.993E-04	5.042E-05	1.268E-04	1.140E-04	4.970E-05
I	7.550E-07	2.819E-06	1.657E-06	7.672E-07	1.966E-06	1.516E-06	1.062E-06
K_2O	3.643E-03	2.527E-02	6.458E-03	5.571E-03	1.049E-02	4.620E-03	7.253E-03
La_2O_3	6.655E-04	1.847E-04	2.491E-03	3.466E-04	4.813E-03	1.842E-03	7.602E-04
Li_2O	4.116E-04	6.225E-04	4.395E-04	9.167E-04	3.228E-04	3.458E-04	9.066E-04
MgO	3.358E-03	3.914E-03	7.970E-03	1.429E-03	2.048E-03	2.374E-03	1.176E-03
MnO	1.822E-02	5.850E-03	2.167E-02	5.289E-03	1.228E-02	8.785E-03	2.030E-02
MoO_3	7.838E-04	1.258E-03	2.630E-04	5.609E-04	4.163E-04	3.895E-04	5.524E-04
Na_2O	1.184E-01	5.398E-01	1.336E-01	1.233E-01	1.426E-01	2.277E-01	1.931E-01
Nb_2O_5	1.173E-09	1.362E-09	1.225E-09	9.086E-10	1.157E-09	8.291E-10	2.454E-09
Nd_2O_3	9.816E-04	7.868E-04	2.038E-03	2.879E-04	2.004E-04	4.689E-04	1.059E-03
NiO	6.381E-03	4.857E-03	2.040E-02	7.765E-03	3.136E-02	1.544E-02	3.864E-03
NpO_2	1.039E-05	7.425E-06	8.707E-06	5.920E-06	1.111E-05	9.865E-06	2.726E-05
P_2O_5	2.156E-02	2.433E-02	1.657E-02	4.418E-02	1.113E-01	1.165E-01	1.114E-01
Pa_2O_5	5.746E-09	1.098E-08	3.726E-09	1.697E-08	2.906E-08	1.458E-08	7.220E-09
PbO	7.985E-03	5.831E-03	1.576E-02	2.794E-03	3.956E-03	4.130E-03	4.184E-03
PdO	3.294E-08	1.175E-07	1.502E-07	7.001E-07	1.504E-06	2.345E-05	2.610E-05
Pr_2O_3	3.305E-07	3.907E-06	2.821E-04	3.054E-06	7.916E-06	3.895E-05	4.786E-05
PuO_2	7.191E-05	6.146E-05	1.751E-04	2.235E-05	3.651E-05	5.096E-05	2.729E-04
RaO	1.728E-12	3.542E-12	9.219E-12	1.453E-12	2.413E-12	3.051E-12	1.167E-12
Rb_2O	6.925E-07	9.527E-06	1.110E-04	6.614E-07	2.260E-05	1.742E-05	1.692E-05
Rh_2O_3	5.102E-07	6.522E-06	1.483E-04	1.109E-06	1.636E-05	1.191E-05	3.253E-05
RuO_2	5.043E-07	3.716E-06	1.577E-03	6.449E-06	7.060E-06	1.797E-04	1.463E-04
SO_3	8.611E-03	3.498E-03	4.380E-03	2.140E-02	2.194E-02	1.096E-02	1.983E-02
Sb_2O_3	3.157E-04	3.856E-04	1.141E-04	3.669E-04	2.832E-04	1.682E-04	2.705E-04
SeO_2	4.670E-05	1.715E-04	2.312E-05	4.122E-05	2.698E-05	2.153E-05	5.154E-05
SiO_2	1.106E-01	8.500E-02	6.684E-02	1.840E-01	5.862E-02	6.146E-02	4.315E-02
Sm_2O_3	1.074E-05	6.835E-06	3.894E-05	5.370E-06	7.554E-06	6.890E-06	1.289E-05
SnO_2	1.669E-06	1.773E-06	5.641E-07	1.329E-06	1.645E-06	1.154E-06	3.854E-06
SrO	3.632E-03	4.118E-03	1.185E-03	5.293E-03	2.434E-02	1.476E-02	5.208E-03
Ta_2O_5	6.495E-09	7.997E-08	1.997E-06	5.408E-08	1.904E-07	3.579E-07	1.257E-06
Tc_2O_7	3.056E-05	5.794E-05	2.836E-05	4.318E-05	3.353E-05	4.569E-05	4.942E-05
TeO_2	1.252E-07	1.432E-06	2.588E-04	9.689E-07	3.001E-06	2.470E-05	1.646E-05
ThO_2	2.562E-03	6.321E-03	1.974E-02	2.219E-03	3.844E-03	4.434E-03	3.204E-04
TiO_2	2.175E-04	1.485E-04	4.568E-04	2.108E-04	1.951E-04	1.799E-04	1.467E-04

Cluster #	**8**	**9**	**10**	**11**	**12**	**13**	**14**
Tl_2O	2.786E-04	1.323E-03	8.650E-05	3.508E-04	7.299E-05	6.515E-04	7.680E-04
UO_3	7.863E-02	3.510E-02	7.591E-02	3.462E-02	7.299E-02	8.037E-02	3.581E-02
V_2O_5	5.918E-04	5.951E-04	1.925E-04	5.806E-04	3.676E-04	3.252E-04	4.361E-04
WO_3	1.214E-07	2.125E-07	8.826E-04	5.783E-06	3.242E-06	6.023E-05	1.877E-04
Y_2O_3	8.329E-06	2.149E-06	2.802E-04	3.596E-05	1.292E-05	2.712E-05	4.174E-05
ZnO	5.645E-04	1.031E-03	9.655E-04	5.562E-04	6.448E-04	5.424E-04	5.363E-04
ZrO_2	2.122E-03	5.230E-03	4.399E-02	6.245E-03	1.301E-02	6.116E-03	1.361E-02
SUM	1	1	1	1	1	1	1
Oxide mass (MT)	1,183.119	143.796	733.959	533.009	275.181	209.397	173.318

Table A.1. (Continued)

Cluster #	15	16	17	18	19	20
Ac_2O_3	2.139E-12	9.739E-13	2.146E-12	9.947E-12	2.254E-11	5.200E-12
Ag_2O	2.797E-04	1.143E-04	1.348E-04	1.165E-03	3.112E-04	2.698E-04
Al_2O_3	1.303E-01	5.719E-01	1.836E-01	2.009E-01	2.846E-01	2.337E-01
Am_2O_3	3.183E-06	9.039E-07	1.703E-05	5.199E-05	1.401E-05	2.036E-06
As_2O_5	2.667E-04	3.762E-04	5.786E-04	3.522E-04	2.148E-04	5.230E-04
B_2O_3	1.983E-03	2.101E-03	1.420E-03	2.679E-03	1.116E-03	3.681E-03
BaO	5.001E-04	2.210E-04	6.212E-04	1.455E-03	1.173E-03	9.286E-04
BeO	2.271E-05	5.245E-05	7.351E-05	1.027E-04	6.692E-05	1.250E-04
Bi_2O_3	5.763E-02	1.445E-02	1.225E-02	3.356E-03	8.542E-03	4.975E-02
CaO	5.348E-02	8.628E-03	8.891E-02	2.214E-02	4.009E-02	3.954E-02
CdO	1.682E-04	4.284E-05	3.601E-03	3.224E-02	2.288E-03	2.705E-04
Ce_2O_3	9.392E-04	3.228E-04	1.574E-03	2.348E-03	1.009E-03	4.756E-04
Cl	2.442E-03	1.447E-03	2.447E-03	2.249E-03	1.817E-03	1.439E-03
Cm_2O_3	1.483E-10	1.240E-11	5.312E-10	2.982E-09	3.500E-10	2.591E-11
CoO	4.997E-05	6.620E-05	6.841E-05	1.206E-04	4.845E-05	2.144E-04
Cr_2O_3	3.810E-03	2.023E-02	1.458E-02	6.172E-03	1.179E-02	1.847E-02
Cs_2O	3.419E-04	7.815E-05	3.951E-04	3.256E-04	2.991E-04	7.742E-05
CuO	3.949E-04	1.800E-04	3.101E-04	4.761E-04	3.344E-04	3.290E-04
Eu_2O_3	1.116E-08	4.573E-10	2.976E-08	7.300E-08	2.044E-08	1.245E-09
F	1.230E-02	2.574E-03	2.545E-03	1.180E-03	1.657E-03	2.258E-02
Fe_2O_3	2.359E-01	5.475E-02	1.382E-01	3.483E-01	1.699E-01	1.432E-01
HgO	1.809E-04	1.000E-04	5.899E-05	6.659E-05	9.738E-05	1.867E-04
I	6.106E-07	7.522E-07	3.508E-06	1.183E-06	3.212E-06	9.656E-07
K_2O	2.133E-02	2.170E-03	9.914E-03	9.598E-03	4.801E-03	4.238E-03
La_2O_3	3.262E-04	9.503E-04	2.169E-03	8.420E-03	1.821E-03	3.198E-03
Li_2O	1.672E-04	2.228E-04	6.235E-04	4.301E-04	3.230E-04	3.880E-04
MgO	1.950E-03	1.929E-03	1.120E-03	2.580E-03	2.336E-03	5.601E-03
MnO	2.420E-02	1.381E-02	1.617E-02	1.234E-02	1.317E-02	1.349E-02
MoO_3	2.299E-04	3.248E-04	6.089E-04	2.615E-04	2.231E-04	6.952E-04
Na_2O	1.284E-01	1.622E-01	3.709E-01	9.553E-02	2.018E-01	1.504E-01
Nb_2O_5	6.318E-10	7.285E-10	8.671E-10	3.634E-10	5.412E-10	7.542E-10
Nd_2O_3	3.741E-04	7.518E-04	3.310E-03	6.412E-03	1.927E-03	6.076E-04
NiO	3.074E-02	3.573E-03	5.730E-03	2.733E-02	1.924E-02	1.542E-02
NpO_2	5.805E-06	5.993E-06	3.955E-05	1.761E-04	3.137E-05	6.276E-06
P_2O_5	5.597E-02	1.393E-02	3.158E-02	9.674E-03	1.302E-02	3.289E-02
Pa_2O_5	2.724E-09	2.149E-09	5.604E-09	3.075E-09	6.252E-09	1.043E-08
PbO	1.226E-02	2.596E-03	3.122E-03	6.782E-03	6.942E-03	8.197E-03
PdO	8.634E-07	2.429E-08	1.925E-04	3.397E-05	2.086E-04	1.205E-07
Pr_2O_3	5.671E-05	7.297E-07	2.405E-04	5.419E-05	2.903E-04	3.995E-07
PuO_2	9.458E-05	4.249E-05	7.171E-05	2.139E-04	1.777E-04	5.540E-05
RaO	3.581E-12	5.831E-13	1.627E-12	8.658E-12	1.115E-11	1.833E-12
Rb_2O	1.579E-05	1.237E-07	1.038E-04	8.812E-05	1.349E-04	1.199E-07
Rh_2O_3	2.017E-05	1.790E-07	2.093E-04	5.439E-05	1.228E-04	1.984E-07
RuO_2	3.512E-04	2.681E-06	4.444E-04	1.492E-04	9.436E-04	1.203E-06
SO_3	1.538E-03	4.985E-03	4.485E-03	1.837E-03	2.623E-03	9.767E-03
Sb_2O_3	1.675E-04	1.708E-04	2.067E-04	1.293E-04	7.047E-05	1.824E-04
SeO_2	2.242E-05	1.679E-05	5.667E-05	3.124E-05	1.669E-05	2.633E-05
SiO_2	1.405E-01	6.917E-02	2.406E-02	3.159E-02	8.062E-02	1.283E-01
Sm_2O_3	1.115E-05	4.548E-06	1.067E-05	4.864E-05	1.598E-05	1.222E-05
SnO_2	1.076E-06	1.129E-06	1.320E-06	5.881E-07	4.925E-07	1.072E-06
SrO	1.555E-03	1.651E-03	2.981E-02	6.831E-04	1.976E-02	1.017E-02
Ta_2O_5	4.062E-07	1.338E-08	4.228E-06	7.798E-07	2.823E-06	1.014E-08
Tc_2O_7	4.231E-05	1.980E-05	4.351E-05	3.384E-05	1.672E-05	3.936E-05
TeO_2	4.291E-05	2.484E-07	9.086E-05	2.710E-05	1.632E-04	1.776E-07
ThO_2	2.919E-03	4.815E-04	1.420E-03	1.709E-02	2.362E-02	2.909E-03
TiO_2	1.325E-04	1.294E-04	1.341E-04	3.350E-04	1.613E-04	2.368E-04

Cluster #	15	16	17	18	19	20
Tl_2O	4.002E-04	1.742E-03	6.497E-04	5.162E-05	2.056E-04	8.883E-04
UO_3	5.014E-02	3.894E-02	2.563E-02	7.475E-02	4.912E-02	9.276E-02
V_2O_5	8.533E-05	2.716E-04	2.467E-04	9.854E-05	1.070E-04	3.700E-04
WO_3	9.984E-05	1.651E-06	4.022E-04	5.502E-06	3.272E-04	2.023E-06
Y_2O_3	4.026E-05	3.720E-06	2.450E-04	2.378E-04	1.646E-04	9.097E-06
ZnO	9.099E-04	3.935E-04	7.566E-04	1.295E-03	4.254E-04	6.876E-04
ZrO_2	2.396E-02	1.808E-03	1.391E-02	6.593E-02	2.967E-02	2.747E-03
SUM	1	1	1	1	1	1
Oxide mass (MT)	327.203	1,453.789	164.666	123.884	249.230	1,350.527

Table A.2. Composition of 20 Clusters in Terms of 41 "Oxide" Components that Are Tracked in 2009 Glass Models (Vienna et al. 2009) (components in bold represent the 15 components used in cluster analysis)

Cluster #	1	2	3	4	5	6	7
Ag_2O	1.331E-03	1.441E-04	1.524E-03	2.014E-04	2.374E-04	5.609E-04	9.114E-05
Al_2O_3	1.396E-01	2.047E-01	1.373E-01	3.732E-01	4.706E-01	2.792E-01	4.494E-01
B_2O_3	2.452E-03	2.132E-03	8.329E-03	1.312E-03	2.359E-03	4.287E-03	1.384E-03
BaO	1.593E-03	4.272E-04	6.923E-04	6.330E-04	2.341E-04	1.360E-03	8.476E-04
Bi_2O_3	6.674E-03	7.259E-02	2.474E-02	9.771E-03	1.860E-02	3.811E-02	5.555E-02
CaO	2.466E-02	5.625E-02	3.875E-02	2.624E-02	1.560E-02	2.003E-02	2.443E-02
CdO	8.557E-04	4.809E-04	4.728E-03	5.184E-03	1.655E-04	5.792E-04	4.747E-05
Ce_2O_3	2.690E-03	8.393E-04	6.909E-04	8.705E-04	2.447E-04	9.537E-04	2.682E-04
Cl	1.721E-03	1.734E-03	2.014E-03	2.454E-03	2.152E-03	1.623E-03	1.707E-03
CoO	1.014E-04	1.022E-04	1.024E-04	1.295E-04	7.149E-05	2.026E-04	8.900E-05
Cr_2O_3	8.171E-03	1.385E-02	1.239E-02	1.310E-02	2.278E-02	2.950E-02	1.852E-02
Cs_2O	9.659E-05	1.551E-04	2.175E-04	3.545E-04	3.317E-04	1.864E-04	1.297E-04
CuO	7.177E-04	1.671E-04	3.613E-04	2.307E-04	1.699E-04	3.550E-04	6.243E-05
F	1.514E-03	2.829E-02	1.615E-03	1.252E-03	1.425E-02	5.538E-03	5.318E-03
Fe_2O_3	3.355E-01	1.141E-01	1.884E-01	1.475E-01	5.826E-02	1.486E-01	1.089E-01
K_2O	7.953E-03	4.906E-03	1.037E-02	5.407E-03	5.862E-03	7.509E-03	4.540E-03
La_2O_3	1.851E-03	4.413E-04	6.736E-03	2.683E-03	2.117E-03	9.713E-03	9.901E-04
Li_2O	1.977E-04	4.101E-04	2.460E-04	3.422E-04	3.871E-04	8.235E-04	2.126E-04
MgO	3.464E-03	1.650E-03	4.086E-03	1.337E-03	1.830E-03	6.146E-03	1.032E-03
MnO	4.799E-02	5.790E-03	2.894E-02	9.733E-03	1.188E-02	3.041E-02	9.480E-03
MoO_3	1.155E-04	3.740E-04	3.220E-04	2.239E-04	2.758E-04	5.394E-04	2.715E-04
Na_2O	2.061E-01	2.481E-01	1.268E-01	1.214E-01	1.484E-01	1.683E-01	1.283E-01
Nd_2O_3	3.170E-03	7.537E-04	1.079E-03	1.923E-03	3.533E-04	1.169E-03	2.865E-04
NiO	1.672E-02	7.794E-03	4.184E-02	2.467E-02	1.291E-02	3.080E-02	6.917E-03
P_2O_5	1.738E-02	6.754E-02	4.281E-02	1.163E-02	4.528E-02	4.359E-02	3.581E-02
PbO	1.312E-02	6.288E-03	6.305E-03	5.784E-03	2.474E-03	7.434E-03	4.204E-03
PdO	2.474E-05	1.972E-05	1.297E-06	2.566E-04	4.549E-06	3.045E-06	1.027E-07
Re_2O_7	1.628E-05	2.920E-05	3.551E-05	3.090E-05	3.338E-05	5.726E-05	3.371E-05
Rh_2O_3	1.179E-04	2.024E-05	2.014E-04	6.279E-05	6.226E-06	5.587E-05	5.631E-07
RuO_2	1.462E-03	8.669E-05	6.325E-05	6.397E-04	1.884E-05	4.539E-04	3.062E-06
SiO_2	6.381E-02	9.362E-02	4.126E-02	1.046E-01	3.430E-02	5.085E-02	7.496E-02
SO_3	4.435E-03	9.069E-03	6.740E-03	2.699E-03	1.221E-02	1.411E-02	8.639E-03
SnO_2	3.378E-06	9.762E-07	7.324E-07	7.285E-07	1.491E-06	2.496E-06	1.368E-06
SrO	7.598E-04	9.799E-03	1.296E-03	2.222E-03	7.351E-03	3.842E-03	1.780E-03
ThO_2	1.604E-02	3.756E-03	5.055E-02	3.060E-02	5.835E-04	8.141E-03	2.548E-04
TiO_2	6.081E-04	1.510E-04	3.804E-04	1.225E-04	2.319E-04	2.772E-04	6.735E-05
UO_3	3.276E-02	3.926E-02	9.487E-02	5.724E-02	5.338E-02	5.497E-02	5.316E-02
V_2O_5	9.357E-05	3.517E-04	2.565E-04	1.566E-04	2.393E-04	4.590E-04	2.242E-04
Y_2O_3	3.208E-04	3.221E-05	6.191E-05	1.008E-04	1.621E-05	8.752E-05	6.018E-06
ZnO	8.631E-04	3.647E-04	1.426E-03	2.869E-04	9.498E-04	8.217E-04	2.022E-04
ZrO_2	3.300E-02	3.390E-03	1.115E-01	3.339E-02	5.290E-02	2.835E-02	1.878E-03
SUM	1	1	1	1	1	1	1
Oxide mass (MT)	405.155	338.933	266.291	220.917	719.021	364.147	1,839.578

Table A.2. (Continued)

Cluster #	8	9	10	11	12	13	14
Ag_2O	2.831E-04	4.452E-04	1.193E-03	1.790E-04	2.611E-04	1.909E-04	1.902E-04
Al_2O_3	4.175E-01	9.350E-02	1.894E-01	2.837E-01	1.640E-01	2.268E-01	3.232E-01
B_2O_3	6.369E-03	5.366E-03	3.114E-03	2.152E-03	2.140E-03	2.368E-03	3.157E-03
BaO	8.530E-04	6.116E-04	3.722E-03	7.194E-04	4.853E-04	5.208E-04	3.294E-04
Bi_2O_3	1.852E-02	1.311E-02	1.707E-02	5.733E-02	3.414E-02	2.470E-02	1.767E-02
CaO	2.472E-02	2.582E-02	2.417E-02	2.486E-02	3.015E-02	2.487E-02	2.167E-02
CdO	2.326E-04	4.130E-04	7.716E-04	3.190E-04	2.408E-04	4.542E-04	7.948E-04
Ce_2O_3	8.586E-04	8.050E-04	1.625E-03	3.970E-04	2.185E-04	3.301E-04	7.644E-04
Cl	1.140E-03	1.733E-03	2.360E-03	2.320E-03	2.013E-03	2.539E-03	2.331E-03
CoO	1.875E-04	1.640E-04	1.120E-04	2.954E-04	1.199E-04	1.265E-04	1.452E-04
Cr_2O_3	1.999E-02	2.742E-02	6.683E-03	2.220E-02	7.714E-02	2.906E-02	7.420E-02
Cs_2O	7.801E-05	1.806E-04	4.827E-04	1.567E-04	1.584E-04	2.635E-04	3.110E-04
CuO	2.136E-04	1.848E-04	7.883E-04	1.456E-04	9.767E-05	2.633E-04	1.435E-04
F	1.086E-02	7.012E-03	4.486E-03	6.083E-02	5.010E-02	2.290E-02	4.400E-03
Fe_2O_3	1.074E-01	6.697E-02	2.996E-01	9.569E-02	1.225E-01	1.015E-01	8.518E-02
K_2O	3.650E-03	2.535E-02	6.474E-03	5.584E-03	1.050E-02	4.629E-03	7.277E-03
La_2O_3	6.669E-04	1.853E-04	2.497E-03	3.474E-04	4.817E-03	1.846E-03	7.628E-04
Li_2O	4.125E-04	6.245E-04	4.407E-04	9.188E-04	3.231E-04	3.465E-04	9.097E-04
MgO	3.365E-03	3.927E-03	7.990E-03	1.432E-03	2.049E-03	2.378E-03	1.180E-03
MnO	1.825E-02	5.869E-03	2.173E-02	5.301E-03	1.229E-02	8.802E-03	2.037E-02
MoO_3	7.854E-04	1.262E-03	2.637E-04	5.621E-04	4.166E-04	3.902E-04	5.543E-04
Na_2O	1.186E-01	5.416E-01	1.339E-01	1.236E-01	1.427E-01	2.281E-01	1.937E-01
Nd_2O_3	9.836E-04	7.893E-04	2.043E-03	2.886E-04	2.006E-04	4.698E-04	1.063E-03
NiO	6.394E-03	4.872E-03	2.045E-02	7.783E-03	3.138E-02	1.547E-02	3.877E-03
P_2O_5	2.160E-02	2.440E-02	1.661E-02	4.428E-02	1.114E-01	1.167E-01	1.118E-01
PbO	8.001E-03	5.850E-03	1.580E-02	2.800E-03	3.960E-03	4.137E-03	4.198E-03
PdO	3.301E-08	1.179E-07	1.506E-07	7.017E-07	1.505E-06	2.350E-05	2.619E-05
Re_2O_7	3.062E-05	5.812E-05	2.843E-05	4.328E-05	3.356E-05	4.578E-05	4.959E-05
Rh_2O_3	5.112E-07	6.543E-06	1.487E-04	1.111E-06	1.638E-05	1.193E-05	3.264E-05
RuO_2	5.054E-07	3.728E-06	1.581E-03	6.464E-06	7.066E-06	1.801E-04	1.468E-04
SiO_2	1.108E-01	8.527E-02	6.701E-02	1.844E-01	5.868E-02	6.157E-02	4.329E-02
SO_3	8.628E-03	3.509E-03	4.391E-03	2.145E-02	2.196E-02	1.098E-02	1.990E-02
SnO_2	1.673E-06	1.779E-06	5.656E-07	1.332E-06	1.646E-06	1.156E-06	3.867E-06
SrO	3.639E-03	4.131E-03	1.188E-03	5.305E-03	2.436E-02	1.479E-02	5.226E-03
ThO_2	2.567E-03	6.342E-03	1.979E-02	2.224E-03	3.847E-03	4.442E-03	3.215E-04
TiO_2	2.179E-04	1.490E-04	4.580E-04	2.113E-04	1.953E-04	1.803E-04	1.472E-04
UO_3	7.879E-02	3.521E-02	7.610E-02	3.470E-02	7.306E-02	8.052E-02	3.593E-02
V_2O_5	5.930E-04	5.970E-04	1.930E-04	5.819E-04	3.679E-04	3.258E-04	4.375E-04
Y_2O_3	8.345E-06	2.156E-06	2.809E-04	3.604E-05	1.293E-05	2.717E-05	4.189E-05
ZnO	5.656E-04	1.034E-03	9.680E-04	5.575E-04	6.453E-04	5.434E-04	5.381E-04
ZrO_2	2.126E-03	5.247E-03	4.410E-02	6.259E-03	1.302E-02	6.128E-03	1.366E-02
SUM	1	1	1	1	1	1	1
Oxide mass (MT)	1,183.119	143.796	733.959	533.009	275.181	209.397	173.318

Table A.2. (Continued)

Cluster #	15	16	17	18	19	20
Ag_2O	2.800E-04	1.146E-04	1.352E-04	1.167E-03	3.118E-04	2.704E-04
Al_2O_3	1.305E-01	5.734E-01	1.840E-01	2.012E-01	2.851E-01	2.341E-01
B_2O_3	1.986E-03	2.107E-03	1.424E-03	2.682E-03	1.118E-03	3.688E-03
BaO	5.008E-04	2.215E-04	6.229E-04	1.457E-03	1.176E-03	9.305E-04
Bi_2O_3	5.771E-02	1.449E-02	1.228E-02	3.360E-03	8.557E-03	4.985E-02
CaO	5.356E-02	8.650E-03	8.914E-02	2.217E-02	4.017E-02	3.962E-02
CdO	1.684E-04	4.295E-05	3.611E-03	3.228E-02	2.292E-03	2.710E-04
Ce_2O_3	9.405E-04	3.236E-04	1.578E-03	2.351E-03	1.010E-03	4.766E-04
Cl	2.445E-03	1.450E-03	2.454E-03	2.252E-03	1.820E-03	1.442E-03
CoO	5.004E-05	6.637E-05	6.859E-05	1.208E-04	4.854E-05	2.148E-04
Cr_2O_3	3.815E-03	2.029E-02	1.462E-02	6.181E-03	1.181E-02	1.851E-02
Cs_2O	3.424E-04	7.834E-05	3.961E-04	3.261E-04	2.996E-04	7.757E-05
CuO	3.955E-04	1.805E-04	3.109E-04	4.768E-04	3.350E-04	3.297E-04
F	1.232E-02	2.581E-03	2.552E-03	1.182E-03	1.660E-03	2.263E-02
Fe_2O_3	2.362E-01	5.489E-02	1.386E-01	3.488E-01	1.702E-01	1.435E-01
K_2O	2.136E-02	2.175E-03	9.940E-03	9.612E-03	4.810E-03	4.246E-03
La_2O_3	3.267E-04	9.527E-04	2.174E-03	8.432E-03	1.824E-03	3.205E-03
Li_2O	1.674E-04	2.234E-04	6.251E-04	4.307E-04	3.236E-04	3.888E-04
MgO	1.953E-03	1.934E-03	1.123E-03	2.584E-03	2.340E-03	5.612E-03
MnO	2.424E-02	1.384E-02	1.621E-02	1.236E-02	1.319E-02	1.352E-02
MoO_3	2.302E-04	3.256E-04	6.105E-04	2.619E-04	2.235E-04	6.966E-04
Na_2O	1.286E-01	1.627E-01	3.718E-01	9.567E-02	2.022E-01	1.508E-01
Nd_2O_3	3.746E-04	7.537E-04	3.319E-03	6.421E-03	1.930E-03	6.088E-04
NiO	3.078E-02	3.582E-03	5.745E-03	2.737E-02	1.928E-02	1.545E-02
P_2O_5	5.605E-02	1.397E-02	3.166E-02	9.687E-03	1.304E-02	3.295E-02
PbO	1.227E-02	2.603E-03	3.130E-03	6.791E-03	6.954E-03	8.213E-03
PdO	8.646E-07	2.435E-08	1.930E-04	3.402E-05	2.090E-04	1.208E-07
Re_2O_7	4.237E-05	1.985E-05	4.362E-05	3.389E-05	1.675E-05	3.944E-05
Rh_2O_3	2.020E-05	1.795E-07	2.099E-04	5.446E-05	1.230E-04	1.988E-07
RuO_2	3.517E-04	2.688E-06	4.456E-04	1.494E-04	9.453E-04	1.205E-06
SiO_2	1.406E-01	6.934E-02	2.412E-02	3.164E-02	8.077E-02	1.285E-01
SO_3	1.540E-03	4.998E-03	4.496E-03	1.839E-03	2.628E-03	9.786E-03
SnO_2	1.078E-06	1.132E-06	1.324E-06	5.890E-07	4.934E-07	1.075E-06
SrO	1.557E-03	1.655E-03	2.989E-02	6.840E-04	1.980E-02	1.019E-02
ThO_2	2.923E-03	4.827E-04	1.424E-03	1.711E-02	2.366E-02	2.915E-03
TiO_2	1.327E-04	1.297E-04	1.345E-04	3.355E-04	1.616E-04	2.373E-04
UO_3	5.021E-02	3.904E-02	2.569E-02	7.485E-02	4.921E-02	9.295E-02
V_2O_5	8.545E-05	2.723E-04	2.473E-04	9.868E-05	1.072E-04	3.707E-04
Y_2O_3	4.032E-05	3.729E-06	2.456E-04	2.381E-04	1.649E-04	9.115E-06
ZnO	9.112E-04	3.945E-04	7.586E-04	1.297E-03	4.262E-04	6.890E-04
ZrO_2	2.400E-02	1.813E-03	1.395E-02	6.602E-02	2.972E-02	2.752E-03
SUM	1	1	1	1	1	1
Oxide mass (MT)	327.203	1,453.789	164.666	123.884	249.230	1,350.527

Appendix B

LAW Glasses Used for Preliminary VHT Model Development

Appendix B: LAW Glasses Used for Preliminary VHT Model Development

Table B.1. Composition and VHT Alteration Rate of Glasses Used for Preliminary VHT Model Development

	WTP Glasses											
Glass ID	**LAWA44R10**	**LAWA53**	**LAWA56**	**LAWA88**	**LAWA102R1**	**LAWA126**	**LAWA128**	**LAWA130**	**LAWM10**	**LAWM15**	**LAWM17**	**LAWM20**
Al_2O_3	6.202E-02	6.092E-02	6.092E-02	6.081E-02	5.928E-02	5.635E-02	6.024E-02	6.024E-02	9.000E-02	9.000E-02	5.000E-02	5.000E-02
B_2O_3	8.904E-02	6.112E-02	1.193E-01	9.701E-02	9.783E-02	9.811E-02	7.063E-02	8.941E-02	1.300E-01	9.360E-02	1.200E-01	7.000E-02
CaO	1.991E-02	7.772E-02	1.951E-02	1.990E-02	4.960E-02	1.988E-02	2.078E-02	2.078E-02	1.000E-01		2.210E-02	8.000E-02
Fe_2O_3	6.983E-02	7.402E-02	7.402E-02	5.531E-02	5.293E-02	5.535E-02	5.784E-02	2.857E-02		6.280E-02	6.500E-02	2.000E-02
K_2O	5.002E-03	4.901E-03	4.901E-03	2.580E-02	2.544E-03	3.877E-02	3.876E-02	3.876E-02			2.000E-02	2.000E-02
Li_2O					2.446E-02				4.500E-02		5.000E-03	2.260E-02
MgO	1.991E-02	1.460E-02	1.460E-02	1.470E-02	1.467E-02	1.479E-02	1.179E-02	1.179E-02		3.720E-02	3.500E-02	3.500E-02
Na_2O	2.001E-01	1.973E-01	1.973E-01	2.000E-01	1.418E-01	1.844E-01	1.844E-01	1.844E-01	1.307E-01	2.200E-01	1.700E-01	1.700E-01
SiO_2	4.457E-01	4.167E-01	4.167E-01	4.399E-01	4.559E-01	4.408E-01	4.604E-01	4.604E-01	4.015E-01	4.348E-01	4.200E-01	4.200E-01
SnO_2												
SO_3	1.000E-03	1.480E-02	1.480E-02	2.100E-03	2.446E-02	3.497E-03	3.497E-03	3.497E-03	2.800E-03	1.600E-03	2.400E-03	2.400E-03
TiO_2	1.991E-02	1.090E-02	1.090E-02	1.990E-02	1.115E-02	1.998E-02	2.088E-02	2.088E-02	3.000E-02	3.000E-02	5.000E-03	5.000E-03
ZnO	2.961E-02	2.951E-02	2.951E-02	2.950E-02	2.994E-02	2.957E-02	3.087E-02	4.136E-02	1.000E-02	1.000E-02	5.000E-02	5.000E-02
ZrO_2	2.991E-02	2.951E-02	2.951E-02	2.990E-02	2.954E-02	2.987E-02	3.127E-02	3.127E-02	4.000E-02		3.500E-02	3.500E-02
BaO									1.000E-04	1.000E-04	2.500E-06	1.000E-04
Br												
CdO									1.000E-04	1.000E-04	2.500E-06	1.000E-04
Ce_2O_3												
Cl	6.503E-03	6.402E-03	6.402E-03	3.300E-03	3.228E-03	1.998E-03	1.998E-03	1.998E-03	8.002E-03	8.002E-03	2.001E-04	8.002E-03
Cr_2O_3	2.001E-04	2.001E-04	2.001E-04	1.000E-04	1.957E-04	1.998E-04	1.998E-04	1.998E-04	3.214E-03	3.214E-03	8.035E-05	3.214E-03
Cs_2O						1.599E-03	1.598E-03	1.598E-03				
F	1.000E-04	1.000E-04	1.000E-04		2.935E-04	2.997E-03	2.997E-03	2.997E-03	2.994E-03	2.994E-03	7.485E-05	2.994E-03
I												
La_2O_3												
MnO												
MoO_3												
NiO									3.000E-04	3.000E-04	7.500E-06	3.000E-04
P_2O_5	3.001E-04	3.001E-04	3.001E-04	7.001E-04	1.272E-03	7.993E-04	7.992E-04	7.992E-04	4.990E-03	4.990E-03	1.248E-04	4.990E-03
PbO									3.000E-04	3.000E-04	7.500E-06	3.000E-04
Re_2O_7	1.000E-03	1.000E-03	1.000E-03	1.000E-03	9.783E-04	9.991E-04	9.990E-04	9.990E-04				
SrO												
V_2O_5												
SUM	1	1	1	1	1	1	1	1	1	1	1	1
r_{alt} (g/m^2/d)	1.00	0.80	1.70	1.40	3.70	2.50	0.90	0.70	12.60	95.10	0.30	13.70
ln(r_{alt})	0.00	-0.22	0.53	0.34	1.31	0.92	-0.11	-0.36	2.53	4.55	-1.20	2.62

Empty cells represent zero concentration

Table B.1. (Continued)

	WTP Glasses											
Glass ID	**LAWM22**	**LAWM24**	**LAWM30**	**LAWM31**	**LAWM33**	**LAWM34**	**LAWM35**	**LAWM38**	**LAWM39**	**LAWM42**	**LAWM45**	**LAWM52 (LAWA88)**
Al_2O_3	8.000E-02	8.000E-02	8.000E-02	5.000E-02	5.000E-02	5.000E-02	5.000E-02	7.000E-02	7.000E-02	6.000E-02	7.000E-02	6.080E-02
B_2O_3	7.000E-02	1.200E-01	1.200E-01	7.000E-02	1.200E-01	8.350E-02	1.200E-01	8.000E-02	9.050E-02	8.000E-02	8.000E-02	9.700E-02
CaO	2.000E-02	2.000E-02	2.000E-02	8.000E-02	8.000E-02	8.000E-02	6.180E-02	7.000E-02	5.000E-02	5.000E-02	5.780E-02	1.990E-02
Fe_2O_3	6.500E-02	6.500E-02	6.500E-02	6.500E-02	6.500E-02	6.290E-02	4.410E-02	3.000E-02	3.000E-02	4.030E-02	5.000E-02	5.530E-02
K_2O	2.000E-02	2.000E-02	1.000E-03	1.000E-03	1.720E-02	2.000E-02	1.000E-03	1.500E-03	1.000E-03	1.000E-03	3.000E-03	2.580E-02
Li_2O	5.000E-03	6.400E-03	2.020E-02	3.000E-02	9.000E-03	3.000E-02	5.000E-03	2.500E-02	2.500E-02	2.500E-02	1.420E-02	
MgO	3.500E-02	1.000E-02	1.000E-02	1.000E-02	1.000E-02	1.000E-02	3.500E-02	1.500E-02	2.500E-02	1.500E-02	1.500E-02	1.470E-02
Na_2O	1.700E-01	1.700E-01	1.700E-01	1.675E-01	1.700E-01	1.700E-01	1.700E-01	1.400E-01	1.400E-01	1.400E-01	1.400E-01	2.000E-01
SiO_2	4.200E-01	4.707E-01	4.200E-01	4.231E-01	4.200E-01	4.200E-01	4.200E-01	4.800E-01	4.800E-01	4.800E-01	4.800E-01	4.399E-01
SnO_2												
SO_3	3.300E-03	2.400E-03	2.400E-03	3.400E-03	3.300E-03	3.300E-03	2.400E-03	3.500E-03	3.500E-03	3.700E-03	3.500E-03	2.100E-03
TiO_2	6.700E-03	5.000E-03	5.900E-03	2.500E-02	2.500E-02	1.480E-02	2.500E-02	1.000E-02	1.000E-02	2.000E-02	2.000E-02	1.990E-02
ZnO	5.000E-02	2.000E-02	5.000E-02	2.000E-02	2.000E-02	2.000E-02	2.000E-02	3.500E-02	3.500E-02	3.500E-02	4.600E-02	2.950E-02
ZrO_2	3.500E-02	1.000E-02	3.500E-02	3.500E-02	1.000E-02	3.500E-02	2.570E-02	2.000E-02	2.000E-02	3.000E-02	2.000E-02	2.990E-02
BaO	1.000E-04	2.500E-06	2.500E-06	1.000E-04	2.500E-06	2.500E-06	1.000E-04	1.000E-04	1.000E-04	1.000E-04	2.500E-06	2.600E-05
Br												
CdO	1.000E-04	2.500E-06	2.500E-06	1.000E-04	2.500E-06	2.500E-06	1.000E-04	1.000E-04	1.000E-04	1.000E-04	2.500E-06	2.600E-05
Ce_2O_3												
Cl	8.002E-03	2.001E-04	2.001E-04	8.002E-03	2.001E-04	2.001E-04	8.002E-03	8.002E-03	8.002E-03	8.002E-03	2.001E-04	2.081E-03
Cr_2O_3	3.214E-03	8.035E-05	8.035E-05	3.214E-03	8.035E-05	8.035E-05	3.214E-03	3.214E-03	3.214E-03	3.214E-03	8.035E-05	8.356E-04
Cs_2O												
F	2.994E-03	7.485E-05	7.485E-05	2.994E-03	7.485E-05	7.485E-05	2.994E-03	2.994E-03	2.994E-03	2.994E-03	7.485E-05	7.784E-04
I												
La_2O_3												
MnO												
MoO_3												
NiO	3.000E-04	7.500E-06	7.500E-06	3.000E-04	7.500E-06	7.500E-06	3.000E-04	3.000E-04	3.000E-04	3.000E-04	7.500E-06	7.800E-05
P_2O_5	4.990E-03	1.248E-04	1.248E-04	4.990E-03	1.248E-04	1.248E-04	4.990E-03	4.990E-03	4.990E-03	4.990E-03	1.248E-04	1.297E-03
PbO	3.000E-04	7.500E-06	7.500E-06	3.000E-04	7.500E-06	7.500E-06	3.000E-04	3.000E-04	3.000E-04	3.000E-04	7.500E-06	7.800E-05
Re_2O_7												
SrO												
V_2O_5												
SUM	1	1	1	1	1	1	1	1	1	1	1	1
r_{alt} (g/m^2/d)	0.20	13.70	21.30	5.50	3.80	48.70	1.00	19.70	12.40	0.80	5.00	3.10
ln(r_{alt})	-1.61	2.62	3.06	1.70	1.34	3.89	0.00	2.98	2.52	-0.22	1.61	1.13

Table B.1. (Continued)

	WTP Glasses											
Glass ID	**LAWM56 (LAWM35)**	**LAWM57**	**LAWM58**	**LAWM59**	**LAWM60**	**LAWM61**	**LAWM62**	**LAWM63**	**LAWM64**	**LAWM65**	**LAWM66**	**LAWM67**
Al_2O_3	5.000E-02	6.999E-02	6.999E-02	6.839E-02	5.000E-02	5.000E-02	5.000E-02	6.999E-02	6.989E-02	5.000E-02	7.589E-02	7.998E-02
B_2O_3	1.200E-01	1.100E-01	9.289E-02	9.009E-02	1.100E-01	1.100E-01	8.999E-02	9.398E-02	1.098E-01	9.000E-02	1.063E-01	1.060E-01
CaO	6.180E-02	2.999E-02	1.030E-02	2.960E-02	1.710E-02	9.999E-03	9.999E-03	1.040E-02	3.000E-02	2.960E-02	9.999E-03	1.550E-02
Fe_2O_3	4.410E-02	4.659E-02	6.499E-02	6.489E-02	4.500E-02	4.500E-02	6.499E-02	4.699E-02	6.499E-02	4.500E-02	6.309E-02	4.599E-02
K_2O	1.000E-03	3.799E-02	3.800E-02	2.000E-02	2.000E-02	3.290E-02	3.380E-02	2.060E-02	2.000E-02	2.000E-02	4.800E-03	5.399E-02
Li_2O	5.000E-03											
MgO	3.500E-02	1.440E-02	1.440E-02	1.440E-02	1.440E-02	1.440E-02	1.440E-02	1.440E-02	1.440E-02	1.440E-02	1.440E-02	1.440E-02
Na_2O	1.700E-01	2.061E-01	2.053E-01	2.000E-01	2.001E-01	2.000E-01	2.000E-01	2.300E-01	2.004E-01	2.279E-01	2.299E-01	2.013E-01
SiO_2	4.200E-01	3.925E-01	4.164E-01	4.454E-01	4.533E-01	4.505E-01	4.433E-01	4.259E-01	3.836E-01	4.359E-01	3.835E-01	3.835E-01
SnO_2												
SO_3	2.400E-03	3.499E-03	3.500E-03	3.500E-03	3.500E-03	3.500E-03	3.500E-03	3.499E-03	3.500E-03	3.500E-03	3.500E-03	3.499E-03
TiO_2	2.500E-02	1.370E-02	1.370E-02	1.370E-02	1.370E-02	1.370E-02	1.370E-02	1.370E-02	1.370E-02	1.370E-02	1.370E-02	1.370E-02
ZnO	2.000E-02	3.029E-02	2.560E-02	2.510E-02	2.800E-02	4.500E-02	3.840E-02	4.499E-02	4.490E-02	2.500E-02	4.500E-02	2.719E-02
ZrO_2	2.570E-02	3.999E-02	4.000E-02	2.000E-02	4.000E-02	2.010E-02	3.300E-02	2.060E-02	3.990E-02	4.000E-02	4.500E-02	4.999E-02
BaO	1.000E-04											
Br												
CdO	1.000E-04											
Ce_2O_3												
Cl	8.002E-03	2.000E-03	2.000E-03	2.000E-03	2.000E-03	2.000E-03	2.000E-03	2.000E-03	2.000E-03	2.000E-03	2.000E-03	2.000E-03
Cr_2O_3	3.214E-03	7.998E-04	7.999E-04	7.999E-04	7.999E-04	7.999E-04	7.999E-04	7.998E-04	7.999E-04	8.000E-04	7.999E-04	7.998E-04
Cs_2O												
F	2.994E-03	7.998E-04	7.999E-04	7.999E-04	7.999E-04	7.999E-04	7.999E-04	7.998E-04	7.999E-04	8.000E-04	7.999E-04	7.998E-04
I												
La_2O_3												
MnO												
MoO_3												
NiO	3.000E-04	9.998E-05	9.999E-05	9.999E-05	9.999E-05	9.999E-05	9.999E-05	9.998E-05	9.999E-05	1.000E-04	9.999E-05	9.998E-05
P_2O_5	4.990E-03	1.200E-03	1.200E-03	1.200E-03	1.200E-03	1.200E-03	1.200E-03	1.200E-03	1.200E-03	1.200E-03	1.200E-03	1.200E-03
PbO	3.000E-04	9.998E-05	9.999E-05	9.999E-05	9.999E-05	9.999E-05	9.999E-05	9.998E-05	9.999E-05	1.000E-04	9.999E-05	9.998E-05
Re_2O_7												
SrO												
V_2O_5												
SUM	1	1	1	1	1	1	1	1	1	1	1	1
r_{alt} (g/m^2/d)	0.70	15.70	17.30	14.80	3.30	39.90	12.70	72.30	3.00	57.60	49.10	28.70
ln(r_{alt})	-0.36	2.75	2.85	2.69	1.19	3.69	2.54	4.28	1.10	4.05	3.89	3.36

Table B.1. (Continued)

	WTP Glasses											
Glass ID	**LAWM68**	**LAWM69**	**LAWM70**	**LAWM71**	**LAWM72**	**LAWM73**	**LAWM74**	**LAWM75**	**LAWM76**	**LAWE2H**	**LAWE3**	**LAWE3H**
Al_2O_3	4.999E-02	7.978E-02	4.999E-02	5.009E-02	7.998E-02	7.998E-02	7.579E-02	7.999E-02	6.400E-02	5.949E-02	6.100E-02	5.939E-02
B_2O_3	8.998E-02	1.099E-01	9.397E-02	8.999E-02	1.100E-01	8.998E-02	8.999E-02	9.149E-02	9.920E-02	9.749E-02	1.000E-01	9.739E-02
CaO	2.999E-02	2.999E-02	1.050E-02	9.999E-03	2.939E-02	2.999E-02	9.999E-03	3.000E-02	1.920E-02	1.970E-02	2.020E-02	1.970E-02
Fe_2O_3	6.499E-02	6.369E-02	6.498E-02	4.500E-02	6.449E-02	4.879E-02	4.500E-02	6.489E-02	5.420E-02	5.359E-02	5.500E-02	5.359E-02
K_2O	4.799E-02	1.830E-02	4.549E-02	5.399E-02	4.179E-02	1.220E-02		1.080E-02	2.600E-02	3.790E-02	4.990E-02	5.409E-02
Li_2O												
MgO	1.440E-02	1.440E-02	1.440E-02	1.440E-02	1.440E-02	1.440E-02	1.440E-02	1.440E-02	1.440E-02	1.440E-02	1.480E-02	1.440E-02
Na_2O	2.001E-01	2.009E-01	2.000E-01	2.000E-01	2.004E-01	2.300E-01	2.132E-01	2.068E-01	2.140E-01	2.078E-01	1.821E-01	1.974E-01
SiO_2	4.080E-01	3.959E-01	4.534E-01	4.494E-01	3.915E-01	4.037E-01	4.535E-01	3.845E-01	4.186E-01	4.244E-01	4.295E-01	4.185E-01
SnO_2												
SO_3	3.499E-03	3.499E-03	3.499E-03	3.500E-03	3.499E-03	3.499E-03	3.500E-03	3.500E-03	3.500E-03	3.200E-03	3.500E-03	3.700E-03
TiO_2	1.370E-02	1.370E-02	1.370E-02	1.370E-02	1.370E-02	1.370E-02	1.370E-02	1.370E-02	1.370E-02	1.370E-02	1.400E-02	1.360E-02
ZnO	3.559E-02	4.499E-02	2.499E-02	4.500E-02	2.500E-02	4.489E-02	2.600E-02	4.500E-02	3.420E-02	3.410E-02	3.500E-02	3.410E-02
ZrO_2	3.679E-02	2.000E-02	2.009E-02	2.000E-02	2.090E-02	2.390E-02	5.000E-02	5.000E-02	3.400E-02	2.930E-02	3.000E-02	2.920E-02
BaO												
Br												
CdO												
Ce_2O_3												
Cl	2.000E-03	2.000E-03	1.999E-03	2.000E-03	2.000E-03	2.000E-03	2.000E-03	2.000E-03	2.000E-03	2.000E-03	2.000E-03	2.000E-03
Cr_2O_3	7.998E-04	7.998E-04	7.998E-04	7.999E-04	7.998E-04	7.998E-04	7.999E-04	7.999E-04	8.000E-04	7.999E-04	8.000E-04	7.999E-04
Cs_2O												
F	7.998E-04	7.998E-04	7.998E-04	7.999E-04	7.998E-04	7.998E-04	7.999E-04	7.999E-04	8.000E-04	7.999E-04	8.000E-04	7.999E-04
I												
La_2O_3												
MnO												
MoO_3												
NiO	9.998E-05	9.998E-05	9.997E-05	9.999E-05	9.998E-05	9.998E-05	9.999E-05	9.999E-05	1.000E-04	9.999E-05	1.000E-04	9.999E-05
P_2O_5	1.200E-03	1.200E-03	1.200E-03	1.200E-03	1.200E-03	1.200E-03	1.200E-03	1.200E-03	1.200E-03	1.200E-03	1.200E-03	1.200E-03
PbO	9.998E-05	9.998E-05	9.997E-05	9.999E-05	9.998E-05	9.998E-05	9.999E-05	9.999E-05	1.000E-04	9.999E-05	1.000E-04	9.999E-05
Re_2O_7												
SrO												
V_2O_5												
SUM	1	1	1	1	1	1	1	1	1	1	1	1
r_{alt} (g/m^2/d)	25.80	31.20	89.80	108.20	54.70	52.10	1.50	0.80	9.90	64.90	14.20	71.10
ln(r_{alt})	3.25	3.44	4.50	4.68	4.00	3.95	0.41	-0.22	2.29	4.17	2.65	4.26

Table B.1. (Continued)

	WTP Glasses											
Glass ID	**LAWE4H**	**LAWE5H**	**LAWE7H**	**LAWE11**	**LAWE12**	**LAWE13**	**LAWE15**	**LAWE16**	**LAWCrP1R**	**LAWCrP2R**	**LAWCrP3R**	**LAWCrP4R**
Al_2O_3	5.969E-02	5.989E-02	6.019E-02	6.100E-02	6.949E-02	6.949E-02	5.939E-02	5.940E-02	6.101E-02	6.101E-02	6.101E-02	6.101E-02
B_2O_3	9.789E-02	9.809E-02	9.869E-02	1.000E-01	8.749E-02	9.749E-02	8.749E-02	8.250E-02	1.000E-01	1.000E-01	1.000E-01	1.000E-01
CaO	2.460E-02	3.610E-02	6.309E-02	2.320E-02	1.970E-02	1.970E-02	1.470E-02	1.470E-02	2.760E-02	2.110E-02	2.760E-02	2.110E-02
Fe_2O_3	5.379E-02	5.399E-02	5.429E-02	5.500E-02	4.360E-02	5.359E-02	5.359E-02	5.360E-02	5.501E-02	5.501E-02	5.501E-02	5.501E-02
K_2O	5.399E-03	5.399E-03	5.399E-03	4.750E-02	5.409E-02	5.409E-02	5.409E-02	5.410E-02	1.300E-03	2.701E-03	1.300E-03	2.700E-03
Li_2O		4.900E-03	3.170E-02									
MgO	1.450E-02	1.450E-02	1.490E-02	1.480E-02	1.440E-02	4.400E-03	9.399E-03	9.400E-03	1.480E-02	1.480E-02	1.480E-02	1.480E-02
Na_2O	2.127E-01	1.897E-01	1.353E-01	1.736E-01	1.974E-01	1.974E-01	1.974E-01	1.974E-01	1.934E-01	2.100E-01	1.934E-01	2.100E-01
SiO_2	4.450E-01	4.505E-01	4.476E-01	4.374E-01	4.184E-01	4.184E-01	4.285E-01	4.284E-01	4.439E-01	4.308E-01	4.345E-01	4.203E-01
SnO_2												
SO_3	4.100E-03	4.600E-03	5.899E-03	3.500E-03	3.500E-03	3.500E-03	3.500E-03	3.500E-03	3.900E-03	3.401E-03	3.900E-03	3.400E-03
TiO_2	1.370E-02	1.370E-02	1.380E-02	1.400E-02	1.370E-02	3.700E-03	1.370E-02	1.370E-02	1.400E-02	1.400E-02	1.400E-02	1.400E-02
ZnO	3.430E-02	3.430E-02	3.460E-02	3.500E-02	3.410E-02	3.410E-02	3.410E-02	3.410E-02	3.500E-02	3.501E-02	3.500E-02	3.500E-02
ZrO_2	2.940E-02	2.940E-02	2.960E-02	3.000E-02	3.920E-02	3.920E-02	3.920E-02	4.420E-02	3.000E-02	3.001E-02	3.000E-02	3.000E-02
BaO												
Br												
CdO												
Ce_2O_3												
Cl	2.000E-03	2.000E-03	2.000E-03	2.000E-03	2.000E-03	2.000E-03	2.000E-03	2.000E-03	1.200E-03	1.900E-03	1.200E-03	1.900E-03
Cr_2O_3	7.999E-04	7.999E-04	7.999E-04	8.000E-04	7.999E-04	7.999E-04	7.999E-04	8.000E-04	3.300E-03	5.901E-03	3.300E-03	5.901E-03
Cs_2O												
F	7.999E-04	7.999E-04	7.999E-04	8.000E-04	7.999E-04	7.999E-04	7.999E-04	8.000E-04	1.100E-03	1.000E-03	1.100E-03	1.000E-03
I												
La_2O_3												
MnO												
MoO_3												
NiO	9.999E-05	9.999E-05	9.999E-05	1.000E-04	9.999E-05	9.999E-05	9.999E-05	1.000E-04				
P_2O_5	1.200E-03	1.200E-03	1.200E-03	1.200E-03	1.200E-03	1.200E-03	1.200E-03	1.200E-03	1.440E-02	1.330E-02	2.380E-02	2.380E-02
PbO	9.999E-05	9.999E-05	9.999E-05	1.000E-04	9.999E-05	9.999E-05	9.999E-05	1.000E-04				
Re_2O_7												
SrO												
V_2O_5												
SUM	1	1	1	1	1	1	1	1	1	1	1	1
r_{alt} (g/m^2/d)	16.20	1.70	16.80	3.60	81.40	67.90	53.60	50.70	3.60	24.10	8.80	22.30
ln(r_{alt})	2.79	0.53	2.82	1.28	4.40	4.22	3.98	3.93	1.28	3.18	2.17	3.10

Table B.1. (Continued)

	WTP Glasses											
Glass ID	**LAWCrP5**	**LAWA49**	**LAWA51**	**LAWA52**	**LAWA60**	**LAWA104**	**LAWA105**	**LAWA125**	**LAWA133**	**LAWA134**	**LAWA135**	**LAWA136**
Al_2O_3	6.099E-02	6.201E-02	6.199E-02	6.180E-02	8.532E-02	6.611E-02	7.031E-02	5.633E-02	6.203E-02	5.644E-02	5.653E-02	5.653E-02
B_2O_3	9.998E-02	8.901E-02	1.197E-01	6.190E-02	1.123E-01	8.592E-02	8.282E-02	9.539E-02	8.899E-02	9.959E-02	1.009E-01	1.009E-01
CaO	5.809E-02			7.880E-02	4.321E-02	1.920E-02	1.850E-02	1.938E-02	5.483E-02	2.018E-02	2.047E-02	3.046E-02
Fe_2O_3	5.499E-02	9.981E-02	6.999E-02	7.510E-02		6.731E-02	6.491E-02	5.384E-02	3.486E-02	5.624E-02	5.693E-02	5.693E-02
K_2O	8.998E-04	5.001E-03	4.500E-03	5.000E-03	5.001E-03	5.501E-03	6.001E-03	4.205E-02	4.295E-03	3.726E-02	3.575E-02	3.575E-02
Li_2O	2.639E-02											
MgO	1.490E-02	1.480E-02	1.480E-02	1.480E-02	1.990E-02	1.920E-02	1.850E-02	1.438E-02	1.998E-02	1.498E-02	1.518E-02	1.518E-02
Na_2O	1.438E-01	2.000E-01	1.800E-01	2.000E-01	2.000E-01	2.200E-01	2.400E-01	1.998E-01	1.998E-01	1.772E-01	1.701E-01	1.701E-01
SiO_2	4.344E-01	4.455E-01	4.657E-01	4.225E-01	4.456E-01	4.300E-01	4.143E-01	4.286E-01	4.453E-01	4.473E-01	4.528E-01	4.428E-01
SnO_2												
SO_3	5.099E-03	1.000E-03	8.999E-04	1.000E-03	1.000E-03	1.000E-03	1.100E-03	3.795E-03	2.197E-03	3.296E-03	3.196E-03	3.196E-03
TiO_2	1.400E-02	1.990E-02	2.000E-02	1.110E-02	1.990E-02	1.920E-02	1.850E-02	1.938E-02	1.998E-02	2.028E-02	2.047E-02	2.047E-02
ZnO	3.499E-02	2.480E-02	2.490E-02	2.990E-02	2.961E-02	2.861E-02	2.761E-02	2.877E-02	2.966E-02	2.997E-02	3.036E-02	3.036E-02
ZrO_2	2.999E-02	2.990E-02	3.000E-02	2.990E-02	2.991E-02	2.891E-02	2.781E-02	2.907E-02	2.996E-02	3.037E-02	3.076E-02	3.076E-02
BaO												
Br												
CdO												
Ce_2O_3												
Cl	1.400E-03	6.501E-03	5.899E-03	6.500E-03	6.501E-03	7.201E-03	7.802E-03	2.197E-03	5.593E-03	1.998E-03	1.898E-03	1.898E-03
Cr_2O_3	5.899E-03	2.000E-04	2.000E-04	2.000E-04	2.000E-04	2.000E-04	2.000E-04	1.998E-04	1.998E-04	1.998E-04	1.997E-04	1.997E-04
Cs_2O								1.798E-03				
F	6.999E-04	1.000E-04	9.999E-05	1.000E-04	1.000E-04	1.000E-04	1.000E-04	3.196E-03	3.995E-04	2.897E-03	2.796E-03	2.796E-03
I												
La_2O_3												
MnO												
MoO_3		1.000E-04	9.999E-05	1.000E-04	1.000E-04	1.000E-04	1.000E-04					
NiO	9.998E-05											
P_2O_5	1.330E-02	3.000E-04	3.000E-04	3.000E-04	3.001E-04	4.001E-04	4.001E-04	8.989E-04	9.988E-04	7.991E-04	6.991E-04	6.991E-04
PbO	9.998E-05											
Re_2O_7		1.000E-03	9.999E-04	1.000E-03	1.000E-03	1.000E-03	1.000E-03	9.988E-04	9.988E-04	9.989E-04	9.987E-04	9.987E-04
SrO												
V_2O_5												
SUM	1	1	1	1	1	1	1	1	1	1	1	1
r_{alt} (g/m^2/d)	0.88	3.40	0.60	7.60	6.20	6.50	39.60	37.90	0.60	0.20	0.30	0.30
ln(r_{alt})	-0.12	1.22	-0.51	2.03	1.82	1.87	3.68	3.63	-0.51	-1.61	-1.20	-1.20

Table B.1. (Continued)

	WTP Glasses											
Glass ID	**LAWC15**	**TFA-BASE**	**A2-AP101**	**A88AP101R1**	**A3-AN104**	**Cl-AN107**	**C22AN107**	**A88Si+15**	**A88Si-15**	**C22Si+15**	**A1C1-1**	**A1C1-2**
Al_2O_3	6.224E-02	7.000E-02	5.619E-02	6.099E-02	6.049E-02	6.059E-02	6.103E-02	6.139E-02	6.051E-02	6.043E-02	6.089E-02	6.072E-02
B_2O_3	8.942E-02	1.000E-01	9.819E-02	9.828E-02	9.919E-02	1.002E-01	1.008E-01	9.479E-02	1.021E-01	9.835E-02	9.118E-02	9.413E-02
CaO	2.008E-02	1.000E-04	1.990E-02	2.000E-02	5.029E-02	5.089E-02	5.113E-02	1.930E-02	2.070E-02	4.992E-02	2.739E-02	3.521E-02
Fe_2O_3	7.014E-02	5.500E-02	5.529E-02	5.549E-02	5.369E-02	5.419E-02	5.583E-02	5.349E-02	5.761E-02	5.353E-02	6.499E-02	6.132E-02
K_2O	1.399E-03	4.100E-03	3.810E-02	2.140E-02	3.300E-03	6.999E-04	9.005E-04	2.370E-02	1.880E-02	1.001E-03	3.499E-03	2.501E-03
Li_2O					2.480E-02	2.500E-02	2.511E-02			2.461E-02	6.199E-03	1.250E-02
MgO	2.008E-02	1.500E-02	1.480E-02	1.480E-02	1.480E-02	1.510E-02	1.511E-02	1.430E-02	1.540E-02	1.481E-02	1.850E-02	1.731E-02
Na_2O	1.998E-01	2.000E-01	1.846E-01	2.000E-01	1.464E-01	1.445E-01	1.443E-01	2.218E-01	1.766E-01	1.619E-01	1.916E-01	1.767E-01
SiO_2	4.476E-01	4.907E-01	4.399E-01	4.412E-01	4.609E-01	4.659E-01	4.659E-01	4.255E-01	4.584E-01	4.556E-01	4.446E-01	4.512E-01
SnO_2												
SO_3	1.299E-03	7.000E-04	4.000E-03	2.799E-03	3.700E-03	3.800E-03	3.102E-03	3.100E-03	2.501E-03	3.402E-03	2.400E-03	2.801E-03
TiO_2	1.998E-02	3.000E-02	1.990E-02	2.000E-02	1.130E-02	1.150E-02	1.141E-02	1.930E-02	2.070E-02	1.121E-02	1.760E-02	1.550E-02
ZnO	2.997E-02	1.500E-02	2.940E-02	2.959E-02	3.040E-02	3.060E-02	3.062E-02	2.850E-02	3.071E-02	3.002E-02	2.949E-02	2.981E-02
ZrO_2	3.007E-02	1.500E-02	2.960E-02	2.999E-02	3.000E-02	3.020E-02	3.022E-02	2.890E-02	3.111E-02	2.961E-02	2.959E-02	2.971E-02
BaO												
Br	7.993E-04											
CdO												
Ce_2O_3												
Cl	7.993E-04	2.800E-03	4.200E-03	1.300E-03	7.899E-03	6.999E-04	8.004E-04	1.400E-03	1.200E-03	9.005E-04	9.098E-03	6.502E-03
Cr_2O_3			2.000E-04	2.000E-04	2.000E-04	9.999E-05	2.001E-04	2.000E-04	1.000E-04	2.001E-04	2.000E-04	1.000E-04
Cs_2O			1.500E-03		1.500E-03	1.500E-03					1.500E-03	1.500E-03
F	4.696E-03	1.000E-04	3.500E-03	2.300E-03	9.999E-05	2.800E-03	1.401E-03	2.500E-03	2.000E-03	1.601E-03	8.998E-04	1.701E-03
I												
La_2O_3												
MnO												
MoO_3												
NiO	3.996E-04					3.000E-04				3.002E-04	9.998E-05	1.000E-04
P_2O_5	1.998E-04	6.000E-04	7.999E-04	6.999E-04	1.100E-03	1.300E-03	1.201E-03	7.999E-04	6.001E-04	1.301E-03	2.999E-04	7.002E-04
PbO						2.000E-04				2.001E-04		
Re_2O_7	9.991E-04	9.000E-04		9.998E-04			1.001E-03	1.100E-03	9.002E-04	1.101E-03		
SrO												
V_2O_5												
SUM	1	1	1	1	1	1	1	1	1	1	1	1
r_{alt} (g/m^2/d)	0.60	9.70	0.80	1.40	0.70	8.80	1.00	32.00	0.40	2.50	0.70	3.40
ln(r_{alt})	-0.51	2.27	-0.22	0.34	-0.36	2.17	0.00	3.47	-0.92	0.92	-0.36	1.22

Table B.1. (Continued)

	WTP Glasses		ORP Glasses									
Glass ID	**A1C1-3**	**A2B1-1**	**ORPLA18**	**ORPLA19**	**ORPLA20**	**ORPLA21**	**ORPLA22**	**ORPLA23**	**ORPLA24**	**ORPLA25**	**ORPLD4**	**ORPLD5**
Al_2O_3	6.052E-02	5.751E-02	9.699E-02	9.699E-02	6.700E-02	6.909E-02	9.460E-02	9.460E-02	9.339E-02	9.170E-02	1.018E-01	1.018E-01
B_2O_3	9.693E-02	9.872E-02	8.799E-02	8.799E-02	8.800E-02	8.639E-02	8.800E-02	8.800E-02	8.549E-02	8.390E-02	1.207E-01	1.003E-01
CaO	4.301E-02	3.181E-02	3.340E-02	3.340E-02	3.340E-02	3.280E-02	3.550E-02	3.550E-02	3.520E-02	3.450E-02	8.032E-02	8.032E-02
Fe_2O_3	5.762E-02	5.471E-02	3.000E-03	3.000E-03	3.000E-03	2.900E-03					3.001E-03	3.001E-03
K_2O	1.600E-03	2.901E-02	5.399E-03	5.399E-03	5.400E-03	5.599E-03	5.400E-03	5.400E-03	5.599E-03	5.800E-03	1.600E-03	1.600E-03
Li_2O	1.871E-02	1.070E-02										
MgO	1.620E-02	1.850E-02	9.299E-03	9.299E-03	9.300E-03	9.099E-03					1.000E-02	1.000E-02
Na_2O	1.616E-01	1.521E-01	2.400E-01	2.400E-01	2.400E-01	2.500E-01	2.400E-01	2.400E-01	2.500E-01	2.600E-01	2.100E-01	2.100E-01
SiO_2	4.577E-01	4.513E-01	3.952E-01	3.952E-01	4.251E-01	4.172E-01	4.029E-01	4.029E-01	3.970E-01	3.910E-01	3.793E-01	3.793E-01
SnO_2			2.760E-02	4.830E-02	2.760E-02	2.710E-02	3.000E-02	5.000E-02	3.000E-02	3.000E-02		
SO_3	3.301E-03	4.601E-03	1.800E-03	1.800E-03	1.800E-03	1.900E-03	1.800E-03	1.800E-03	1.900E-03	2.000E-03	9.602E-03	9.602E-03
TiO_2	1.350E-02	1.840E-02										
ZnO	3.011E-02	3.411E-02	2.760E-02	2.760E-02	2.760E-02	2.710E-02	3.000E-02	3.000E-02	2.940E-02	2.890E-02	3.011E-02	3.011E-02
ZrO_2	2.991E-02	3.011E-02	5.999E-02	3.930E-02	6.000E-02	5.879E-02	6.000E-02	4.000E-02	5.999E-02	6.000E-02	3.011E-02	4.051E-02
BaO												
Br												
CdO												
Ce_2O_3												
Cl	3.901E-03	3.201E-03	6.799E-03	6.799E-03	6.800E-03	7.099E-03	6.800E-03	6.800E-03	7.099E-03	7.300E-03	3.301E-03	3.301E-03
Cr_2O_3	1.000E-04	2.000E-04	5.000E-03	5.000E-03	5.000E-03	5.000E-03	5.000E-03	5.000E-03	5.000E-03	4.900E-03	5.001E-03	5.001E-03
Cs_2O	1.500E-03	1.500E-03										
F	2.501E-03	2.801E-03									1.700E-03	1.700E-03
I												
La_2O_3												
MnO												
MoO_3												
NiO	2.001E-04										4.001E-04	4.001E-04
P_2O_5	1.000E-03	7.001E-04									2.901E-03	2.901E-03
PbO											1.000E-04	1.000E-04
Re_2O_7												
SrO												
V_2O_5											1.000E-02	2.000E-02
SUM	1	1	1	1	1	1	1	1	1	1	1	1
r_{alt} (g/m^2/d)	0.70	0.50	36.00	22.00	7.00	43.00	3.00	12.00	12.00	42.00	13.00	14.00
ln(r_{alt})	-0.36	-0.69	3.58	3.09	1.95	3.76	1.10	2.48	2.48	3.74	2.56	2.64

Table B.1. (Continued)

	ORP Glasses											
Glass ID	**ORPLD6**	**ORPLD7**	**ORPLD8**	**ORPLD9**	**ORPLF5**	**ORPLF6**	**ORPLG1**	**ORPLG2**	**ORPLG3**	**ORPLG4**	**ORPLG5**	**ORPLG6**
Al_2O_3	1.012E-01	1.008E-01	1.003E-01	8.569E-02	9.620E-02	8.479E-02	1.004E-01	9.989E-02	9.950E-02	9.950E-02	9.949E-02	6.769E-02
B_2O_3	9.869E-02	9.870E-02	9.499E-02	9.499E-02	9.340E-02	9.359E-02	8.900E-02	8.819E-02	8.740E-02	8.740E-02	8.739E-02	8.698E-02
CaO	7.909E-02	7.910E-02	7.349E-02	7.349E-02	9.580E-02	9.579E-02	2.230E-02	2.200E-02	2.180E-02	2.180E-02	2.770E-02	2.749E-02
Fe_2O_3	3.000E-03	3.000E-03	2.900E-03	2.900E-03	2.900E-03	2.900E-03	3.000E-03	2.900E-03	2.900E-03	2.900E-03		2.899E-03
K_2O	1.700E-03	1.700E-03	1.800E-03	1.800E-03	5.400E-03	5.399E-03	5.060E-02	5.199E-02	5.340E-02	5.340E-02	5.339E-02	5.399E-02
Li_2O					3.590E-02	3.450E-02						
MgO	9.899E-03	9.900E-03	9.699E-03	9.699E-03	9.700E-03	9.699E-03	9.600E-03	9.599E-03	9.500E-03	9.500E-03		9.798E-03
Na_2O	2.200E-01	2.200E-01	2.300E-01	2.300E-01	1.300E-01	1.300E-01	1.850E-01	1.900E-01	1.950E-01	1.950E-01	1.950E-01	1.975E-01
SiO_2	3.733E-01	3.733E-01	3.674E-01	3.674E-01	4.154E-01	4.154E-01	4.127E-01	4.089E-01	4.050E-01	4.050E-01	4.079E-01	4.174E-01
SnO_2		1.000E-02	9.999E-03	9.999E-03	8.400E-03	8.399E-03	2.970E-02	2.940E-02	2.910E-02	4.800E-02	2.910E-02	2.899E-02
SO_3	1.010E-02	1.010E-02	1.060E-02	1.060E-02	2.090E-02	2.090E-02	3.600E-03	3.700E-03	3.800E-03	3.800E-03	3.800E-03	3.799E-03
TiO_2												
ZnO	2.970E-02	2.970E-02	2.990E-02	2.990E-02	2.870E-02	2.870E-02	2.450E-02	2.430E-02	2.400E-02	2.400E-02	2.770E-02	3.479E-02
ZrO_2	3.990E-02	3.990E-02	4.020E-02	4.020E-02	3.830E-02	3.830E-02	5.930E-02	5.879E-02	5.820E-02	3.930E-02	5.819E-02	5.799E-02
BaO												
Br												
CdO												
Ce_2O_3												
Cl	3.500E-03	3.500E-03	3.600E-03	3.600E-03	1.000E-04	9.999E-05	2.000E-03	2.100E-03	2.100E-03	2.100E-03	2.100E-03	2.200E-03
Cr_2O_3	5.000E-03	5.000E-03	5.000E-03	5.000E-03	5.600E-03	5.599E-03	6.000E-03	5.999E-03	6.000E-03	6.000E-03	5.999E-03	5.999E-03
Cs_2O												
F	1.800E-03	1.800E-03	1.900E-03	1.900E-03	9.000E-04	8.999E-04	8.000E-04	7.999E-04	8.000E-04	8.000E-04	7.999E-04	8.998E-04
I												
La_2O_3												
MnO												
MoO_3												
NiO	4.000E-04	4.000E-04	4.000E-04	4.000E-04			1.000E-04	9.999E-05	1.000E-04	1.000E-04	9.999E-05	9.998E-05
P_2O_5	3.000E-03	3.000E-03	3.100E-03	3.100E-03	4.000E-04	4.000E-04	1.300E-03	1.300E-03	1.300E-03	1.300E-03	1.300E-03	1.400E-03
PbO	9.999E-05	1.000E-04	2.000E-04	2.000E-04			1.000E-04	9.999E-05	1.000E-04	1.000E-04	9.999E-05	9.998E-05
Re_2O_7												
SrO												
V_2O_5	1.970E-02	1.000E-02	1.460E-02	2.920E-02	1.200E-02	2.470E-02						
SUM	1	1	1	1	1	1	1	1	1	1	1	1
r_{alt} ($g/m^2/d$)	18.00	15.00	13.00	42.00	22.00	17.00	2.00	2.00	12.00	20.00	4.00	11.00
$\ln(r_{alt})$	2.89	2.71	2.56	3.74	3.09	2.83	0.69	0.69	2.48	3.00	1.39	2.40

Table B.1. (Continued)

	ORP Glasses											
Glass ID	**ORPLG7**	**ORPLG8**	**ORPLG9**	**ORPLG10**	**ORPLG11**	**ORPLG12**	**ORPLA2**	**ORPLA3**	**ORPLA4**	**ORPLA5**	**ORPLA6**	**ORPLA7**
Al_2O_3	6.770E-02	6.749E-02	6.739E-02	6.720E-02	6.749E-02	6.749E-02	1.000E-01	9.999E-02	7.999E-02	1.000E-01	1.088E-01	1.088E-01
B_2O_3	8.650E-02	8.569E-02	8.489E-02	8.400E-02	8.569E-02	8.568E-02	9.000E-02	8.999E-02	8.999E-02	7.002E-02	7.780E-02	7.781E-02
CaO	2.740E-02	2.710E-02	2.690E-02	2.660E-02	3.960E-02	2.709E-02	2.500E-02	3.040E-02	3.500E-02	1.000E-02	1.000E-02	1.470E-02
Fe_2O_3	2.900E-03	2.900E-03	2.800E-03	2.800E-03		2.899E-03	1.010E-02	1.010E-02	3.020E-02	1.010E-02	9.400E-03	9.401E-03
K_2O	5.470E-02	5.609E-02	5.749E-02	5.880E-02	5.609E-02	5.609E-02	5.600E-03	5.599E-03	5.599E-03	5.602E-03	5.600E-03	5.601E-03
Li_2O												
MgO	9.700E-03	9.599E-03	9.499E-03	9.400E-03		9.598E-03	1.350E-02	1.350E-02	1.350E-02	1.350E-02	9.100E-03	9.101E-03
Na_2O	2.000E-01	2.050E-01	2.100E-01	2.150E-01	2.050E-01	2.050E-01	2.500E-01	2.500E-01	2.500E-01	2.501E-01	2.500E-01	2.500E-01
SiO_2	4.155E-01	4.115E-01	4.075E-01	4.035E-01	4.115E-01	4.114E-01	4.131E-01	4.131E-01	4.131E-01	4.332E-01	4.192E-01	4.050E-01
SnO_2	2.880E-02	2.860E-02	2.830E-02	2.800E-02	2.860E-02	2.859E-02	1.000E-02			1.000E-02	1.000E-02	1.000E-02
SO_3	3.900E-03	4.000E-03	4.100E-03	4.200E-03	4.000E-03	3.999E-03	1.900E-03	1.900E-03	1.900E-03	1.901E-03	1.900E-03	1.900E-03
TiO_2												
ZnO	3.460E-02	3.430E-02	3.390E-02	3.360E-02	3.430E-02	3.429E-02	2.360E-02	2.360E-02	2.360E-02	3.361E-02	2.360E-02	2.360E-02
ZrO_2	5.770E-02	5.709E-02	5.659E-02	5.600E-02	5.709E-02	3.859E-02	4.800E-02	4.800E-02	4.800E-02	4.801E-02	6.070E-02	6.071E-02
BaO												
Br												
CdO												
Ce_2O_3												
Cl	2.200E-03	2.300E-03	2.300E-03	2.400E-03	2.300E-03	2.300E-03	7.100E-03	7.099E-03	7.099E-03	7.102E-03	7.100E-03	7.101E-03
Cr_2O_3	5.900E-03	5.899E-03	5.899E-03	5.900E-03	5.899E-03	5.899E-03	2.000E-04	4.900E-03	2.000E-04	4.901E-03	4.900E-03	4.900E-03
Cs_2O							1.900E-03	1.900E-03	1.900E-03	1.901E-03	1.900E-03	1.900E-03
F	9.000E-04	8.999E-04	8.999E-04	9.000E-04	8.999E-04	8.998E-04						
I												
La_2O_3												
MnO												
MoO_3												
NiO	1.000E-04	9.999E-05	9.999E-05	1.000E-04	9.999E-05	9.998E-05						
P_2O_5	1.400E-03	1.400E-03	1.400E-03	1.500E-03	1.400E-03	2.000E-02						
PbO	1.000E-04	9.999E-05	9.999E-05	1.000E-04	9.999E-05	9.998E-05						
Re_2O_7												
SrO												
V_2O_5												9.401E-03
SUM	1	1	1	1	1	1	1	1	1	1	1	1
r_{alt} (g/m^2/d)	22.00	44.00	50.00	91.00	9.00	102.00	130.00	115.00	114.00	103.00	91.00	68.00
ln(r_{alt})	3.09	3.78	3.91	4.51	2.20	4.62	4.87	4.74	4.74	4.63	4.51	4.22

Table B.1. (Continued)

	ORP Glasses											
Glass ID	**ORPLA8**	**ORPLA9**	**ORPLA10**	**ORPLA12**	**ORPLA13**	**ORPLA14**	**ORPLA15**	**ORPLA16**	**ORPLA17**	**ORPLB2**	**ORPLB3**	**ORPLB4**
Al_2O_3	5.820E-02	1.090E-01	1.090E-01	1.077E-01	1.083E-01	1.070E-01	9.459E-02	9.871E-02	9.890E-02	1.000E-01	9.881E-02	1.003E-01
B_2O_3	8.480E-02	7.801E-02	7.800E-02	7.129E-02	7.071E-02	7.200E-02	8.649E-02	7.781E-02	8.780E-02	7.301E-02	8.571E-02	8.521E-02
CaO		6.521E-02	6.520E-02	2.030E-02	2.010E-02	2.050E-02	3.340E-02	1.470E-02	2.990E-02	1.100E-02	3.000E-02	1.900E-02
Fe_2O_3	2.700E-02	9.101E-03	9.100E-03	9.298E-03	9.201E-03	9.400E-03	9.299E-03	9.401E-03	9.400E-03	1.100E-02	9.601E-03	9.601E-03
K_2O	5.600E-03	5.601E-03	5.600E-03	5.399E-03	5.501E-03	5.300E-03	5.399E-03	5.601E-03	5.400E-03	1.200E-03	1.100E-03	1.100E-03
Li_2O												
MgO	3.370E-02	9.101E-03	9.100E-03	9.298E-03	9.201E-03	9.400E-03	9.299E-03	9.101E-03	9.100E-03	1.100E-02	9.301E-03	9.301E-03
Na_2O	2.500E-01	2.500E-01	2.500E-01	2.400E-01	2.450E-01	2.350E-01	2.400E-01	2.500E-01	2.400E-01	2.500E-01	2.400E-01	2.400E-01
SiO_2	4.210E-01	3.551E-01	3.578E-01	4.099E-01	4.061E-01	4.138E-01	3.950E-01	4.158E-01	4.003E-01	3.998E-01	4.006E-01	4.006E-01
SnO_2	1.940E-02	2.000E-02	2.680E-02	2.749E-02	2.720E-02	2.780E-02	2.750E-02	1.000E-02	1.000E-02	1.080E-02	1.000E-02	1.000E-02
SO_3	1.900E-03	1.900E-03	1.900E-03	1.800E-03	1.900E-03	1.800E-03	1.800E-03	1.900E-03	1.800E-03	5.201E-03	5.001E-03	5.001E-03
TiO_2	1.550E-02											
ZnO	1.000E-02	2.360E-02	2.360E-02	2.450E-02	2.420E-02	2.470E-02	2.450E-02	2.360E-02	2.360E-02	3.650E-02	2.370E-02	2.370E-02
ZrO_2	5.900E-02	5.001E-02	5.000E-02	5.949E-02	5.891E-02	6.000E-02	5.949E-02	6.001E-02	6.070E-02	5.441E-02	6.041E-02	6.041E-02
BaO												
Br												
CdO												
Ce_2O_3												
Cl	7.100E-03	7.101E-03	7.100E-03	6.799E-03	6.901E-03	6.600E-03	6.799E-03	7.101E-03	6.800E-03	1.100E-03	1.100E-03	1.100E-03
Cr_2O_3	4.900E-03	4.900E-03	4.900E-03	4.999E-03	4.900E-03	5.000E-03	5.000E-03	4.900E-03	5.000E-03	5.201E-03	5.301E-03	5.301E-03
Cs_2O	1.900E-03	1.900E-03	1.900E-03	1.800E-03	1.800E-03	1.700E-03	1.500E-03	1.900E-03	1.500E-03	1.500E-03	1.400E-03	1.400E-03
F										4.900E-03	4.700E-03	4.700E-03
I												
La_2O_3												
MnO										6.001E-04	6.001E-04	6.001E-04
MoO_3												
NiO										4.000E-04	4.000E-04	4.000E-04
P_2O_5										2.300E-03	2.200E-03	2.200E-03
PbO												
Re_2O_7												
SrO												
V_2O_5		9.401E-03						9.401E-03	9.800E-03	2.000E-02	1.000E-02	2.000E-02
SUM	1	1	1	1	1	1	1	1	1	1	1	1
r_{alt} (g/m^2/d)	99.00	57.00	15.00	16.00	20.00	9.00	25.00	108.00	74.00	110.00	38.00	41.00
ln(r_{alt})	4.60	4.04	2.71	2.77	3.00	2.20	3.22	4.68	4.30	4.70	3.64	3.71

Table B.1. (Continued)

	ORP Glasses											
Glass ID	**ORPLC1**	**ORPLC5**	**ORPLD1**	**ORPLD2**	**ORPLD3**	**ORPLE1**	**ORPLE2**	**ORPLE3**	**ORPLE4**	**ORPLE5**	**ORPLE6**	**ORPLE7**
Al_2O_3	9.497E-02	1.004E-01	1.016E-01	9.110E-02	8.110E-02	7.599E-02	1.001E-01	1.001E-01	7.641E-02	7.599E-02	7.600E-02	7.599E-02
B_2O_3	6.058E-02	8.520E-02	1.205E-01	7.610E-02	8.610E-02	9.849E-02	1.146E-01	1.146E-01	9.811E-02	9.609E-02	9.850E-02	9.849E-02
CaO	2.999E-02	1.910E-02	8.021E-02	8.020E-02	1.002E-01	1.046E-01	8.040E-02	1.046E-01	1.043E-01	1.024E-01	9.970E-02	1.046E-01
Fe_2O_3	9.997E-03	9.700E-03	1.000E-02	7.500E-03	7.500E-03	2.400E-03	2.400E-03	2.400E-03	2.300E-03	2.300E-03	2.400E-03	2.400E-03
K_2O	5.798E-03	5.400E-03	1.600E-03	1.600E-03	1.600E-03	5.499E-03	5.500E-03	5.499E-03	6.101E-03	6.799E-03	5.500E-03	5.499E-03
Li_2O				7.500E-03	7.500E-03	3.000E-02	3.000E-02	3.000E-02	2.100E-02	1.100E-02	3.000E-02	2.600E-02
MgO	9.997E-03	9.300E-03	1.000E-02	1.000E-02	1.000E-02	1.050E-02	1.050E-02	1.050E-02	1.050E-02	9.899E-03	1.050E-02	1.050E-02
Na_2O	2.499E-01	2.357E-01	2.100E-01	2.100E-01	2.100E-01	1.600E-01	1.600E-01	1.600E-01	1.800E-01	2.000E-01	1.600E-01	1.600E-01
SiO_2	3.831E-01	4.010E-01	3.717E-01	3.940E-01	3.940E-01	4.141E-01	3.980E-01	3.739E-01	4.034E-01	3.995E-01	4.141E-01	4.141E-01
SnO_2	1.999E-02	1.000E-02		1.000E-02								
SO_3	5.498E-03	5.200E-03	9.601E-03	9.600E-03	9.600E-03	1.250E-02	1.250E-02	1.250E-02	1.250E-02	1.250E-02	1.250E-02	1.250E-02
TiO_2	9.997E-03											
ZnO	2.999E-02	2.370E-02	3.000E-02	2.510E-02	2.510E-02	3.220E-02	3.220E-02	3.220E-02	3.130E-02	2.960E-02	3.220E-02	3.220E-02
ZrO_2	4.499E-02	6.040E-02	3.00E-02	5.260E-02	4.260E-02	3.540E-02	3.540E-02	3.540E-02	3.530E-02	3.510E-02	3.620E-02	3.540E-02
BaO												
Br												
CdO												
Ce_2O_3												
Cl	6.598E-03	6.200E-03	3.300E-03	3.300E-03	3.300E-03	2.000E-04	2.000E-04	2.000E-04	3.000E-04	3.000E-04	2.000E-04	2.000E-04
Cr_2O_3	4.999E-03	5.300E-03	5.001E-03	5.000E-03	5.000E-03	9.999E-04	1.000E-03	9.999E-04	1.100E-03	1.300E-03	5.000E-03	5.000E-03
Cs_2O	1.500E-03	1.400E-03	1.300E-03	1.300E-03	1.300E-03	1.500E-03	1.500E-03	1.500E-03	1.500E-03	1.500E-03	1.500E-03	1.500E-03
F	9.997E-05	1.000E-04	1.700E-03	1.700E-03	1.700E-03	2.000E-03	2.000E-03	2.000E-03	2.300E-03	2.500E-03	2.000E-03	2.000E-03
I												
La_2O_3												
MnO												
MoO_3												
NiO			4.000E-04	4.000E-04	4.000E-04							
P_2O_5	1.999E-03	1.900E-03	2.900E-03	2.900E-03	2.900E-03	1.200E-03	1.200E-03	1.200E-03	1.400E-03	1.500E-03	1.200E-03	1.200E-03
PbO			1.000E-04	1.000E-04	1.000E-04							
Re_2O_7												
SrO												
V_2O_5	2.999E-02	2.000E-02	1.000E-02	1.000E-02	1.000E-02	1.250E-02	1.250E-02	1.250E-02	1.210E-02	1.180E-02	1.250E-02	1.250E-02
SUM	1	1	1	1	1	1	1	1	1	1	1	1
r_{alt} (g/m^2/d)	123.00	40.00	14.00	25.00	13.00	19.90	29.20	18.90	41.50	104.90	24.40	40.60
ln(r_{alt})	4.81	3.69	2.64	3.22	2.56	2.99	3.37	2.94	3.73	4.65	3.19	3.70

Table B.1. (Continued)

	ORP Glasses											
Glass ID	**ORPLE8**	**ORPLE9**	**ORPLE10**	**ORPLE11**	**ORPLE12**	**LAWA173**	**LAWA174**	**LAWA175**	**LAWA176**	**LAWA180**	**LAWA183**	**LAWA184**
Al_2O_3	7.599E-02	7.599E-02	8.799E-02	7.599E-02	7.600E-02	1.065E-01	1.065E-01	1.215E-01	1.365E-01	1.085E-01	1.065E-01	1.065E-01
B_2O_3	9.449E-02	9.049E-02	1.046E-01	9.849E-02	9.850E-02	1.129E-01	9.788E-02	1.129E-01	9.788E-02	7.759E-02	9.788E-02	9.419E-02
CaO	1.005E-01	9.649E-02	9.249E-02	1.046E-01	1.005E-01	7.988E-02	7.988E-02	7.988E-02	7.988E-02	7.979E-02	7.988E-02	7.659E-02
Fe_2O_3	1.050E-02	1.050E-02	2.400E-03	2.400E-03	2.400E-03	9.098E-03	9.098E-03	9.098E-03	9.098E-03	9.099E-03	9.098E-03	9.099E-03
K_2O	5.499E-03	5.499E-03	5.499E-03	5.499E-03	5.500E-03	5.099E-03	5.099E-03	5.099E-03	5.099E-03	5.599E-03	5.099E-03	5.099E-03
Li_2O	3.000E-02	3.000E-02	3.000E-02	2.500E-02	2.500E-02							
MgO	1.050E-02	1.050E-02	1.050E-02	1.050E-02	1.050E-02	9.098E-03	9.098E-03	9.098E-03	9.098E-03	9.099E-03	9.098E-03	9.099E-03
Na_2O	1.600E-01	1.600E-01	1.600E-01	1.600E-01	1.600E-01	2.300E-01	2.300E-01	2.300E-01	2.300E-01	2.500E-01	2.300E-01	2.300E-01
SiO_2	4.141E-01	4.141E-01	4.081E-01	4.141E-01	4.141E-01	3.485E-01	3.485E-01	3.485E-01	3.485E-01	3.532E-01	3.433E-01	3.658E-01
SnO_2												
SO_3	1.250E-02	1.250E-02	1.250E-02	1.250E-02	1.250E-02	7.499E-03	7.499E-03	7.499E-03	7.499E-03	7.499E-03	7.499E-03	7.499E-03
TiO_2												
ZnO	3.220E-02	3.220E-02	3.220E-02	3.220E-02	3.220E-02	2.999E-02	2.999E-02	2.999E-02	2.999E-02	2.350E-02	2.999E-02	1.450E-02
ZrO_2	3.540E-02	3.940E-02	3.540E-02	3.540E-02	3.540E-02	4.499E-02	5.999E-02	2.999E-02	2.999E-02	5.949E-02	5.999E-02	5.999E-02
BaO												
Br												
CdO												
Ce_2O_3												
Cl	2.000E-04	2.000E-04	2.000E-04	2.000E-04	2.000E-04	6.499E-03	6.499E-03	6.499E-03	6.499E-03	7.099E-03	6.499E-03	6.499E-03
Cr_2O_3	9.999E-04	5.000E-03	9.999E-04	9.999E-04	5.000E-03	2.000E-04	2.000E-04	2.000E-04	2.000E-04	2.000E-04	2.000E-04	2.000E-04
Cs_2O	1.500E-03	1.500E-03	1.500E-03	1.500E-03	1.500E-03							
F	2.000E-03	2.000E-03	2.000E-03	2.000E-03	2.000E-03							
I												
La_2O_3												
MnO												
MoO_3												
NiO												
P_2O_5	1.200E-03	1.200E-03	1.200E-03	1.200E-03	1.200E-03							
PbO												
Re_2O_7												
SrO												
V_2O_5	1.250E-02	1.250E-02	1.250E-02	1.750E-02	1.750E-02	9.798E-03	9.798E-03	9.798E-03	9.798E-03	9.399E-03	1.500E-02	1.500E-02
SUM	1	1	1	1	1	1	1	1	1	1	1	1
r_{alt} (g/m^2/d)	34.80	27.40	32.40	31.50	30.60	77.00	28.00	45.00	17.00	65.00	26.00	8.00
ln(r_{alt})	3.55	3.31	3.48	3.45	3.42	4.34	3.33	3.81	2.83	4.17	3.26	2.08

Table B.1. (Continued)

	ORP Glasses											
Glass ID	**LAWA185**	**LAWA186**	**LAWA187**	**LAWA188**	**LAWA189**	**LAWA190**	**LAWA191**	**LAWA192**	**LAWA193**	**LAWA194**	**LAWA195**	**LAWA196**
Al_2O_3	1.215E-01	1.164E-01	1.065E-01	1.065E-01	1.065E-01	1.215E-01	1.215E-01	1.215E-01	1.215E-01	1.085E-01	1.085E-01	1.185E-01
B_2O_3	9.789E-02	9.299E-02	1.279E-01	1.279E-01	1.129E-01	1.129E-01	1.129E-01	1.129E-01	1.129E-01	7.759E-02	7.758E-02	7.759E-02
CaO	7.989E-02	7.989E-02	6.479E-02	5.479E-02	7.489E-02	5.979E-02	7.489E-02	5.979E-02	5.479E-02	6.979E-02	6.479E-02	5.979E-02
Fe_2O_3	9.099E-03	9.099E-03	9.099E-03	9.098E-03	9.098E-03	9.099E-03	9.098E-03	9.099E-03	9.099E-03	9.099E-03	9.098E-03	9.099E-03
K_2O	5.099E-03	5.099E-03	5.099E-03	5.099E-03	5.099E-03	5.099E-03	5.099E-03	5.099E-03	5.099E-03	5.599E-03	5.599E-03	5.599E-03
Li_2O												
MgO	9.099E-03	9.099E-03	9.099E-03	9.098E-03	9.098E-03	9.099E-03	9.098E-03	9.099E-03	9.099E-03	9.099E-03	9.098E-03	9.099E-03
Na_2O	2.300E-01	2.300E-01	2.300E-01	2.300E-01	2.300E-01	2.300E-01	2.300E-01	2.300E-01	2.300E-01	2.500E-01	2.500E-01	2.500E-01
SiO_2	3.688E-01	3.688E-01	3.486E-01	3.485E-01	3.485E-01	3.486E-01	3.485E-01	3.586E-01	3.586E-01	3.532E-01	3.531E-01	3.632E-01
SnO_2			9.999E-03	2.010E-02						9.999E-03	9.998E-03	
SO_3	7.499E-03	7.499E-03	7.499E-03	7.499E-03	7.499E-03	7.499E-03	7.499E-03	7.499E-03	7.499E-03	7.499E-03	7.499E-03	7.499E-03
TiO_2												
ZnO	1.950E-02	1.450E-02	3.000E-02	2.999E-02	2.999E-02	3.000E-02	2.999E-02	3.000E-02	3.000E-02	2.350E-02	2.350E-02	2.350E-02
ZrO_2	3.000E-02	4.500E-02	3.000E-02	2.999E-02	4.499E-02	4.500E-02	2.999E-02	4.000E-02	4.000E-02	5.949E-02	5.949E-02	5.949E-02
BaO												
Br												
CdO												
Ce_2O_3												
Cl	6.499E-03	6.499E-03	6.499E-03	6.499E-03	6.499E-03	6.499E-03	6.499E-03	6.499E-03	6.499E-03	7.099E-03	7.099E-03	7.099E-03
Cr_2O_3	2.000E-04	2.000E-04	5.199E-03	5.199E-03	5.199E-03	5.199E-03	5.199E-03	2.000E-04	5.199E-03	2.000E-04	5.299E-03	2.000E-04
Cs_2O												
F												
I												
La_2O_3												
MnO												
MoO_3												
NiO												
P_2O_5												
PbO												
Re_2O_7												
SrO												
V_2O_5	1.500E-02	1.500E-02	9.799E-03	9.798E-03	9.798E-03	9.799E-03	9.798E-03	9.799E-03	9.799E-03	9.399E-03	9.398E-03	9.399E-03
SUM	1	1	1	1	1	1	1	1	1	1	1	1
r_{alt} (g/m^2/d)	14.00	10.00	25.00	11.00	15.00	27.00	19.00	28.00	23.00	23.00	26.00	79.00
ln(r_{alt})	2.64	2.30	3.22	2.40	2.71	3.30	2.94	3.33	3.14	3.14	3.26	4.37

Table B.1. (Continued)

	ORP Glass	HLP Glasses										
Glass ID	**LAWA197**	**HLP-01 (baseline)**	**HLP-03**	**HLP-04**	**HLP-05**	**HLP-06**	**HLP-07**	**HLP-08**	**HLP-09**	**HLP-10**	**HLP-11**	**HLP-12**
Al_2O_3	1.185E-01	7.000E-02	6.601E-02	8.239E-02	4.000E-02	1.194E-01	9.002E-02	7.309E-02	6.841E-02	7.151E-02	7.409E-02	6.741E-02
B_2O_3	7.758E-02	1.000E-01	9.431E-02	1.178E-01	1.032E-01	9.471E-02	9.792E-02	5.999E-02	1.200E-01	8.002E-02	1.058E-01	9.632E-02
CaO	5.479E-02	1.000E-04	1.000E-04	9.999E-05	9.999E-05	1.000E-04	1.000E-04	9.999E-05	1.000E-04	1.000E-04	9.999E-05	1.000E-04
Fe_2O_3	9.098E-03	5.500E-02	5.191E-02	6.479E-02	5.679E-02	5.211E-02	5.381E-02	5.749E-02	5.381E-02	5.631E-02		9.002E-02
K_2O	5.599E-03	4.100E-03	3.900E-03	4.900E-03	4.300E-03	3.900E-03	4.001E-03	4.300E-03	4.000E-03	4.201E-03	4.400E-03	4.001E-03
Li_2O												
MgO	9.098E-03	1.500E-02	1.410E-02	1.770E-02	1.550E-02	1.420E-02	1.470E-02	1.570E-02	1.470E-02	1.530E-02	1.590E-02	1.440E-02
Na_2O	2.500E-01	2.000E-01	1.885E-01	2.357E-01	2.065E-01	1.894E-01	1.957E-01	2.089E-01	1.956E-01	2.045E-01	2.117E-01	1.926E-01
SiO_2	3.631E-01	4.907E-01	5.201E-01	4.000E-01	5.064E-01	4.646E-01	4.802E-01	5.124E-01	4.798E-01	5.017E-01	5.192E-01	4.726E-01
SnO_2												
SO_3	7.499E-03	7.000E-04	7.001E-04	8.999E-04	7.999E-04	7.001E-04	7.001E-04	7.999E-04	7.001E-04	7.001E-04	7.999E-04	7.001E-04
TiO_2		3.000E-02	2.820E-02	3.530E-02	3.090E-02	2.840E-02	2.931E-02	3.130E-02	2.930E-02	3.061E-02	3.170E-02	2.891E-02
ZnO	2.350E-02	1.500E-02	1.410E-02	1.770E-02	1.550E-02	1.420E-02	1.470E-02	1.570E-02	1.470E-02	1.530E-02	1.590E-02	1.440E-02
ZrO_2	5.949E-02	1.500E-02	1.410E-02	1.770E-02	1.550E-02	1.420E-02	1.470E-02	1.570E-02	1.470E-02	1.530E-02	1.590E-02	1.440E-02
BaO												
Br												
CdO												
Ce_2O_3												
Cl	7.099E-03	2.800E-03	2.600E-03	3.300E-03	2.900E-03	2.600E-03	2.701E-03	2.900E-03	2.700E-03	2.801E-03	2.900E-03	2.701E-03
Cr_2O_3	5.299E-03	8.000E-04	7.001E-04	8.999E-04	7.999E-04	7.001E-04	7.001E-04	7.999E-04	7.001E-04	8.002E-04	7.999E-04	7.001E-04
Cs_2O												
F		1.000E-04	1.000E-04	9.999E-05	9.999E-05	1.000E-04	1.000E-04	9.999E-05	1.000E-04	1.000E-04	9.999E-05	1.000E-04
I												
La_2O_3												
MnO												
MoO_3												
NiO												
P_2O_5		6.000E-04	5.001E-04	6.999E-04	5.999E-04	5.001E-04	5.001E-04	5.999E-04	5.001E-04	6.001E-04	5.999E-04	5.001E-04
PbO												
Re_2O_7		1.000E-04	1.000E-04	9.999E-05	9.999E-05	1.000E-04	1.000E-04	9.999E-05	1.000E-04	1.000E-04	9.999E-05	1.000E-04
SrO												
V_2O_5	9.398E-03											
SUM	1	1	1	1	1	1	1	1	1	1	1	1
r_{alt} (g/m^2/d)	24.00	11.74	11.91	60.38	7.58	18.66	28.03	16.84	18.47	12.44	36.81	24.57
ln(r_{alt})	3.18	2.46	2.48	4.10	2.03	2.93	3.33	2.82	2.92	2.52	3.61	3.20

Table B.1. (Continued)

	HLP Glasses											
Glass ID	**HLP-13**	**HLP-14**	**HLP-15**	**HLP-16**	**HLP-17**	**HLP-18**	**HLP-20**	**HLP-21**	**HLP-22**	**HLP-23**	**HLP-24**	**HLP-25 (baseline)**
Al_2O_3	7.180E-02	7.209E-02	6.781E-02	7.101E-02	6.821E-02	7.101E-02	7.101E-02	6.821E-02	7.370E-02	6.720E-02	7.179E-02	7.000E-02
B_2O_3	1.027E-01	1.031E-01	9.692E-02	1.015E-01	9.752E-02	1.015E-01	1.015E-01	9.752E-02	1.053E-01	9.610E-02	1.027E-01	1.000E-01
CaO	1.000E-04	9.998E-05	1.000E-04	1.000E-04	1.000E-04	1.000E-04	1.000E-04	1.000E-04	1.000E-04	1.000E-04	9.999E-05	1.000E-04
Fe_2O_3	3.000E-02	5.669E-02	5.331E-02	5.591E-02	5.361E-02	5.591E-02	5.591E-02	5.361E-02	5.790E-02	5.290E-02	5.649E-02	5.500E-02
K_2O	4.200E-03	4.299E-03	4.001E-03	4.200E-03	4.001E-03	4.200E-03	4.200E-03	4.001E-03	3.300E-03	4.700E-03	3.700E-03	4.100E-03
Li_2O												
MgO	1.540E-02	1.550E-02	1.450E-02	1.520E-02	1.460E-02	1.520E-02		4.001E-02	1.580E-02	1.440E-02	1.540E-02	1.500E-02
Na_2O	2.053E-01	2.062E-01	1.939E-01	2.031E-01	1.950E-01	2.031E-01	2.031E-01	1.950E-01	1.600E-01	2.300E-01	1.800E-01	2.000E-01
SiO_2	5.037E-01	5.058E-01	4.756E-01	4.982E-01	4.783E-01	4.982E-01	4.982E-01	4.783E-01	5.167E-01	4.713E-01	5.036E-01	4.907E-01
SnO_2												
SO_3	8.000E-04	7.998E-04	7.001E-04	7.001E-04	7.001E-04	7.001E-04	7.001E-04	7.001E-04	6.000E-04	8.000E-04	6.999E-04	7.000E-04
TiO_2	3.080E-02		6.001E-02	3.040E-02	2.921E-02	3.040E-02	3.040E-02	2.921E-02	3.160E-02	2.880E-02	3.080E-02	3.000E-02
ZnO	1.540E-02	1.550E-02	1.450E-02		4.001E-02	1.520E-02	1.520E-02	1.460E-02	1.580E-02	1.440E-02	1.540E-02	1.500E-02
ZrO_2	1.540E-02	1.550E-02	1.450E-02	1.520E-02	1.460E-02		1.520E-02	1.460E-02	1.580E-02	1.440E-02	1.540E-02	1.500E-02
BaO												
Br												
CdO												
Ce_2O_3												
Cl	2.800E-03	2.899E-03	2.701E-03	2.800E-03	2.701E-03	2.800E-03	2.800E-03	2.701E-03	2.200E-03	3.200E-03	2.500E-03	2.800E-03
Cr_2O_3	8.000E-04	7.998E-04	7.001E-04	8.001E-04	7.001E-04	8.001E-04	8.001E-04	7.001E-04	6.000E-04	9.000E-04	6.999E-04	8.000E-04
Cs_2O												
F	1.000E-04	9.998E-05	1.000E-04	1.000E-04	1.000E-04	1.000E-04	1.000E-04	1.000E-04	1.000E-04	1.000E-04	9.999E-05	1.000E-04
I												
La_2O_3												
MnO												
MoO_3												
NiO												
P_2O_5	6.000E-04	5.999E-04	5.001E-04	6.001E-04	5.001E-04	6.001E-04	6.001E-04	5.001E-04	4.000E-04	6.000E-04	5.000E-04	6.000E-04
PbO												
Re_2O_7	1.000E-04	9.998E-05	1.000E-04	1.000E-04	1.000E-04	1.000E-04	1.000E-04	1.000E-04	1.000E-04	1.000E-04	9.999E-05	1.000E-04
SrO												
V_2O_5												
SUM	1	1	1	1	1	1	1	1	1	1	1	1
r_{alt} (g/m^2/d)	21.25	34.32	6.61	16.66	5.78	31.16	19.03	8.70	3.80	50.66	10.43	14.87
ln(r_{alt})	3.06	3.54	1.89	2.81	1.75	3.44	2.95	2.16	1.33	3.93	2.34	2.70

Table B.1. (Continued)

	HLP Glasses											
Glass ID	**HLP-26 (baseline)**	**HLP-28**	**HLP-29**	**HLP-30**	**HLP-32**	**HLP-33**	**HLP-34**	**HLP-35**	**HLP-39**	**HLP-41**	**HLP-43 (baseline)**	**HLP-44 (reduced)**
Al_2O_3	7.000E-02	1.194E-01	1.194E-01	1.194E-01	4.000E-02	4.000E-02	4.000E-02	1.194E-01	4.001E-02	4.001E-02	7.000E-02	7.000E-02
B_2O_3	1.000E-01	1.200E-01	6.001E-02	5.999E-02	1.200E-01	6.001E-02	6.001E-02	1.200E-01	1.200E-01	6.002E-02	1.000E-01	1.000E-01
CaO	1.000E-04	1.000E-04	1.000E-04	9.999E-05	1.000E-04	1.000E-04	1.000E-04	1.000E-04	1.000E-04	1.000E-04	1.000E-04	1.000E-04
Fe_2O_3	5.500E-02	3.100E-02	2.541E-02	5.639E-02	6.460E-02	5.901E-02	9.001E-02	6.770E-02	1.013E-01	1.267E-01	5.500E-02	5.500E-02
K_2O	4.100E-03	3.300E-03	4.701E-03	3.300E-03	3.300E-03	4.700E-03	3.300E-03	4.700E-03	4.701E-03	4.701E-03	4.100E-03	4.100E-03
Li_2O												
MgO	1.500E-02	8.401E-03	6.901E-03	1.540E-02	1.760E-02	1.610E-02	2.450E-02	1.850E-02	2.761E-02	3.451E-02	1.500E-02	1.500E-02
Na_2O	2.000E-01	1.600E-01	2.300E-01	1.600E-01	1.600E-01	2.300E-01	1.600E-01	2.300E-01	2.300E-01	2.301E-01	2.000E-01	2.000E-01
SiO_2	4.907E-01	5.201E-01	5.201E-01	5.199E-01	5.200E-01	5.201E-01	5.201E-01	3.600E-01	3.601E-01	3.601E-01	4.907E-01	4.907E-01
SnO_2												
SO_3	7.000E-04	6.001E-04	8.002E-04	5.999E-04	6.000E-04	8.001E-04	6.001E-04	8.000E-04	8.002E-04	8.002E-04	7.000E-04	7.000E-04
TiO_2	3.000E-02	1.690E-02	1.380E-02	3.070E-02	3.520E-02	3.210E-02	4.900E-02	3.690E-02	5.521E-02	6.902E-02	3.000E-02	3.000E-02
ZnO	1.500E-02	8.401E-03	6.901E-03	1.540E-02	1.760E-02	1.610E-02	2.450E-02	1.850E-02	2.761E-02	3.451E-02	1.500E-02	1.500E-02
ZrO_2	1.500E-02	8.401E-03	6.901E-03	1.540E-02	1.760E-02	1.610E-02	2.450E-02	1.850E-02	2.761E-02	3.451E-02	1.500E-02	1.500E-02
BaO												
Br												
CdO												
Ce_2O_3												
Cl	2.800E-03	2.200E-03	3.201E-03	2.200E-03	2.200E-03	3.200E-03	2.200E-03	3.200E-03	3.201E-03	3.201E-03	2.800E-03	2.800E-03
Cr_2O_3	8.000E-04	6.001E-04	9.002E-04	5.999E-04	6.000E-04	9.001E-04	6.001E-04	9.000E-04	9.002E-04	9.003E-04	8.000E-04	8.000E-04
Cs_2O												
F	1.000E-04	1.000E-04	1.000E-04	9.999E-05	1.000E-04	1.000E-04	1.000E-04	1.000E-04	1.000E-04	1.000E-04	1.000E-04	1.000E-04
I												
La_2O_3												
MnO												
MoO_3												
NiO												
P_2O_5	6.000E-04	4.000E-04	6.001E-04	4.000E-04	4.000E-04	6.001E-04	4.000E-04	6.000E-04	6.001E-04	6.002E-04	6.000E-04	6.000E-04
PbO												
Re_2O_7	1.000E-04	1.000E-04	1.000E-04	9.999E-05	1.000E-04	1.000E-04	1.000E-04	1.000E-04	1.000E-04	1.000E-04	1.000E-04	1.000E-04
SrO												
V_2O_5												
SUM	1	1	1	1	1	1	1	1	1	1	1	1
r_{alt} (g/m^2/d)	20.52	15.39	87.76	45.10	2.42	64.51	5.51	51.10	7.71	5.89	11.58	14.12
ln(r_{alt})	3.02	2.73	4.47	3.81	0.88	4.17	1.71	3.93	2.04	1.77	2.45	2.65

Table B.1. (Continued)

	HLP Glasses											
Glass ID	**HLP-45 (reduced)**	**HLP-47 (LRM)**	**HLP-48 (LAW-A33)**	**HLP-51 (LAW-ABP1)**	**HLP-54 (L4-912)**	**HLP-55 (L4-99)**	**HLP-56 (LAW-A44)**	**HLP-58**	**HLP-59**	**HLP-61**	**HLP-62**	**HLP-64**
Al_2O_3	7.000E-02	1.001E-01	1.197E-01	1.000E-01	1.200E-01	9.003E-02	6.202E-02	6.861E-02	6.648E-02	4.000E-02	4.000E-02	4.000E-02
B_2O_3	1.000E-01	8.009E-02	8.850E-02	9.250E-02	9.003E-02	9.003E-02	8.903E-02	9.801E-02	9.497E-02	1.257E-01	1.257E-01	6.000E-02
CaO	1.000E-04	5.006E-03					1.991E-02	2.000E-02	4.999E-02	5.000E-02	5.000E-02	1.000E-04
Fe_2O_3	5.500E-02	1.001E-02	5.770E-02	2.500E-02			6.982E-02	5.391E-02	5.228E-02			
K_2O	4.100E-03	1.502E-02	3.100E-02	2.200E-02	3.301E-03	3.301E-03	5.002E-03	4.000E-03	3.899E-03	5.000E-02	3.300E-03	5.000E-02
Li_2O		1.001E-03										
MgO	1.500E-02	1.001E-03	1.990E-02	1.000E-02			1.991E-02	1.470E-02	1.430E-02	4.300E-02		4.300E-02
Na_2O	2.000E-01	2.002E-01	2.000E-01	2.000E-01	2.001E-01	2.001E-01	2.001E-01	1.960E-01	1.899E-01	1.600E-01	1.600E-01	1.600E-01
SiO_2	4.907E-01	5.443E-01	3.825E-01	4.189E-01	5.680E-01	5.980E-01	4.456E-01	4.809E-01	4.661E-01	3.965E-01	4.692E-01	5.200E-01
SnO_2												
SO_3	7.000E-04	2.002E-03	1.000E-03	1.000E-03	3.201E-03	3.201E-03	1.000E-03	7.001E-04	6.998E-04	9.000E-04	9.000E-04	9.000E-04
TiO_2	3.000E-02	1.001E-03	2.490E-02	2.490E-02			1.991E-02	2.940E-02	2.849E-02	8.590E-02	8.590E-02	
ZnO	1.500E-02		4.270E-02	2.600E-02			2.961E-02	1.470E-02	1.430E-02	4.300E-02		4.140E-02
ZrO_2	1.500E-02	1.001E-02	2.490E-02	5.250E-02			2.991E-02	1.470E-02	1.430E-02		6.000E-02	6.000E-02
BaO		5.006E-05										
Br												
CdO		2.002E-03										
Ce_2O_3												
Cl	2.800E-03	8.009E-03	5.800E-03	5.800E-03	9.003E-04	9.003E-04	6.502E-03	2.700E-03	2.699E-03	3.500E-03	3.500E-03	3.500E-03
Cr_2O_3	8.000E-04	2.002E-03	2.000E-04	2.000E-04	4.001E-04	4.001E-04	2.001E-04	8.001E-04	7.998E-04	9.000E-04	9.000E-04	9.000E-04
Cs_2O												
F	1.000E-04	1.001E-02	4.000E-04	4.000E-04	2.101E-03	2.101E-03	1.000E-04	1.000E-04	9.997E-05	1.000E-04	1.000E-04	1.000E-04
I		2.002E-05										
La_2O_3		1.001E-04		2.000E-02	1.000E-04	1.000E-04						
MnO		1.001E-03										
MoO_3							1.000E-04					
NiO		1.001E-03										
P_2O_5	6.000E-04	5.006E-03	8.000E-04	8.000E-04	1.190E-02	1.190E-02	3.001E-04	6.001E-04	5.998E-04	4.000E-04	4.000E-04	2.000E-02
PbO		1.001E-03										
Re_2O_7	1.000E-04						1.000E-03	1.000E-04	9.997E-05	1.000E-04	1.000E-04	1.000E-04
SrO												
V_2O_5												
SUM	1	1	1	1	1	1	1	1	1	1	1	1
r_{alt} (g/m^2/d)	18.16	72.61	73.88	21.69	53.70	69.32	0.71	2.68	3.07	6.98	0.37	7.08
ln(r_{alt})	2.90	4.29	4.30	3.08	3.98	4.24	-0.34	0.98	1.12	1.94	-1.00	1.96

Table B.1. (Continued)

	HLP Glasses				ICV Glasses							
Glass ID	**HLP-65**	**HLP-68**	**HLP-69**	**HLP-75**	**AMBG-13**	**AMBG-15**	**ASCM-04**	**ASCM-05**	**AMOG-01**	**AMOG-02**	**AMOG-03**	**AMP1-01**
Al_2O_3	4.000E-02	9.640E-02	1.194E-01	7.429E-02	9.890E-02	9.460E-02	9.610E-02	9.330E-02	9.610E-02	9.610E-02	9.610E-02	9.130E-02
B_2O_3	6.000E-02	6.000E-02	6.000E-02	8.929E-02	5.000E-02	5.000E-02	5.000E-02	5.000E-02	5.000E-02	5.000E-02	5.000E-02	5.000E-02
CaO	5.000E-02	5.000E-02	1.000E-04	2.310E-02	3.750E-02	3.580E-02	3.620E-02	3.500E-02	3.620E-02	3.620E-02	3.620E-02	2.770E-02
Fe_2O_3	9.820E-02	1.577E-01	2.400E-03	5.539E-02	6.330E-02	6.040E-02	6.110E-02	5.900E-02	6.110E-02	6.110E-02	6.110E-02	4.340E-02
K_2O	3.300E-03	5.000E-02	3.300E-03	2.490E-02	1.760E-02	1.680E-02	1.710E-02	1.660E-02	1.710E-02	1.710E-02	1.710E-02	1.510E-02
Li_2O												
MgO	4.300E-02			2.000E-02	9.700E-03	9.300E-03	9.400E-03	9.100E-03	9.400E-03	9.400E-03	9.400E-03	1.350E-02
Na_2O	1.600E-01	1.600E-01	1.600E-01	1.984E-01	2.000E-01	2.000E-01	2.200E-01	2.400E-01	2.200E-01	2.200E-01	2.200E-01	2.000E-01
SiO_2	5.200E-01	3.600E-01	5.200E-01	4.155E-01	4.255E-01	4.061E-01	4.111E-01	3.966E-01	4.111E-01	4.111E-01	4.111E-01	4.679E-01
SnO_2												
SO_3	9.000E-04	9.000E-04	9.000E-04	8.999E-04	8.300E-03	8.300E-03	9.300E-03	1.020E-02	9.300E-03	9.300E-03	9.300E-03	3.700E-03
TiO_2			8.590E-02	3.680E-02	9.700E-03	1.930E-02	9.400E-03	9.100E-03	9.400E-03	9.400E-03	9.400E-03	7.900E-03
ZnO			4.300E-02	2.000E-02								
ZrO_2		6.000E-02		2.700E-02	7.000E-02	6.000E-02	7.000E-02	7.000E-02	7.000E-02	7.000E-02	7.000E-02	7.000E-02
BaO												5.000E-04
Br												
CdO												
Ce_2O_3												
Cl	3.500E-03	3.500E-03	3.500E-03	3.500E-03	1.800E-03	1.800E-03	2.000E-03	2.200E-03	2.000E-03	2.000E-03	2.000E-03	3.000E-04
Cr_2O_3	9.000E-04	9.000E-04	9.000E-04	8.999E-04	9.000E-04	9.000E-04	1.000E-03	1.100E-03	1.000E-03	1.000E-03	1.000E-03	1.400E-03
Cs_2O												
F	1.000E-04	1.000E-04	1.000E-04	9.999E-05	7.000E-04	7.000E-04	8.000E-04	9.000E-04	8.000E-04	8.000E-04	8.000E-04	1.000E-04
I												
La_2O_3						2.000E-02						
MnO												7.000E-04
MoO_3												
NiO												
P_2O_5	2.000E-02	4.000E-04	4.000E-04	9.899E-03	6.000E-03	1.590E-02	6.400E-03	6.800E-03	6.400E-03	6.400E-03	6.400E-03	6.200E-03
PbO												
Re_2O_7	1.000E-04	1.000E-04	1.000E-04	9.999E-05	1.000E-04	1.000E-04	1.000E-04	1.000E-04	1.000E-04	1.000E-04	1.000E-04	
SrO												3.000E-04
V_2O_5												
SUM	1	1	1	1	1	1	1	1	1	1	1	1
r_{alt} (g/m^2/d)	5.84	8.91	7.47	17.52	7.73	75.01	15.82	99.34	3.24	10.56	11.42	1.03
ln(r_{alt})	1.76	2.19	2.01	2.86	2.04	4.32	2.76	4.60	1.18	2.36	2.44	0.03

Table B.1. (Continued)

	ICV Glasses											
Glass ID	**AMP1-03**	**AMP1-04**	**AMP1-09**	**AMP1-10**	**AMP1-11**	**AMP1-12**	**AMP2-03**	**AMP2-10**	**AMP2-02**	**AMP2-11**	**AMP2-16**	**S22-01**
Al_2O_3	9.680E-02	9.400E-02	8.620E-02	1.169E-01	1.424E-01	1.679E-01	8.000E-02	1.468E-01	8.000E-02	1.595E-01	8.000E-02	8.000E-02
B_2O_3	5.000E-02	4.170E-02	5.000E-02	4.850E-02	4.700E-02	4.550E-02	6.000E-02	6.000E-02	6.000E-02	6.000E-02	6.000E-02	6.000E-02
CaO	5.100E-02	2.860E-02	2.600E-02	2.740E-02	2.700E-02	2.670E-02	2.500E-02	5.500E-02	2.500E-02	2.500E-02	5.500E-02	2.500E-02
Fe_2O_3	6.490E-02	4.470E-02	4.070E-02	4.210E-02	4.080E-02	3.950E-02	1.100E-01	4.000E-02	1.100E-01	1.100E-01	4.000E-02	1.100E-01
K_2O	9.900E-03	1.550E-02	1.420E-02	1.460E-02	1.420E-02	1.370E-02	2.500E-02	2.500E-02	2.500E-02	9.000E-03	9.000E-03	
Li_2O												
MgO	2.770E-02	1.390E-02	1.260E-02	1.430E-02	1.510E-02	1.590E-02	9.000E-03	3.000E-02	3.000E-02	9.000E-03	3.000E-02	3.000E-02
Na_2O	2.000E-01	2.000E-01	2.400E-01	1.940E-01	1.880E-01	1.820E-01	1.800E-01	1.800E-01	1.800E-01	1.800E-01	2.052E-01	1.700E-01
SiO_2	4.079E-01	4.819E-01	4.377E-01	4.538E-01	4.398E-01	4.260E-01	4.385E-01	3.900E-01	4.400E-01	3.900E-01	4.483E-01	4.132E-01
SnO_2												
SO_3	1.800E-03	3.600E-03	4.500E-03	3.500E-03	3.400E-03	3.300E-03	9.500E-03	1.000E-03	1.000E-03	1.000E-03	1.000E-03	9.500E-03
TiO_2	1.010E-02	8.200E-03	7.400E-03	7.700E-03	7.500E-03	7.200E-03	2.000E-02	7.000E-03	2.000E-02	2.000E-02	2.000E-02	
ZnO												
ZrO_2	7.000E-02	5.830E-02	7.000E-02	6.790E-02	6.580E-02	6.370E-02	2.000E-02	4.220E-02	2.000E-02	2.750E-02	2.850E-02	8.000E-02
BaO	5.000E-04	5.000E-04	4.000E-04	5.000E-04	5.000E-04	4.000E-04						4.500E-04
Br												
CdO												
Ce_2O_3												1.900E-04
Cl	1.000E-04	3.000E-04	4.000E-04	3.000E-04	3.000E-04	3.000E-04	1.000E-03	1.000E-03	1.000E-03	1.000E-03	1.000E-03	5.000E-03
Cr_2O_3	5.800E-03	1.400E-03	1.700E-03	1.300E-03	1.300E-03	1.300E-03	4.000E-03	4.000E-03	4.000E-03	4.000E-03	4.000E-03	5.800E-03
Cs_2O												
F	1.000E-04	1.000E-04	1.000E-04	1.000E-04	1.000E-04	1.000E-04	1.000E-03	1.000E-03	1.000E-03	1.000E-03	1.000E-03	1.000E-02
I												
La_2O_3												
MnO	9.000E-04	7.000E-04	6.000E-04	7.000E-04	6.000E-04	6.000E-04	1.000E-03	1.000E-03	1.000E-03	1.000E-03	1.000E-03	6.500E-04
MoO_3												
NiO												
P_2O_5	2.200E-03	6.300E-03	7.200E-03	6.100E-03	5.900E-03	5.700E-03	1.600E-02	1.600E-02	2.000E-03	2.000E-03	1.600E-02	
PbO												
Re_2O_7												
SrO	3.000E-04	3.000E-04	3.000E-04	3.000E-04	3.000E-04	2.000E-04						2.600E-04
V_2O_5												
SUM	1	1	1	1	1	1	1	1	1	1	1	1
r_{alt} (g/m^2/d)	0.61	1.42	80.52	0.91	1.40	9.12	40.10	23.77	12.13	25.30	14.05	0.64
ln(r_{alt})	-0.49	0.35	4.39	-0.10	0.34	2.21	3.69	3.17	2.50	3.23	2.64	-0.45

Table B.1. (Continued)

	ICV Glasses											
Glass ID	**S22-03**	**S22-05**	**S22-10**	**S22-13**	**S22-15**	**S22-16**	**S22-17**	**S22-20**	**S22-21**	**S22-22**	**S22-24**	**S22-26**
Al_2O_3	8.000E-02	1.661E-01	9.891E-02	1.020E-01	1.020E-01	1.256E-01	1.020E-01	8.000E-02	1.020E-01	1.093E-01	1.679E-01	8.000E-02
B_2O_3	6.000E-02	6.000E-02	5.001E-02	5.125E-02	5.125E-02	6.000E-02	5.125E-02	5.590E-02	5.125E-02	4.224E-02	6.000E-02	6.000E-02
CaO	5.500E-02	2.500E-02	3.750E-02	4.750E-02	3.250E-02	2.500E-02	3.250E-02	5.500E-02	4.750E-02	3.812E-02	5.500E-02	5.500E-02
Fe_2O_3	9.840E-02	3.950E-02	6.331E-02	5.713E-02	9.238E-02	3.950E-02	5.713E-02	1.100E-01	5.713E-02	6.637E-02	3.950E-02	3.950E-02
K_2O			1.760E-02	6.250E-03	6.250E-03	2.500E-02	1.875E-02		1.875E-02	9.370E-03		
Li_2O												
MgO			9.701E-03	7.500E-03	7.500E-03	3.000E-02	2.250E-02	3.000E-02	7.500E-03	1.125E-02		
Na_2O	1.700E-01	2.300E-01	2.000E-01	2.150E-01	1.850E-01	2.300E-01	1.850E-01	2.300E-01	1.850E-01	1.925E-01	1.700E-01	2.300E-01
SiO_2	4.001E-01	4.001E-01	4.255E-01	4.543E-01	4.558E-01	4.001E-01	4.612E-01	4.001E-01	4.612E-01	4.449E-01	4.083E-01	4.565E-01
SnO_2												
SO_3		9.500E-03	8.301E-03	2.380E-03	2.380E-03		2.380E-03		2.380E-03	3.560E-03	9.500E-03	
TiO_2	2.000E-02		9.701E-03	5.000E-03	1.500E-02		5.000E-03		5.000E-03	1.000E-02	2.000E-02	2.000E-02
ZnO												
ZrO_2	8.000E-02	2.750E-02	7.001E-02	4.063E-02	4.063E-02	2.750E-02	4.063E-02	2.750E-02	4.063E-02	4.394E-02	2.750E-02	2.750E-02
BaO	4.500E-04	4.500E-04		4.500E-04	4.500E-04	4.500E-04	4.500E-04	4.500E-04	4.500E-04	4.500E-04	4.500E-04	4.500E-04
Br												
CdO												
Ce_2O_3	1.900E-04	1.900E-04		1.900E-04	1.900E-04	1.900E-04	1.900E-04	1.900E-04	1.900E-04	1.900E-04	1.900E-04	1.900E-04
Cl			1.800E-03	2.500E-03	8.300E-04	5.000E-03	2.500E-03		2.500E-03	3.130E-03		5.000E-03
Cr_2O_3		5.800E-03	9.001E-04	8.300E-04	8.300E-04	5.800E-03	8.300E-04		8.300E-04	2.900E-03	5.800E-03	
Cs_2O												
F	1.000E-02	1.000E-02	7.001E-04	8.300E-04	8.300E-04		8.300E-04	1.000E-02	8.300E-04	6.880E-03	1.000E-02	
I												
La_2O_3												
MnO	6.500E-04	6.500E-04		6.500E-04	6.500E-04	6.500E-04	6.500E-04	6.500E-04	6.500E-04	6.500E-04	6.500E-04	6.500E-04
MoO_3												
NiO												
P_2O_5	2.500E-02	2.500E-02	6.001E-03	5.330E-03	5.330E-03	2.500E-02	1.600E-02		1.600E-02	1.406E-02	2.500E-02	2.500E-02
PbO												
Re_2O_7												
SrO	2.600E-04	2.600E-04		2.600E-04	2.600E-04	2.600E-04	2.600E-04	2.600E-04	2.600E-04	2.600E-04	2.600E-04	2.600E-04
V_2O_5												
SUM	1	1	1	1	1	1	1	1	1	1	1	1
r_{alt} (g/m^2/d)	0.32	85.24	3.56	45.25	18.77	137.06	30.74	147.14	45.27	82.95	41.09	125.09
ln(r_{alt})	-1.15	4.45	1.27	3.81	2.93	4.92	3.43	4.99	3.81	4.42	3.72	4.83

Table B.1. (Continued)

	ICV Glasses				
Glass ID	**S22-31**	**S22-32**	**S22-36**	**S22-38**	**S22-40**
Al_2O_3	8.000E-02	1.093E-01	1.020E-01	1.263E-01	1.020E-01
B_2O_3	6.000E-02	3.988E-02	5.125E-02	5.125E-02	5.125E-02
CaO	5.500E-02	3.775E-02	3.250E-02	3.250E-02	3.250E-02
Fe_2O_3	3.950E-02	6.770E-02	5.713E-02	5.713E-02	5.713E-02
K_2O	2.500E-02	8.130E-03	1.875E-02	6.250E-03	6.250E-03
Li_2O					
MgO		1.275E-02	2.250E-02	2.250E-02	7.500E-03
Na_2O	1.700E-01	1.895E-01	1.850E-01	1.850E-01	1.850E-01
SiO_2	4.387E-01	4.613E-01	4.564E-01	4.500E-01	5.010E-01
SnO_2					
SO_3	9.500E-03	4.040E-03	7.130E-03	2.380E-03	2.380E-03
TiO_2	2.000E-02	8.000E-03	5.000E-03	1.500E-02	5.000E-03
ZnO					
ZrO_2	8.000E-02	4.586E-02	4.063E-02	4.063E-02	4.063E-02
BaO	4.500E-04	4.500E-04	4.500E-04	4.500E-04	4.500E-04
Br					
CdO					
Ce_2O_3	1.900E-04	1.900E-04	1.900E-04	1.900E-04	1.900E-04
Cl	5.000E-03	1.670E-03	2.500E-03	2.500E-03	8.300E-04
Cr_2O_3	5.800E-03	9.200E-04	8.300E-04	8.300E-04	8.300E-04
Cs_2O					
F	1.000E-02	1.000E-03	8.300E-04	8.300E-04	8.300E-04
I					
La_2O_3					
MnO	6.500E-04	6.500E-04	6.500E-04	6.500E-04	6.500E-04
MoO_3					
NiO					
P_2O_5		1.067E-02	1.600E-02	5.330E-03	5.330E-03
PbO					
Re_2O_7					
SrO	2.600E-04	2.600E-04	2.600E-04	2.600E-04	2.600E-04
V_2O_5					
SUM	1	1	1	1	1
r_{alt} ($g/m^2/d$)	0.62	17.75	40.35	16.99	4.35
$\ln(r_{alt})$	-0.48	2.88	3.70	2.83	1.47

Appendix C

SEM Micrographs of VHT Samples of CCIM-AN Glasses

Appendix C: SEM Micrographs of VHT Samples of CCIM-AN Glasses

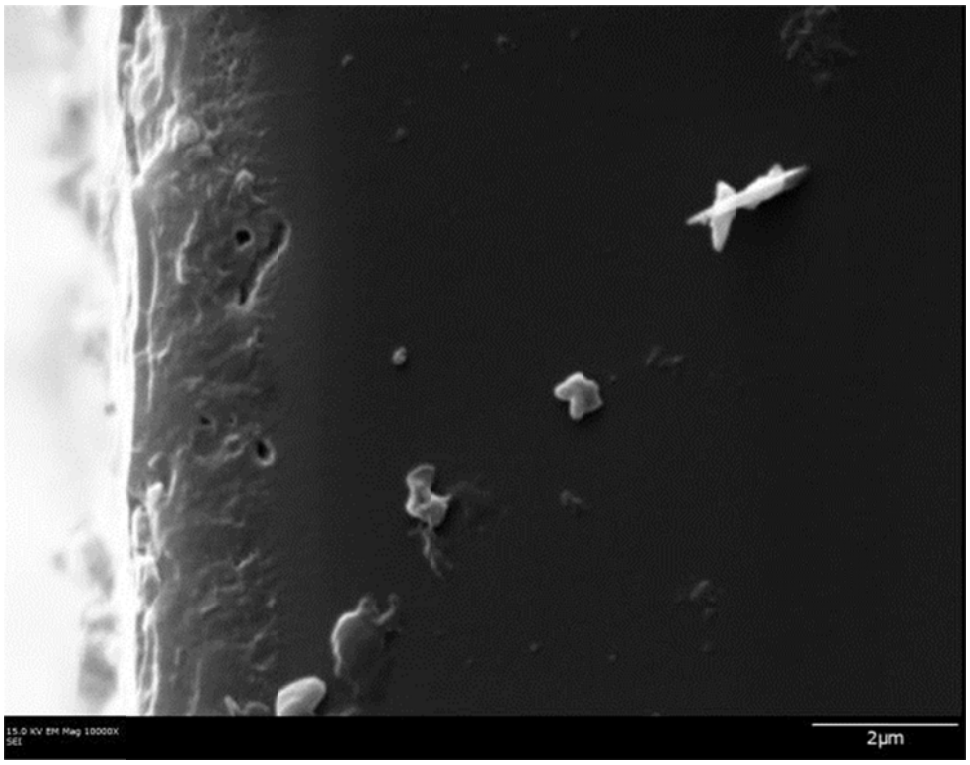

CCIM-AN-02Q

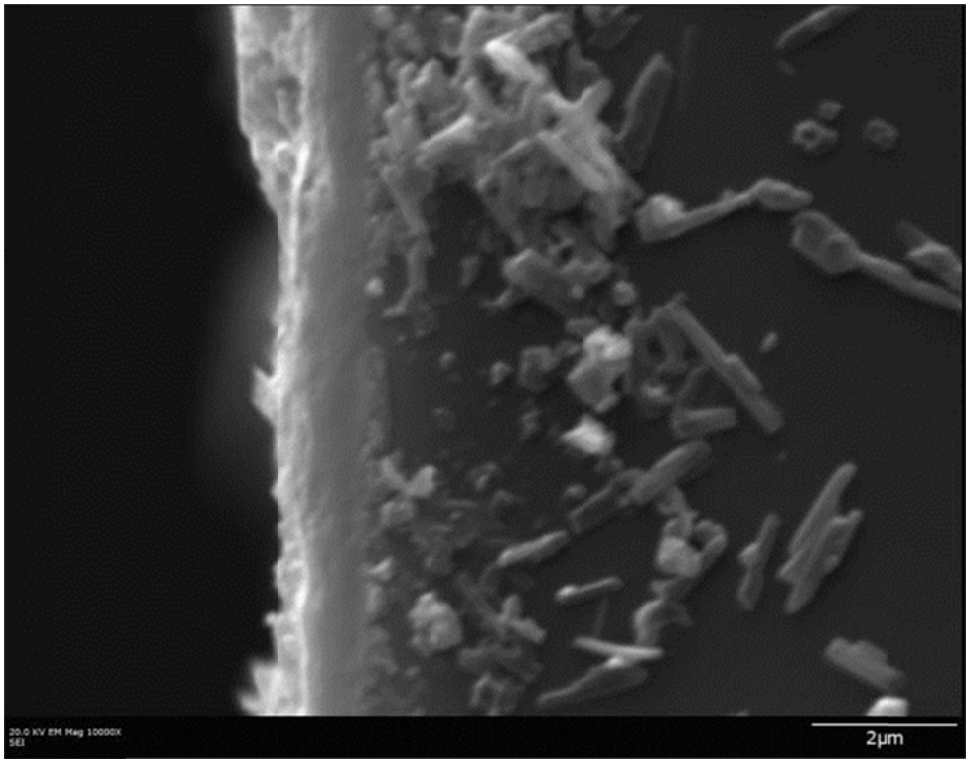

CCIM-AN-04Q

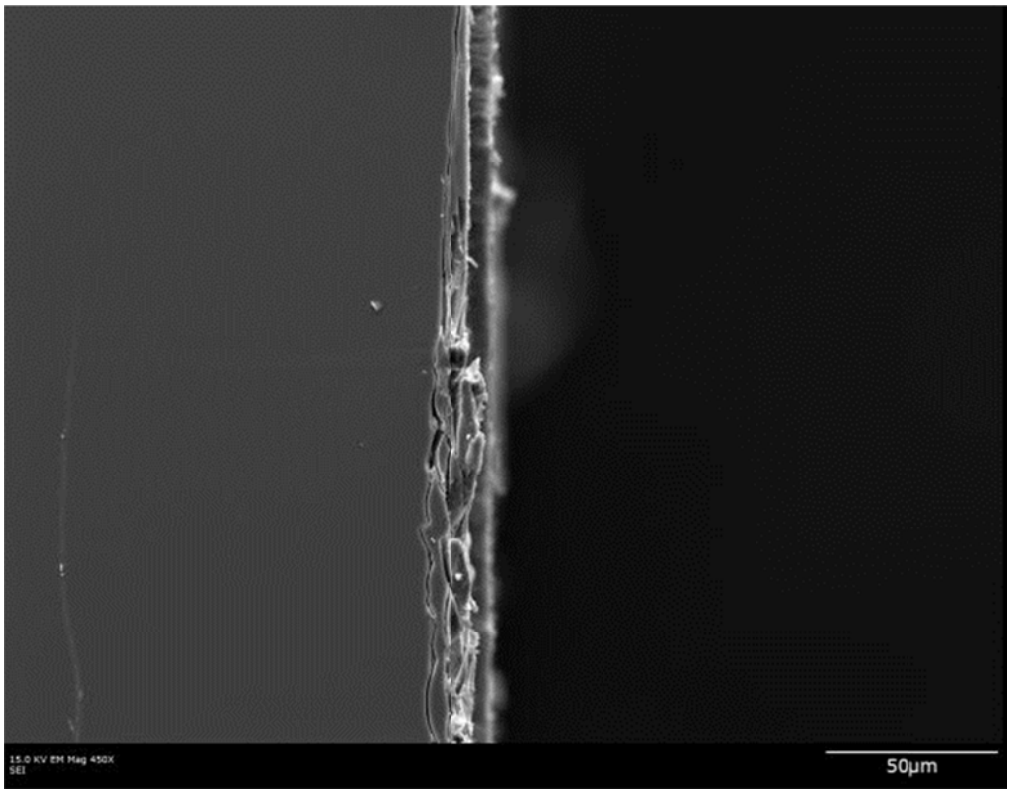

CCIM-AN-09Q

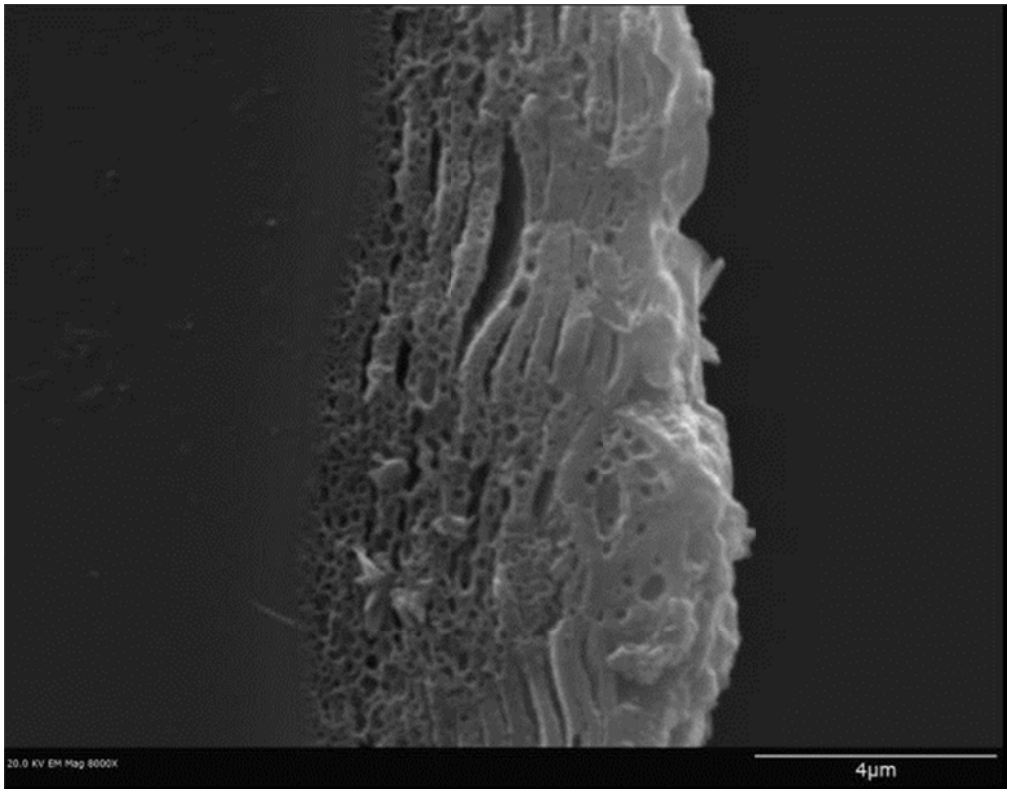

CCIM-AN-11Q

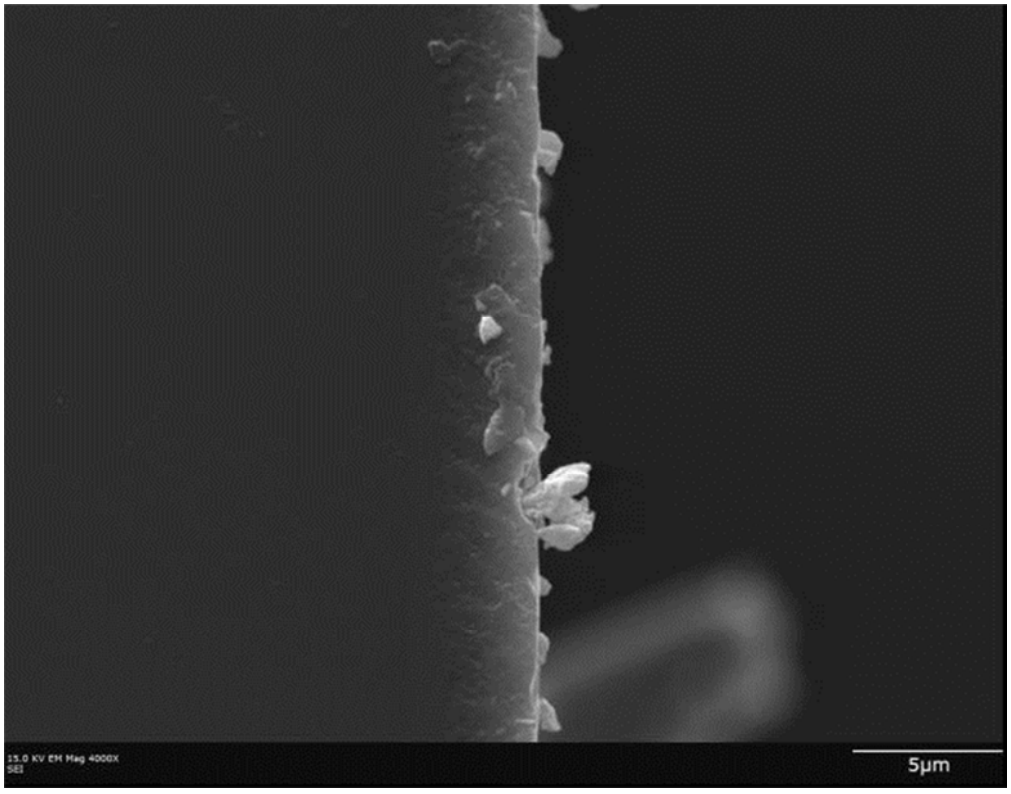

CCIM-AN-18Q

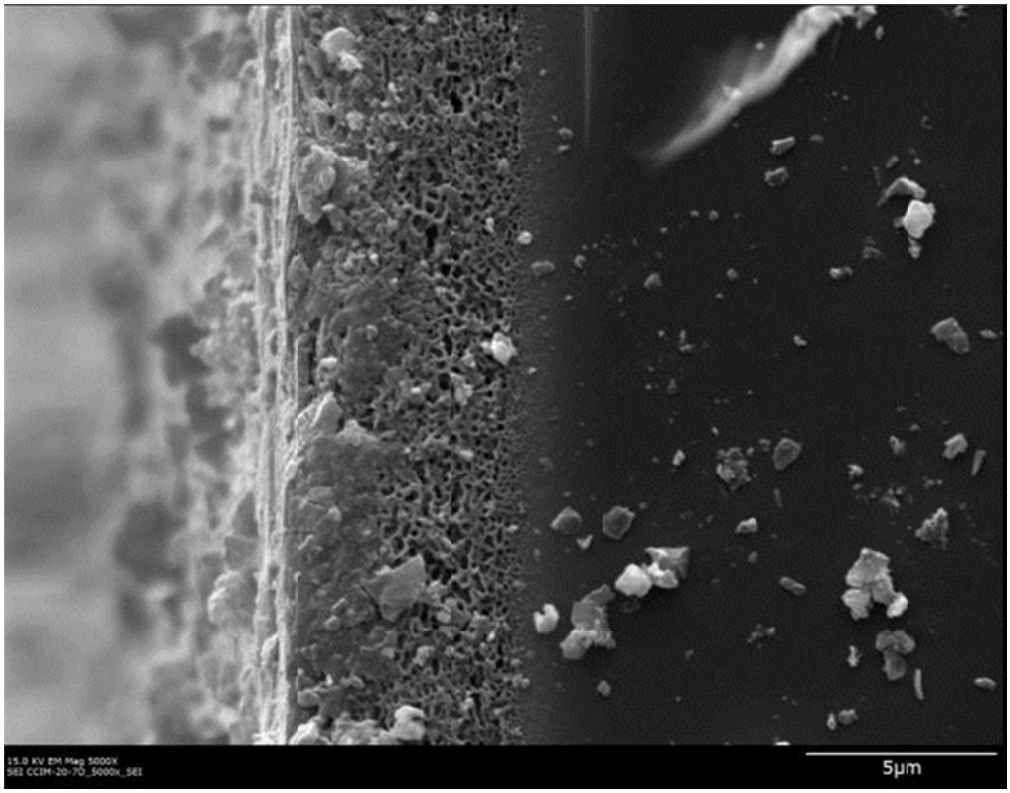

CCIM-AN-20Q

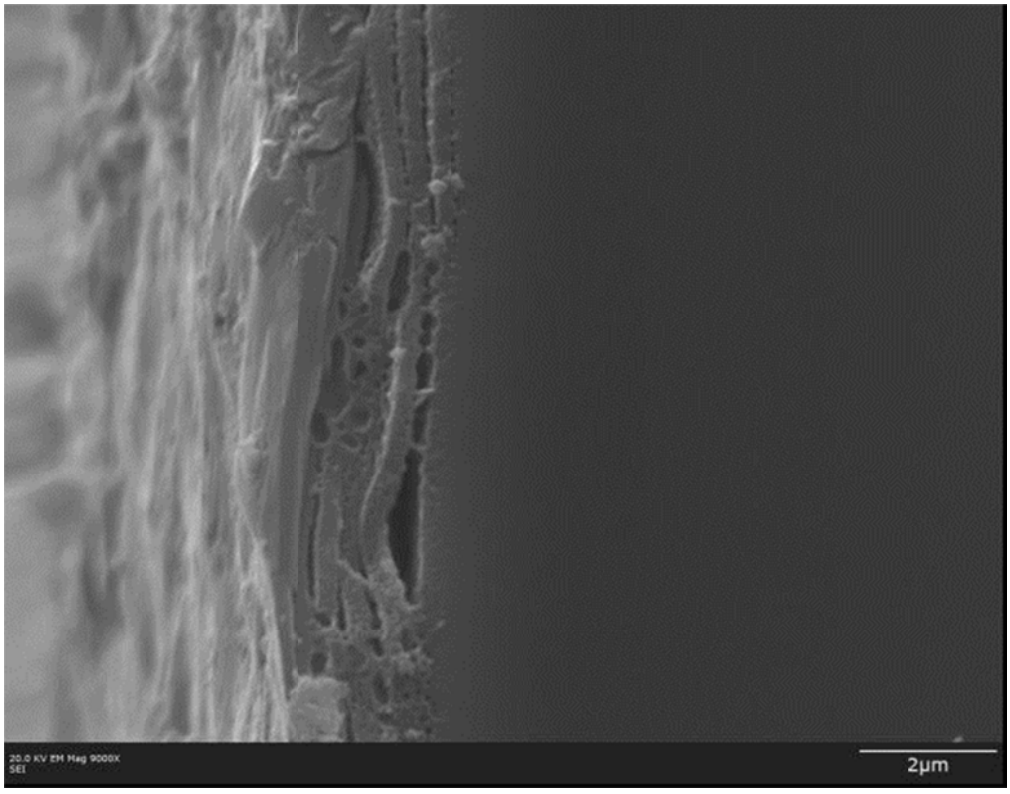

CCIM-AN-02CCC

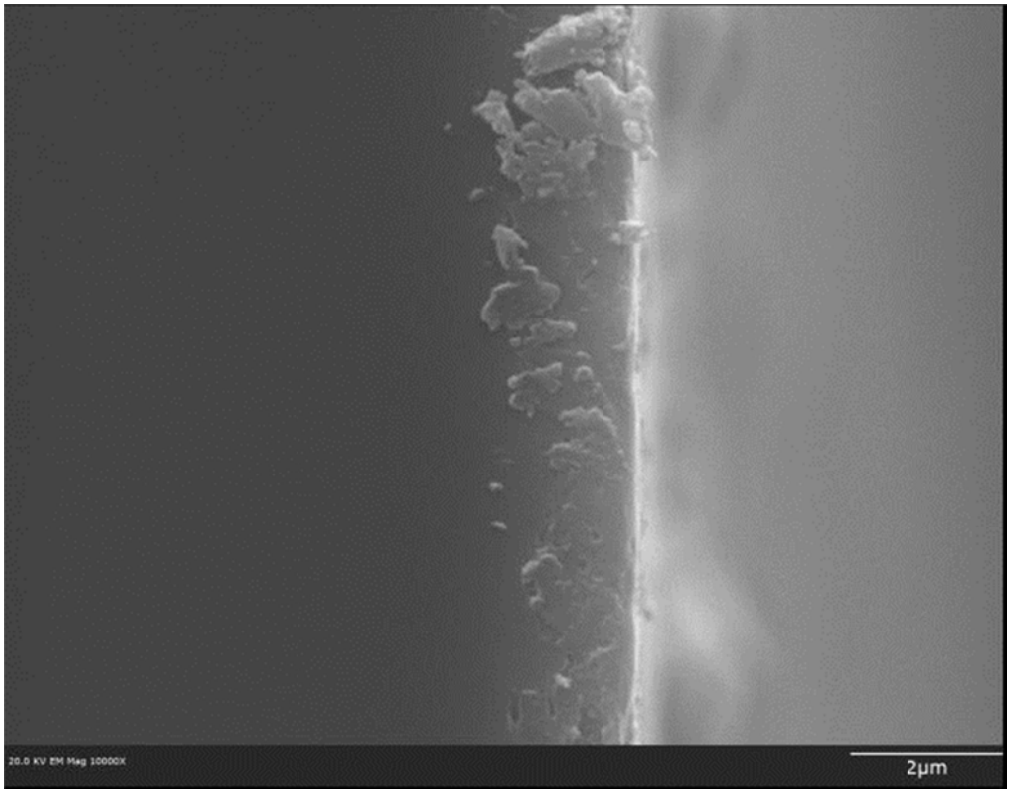

CCIM-AN-04 CCC

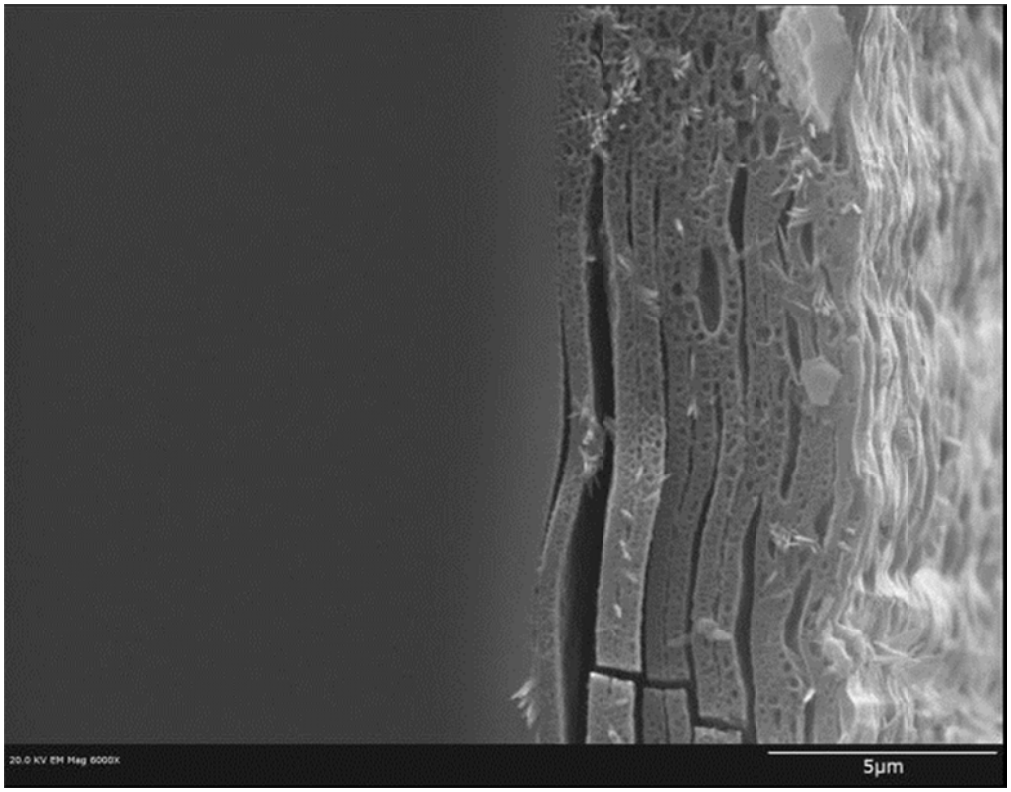

CCIM-AN-09 CCC

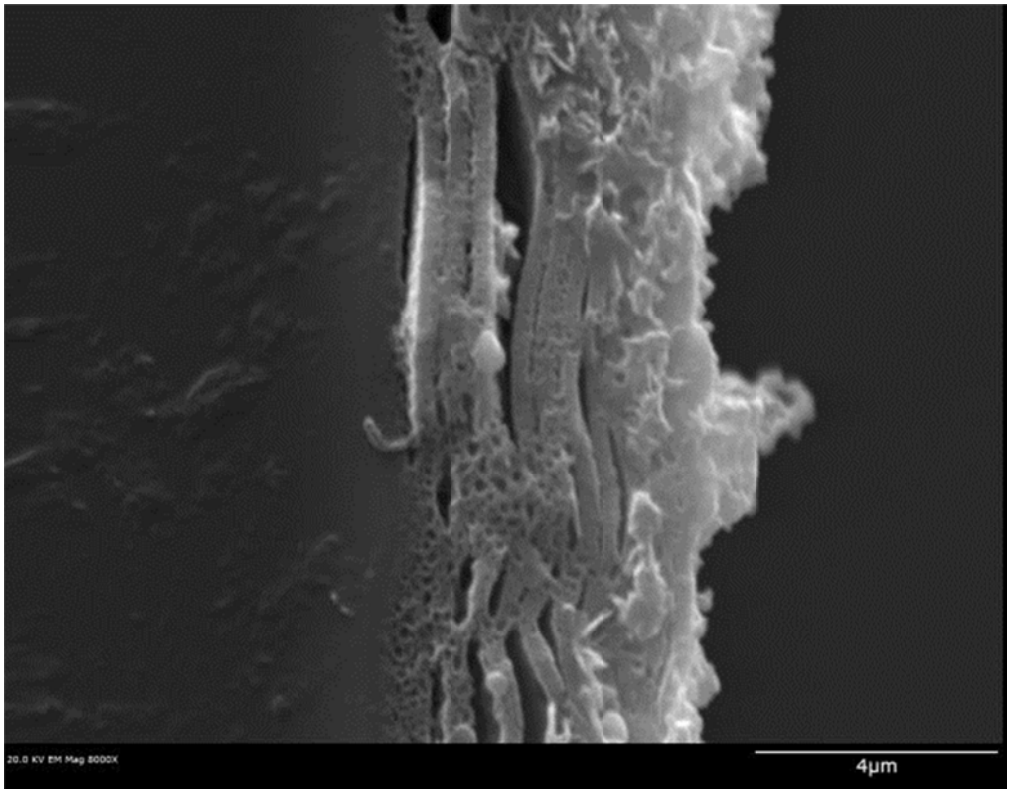

CCIM-AN-11 CCC

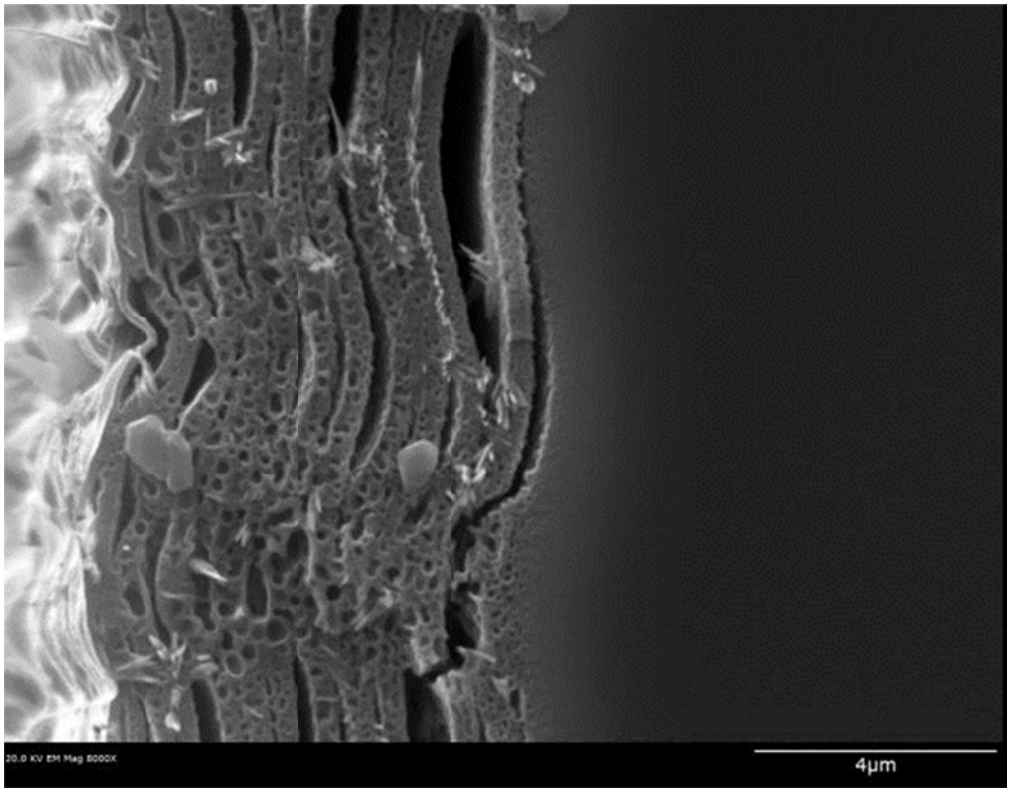

CCIM-AN-18 CCC

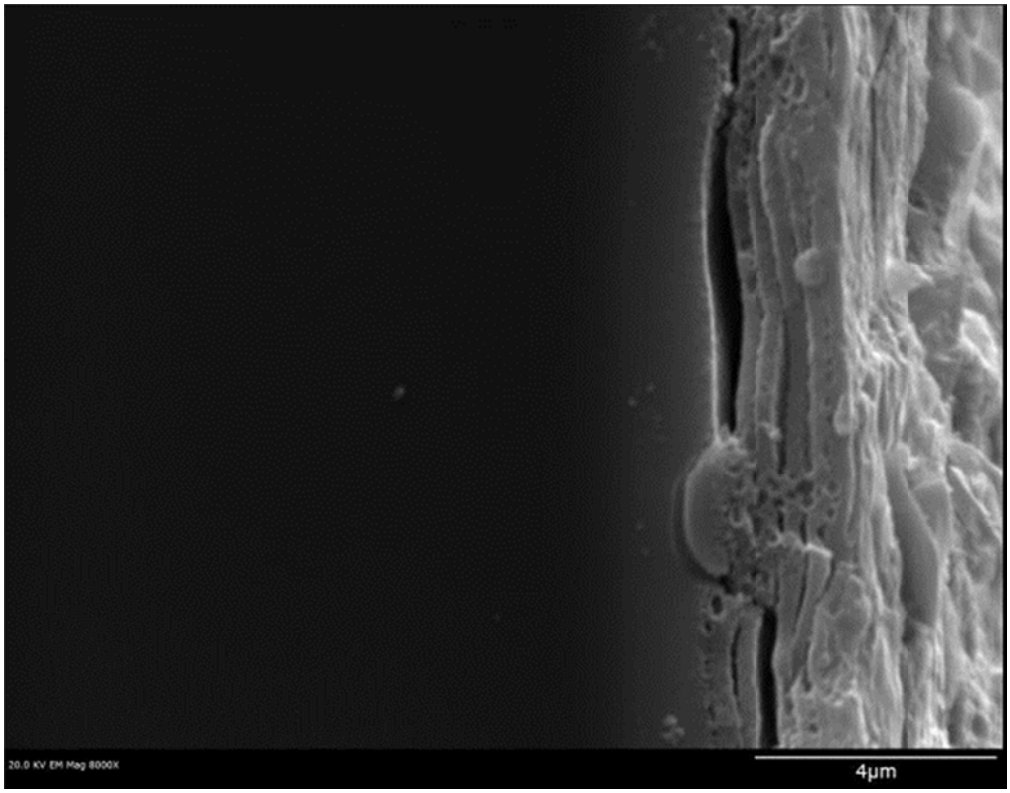

CCIM-AN-20 CCC

Appendix D

Candidate Matrix Glasses

Appendix D: Candidate Matrix Glasses

Table D.1. Composition and Predicted Properties of 51 Candidate Matrix Glasses

Comp.	1	2	3	4	5	6	7	8	9
Al_2O_3	0.20297	0.18032	0.22537	0.19789	0.18136	0.19367	0.18392	0.22464	0.18969
B_2O_3	0.15964	0.20737	0.17553	0.14580	0.14241	0.21385	0.20329	0.14905	0.17301
Bi_2O_3	0.02818	0.00434	0.02972	0.01046	0.01932	0.02111	0.00497	0.01287	0.00419
CaO	0.03409	0.09341	0.08263	0.05825	0.07286	0.01180	0.01083	0.02710	0.08416
CdO	0.00178	0.00112	0.00183	0.00199	0.00242	0.00102	0.00267	0.00230	0.00131
Cr_2O_3	0.00949	0.00783	0.00878	0.00441	0.00583	0.01206	0.00461	0.00334	0.00779
F	0.00167	0.00372	0.00524	0.00439	0.00966	0.00353	0.00724	0.00481	0.00985
Fe_2O_3	0.04666	0.04736	0.03465	0.02316	0.02644	0.03043	0.04174	0.04712	0.04938
K_2O	0.02488	0.03570	0.00006	0.02855	0.01360	0.00433	0.01283	0.03106	0.02501
La_2O_3	0.00905	0.00728	0.00182	0.00270	0.00543	0.00200	0.00221	0.00593	0.00139
Li_2O	0.02355	0.05417	0.02655	0.01344	0.04822	0.01322	0.04986	0.04672	0.05272
MgO	0.00972	0.00222	0.00174	0.00955	0.00465	0.00917	0.00583	0.00455	0.00900
MnO	0.00185	0.00390	0.00638	0.01184	0.00949	0.00589	0.00343	0.01163	0.01432
Na_2O	0.08590	0.07087	0.07714	0.08455	0.09204	0.11495	0.05159	0.11546	0.05268
Nd_2O_3	0.00139	0.00189	0.00177	0.00130	0.00151	0.00109	0.00183	0.00197	0.00178
NiO	0.00129	0.00389	0.00402	0.00118	0.00477	0.00695	0.00393	0.00706	0.00525
P_2O_5	0.00653	0.01154	0.02146	0.00544	0.01928	0.02142	0.01828	0.01478	0.00653
PbO	0.00352	0.00494	0.00520	0.00108	0.00839	0.00576	0.00158	0.00104	0.00521
RuO_2	0.00002	0.00004	0.00003	0.00001	0.00002	0.00004	0.00005	0.00001	0.00003
SiO_2	0.32913	0.23220	0.27130	0.35733	0.27966	0.27634	0.35169	0.27677	0.27566
SO_3	0.00592	0.00396	0.00693	0.00433	0.00690	0.00516	0.00221	0.00170	0.00389
SrO	0.00294	0.00409	0.00876	0.00291	0.00880	0.00738	0.00899	0.00371	0.00358
ZrO_2	0.00985	0.01783	0.00307	0.02944	0.03693	0.03884	0.02641	0.00637	0.02356
Total	1	1	1	1	1	1	1	1	1
Multicomponent constraints									
Al_2O_3+Fe_2O_3+ZrO_2	0.25948	0.24552	0.26309	0.25049	0.24473	0.26294	0.25208	0.27813	0.26263
Al_2O_3+ Fe_2O_3	0.24963	0.22768	0.26003	0.22105	0.20780	0.22410	0.22566	0.27176	0.23907
Al_2O_3+ ZrO_2	0.21282	0.19815	0.22844	0.22733	0.21829	0.23251	0.21033	0.23101	0.21325
Fe_2O_3+ ZrO_2	0.05651	0.06520	0.03772	0.05260	0.06337	0.06926	0.06816	0.05349	0.07294
Predicted properties (Vienna et al. 2009)									
η_{1150}, Pa.s	8.06	0.54	3.90	14.06	1.25	6.38	6.27	2.27	1.22
T at 5 Pas, °C	1204.3	925.7	1122.0	1268.5	1008.1	1174.0	1175.2	1047.0	1000.9
$T_{1\%}$-Sp, °C	1014.3	917.4	1065.5	940.3	940.5	1047.8	919.7	992.8	1064.7
ε_{1150}, S/m	16.4	35.7	16.4	11.4	33.4	19.4	22.9	38.9	26.6
Nepheline formation criteria									
N_{Si}	0.533	0.480	0.473	0.559	0.506	0.472	0.599	0.449	0.532
OB	0.570	0.587	0.570	0.572	0.594	0.556	0.542	0.592	0.585

Table D.1. (Continued)

Comp.	10	11	12	13	14	15	16	17	18
Al_2O_3	0.23499	0.19171	0.20149	0.21108	0.22020	0.24868	0.22532	0.23021	0.22028
B_2O_3	0.15461	0.14234	0.17230	0.21673	0.17137	0.16750	0.14907	0.14291	0.16149
Bi_2O_3	0.02037	0.01789	0.00427	0.00756	0.00555	0.01494	0.00179	0.01832	0.00230
CaO	0.03888	0.08265	0.09341	0.03618	0.01980	0.09086	0.07290	0.03119	0.06603
CdO	0.00228	0.00166	0.00145	0.00109	0.00220	0.00250	0.00247	0.00280	0.00221
Cr_2O_3	0.01261	0.01269	0.00899	0.00254	0.00402	0.00145	0.01025	0.00249	0.00879
F	0.00889	0.00900	0.00777	0.00693	0.00183	0.00438	0.00373	0.00412	0.00373
Fe_2O_3	0.01012	0.04468	0.05142	0.06467	0.04040	0.01824	0.02590	0.02279	0.04041
K_2O	0.01394	0.02792	0.03371	0.01755	0.03761	0.03933	0.01023	0.00208	0.03567
La_2O_3	0.00454	0.00764	0.00548	0.00352	0.00559	0.00946	0.00150	0.00315	0.00660
Li_2O	0.03145	0.05455	0.04188	0.05106	0.04265	0.01622	0.05085	0.02545	0.03787
MgO	0.00816	0.00787	0.00838	0.00428	0.00419	0.00422	0.00639	0.00990	0.00919
MnO	0.00420	0.00541	0.01193	0.00397	0.00884	0.00443	0.00276	0.00704	0.00717
Na_2O	0.05440	0.06146	0.08187	0.08884	0.07626	0.11700	0.09681	0.11996	0.10801
Nd_2O_3	0.00154	0.00160	0.00176	0.00140	0.00163	0.00107	0.00109	0.00130	0.00169
NiO	0.00279	0.00649	0.00572	0.00788	0.00826	0.00461	0.00143	0.00308	0.00176
P_2O_5	0.00888	0.01412	0.01120	0.01132	0.00704	0.01070	0.02140	0.01515	0.02357
PbO	0.00934	0.00405	0.00366	0.00515	0.00716	0.00852	0.00845	0.00816	0.00414
RuO_2	0.00003	0.00005	0.00002	0.00004	0.00003	0.00003	0.00003	0.00002	0.00003
SiO_2	0.36647	0.29425	0.23356	0.24027	0.29802	0.21230	0.26677	0.31257	0.24329
SO_3	0.00537	0.00578	0.00482	0.00384	0.00194	0.00428	0.00486	0.00556	0.00619
SrO	0.00110	0.00254	0.00797	0.00743	0.00884	0.00869	0.00671	0.00411	0.00226
ZrO_2	0.00504	0.00366	0.00692	0.00666	0.02658	0.01061	0.02929	0.02762	0.00734
Total	1	1	1	1	1	1	1	1	1
Multicomponent constraints									
Al_2O_3+Fe_2O_3+ZrO_2	0.25015	0.24004	0.25983	0.28241	0.28717	0.27753	0.28052	0.28062	0.26803
Al_2O_3+ Fe_2O_3	0.24511	0.23639	0.25291	0.27576	0.26059	0.26692	0.25122	0.25300	0.26069
Al_2O_3+ ZrO_2	0.24003	0.19536	0.20841	0.21774	0.24677	0.25929	0.25462	0.25783	0.22762
Fe_2O_3+ ZrO_2	0.01516	0.04834	0.05834	0.07133	0.06697	0.02885	0.05519	0.05041	0.04775
Predicted properties (Vienna et al. 2009)									
η_{1150}, Pa.s	13.86	1.37	0.84	1.13	4.25	2.15	1.75	7.94	1.55
T at 5 Pas, °C	1263.7	1005.2	958.7	970.0	1131.8	1055.0	1034.5	1197.2	1008.5
$T_{1\%}$-Sp, °C	1074.3	1088.6	1063.4	989.6	1031.8	943.9	1021.2	973.5	996.5
ε_{1150}, S/m	12.5	29.7	27.6	37.0	23.8	20.9	34.9	23.1	31.5
Nepheline formation criteria									
N_{Si}	0.559	0.538	0.452	0.445	0.501	0.367	0.453	0.472	0.426
OB	0.553	0.591	0.599	0.571	0.574	0.603	0.591	0.577	0.594

Table D.1. (Continued)

Comp.	19	20	21	22	23	24	25	26	27
Al_2O_3	0.24206	0.22837	0.20813	0.25557	0.18659	0.20646	0.23783	0.21598	0.20497
B_2O_3	0.17465	0.20640	0.14247	0.21281	0.19479	0.19927	0.21524	0.17618	0.20347
Bi_2O_3	0.02755	0.01096	0.01392	0.00686	0.01902	0.00254	0.02269	0.02731	0.02837
CaO	0.03461	0.01669	0.03505	0.00173	0.09811	0.01140	0.01549	0.02327	0.01530
CdO	0.00165	0.00231	0.00259	0.00236	0.00235	0.00207	0.00150	0.00290	0.00180
Cr_2O_3	0.00423	0.00279	0.01237	0.00385	0.00917	0.00532	0.00402	0.00332	0.00125
F	0.00557	0.00622	0.00635	0.00509	0.00188	0.00330	0.00769	0.00166	0.00845
Fe_2O_3	0.05764	0.01911	0.06137	0.05954	0.04985	0.01206	0.04794	0.04081	0.02729
K_2O	0.01185	0.00552	0.00431	0.03777	0.03454	0.03972	0.01975	0.00898	0.02475
La_2O_3	0.00316	0.00542	0.00808	0.00881	0.00891	0.00849	0.00871	0.00711	0.00202
Li_2O	0.04209	0.04925	0.02879	0.03047	0.03567	0.05421	0.01723	0.05977	0.04780
MgO	0.00860	0.00225	0.00771	0.00549	0.00327	0.00885	0.00221	0.00508	0.00968
MnO	0.01337	0.00679	0.01341	0.00370	0.00167	0.00705	0.00570	0.00517	0.01439
Na_2O	0.09796	0.07708	0.07374	0.10953	0.08743	0.09176	0.09241	0.05072	0.06660
Nd_2O_3	0.00199	0.00154	0.00161	0.00116	0.00103	0.00181	0.00168	0.00138	0.00126
NiO	0.00261	0.00203	0.00227	0.00221	0.00273	0.00619	0.00930	0.00159	0.00876
P_2O_5	0.01827	0.00888	0.02476	0.01312	0.01055	0.02045	0.01940	0.00998	0.01272
PbO	0.00288	0.00626	0.00374	0.00609	0.00400	0.00288	0.00489	0.00788	0.00860
RuO_2	0.00002	0.00005	0.00003	0.00002	0.00002	0.00005	0.00004	0.00001	0.00002
SiO_2	0.22925	0.31536	0.32813	0.20843	0.22176	0.28230	0.22645	0.32795	0.26310
SO_3	0.00314	0.00138	0.00561	0.00572	0.00418	0.00113	0.00565	0.00142	0.00302
SrO	0.00559	0.00576	0.00742	0.00142	0.00497	0.00330	0.00990	0.00386	0.00951
ZrO_2	0.01125	0.01958	0.00814	0.01825	0.01752	0.02941	0.02426	0.01767	0.03688
Total	1	1	1	1	1	1	1	1	1
Multicomponent constraints									
Al_2O_3+Fe_2O_3+ZrO_2	0.31094	0.26705	0.27765	0.33336	0.25395	0.24792	0.31003	0.27447	0.26914
Al_2O_3+ Fe_2O_3	0.29970	0.24748	0.26951	0.31511	0.23644	0.21851	0.28577	0.25680	0.23225
Al_2O_3+ ZrO_2	0.25330	0.24794	0.21628	0.27382	0.20410	0.23586	0.26209	0.23365	0.24185
Fe_2O_3+ ZrO_2	0.06889	0.03869	0.06952	0.07779	0.06737	0.04147	0.07220	0.05848	0.06417
Predicted properties (Vienna et al. 2009)									
η_{1150}, Pa.s	2.22	4.51	8.53	3.25	0.84	2.11	5.93	4.07	2.31
T at 5 Pas, °C	1055.0	1138.6	1210.8	1098.1	965.0	1046.2	1167.9	1128.4	1070.8
$T_{1\%}$-Sp, °C	1084.0	880.2	1169.9	1031.3	957.5	875.2	1100.3	958.8	980.9
ε_{1150}, S/m	32.0	27.5	16.4	28.8	26.4	38.1	16.9	29.9	27.3
Nepheline formation criteria									
N_{Si}	0.403	0.508	0.538	0.363	0.447	0.486	0.407	0.552	0.492
OB	0.585	0.551	0.567	0.573	0.595	0.569	0.561	0.560	0.566

Table D.1. (Continued)

Comp.	28	29	30	31	32	33	34	35	36
Al_2O_3	0.25920	0.22360	0.23863	0.21606	0.19754	0.21111	0.21611	0.25384	0.21796
B_2O_3	0.17329	0.14351	0.14714	0.15590	0.18371	0.16801	0.16620	0.18840	0.17580
Bi_2O_3	0.02311	0.01774	0.00609	0.02455	0.01686	0.01339	0.00846	0.02508	0.01766
CaO	0.04830	0.08156	0.07082	0.02767	0.07407	0.07644	0.01839	0.02794	0.00531
CdO	0.00134	0.00203	0.00154	0.00155	0.00190	0.00168	0.00257	0.00202	0.00131
Cr_2O_3	0.00250	0.00141	0.01190	0.00903	0.00581	0.01052	0.00918	0.00394	0.00851
F	0.00483	0.00140	0.00156	0.00411	0.00723	0.00301	0.00141	0.00217	0.00742
Fe_2O_3	0.04805	0.05170	0.05481	0.05238	0.02006	0.01819	0.05547	0.03159	0.04866
K_2O	0.03015	0.01435	0.01171	0.00269	0.01799	0.03126	0.00868	0.01369	0.02548
La_2O_3	0.00563	0.00935	0.00466	0.00183	0.00599	0.00275	0.00462	0.00693	0.00900
Li_2O	0.02536	0.01570	0.04754	0.05354	0.03318	0.02375	0.02504	0.03347	0.01054
MgO	0.00824	0.00517	0.00167	0.00209	0.00771	0.00336	0.00141	0.00242	0.00516
MnO	0.00622	0.01193	0.00559	0.00119	0.00915	0.00614	0.01152	0.00130	0.01499
Na_2O	0.08094	0.05236	0.08746	0.08545	0.11334	0.11921	0.07690	0.10604	0.08536
Nd_2O_3	0.00114	0.00133	0.00132	0.00178	0.00135	0.00113	0.00126	0.00132	0.00103
NiO	0.00635	0.00921	0.00341	0.00242	0.00106	0.00989	0.00309	0.00311	0.00631
P_2O_5	0.00867	0.02067	0.02124	0.02222	0.02144	0.02044	0.02124	0.01457	0.02484
PbO	0.00531	0.00382	0.00366	0.00121	0.00371	0.00716	0.00351	0.00420	0.00562
RuO_2	0.00002	0.00005	0.00002	0.00001	0.00004	0.00002	0.00003	0.00004	0.00004
SiO_2	0.24242	0.30693	0.25890	0.31479	0.25504	0.25946	0.33312	0.24743	0.31408
SO_3	0.00219	0.00146	0.00413	0.00154	0.00254	0.00433	0.00414	0.00402	0.00209
SrO	0.00321	0.00659	0.00482	0.00985	0.00304	0.00164	0.00722	0.00125	0.00614
ZrO_2	0.01353	0.01815	0.01138	0.00814	0.01726	0.00713	0.02043	0.02524	0.00671
Total	1	1	1	1	1	1	1	1	1
Multicomponent constraints									
Al_2O_3+Fe_2O_3+ZrO_2	0.32077	0.29345	0.30482	0.27658	0.23486	0.23643	0.29201	0.31066	0.27333
Al_2O_3+ Fe_2O_3	0.30724	0.27530	0.29343	0.26844	0.21760	0.22930	0.27158	0.28543	0.26662
Al_2O_3+ ZrO_2	0.27273	0.24175	0.25001	0.22420	0.21480	0.21824	0.23654	0.27907	0.22467
Fe_2O_3+ ZrO_2	0.06158	0.06985	0.06619	0.06052	0.03732	0.02532	0.07590	0.05683	0.05537
Predicted properties (Vienna et al. 2009)									
η_{1150}, Pa.s	5.33	12.05	2.36	3.80	1.37	2.09	13.65	4.68	14.51
T at 5 Pas, °C	1157.3	1246.3	1059.9	1117.6	1006.4	1047.8	1260.1	1142.5	1262.4
$T_{1\%}$-Sp, °C	1131.1	1172.4	1155.9	1023.8	858.9	1008.6	1106.4	999.4	1110.0
ε_{1150}, S/m	16.5	8.5	30.4	34.1	29.9	24.5	15.0	26.4	12.2
Nepheline formation criteria									
N_{Si}	0.416	0.527	0.443	0.511	0.451	0.440	0.532	0.407	0.509
OB	0.583	0.575	0.590	0.570	0.585	0.589	0.555	0.573	0.555

Table D.1. (Continued)

Comp.	37	38	39	40	41	42	43	44	45
Al_2O_3	0.18696	0.24973	0.25923	0.19551	0.20295	0.23550	0.23519	0.22875	0.20433
B_2O_3	0.19466	0.21567	0.16126	0.17537	0.21556	0.20962	0.21019	0.18993	0.21262
Bi_2O_3	0.00888	0.02257	0.02873	0.01883	0.02486	0.02126	0.01473	0.00362	0.00120
CaO	0.05617	0.03965	0.08985	0.01745	0.05148	0.01806	0.05879	0.09434	0.08060
CdO	0.00251	0.00216	0.00102	0.00204	0.00286	0.00177	0.00256	0.00178	0.00219
Cr_2O_3	0.00320	0.00370	0.00897	0.00726	0.00328	0.00885	0.01187	0.00946	0.00279
F	0.00980	0.00147	0.00188	0.00957	0.00460	0.00703	0.00627	0.00981	0.00315
Fe_2O_3	0.02524	0.01244	0.01168	0.06158	0.03107	0.01640	0.02874	0.02764	0.03774
K_2O	0.01467	0.01795	0.00203	0.03183	0.03983	0.00657	0.00875	0.03979	0.02951
La_2O_3	0.00549	0.00738	0.00854	0.00761	0.00164	0.00637	0.00747	0.00990	0.00875
Li_2O	0.02312	0.04004	0.01320	0.00348	0.04628	0.03773	0.02887	0.02464	0.03715
MgO	0.00182	0.00913	0.00890	0.00275	0.00259	0.00797	0.00322	0.00465	0.00619
MnO	0.01071	0.00605	0.00776	0.01301	0.00187	0.01127	0.00418	0.01484	0.01187
Na_2O	0.06551	0.11328	0.10069	0.09427	0.06020	0.10591	0.07605	0.05154	0.07742
Nd_2O_3	0.00170	0.00197	0.00193	0.00193	0.00146	0.00125	0.00174	0.00183	0.00160
NiO	0.00229	0.00729	0.00297	0.00189	0.00998	0.00756	0.00313	0.00422	0.00800
P_2O_5	0.00758	0.01995	0.01314	0.01682	0.01568	0.01872	0.01519	0.00575	0.01459
PbO	0.00484	0.00259	0.00601	0.00222	0.00825	0.00278	0.00816	0.00334	0.00280
RuO_2	0.00004	0.00001	0.00002	0.00004	0.00003	0.00003	0.00001	0.00002	0.00005
SiO_2	0.34072	0.21303	0.25942	0.31453	0.26192	0.24223	0.26364	0.25280	0.20954
SO_3	0.00165	0.00604	0.00688	0.00195	0.00568	0.00395	0.00232	0.00126	0.00475
SrO	0.00896	0.00270	0.00213	0.00506	0.00412	0.00607	0.00755	0.00963	0.00452
ZrO_2	0.02348	0.00520	0.00377	0.01501	0.00382	0.02312	0.00138	0.01046	0.03866
Total	1	1	1	1	1	1	1	1	1
Multicomponent constraints									
Al_2O_3+Fe_2O_3+ZrO_2	0.23568	0.26736	0.27468	0.27209	0.23784	0.27502	0.26531	0.26685	0.28073
Al_2O_3+ Fe_2O_3	0.21220	0.26217	0.27091	0.25708	0.23402	0.25190	0.26393	0.25639	0.24207
Al_2O_3+ ZrO_2	0.21045	0.25493	0.26300	0.21052	0.20677	0.25862	0.23657	0.23921	0.24299
Fe_2O_3+ ZrO_2	0.04872	0.01763	0.01545	0.07659	0.03489	0.03952	0.03012	0.03810	0.07640
Predicted properties (Vienna et al. 2009)									
η_{1150}, Pa.s	6.95	1.72	6.21	12.89	1.69	2.88	3.67	3.09	1.25
T at 5 Pas, °C	1185.2	1016.6	1175.3	1252.2	1027.3	1085.7	1114.6	1092.6	1005.0
$T_{1\%}$-Sp, °C	874.1	950.8	1095.9	1021.7	923.3	1045.1	1053.9	1085.0	1007.0
ε_{1150}, S/m	12.5	34.3	14.4	12.1	25.0	29.8	17.4	12.0	23.6
Nepheline formation criteria									
N_{Si}	0.574	0.370	0.419	0.520	0.499	0.415	0.459	0.474	0.427
OB	0.553	0.574	0.582	0.562	0.563	0.566	0.560	0.580	0.584

Table D.1. (Continued)

Comp.	46	47	48	49	50	Centroid	Min	Max
Al_2O_3	0.23901	0.22314	0.21019	0.24000	0.23315	0.22000	0.18032	0.25923
B_2O_3	0.20708	0.21072	0.20103	0.16638	0.17948	0.18000	0.14234	0.21673
Bi_2O_3	0.01926	0.00628	0.00773	0.02974	0.00419	0.01550	0.00120	0.02974
CaO	0.00733	0.07134	0.04770	0.09639	0.01832	0.05000	0.00173	0.09811
CdO	0.00198	0.00267	0.00229	0.00127	0.00220	0.00200	0.00102	0.00290
Cr_2O_3	0.01071	0.00572	0.01119	0.00144	0.00697	0.00700	0.00125	0.01269
F	0.00173	0.00272	0.00841	0.00853	0.00120	0.00550	0.00120	0.00985
Fe_2O_3	0.06817	0.02998	0.01140	0.03177	0.01732	0.04000	0.01012	0.06817
K_2O	0.02445	0.03183	0.01091	0.02879	0.02906	0.02000	0.00006	0.03983
La_2O_3	0.00512	0.00227	0.00365	0.00266	0.00810	0.00550	0.00139	0.00990
Li_2O	0.03556	0.00803	0.04206	0.04598	0.03927	0.03000	0.00348	0.05977
MgO	0.00158	0.00472	0.00842	0.00825	0.00781	0.00550	0.00141	0.00990
MnO	0.00525	0.00491	0.01114	0.00786	0.00992	0.00800	0.00119	0.01499
Na_2O	0.11187	0.09668	0.10029	0.07741	0.05257	0.08500	0.05072	0.11996
Nd_2O_3	0.00165	0.00198	0.00103	0.00167	0.00147	0.00150	0.00103	0.00199
NiO	0.00483	0.00172	0.00294	0.00905	0.00643	0.00550	0.00106	0.00998
P_2O_5	0.01985	0.00902	0.02250	0.00564	0.01955	0.01500	0.00544	0.02484
PbO	0.00497	0.00183	0.00109	0.00897	0.00279	0.00550	0.00104	0.00934
RuO_2	0.00002	0.00004	0.00005	0.00002	0.00002	0.00003	0.00001	0.00005
SiO_2	0.21784	0.23658	0.25727	0.20686	0.31925	0.26897	0.20686	0.36647
SO_3	0.00245	0.00660	0.00501	0.00344	0.00499	0.00400	0.00113	0.00693
SrO	0.00921	0.00888	0.00141	0.00781	0.00608	0.00550	0.00110	0.00990
ZrO_2	0.00008	0.03235	0.03230	0.01006	0.02986	0.02000	0.00008	0.03884
Total	1	1	1	1	1	1	1	1
Multicomponent constraints								
Al_2O_3+Fe_2O_3+ZrO_2	0.30727	0.28547	0.25388	0.28183	0.28032	0.28000	0.23486	0.33336
Al_2O_3+ Fe_2O_3	0.30718	0.25312	0.22159	0.27177	0.25046	0.26000	0.20780	0.31511
Al_2O_3+ ZrO_2	0.23909	0.25549	0.24249	0.25006	0.26301	0.24000	0.19536	0.27907
Fe_2O_3+ ZrO_2	0.06826	0.06233	0.04369	0.04184	0.04717	0.06000	0.01516	0.07779
Predicted properties (Vienna et al. 2009)								
η_{1150}, Pa.s	2.28	5.16	1.99	0.84	10.68	3.72	0.54	14.51
T at 5 Pas, °C	1048.8	1153.5	1043.8	964.7	1237.4	1117.1	925.7	1268.5
$T_{1\%}$-Sp, °C	1101.7	969.2	968.8	1057.6	1066.5	1057.3	858.9	1172.4
ε_{1150}, S/m	33.8	13.7	31.2	28.0	16.4	19.7	8.5	38.9
Nepheline formation criteria								
N_{Si}	0.383	0.425	0.453	0.395	0.528	0.469	0.363	0.599
OB	0.574	0.573	0.570	0.606	0.555	0.574	0.542	0.606

Distribution*

U.S. Department of Energy
Office of Environmental Management
Kurt Gerdes
Steve Schneider
Gary Smith

U.S. Department of Energy
Office of River Protection
Rob Gilbert
Albert Kruger
Billie Mauss

Idaho National Laboratory
Nick Soelberg

Savannah River National Laboratory
Fabienne Johnson
Jim Marra
David Peeler

Vitreous State Laboratory
Wing Kot
Ian Pegg

Washington River Protection Solutions
Paul Certa
Gene Ramsey
Terry Sams

Waste Treatment and Immobilization Plant
Steve Barnes
Ernie Lee
Jim Nelson
Larry Petkus

AREVA Federal Services
Eric Tchemitcheff
Catherine Veyer

Pacific Northwest National Laboratory
Paul Bredt
Jim Buelt
Jaehun Chun
Jarrod Crum
Ashutosh Goel
Pavel Hrma
Brad Johnson
Gary Josephson
Jesse Lang
Will Lepry
Dongsang Kim
Pepa Matyas
John McCloy
Reid Peterson
Loni Peurrung
Greg Piepel
Brian Riley
Carmen Rodriguez
Joseph Ryan
Mike Schweiger
Dan Skorski
John Vienna
Joseph Westsik, Jr.

*Distribution will be made electronically

Pacific Northwest
NATIONAL LABORATORY

U.S. DEPARTMENT OF
ENERGY

902 Battelle Boulevard
P.O. Box 999
Richland, WA 99352
1-888-375-PNNL (7665)
www.pnl.gov